

# **Reaction and Protein Engineering Employing a Carbonyl Reductase from *Candida parapsilosis***

Von der Fakultät für Mathematik, Informatik und Naturwissenschaften der RWTH  
Aachen University zur Erlangung des akademischen Grades eines Doktors der  
Naturwissenschaften genehmigte Dissertation

vorgelegt von

Diplom-Biotechnologe

Andre Jakoblinnert

aus

Ostercappeln

Berichter:   Universitätsprofessor Dr. Ulrich Schwaneberg  
              Universitätsprofessorin Dr. Marion B. Ansorge-Schumacher

Tag der mündlichen Prüfung: 21.09.2012

Diese Dissertation ist auf den Internetseiten der Hochschulbibliothek  
online verfügbar.





*“Früher war ichforsch, heute bin ich Forscher.”*

---

***Parts of this thesis have been published as the following journal contributions***

*"Asymmetric reduction of ketones with recombinant E. coli whole cells in neat substrates."*

from: **Jakoblinnert, A.**; Mladenov, R.; Paul, A.; Sibilla, F.; Schwaneberg, U.; Ansorge-Schumacher, M. B.\*; de Maria, P. D.\*  
in: Chemical Communications **47**: 12230-12232, **2011**

*"Who's Who? Allocation of Carbonyl Reductase Isoenzymes from Candida parapsilosis by Combining Bio- and Computational Chemistry."*

from: **Jakoblinnert, A.**; Bocola, M.; Bhattacharjee, M.; Steinsiek, S.; Bonitz-Dulat, M.; Schwaneberg, U.; Ansorge-Schumacher, M. B.\*  
in: Chembiochem **13**: 803-809, **2012**

*"Reengineered carbonyl reductase for reducing methyl-substituted cyclohexanones"*

from: **Jakoblinnert, A.**; Wachtmeister, J.; Schukur, L.; Shivange, A.V.; Bocola, M.; Ansorge-Schumacher, M. B.\*; Schwaneberg, U.\*  
in: Protein Engineering, Design & Selection, *in press*  
published online: Jan. 24, **2013** (doi: 10.1093/protein/gzt001)

*"Design of an Activity and Stability Improved Carbonyl Reductase from Candida parapsilosis"*

from: **Jakoblinnert, A.**; van den Wittenboer, A.; Shivange, A. V.; Bocola, M.; Hefele, L.; Ansorge-Schumacher, M. B.\*; Schwaneberg, U.\*  
in: Journal of Biotechnology, *accepted*

---

## Acknowledgement

This thesis was carried out in the framework of the graduate school *BioNoCo* (Biocatalysis in non-conventional media) financed by the Deutsche Forschungsgemeinschaft at the Lehrstuhl für Biotechnologie at RWTH Aachen University.

In the first place, I would like to thank my supervising professors Prof. Ulrich Schwaneberg (RWTH Aachen) & Prof. Marion B. Ansorge-Schumacher (TU Berlin) for giving the opportunity to execute this work and for their valuable counseling throughout the whole project. Prof. Conrath I thank for being the chairman of the Promotionskommission, and Prof. Blank for being my third examiner. Especially, Prof. Schwaneberg, who was the professor at the site, I convey my appreciation for all the support on the professional and personal level. I would like to express my gratitude to my direct supervisors Dr. Amol Shivange and Dr. Marco Bocola, who supported and guided me in the course of my practical work but also in the development to become a researcher. As the scientific head of most successful collaboration during this project, I acknowledge Dr. Pablo Dominguez de Maria. He not only supported me in scientific manner but also had a sympathetic ear for all my concerns and always time for *“commando cerveza”*.

Without the help, suggestions and critical questions of my office colleagues, I would have not been able to finish this work as it is. For all the honesty, the fun and the madness in the lab and in the office I thank Dr. Jan Marienhagen, Alexander Dennig, Christina Müller, Paula Bracco, Ramona (Barona) Knab, Dr. Tamara Dworeck and Marcus Schallmeyer. (*“The thing is...; Nehe; Deine Mutter,...; Eberkralle; 6-Minuten-Ei; Schwanumaaaaaaaaaaaaan;.....”*

For support in practical and scientific issues I convey my gratitude to Dr. Anne van den Wittenboer (now BASF) for introducing me into the topic, Dr. Lars Regestein (AVT, RWTH Aachen) for giving the chance to perform several fermentations, Thomas Ostapowicz (ITMC, RWTH Aachen) for preparing standards for analytics and Nicole Herr as well as Ronny Wesche (TC4, TU Berlin) for performing kinetic resolutions for me.

I always admired the collaboration with students and the graduate school BioNoCo gave me the chance to construct small projects and hire dedicated students to fulfill the tasks. For the contributions to my final thesis, I would like to thank Patricia Tilstam (Master thesis), Jochen Wachtmeister (Bachelor thesis), Jörg Müller (Bachelor thesis), Radoslav Mladenov (research project), Albert Paul (research project), Lina Schukur (research project), Lora Hefele and Nils Lippmann (research project).

---

## Zusammenfassung

Die Herstellung chiraler Alkohole als Bausteine für die Synthese von Pharmazeutika und Feinchemikalien gewinnt an Bedeutung in der chemischen Industrie. Biokatalytische Verfahren zur Bereitstellung dieser Komponenten durch asymmetrische Reduktion von preiswerten Ketonen stellt eine kompetitive Syntheseroute im Hinblick auf Selektivität, Produktivität, Kosteneffizienz und Nachhaltigkeit dar. Die Hauptherausforderungen zur Implementierung eines ökonomisch machbaren biokatalytischen Prozesses zur Ketonreduktion werden hier behandelt. Einerseits werden die äußeren Reaktionsbedingungen so verändert, dass die Ressourcen effizient genutzt werden und hohe Raum-Zeit-Ausbeuten möglich sind. Andererseits wird das Enzym, welches die Reaktion katalysiert, mittels Proteinengineering so entwickelt, dass es den Prozesskenngrößen besser gerecht werden kann.

Diese Thesis hat die Carbonylreduktase aus der Hefe *Candida parapsilosis* (CPCR2) zum Gegenstand, welche in der Lage ist ein breites Spektrum an Ketonen selektiv zu den entsprechenden chiralen Alkoholen umzusetzen. Zuerst musste die molekulare Identität der CPCR2 geklärt werden. Computergestützte Modellierung machte die Voraussage von Indikatorsubstraten möglich, die wiederum, experimentell verifiziert, eine Zuordnung von Sequenz und Funktion zweier Isoenzyme (CPCR1 & CPCR2) ermöglichte.

Die Verwendung von CPCR2 in einem neuartigen Reaktionskonzept für die Produktion von chiralen Alkoholen in molaren Mengen durch ein apparativ schlichtes Verfahren und unkomplizierte Produktaufarbeitung wurde hier erstmals gezeigt. Die Entwicklung des sogenannten „*Neat Substrate System*“ oder „*Reinsubstratsystem*“, worin ausschließlich reine Substrate und der Ganzzellkatalysator verwendet werden, beinhaltete die Identifizierung der beeinflussenden Reaktionsparameter und der Optimierung. Zudem wurde dieses Konzept erweitert auf die Verwendung verschiedener Substrate, zwei weiterer Enzyme zur Ketonreduktion und eines alternativen Reaktionsmodus. Das „*Neat Substrate System*“ ist das erste Beispiel für eine biokatalytische Alkoholproduktion in einem Reaktionsmedium ohne jegliches zusätzliches Lösungsmittel. Die Vielseitigkeit und Effektivität dieses System, welches hier entwickelt wurde, macht eine breite Anwendung in der organischen Synthese zur Herstellung chiraler Zwischenstufen möglich.

Proteinengineering wurde in den letzten Jahren sehr erfolgreich verwendet um maßgeschneiderte Enzyme für industrielle Prozesse bereitzustellen. Hierin spielen die Verbesserung von Aktivität, Stabilität sowie Selektivität die Hauptrolle. In dieser Thesis wird das Enzym CPCR2 zum ersten Mal einem semi-rationalen Proteinengineering unterzogen. Die Etablierung eines Proteinexpressionsverfahrens sowie Aktivitätstests im Microlitermassstab sind dafür eine Voraussetzung um

---

Mutantenbibliotheken von CPCR2 durchzumustern. Die zwei Ziele des Engineering waren die Erweiterung des Substratspektrums, sowie die Erhöhung der Enzymstabilität. Ein semi-rationaler Ansatz führte dabei zu einer erheblichen Aktivitätssteigerung hinsichtlich der Umsetzung von methyl-substituierten Cyclohexanonen. Hierbei wurde eine CPCR2-Variante identifiziert mit einem Aminosäureaustausch an Position 119 von Leucin zu Methionin (CPCR2-L119M), welche im Vergleich zum Wildtyp eine siebenfache höhere Aktivität zu 2-Methylcyclohexanon aufwies. Dieser experimentelle Befund konnte anhand von computergestützten Simulationen erklärt werden. Für CPCR2 konnte gezeigt werden, dass strukturell konservative Austausche wohlmöglich besser geeignet sind um das Substratspektrum zu beeinflussen. Die Hypothese liefert einen weiteren Ansatzpunkt für die Interpretation von Struktur-Funktions-Beziehungen in Enzymen und kann zukünftige Strategien zur Erweiterung von Substratspektren voranbringen.

Vorrausgehende Untersuchungen zur Stabilität von CPCR2 zeigten eine starke Inaktivierung an wässrig-organischen Grenzflächen. Für den Versuch der Enzymstabilisierung durch Protein-engineering wurde zuerst ein rein rationaler Ansatz gewählt, welcher zu der Doppelmutante CPCR2-A275N-L276Q führte, die sowohl in Aktivität als auch in Stabilität verbessert war. Die Variante diente als Ausgangspunkt für eine semi-rationale Optimierung durch einzelne und simultane Sättigungsmutagenese der Positionen 275 & 276. Die beste Variante CPCR2-A275S-L276Q zeigte eine Erhöhung der Aktivität um den Faktor 1,4, sowie eine Verbesserung der Thermoresistenz ( $\Delta T_{50}$ ) um +5.2°C. Zusätzlich wurde die Grenzflächenstabilität um den Faktor 1,6 erhöht. Die eingehende Analyse der Mutationen zeigte eine Kooperativität der Positionen 275 und 276, welche beide an der Interaktionsfläche des Dimers bzw. nahe der Bindungstasche liegen. Experimentelle Daten sowie computergestützte Analysen zeigten, dass die Stabilisierung hauptsächlich durch die Position 275 beeinflusst wurde, wohingegen die Aktivierung maßgeblich von Position 276 verursacht wurde. Strukturelle Untersuchungen eines Homologiemodells zeigten zudem, dass die stabilste Einzelmutante CPCR2-A275T eine Wasserstoffbrücke zwischen den Monomeren ausbildet, welche die erhöhte Stabilität erklärt. Der Einfluss von Position 276 konnte insoweit rationalisiert werden, dass die Aminosäuren an dieser Positionen in direktem Kontakt zum Substratmolekül stehen und somit die Aktivität modulieren können.

In dieser Arbeit wurde die Zuordnung von Sequenz zu Funktion für die Identifizierung von CPCR1 und CPCR2 erreicht. Des Weiteren wurde ein neuartiges Reaktionskonzept, das „*Neat Substrate System*“, entwickelt und erweitert für mögliche breite Anwendung. Außerdem wurden mittels Protein-engineering Varianten von CPCR2 erzeugt mit erweitertem Substratspektrum, sowie deutlich erhöhter Stabilität und Aktivität.

---

## Summary

Biocatalytic manufacturing of chiral alcohols as building blocks for the synthesis of pharmaceuticals and fine chemicals is of growing relevance in the chemical industry. The biocatalytic route to provide these compounds by asymmetric reduction of cheap ketones constitutes a competitive synthesis route with respect to selectivity, productivity, cost-effectiveness and sustainability. Major challenges to establish economically feasible biocatalytic processes are addressed; on the one hand by reaction engineering facilitating efficient use of the resources and high space-time yields and on the other hand by protein engineering to supply appropriate enzymes to meet the process benchmarks.

In this thesis, the characterization of a promising carbonyl reductase from the yeast *Candida parapsilosis* (CPCR2), which is able to selectively reduce various ketones to the corresponding alcohols, is presented. Molecular modeling permitted the prediction of indicator substrates and experimental verification enabled the assignment of sequence to function of two CPCR isoenzymes (CPCR1 & CPCR2). Applying CPCR2, a novel concept for producing chiral alcohols in molar amounts via an easy operation mode and straightforward work-up is introduced. Throughout the development of this so-called “neat substrate system”, which is composed of pure substrates and the whole cell catalyst, the key reaction parameters were elucidated and optimized. Moreover, the concept was further expanded towards different substrates, other ketone reducing enzymes and alternative operation modes. The “neat substrate system” demonstrates the first example for efficient biocatalytic alcohol production in a reaction medium lacking any bulk solvent. The versatility and efficiency of this system, developed here, might leverage this technique to become widely applicable.

Protein engineering has become a powerful tool for tailoring enzymes to meet certain requirements like increased activity, stability or selectivity. In this thesis, CPCR2 was subjected to semi-rational protein engineering for the first time. The establishment of an appropriate protein expression procedure and a NADH-depletion activity assay in microliter formate enabled screening of CPCR2 variant libraries. The main engineering goals were the enlargement of the substrate spectrum and stabilization of the enzyme.

A semi-rational approach led to substantial activity increase towards cyclohexanone substrates by exchange of leucine to methionine located in the substrate binding pocket (CPCR2-L119M). In particular,  $k_{\text{cat}}$  for the reduction of 2-methyl cyclohexanone was increased more than 7-fold. The effect was explained on the molecular level by *in silico* substrate docking. The overall findings led to the assumption that more conservative amino acid substitutions might be more appropriate for altering the substrate scope of CPCR2. This may guide future strategies to modify the substrate acceptance of this enzyme class.



---

Former studies on CPCR2 revealed severe inactivation at water-organic interfaces, which limits the application of the enzyme in biphasic systems. Previous attempts to stabilize the enzyme by rational protein engineering led to the double mutant CPCR2-(A275N, L276Q) showed increased stability as well as activity. This variant was adopted as a starting point for semi-rational optimization. Simultaneous site saturation and screening of these two positions revealed variants with improved activity and stability superior to the previous variant. The best variant found was CPCR2-(A275S, L276Q) exhibiting 1.4-fold higher activity, a  $\Delta T_{50}$  of +5.2 °C in thermoresistance and 1.6-fold increased interfacial stability. Analysis of the single mutations suggested cooperativity of the amino acids at position 275 and 276, which are located at the dimer interface and close to the binding pocket. Experimental data as well as computational analysis indicated a contribution to stability by position 275 and an impact on activity by position 276. Structural investigation of the model predicted the establishment of an inter-subunit hydrogen bond by threonine at position 275 being responsible for stabilization and direct interactions of residue 276 with the substrate modulating activity.

Taken together, a sequence to function assignment was achieved for identification of CPCR1 and CPCR2. A novel concept for biocatalytic alcohol manufacture, the “neat substrate system”, was developed and expanded to possible broad applications. CPCR2 was subjected to protein engineering yielding new variants with enlarged substrate scope, increased activity and stability.

## Table of Contents

<b>1. General Introduction.....</b>	<b>1</b>
<b>1.1. Biocatalysis in Organic Synthesis .....</b>	<b>1</b>
1.1.1. Importance of Biocatalysis in Industry in the 21th Century.....	1
1.1.2. Advantages and Drawbacks of Biocatalysis.....	2
1.1.3. Biocatalysis for the Production of Chiral Compounds.....	3
<b>1.2. Chiral Alcohols through Biocatalysis .....</b>	<b>3</b>
1.2.1. Chemical versus Biocatalytic Synthesis of Chiral Alcohols .....	3
1.2.2. Biocatalytic Routes to Chiral Alcohols.....	4
<b>1.3. Asymmetric Reduction of Prochiral Ketones by Biocatalysis .....</b>	<b>6</b>
1.3.1. General Aspects.....	6
1.3.2. Cofactor Regeneration .....	7
1.3.3. Whole Cells vs. Isolated Enzymes.....	7
1.3.4. Large-Scale Production of Chiral Alcohols.....	8
1.3.5. Alcohol Dehydrogenases in Non-conventional Media.....	11
<b>1.4. Biochemical Properties of Alcohol Dehydrogenases .....</b>	<b>15</b>
1.4.1. Classification of NAD(P)H-dependent Alcohol Dehydrogenases.....	15
1.4.2. Catalytic Mechanism and Enantioselectivity.....	15
1.4.3. Structural Motifs & Substrate Specificity .....	17
1.4.4. Limitations of Using Alcohol Dehydrogenases in Industrial Applications .....	19
<b>1.5. Carbonyl Reductase from <i>Candida parapsilosis</i>, a Powerful Catalyst with a Moving History .....</b>	<b>20</b>
1.5.1. Discovery and Impact .....	20
1.5.2. Substrate Scope and Selectivity .....	20
1.5.3. Temperature, pH Optimum and Stability.....	21
1.5.4. Comparison to Other Carbonyl Reductases from <i>Candida spp.</i> .....	22
1.5.5. Synthetic and Preparative Applications of CPCR Preparations .....	24
1.5.6. Patent Situation.....	24
<b>1.6. Enzyme Engineering for Improving Enzyme Performance .....</b>	<b>25</b>
1.6.1. General Concepts for Enzyme Improvement.....	25
1.6.2. Rational Protein Design & Computational Methods.....	26
1.6.3. Directed Evolution.....	27
1.6.4. Selection and Screening for Improved Variants.....	28
1.6.5. Enzyme Engineering of Alcohol Dehydrogenases .....	29

---

<b>1.7. Aim of This Thesis .....</b>	<b>33</b>
<b>1.8. References.....</b>	<b>34</b>
<b>2. Experimental .....</b>	<b>39</b>
<b>2.1. Molecular Biology Techniques.....</b>	<b>39</b>
2.1.1. Used Strains and Plasmids.....	39
2.1.2. Design of CPCR2 Gene Construct .....	40
2.1.3. Generation of Site-specific CPCR2 Mutants .....	41
2.1.4. Construction of CPCR2 Site-saturation Libraries .....	41
2.1.5. Transformation of Plasmid Constructs to <i>E. coli</i> .....	42
<b>2.2. Protein Chemistry Techniques.....</b>	<b>43</b>
2.2.1. CPCR2 Protein Expression in Flask Scale .....	43
2.2.2. CPCR2 Protein Expression in Fermenter .....	43
2.2.3. CPCR2 Protein Expression in 96-well Multititer Plates.....	44
2.2.4. Cell Lysis & CPCR2 Protein Purification .....	45
2.2.5. Cell Lysis in 96-well Plate-scale.....	46
2.2.6. NADH-depletion Assay for Activity Determination in Cuvette-scale .....	46
2.2.7. NADH-depletion Assay for Activity Determination in Microtiter Plate.....	47
2.2.8. Inactivation Assays for CPCR2 .....	48
2.2.8.1. Inactivation by Temperature .....	48
2.2.8.2. Inactivation by Detergents .....	49
2.2.8.3. Inactivation by Organic Solvents .....	50
2.2.9. Screening Strategy for Identification of More Stable CPCR2 Variants.....	51
<b>2.3. CPCR2 Biotransformations.....</b>	<b>51</b>
2.3.1. Biotransformation with Purified CPCR2 Enzyme.....	51
2.3.2. Biotransformation with Whole Cells with CPCR2-overexpressed.....	52
2.3.3. Biotransformation in Neat Substrates.....	52
<b>2.4. Computational Methods.....</b>	<b>54</b>
2.4.1. DNA & Protein Design and Sequence Analysis.....	54
2.4.2. DNA & Protein Alignments .....	54
2.4.3. Data Analysis and Fitting .....	54
<b>2.5. References.....</b>	<b>54</b>

---

<b>3</b>	<b>Results &amp; Discussion</b> .....	<b>55</b>
<b>3.1</b>	<b>Who's who? – Allocation of Carbonyl Reductase Isoenzymes from <i>Candida parapsilosis</i> by Combination of Bio- and Computational Chemistry</b> .....	<b>55</b>
3.1.1	Abstract .....	55
3.1.2	Introduction.....	55
3.1.3	Experimental .....	56
3.1.3.1	Preparation of CPCR from <i>C. parapsilosis</i> .....	56
3.1.3.2	Biochemical Characterization of CPCR1 .....	57
3.1.3.3	Cloning and Sequencing of CpSADH and CPCR1 .....	58
3.1.3.4	Measurement of Activity on Indicator Substrates .....	58
3.1.3.5	Computational Analysis.....	59
3.1.4	Results and Discussion.....	60
3.1.4.1	Biochemical and Molecular Characteristics of CPCR Preparations .....	60
3.1.4.2	Identification and Analysis of the Amino Acid Sequence.....	61
3.1.4.3	Computational analysis of CPCR Structure and Binding of Substrates .....	63
3.1.5	Conclusion .....	65
3.1.6	Supplementary Information .....	66
3.1.7	References.....	70
<b>3.2</b>	<b>Asymmetric Reduction of Ketones with Recombinant <i>E. coli</i> Whole Cells in Neat Substrates</b>	<b>71</b>
3.2.1	Abstract .....	71
3.2.2	Introduction.....	71
3.2.3	Results and Discussion.....	72
3.2.4	Summary and Outlook.....	75
3.2.5	References & Notes.....	76
<b>3.3</b>	<b>Synthetic Toolbox to Chiral Alcohols via Asymmetric Ketone Reduction with Recombinant <i>E. coli</i> Cells in Neat Substrates</b> .....	<b>78</b>
3.3.1	Introduction.....	78
3.3.1.1	Selection of Biocatalysts.....	79
3.3.1.2	Selection of Benchmark Substrates.....	79
3.3.1.3	Mass Transfer Limitation, Cofactor Availability & Process Stability.....	80
3.3.1.4	Deracemization for Production of Chiral Alcohols .....	80
3.3.2	Materials and Methods .....	82
3.3.2.1	Supply of Biocatalysts.....	82
3.3.2.2	Pre-treatment of Whole Cells & Liquid Substrates .....	82
3.3.2.3	General Setup of the Neat Substrate System.....	83

3.3.2.4	Permeabilization of Whole Cells & Cofactor Addition .....	83
3.3.2.5	Repeated Batch Operation .....	83
3.3.2.6	Deracemization of 1-phenylethanol.....	84
3.3.2.7	Chiral Gas Chromatography .....	84
3.3.3	Results and Discussion.....	85
3.3.3.1	Application of Three Different ADHs in Neat Substrates and Effect of $a_w$ .....	85
3.3.3.2	Conversion of Structurally Diverse Ketones & Stereoselectivity of the Alcohols .....	86
3.3.3.3	Mass Transfer Limitations of the Reaction System .....	90
3.3.3.4	Cofactor Limitations of the Reaction System .....	91
3.3.3.5	Influence of Temperature on the Reaction System .....	93
3.3.3.6	Operational Stability of the Catalyst in the Reaction System .....	94
3.3.3.7	Sequential Deracemization in Neat Substrates .....	95
3.3.4	Conclusion .....	98
3.3.5	References .....	99
<b>3.4</b>	<b>Reengineered Carbonyl Reductase for Reducing Methyl-substituted Cyclohexanones.....</b>	<b>103</b>
3.4.1	Abstract .....	103
3.4.2	Introduction.....	103
3.4.3	Materials & Methods.....	105
3.4.3.1	Preparation of Chiral Standards .....	105
3.4.3.2	Molecular Modeling .....	105
3.4.3.3	Cloning of CPCR2 into pET22 .....	106
3.4.3.4	Site Saturation Mutagenesis .....	106
3.4.3.5	Mutant Library Generation .....	107
3.4.3.6	CPCR2 Protein Expression in Microtiter Plate .....	107
3.4.3.7	CPCR2 Protein Expression in Flasks .....	107
3.4.3.8	CPCR2 Protein Purification .....	108
3.4.3.9	CPCR2 Activity Assay in Microtiter Plate .....	108
3.4.3.10	CPCR2 Activity Assay in Cuvette .....	108
3.4.3.11	Determination of Kinetic Parameters $K_M$ and $v_{max}$ .....	108
3.4.3.12	Determination of Temperature and pH-optimum .....	108
3.4.3.13	Asymmetric Reduction of 2-methylcyclohexanone .....	109
3.4.3.14	Determination of Conversion, Enantiomeric & Diastereomeric Excess .....	109
3.4.4	Results & Discussion .....	110
3.4.4.1	Rational Site Selection .....	110
3.4.4.2	Screening with Acetophenone & 2-butanone.....	111

3.4.4.3	Screening with Poorly Accepted Substrates & Identification Improved Variants...	112
3.4.4.4	Substrate Specificity and Selectivity of CPCR2-L119M.....	113
3.4.4.5	Structure-function Relationships & Substrate Docking.....	114
3.4.5	Conclusion .....	116
3.4.6	Supplementary Information .....	117
3.4.7	References.....	120
<b>3.5</b>	<b>Design of a Carbonyl Reductase from <i>Candida parapsilosis</i> Towards Enhanced Activity and Stability.....</b>	<b>122</b>
3.5.1	Abstract .....	122
3.5.2	Introduction.....	122
3.5.3	Materials and Methods .....	124
3.5.3.1	Chemicals, Oligo Nucleotides and Enzymes .....	124
3.5.3.2	Cloning of CPCR2 and Generation of CPCR2 Variants .....	124
3.5.3.3	Construction of CPCR2 Variants and Site-saturation Libraries.....	124
3.5.3.4	NADH-depletion Assays for CPCR2 Activity.....	125
3.5.3.5	Kinetic Parameters, Stereoselectivity, T <sub>50</sub> -value and Interfacial Stability .....	125
3.5.3.6	Screening for Improved Stability .....	127
3.5.4	Results & Discussion.....	128
3.5.4.1	Interfacial Stability of CPCR2 .....	128
3.5.4.2	Rational Site Selection for CPCR2 Variants.....	129
3.5.4.3	Activity & Stability of Rationally Designed CPCR2 Variants.....	129
3.5.4.4	Cooperativity of Position 275 and 276 in CPCR2.....	131
3.5.4.5	Screening Procedure of Increased Activity and Stability.....	132
3.5.4.6	CPCR2 Variants Found by Screening.....	134
3.5.4.7	Characterization of Purified CPCR2 Variants.....	136
3.5.4.8	Computational Analysis of the Mutations.....	137
3.5.4.9	Hypotheses of activating or stabilizing role of position 275 and 276 in CPCR2 .....	139
3.5.5	Conclusion .....	141
3.5.6	Supplementary Information .....	142
3.5.7	References.....	146
<b>4.</b>	<b>Conclusion .....</b>	<b>148</b>
<b>5</b>	<b>Appendix .....</b>	<b>154</b>
<b>5.1</b>	<b>List of Abbreviations .....</b>	<b>154</b>
<b>5.2</b>	<b>List of Figures.....</b>	<b>157</b>
<b>5.3</b>	<b>List of Tables.....</b>	<b>159</b>

# 1. General Introduction

## 1.1. Biocatalysis in Organic Synthesis

Biocatalysis is one of the main pillars of applied biotechnology, defined by the European Federation of Biotechnology as the *“integration of natural sciences and engineering sciences in order to achieve the application of organisms, cells, parts thereof and molecular analogs for products and services”*.<sup>[1]</sup>

In this thesis, the focus is laid on biocatalysis with regard to application in white/industrial biotechnology to produce value-added compounds mainly applying biotransformation involving only one or few synthetic steps.

### 1.1.1. Importance of Biocatalysis in Industry in the 21th Century

Biocatalysis is used by mankind since 6000 years for preparation of food and drinks; at the outset without knowing about the microorganisms facilitating these useful conversions like ethanol production from sugars during brewing. Traditionally, biocatalysis played a crucial role in the food sector but started to gain significance around hundred years ago in other areas like the laundry, pulp and leather industry. Fundamental discoveries led to the understanding that microorganisms and the enzymes therein are the catalysts accelerating the chemical reactions. With the advent of recombinant DNA technology in the late 1980s' as well as the advancements in protein chemistry and reaction engineering, biocatalysis became a valuable tool in organic synthesis. Some processes employing enzymes have been established in multi-ton scale e.g. for the production of sweeteners, vitamins, amino acids or acrylamide (see Table 1). The number of industrial processes with biocatalysis involved is rapidly increasing especially in the fields of biofuels, biomaterials and active pharmaceutical intermediates.

**Table 1 Selected large-scale biotransformations (not whole cells), adapted from**<sup>[2]</sup>.

Scale (t a <sup>-1</sup> )	Product	Enzyme	Application	Company
>1,000,000	high-fructose corn syrup	glucose isomerase	sweetener in drinks	various
>100,000	lactose-free milk	lactase	food & drinks	various
>10,000	acrylamide	nitrilase	polymer industry	Nitto Co.
>10,000	cocoa butter	lipase	Food industry	Fuji Oil

In 2003, McKinsey & Co. predicted that by 2010, industrial biotechnology will account for 10 % of the sales within the chemical industry, amounting to 125 billion US\$.<sup>[3]</sup> This value was almost met with 121 billion US\$ and sales are estimated to reach up to 675 billion US\$ in 2020.<sup>[4]</sup> This development is also reflected by the doubling of biocatalytic processes implemented in industry, wherein 150 processes were counted in 2005<sup>[5]</sup> and 300 processes are reported in 2010.<sup>[6]</sup> Biocatalysis is especially

suited for drug synthesis and in this multi-billion dollar market actually 10 % of the total drug synthesis depend on enzymatic steps as announced in 2009.<sup>[7]</sup>

### 1.1.2. Advantages and Drawbacks of Biocatalysis

Nowadays, not only economic drivers foster the substitution of established chemical processes but also political and ecologic issues are taken into account. At best, a process has to be efficient and sustainable at the same time and biocatalysis can contribute to this overall goal in a substantial manner due to its inherent characteristics. One development is the use of non-fossil carbon sources for the production of bulk chemicals and fuel components to be less dependent on the depleting oil sources. Especially the recycling of cheap waste material by biocatalysis lowers the cost of raw materials.<sup>[8]</sup> The application of bio-based starting material directly counteracts the use of toxic chemicals and reduces emission of greenhouse gases and waste water.<sup>[8]</sup> Another environmental aspect is that biocatalysts themselves are biodegradable.<sup>[9]</sup>

Compared to classical chemical catalysis, biocatalysis usually operates at mild reaction conditions such as ambient pressure and temperature as well as mostly in aqueous buffer systems. These features increase the safety at the working place, decrease energy costs and unwanted side-reactions.<sup>[9]</sup> Additionally, enzymes are very efficient catalyst accelerating reaction exceeding factor  $10^{15}$  at loads of usually 0.1–1 % and total turnover numbers up to  $10^5$ .<sup>[9]</sup>

A key feature of biocatalysis is its chemo-, regio- and stereoselectivity, which are usually superior to chemical catalysis. Especially in pharmaceutical industry enantiomeric purity of the products is most important and 80 % of all active components are chiral.<sup>[10]</sup> Biocatalysis, furthermore, provides excellent product qualities.<sup>[10-11]</sup> The innate chemoselectivity of enzymes makes the use of intensive protection-group chemistry obsolete, reducing the number of reaction steps and waste production.<sup>[11]</sup>

Recent developments aim at the implementation of biocatalytic processes in multi-step reactions since enzymes are typically compatible and these arrangements enforce productivity and reduce inhibition phenomena.<sup>[8]</sup> Also combinations of chemo- and biocatalytic steps in one pot are established to increase yields and simplify the reaction sequences.<sup>[8, 12]</sup>

Even though biocatalysis is endowed with several advantageous features compared to chemical catalysis the choice for a biocatalytic route in organic synthesis is often impaired. This is because many reservations are voiced including limited substrate specificity and general catalyst availability, instability and inhibition as well as low productivity and dependency on expensive cofactors.<sup>[2, 9]</sup> Furthermore, enzymes are most active in aqueous environments and water is in many cases the least suitable solvent or agent in organic chemistry since water is nucleophilic and acts as acid or base.<sup>[9]</sup> Also most organic compounds are only poorly soluble in water.<sup>[9]</sup>



However, recent scientific developments in the field of protein engineering have facilitated the tailoring of enzyme properties towards specific process requirements. Many examples show the application of powerful techniques such as directed evolution, rational design and combinations thereof to provide suitable catalysts for industrial application.<sup>[6, 10, 12-13]</sup> Herein, substantial improvements in activity, selectivity and process stability have been achieved. Process engineering helped overcoming inactivation and inhibition phenomena by design of appropriate reactors or catalyst immobilization, which dramatically increased space-time yields and catalyst stability.<sup>[8]</sup> The dependence on expensive auxiliary compounds such as nicotinamide cofactor was tackled by recycling and is efficiently applied on industrial scale.<sup>[14]</sup>

Current trends in biocatalysis are expected to emerge from the fields of metabolic engineering and synthetic biology. Metabolic engineering aims at optimization of enzymatic, transport and regulatory functions of a production microorganism to provide high value-added products from cheap feed stocks. In synthetic biology, for example, microorganisms with a minimal synthetic genome are generated with customized gene expression abilities for an application.

### **1.1.3. Biocatalysis for the Production of Chiral Compounds**

In recent years, chiral chemicals for pharmaceuticals, agrochemicals and food ingredients are more and more manufactured via biocatalysis.<sup>[15]</sup> Most of the industrial relevant processes involve introduction of chiral centers to product molecules.<sup>[16]</sup> The importance of enantiopurity in this multi-billion dollar market is further fueled by the Food & Drug Administration (FDA). Due to the critical role of enantiomeric purity of drugs in selectivity and toxicity, the FDA demands additional toxicological studies on all drug components that comprise more than 1 % of the total agent (docket No. 97D-0448).<sup>[2]</sup> Most important compounds are chiral alcohols, amine, carboxylic acids and epoxides.<sup>[13b]</sup>

## **1.2. Chiral Alcohols through Biocatalysis**

### **1.2.1. Chemical versus Biocatalytic Synthesis of Chiral Alcohols**

Asymmetric reduction of simple prochiral ketones, such as 2-butanone or 3-butanone, to the corresponding chiral alcohols is still a lively research area. In 2001, the Nobel Prize in Chemistry was awarded for development of Rhodium/Ruthenium catalysts for this purpose to K. B. Sharpless, W. S. Knowles and R. Noyori. Industrial processes in ton scale have been established employing this type of catalysts.<sup>[10]</sup>

The Rhodium/Ruthenium catalysts constitute a breakthrough in homogeneous catalysis towards chiral alcohols; however, the technology is hampered by the rather expensive, rare and toxic transition metals.<sup>[18]</sup> Additionally, the complex chiral ligands are difficult to produce and cannot be

reused. Furthermore, enantioselectivity of most chemical hydrogenation methods is only moderate for simple dialkyl ketones or diketones.<sup>[19]</sup> Progress was made by using organic H-donor instead of molecular hydrogen, since this is comparably expensive and explosive.<sup>[10]</sup> Chiral modified borane compounds can deliver a broad variety of enantiopure alcohols, but large amounts of borane are difficult to handle.<sup>[10]</sup>

Nowadays classical chemical synthetic approaches are in competition with biocatalytic processes due to the numerous advantages of biocatalysis stated earlier. Especially in the field for the preparation of enantiopure alcohols, the selectivity of enzymes coupled with the benign reaction mode have the potential to outperform chemical catalysts.<sup>[2, 17]</sup>

### 1.2.2. Biocatalytic Routes to Chiral Alcohols

The demand for production processes of chiral alcohol is enormous, since in five years 57 patents have been filed using biocatalysis for this purpose.<sup>[16]</sup> Chiral alcohols can be accessed by different pathways using various precursor molecules and enzymes (see Figure 1).

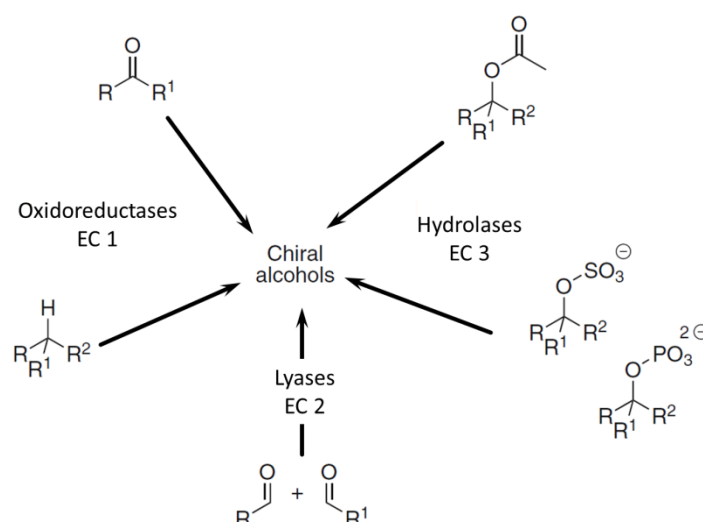


**Figure 1** Examples for different biocatalytic routes for the production of chiral alcohols. The substrate structures are depicted, which result in chiral alcohols when transformed by the respective enzyme class (EC = Enzyme Commission number) indicated. Adapted from<sup>[20]</sup>.

Hydrolases (EC 3) play the most important role in industrial processes today.<sup>[21]</sup> Very prominent among these are lipases performing kinetic racemate resolution by stereoselective esterification and hydrolysis. Here, an acyl donor is connected to only one of the stereoisomers of the racemic alcohol. The ester and the remaining alcohol can be separated by distillation. The enantiopure esterified enantiomer can be recovered by ester hydrolysis. Furthermore, lipases offer a broad substrate spectrum, are commercially available and operate in organic solvents, which provides high solubility of organic substrate and product.<sup>[9]</sup> Additionally, other hydrolases such as phosphatases and sulfatases are described to yield chiral alcohols.<sup>[20]</sup> However, the maximum possible yield of kinetic

resolution is 50 % and enantiomeric excess of the product is reduced with conversion higher than 50 %.<sup>[9]</sup> Recently, an interesting approach combining a lipase for racemate resolution and a Ruthenium catalyst for racemization of the unwanted enantiomer was realized.<sup>[22]</sup>

Chiral hydroxyketones can be obtained by lyases (EC 4) such as benzaldehyde lyase, pyruvate decarboxylase and deoxyriboaldolase or hydroxynitrile lyases.<sup>[20]</sup> In this reaction a new carbon-carbon bond is established between two aldehydes and chiral hydroxyketones are produced.

Among the oxidoreductases (EC 1), alcohol dehydrogenases (ADHs) or carbonyl reductases play the most important role. To access chiral alcohols asymmetric reduction of prochiral ketones to the corresponding alcohols is performed. The main advantage compared to kinetic resolution by lipases is that the theoretical yield can be 100 %. Furthermore, no auxiliary compounds (e.g. acyl donor) are required rendering this process efficient with regard to atom economy.<sup>[23]</sup> However, a major drawback is that ADHs almost exclusively depend on the expensive nicotinamide cofactor in stoichiometric amounts. The solution to this is cofactor recycling, which is outline in chapter 1.3.2.

As ketone reduction is reversible, asymmetric oxidation of alcohols can also be used to kinetically resolve a racemic mixture but yields can again not exceed 50 %. Nevertheless, a combination of enzymes exhibiting different cofactor preference and opposite enantioselectivity was applied in a one-pot reaction to give 100 % enantiopure alcohol from the racemate.<sup>[24]</sup> Also stereoinversion was reported wherein microorganisms resolve racemic mixtures to only one enantiomer (see Figure 2).<sup>[9]</sup> Furthermore, ADHs are not as tolerant to organic solvents as lipases, but many of them are commercially available tendering the two possible stereoselectivities.

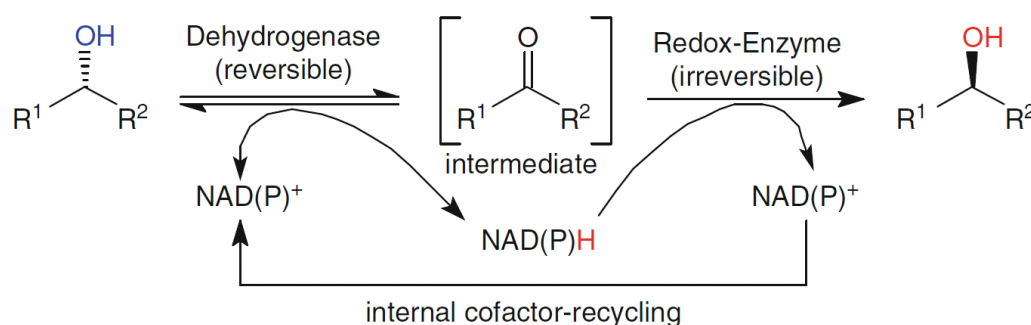


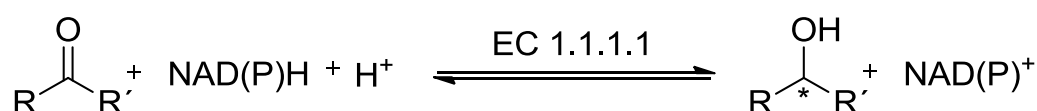
**Figure 2** Deracemization of secondary alcohol via microbial stereoinversion applying two enzymes of opposite enantioselectivity. Taken from <sup>[9]</sup>.

A second enzyme class performing oxidoreductions are monooxygenases, which are able to incorporate hydroxyl functions into non-activated alkyl chains yielding chiral alcohols.<sup>[25]</sup> However, larger scale applications of this enzyme class are lacking.

### 1.3. Asymmetric Reduction of Prochiral Ketones by Biocatalysis

#### 1.3.1. General Aspects

The interconversion of ketones to the corresponding alcohols and vice versa is the most common redox reaction in organic chemistry.<sup>[18]</sup> Compared to the other biocatalytic methods to prepare chiral alcohols, asymmetric reduction of prochiral ketones with NAD(P)H-dependent alcohol dehydrogenases -also termed carbonyl reductases- (E.C. 1.1.1.1) is distinctly attractive. This is due to the cheap prochiral ketonic starting material and the theoretically yield of 100 % of enantiopure alcohol (see Scheme 1). The introduction of chirality in to non-chiral compounds is generally connected to a high increase of value. The high value-added product from asymmetric ketone reduction is the driving force for the development of new biocatalytic production processes. This technique is now considered as fully complementary to chemical methods for large-scale pharmaceutical manufacturing.<sup>[17]</sup>



**Scheme 1** Interconversion of a ketone to the corresponding alcohol with NAD(P)H as cofactor catalyzed by alcohol dehydrogenase (EC 1.1.1.1). R and R' indicate different substitutions of the molecule. The asterisk designates a chiral carbon atom.

Since the early days of biotechnology, whole cell microorganisms, such as *Saccharomyces cerevisiae*, were used to reduce carbonyl compounds enantioselectively in industrial scale due to the easy process handling, cheap raw materials and *in vivo* cofactor recycling.<sup>[10]</sup> However, an economic fermentation process usually requires substrate concentrations >30 g L<sup>-1</sup> and easy product downstream processing, which is not always feasible.<sup>[10]</sup>

Shortcomings in aqueous biocatalysis like low solubility of the organic substrate and product molecules are tackled by process engineering such as aqueous-organic two-phase setups, monophasic aqueous-organic mixtures or enzyme-membrane and packed-bed reactors.<sup>[16-17]</sup> Most importantly, these processes were proven to be scalable for industrial application.<sup>[13b]</sup> Recently, “one-pot” syntheses of multi-step process involving biocatalytic asymmetric reduction were shown to work.<sup>[14b, 17]</sup> Such developments are desirable since time, effort and solvent can be saved.

Oxidation of alcohols by ADHs is rare, since this destroys stereocenters and can easily be achieved by classical chemical methods. However, aldehydes are notoriously instable in conventional chemical oxidation conditions; hence, some biocatalytic methods have been developed to produce aldehydes from the corresponding primary alcohols.<sup>[26]</sup>

### 1.3.2. Cofactor Regeneration

The economic drawback that costly nicotinamide cofactors (NAD(P)H) are needed in stoichiometric amount was overcome by several strategies to regenerate the cofactor *in situ*.<sup>[14b]</sup> Herein, two main approaches appear also in industrial scale, namely the *substrate-coupled* and the *enzyme-coupled* cofactor regeneration (see Figure 3).

In the substrate-coupled approach, a single ADH oxidizes an auxiliary cheap alcohol (H-donor), mostly isopropanol, while reducing NAD(P)<sup>+</sup> to NAD(P)H (see Figure 3, left).<sup>[18]</sup> The same ADH also carries out the stereoselective reduction reaction. Herein, the H-donor must be in excess to shift the equilibrium to the product side, which can result in substrate-inhibition or biocatalyst inactivation.<sup>[18]</sup> However, there are solvent-tolerant enzymes and cells, which can deal with up to 80 and 50 % (v/v) of isopropanol, respectively.<sup>[27]</sup> In principle, the reaction can also be run in the oxidation direction with an excess of acetone. However, biocatalysts have been shown to be susceptible to acetone inactivation at higher concentrations.<sup>[28]</sup>

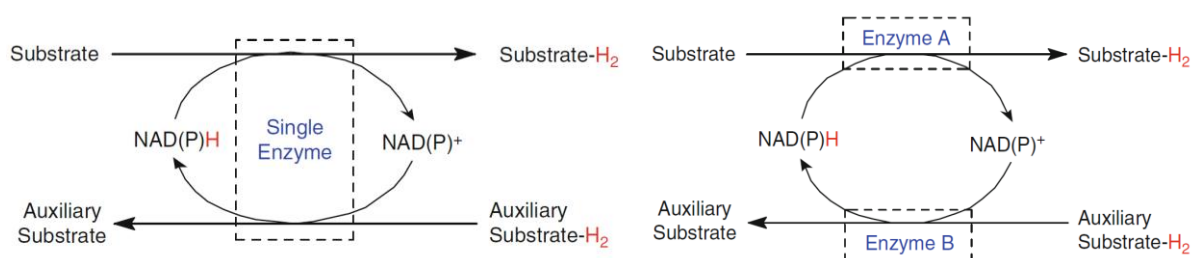


**Figure 3** Cofactor regeneration systems for alcohol dehydrogenases. Left: Substrate-coupled mode with a single enzyme catalyzing substrate reduction and auxiliary substrate oxidation. Right: Enzyme-coupled mode wherein enzyme A reduces the substrate and a second enzyme (B) takes over the part of auxiliary substrate oxidation. Taken from <sup>[9]</sup>.

In the enzyme-coupled approach one enzyme has the reducing the other the oxidizing part (see Figure 3, right). With different substrates and activities the performance and equilibrium of these systems can be triggered. A prominent method is the use of dehydrogenases oxidizing formate, glucose and glucose-6-phosphate for cofactor reduction.<sup>[9]</sup> The oxidized species are in the following eliminated from the equilibrium promoting alcohol formation. Additionally, phosphite and other ADHs have been exploited for cofactor regeneration as well.<sup>[9]</sup> Alternatively, hydrogenases were shown to utilize molecular hydrogen for regeneration of nicotinamide cofactors.<sup>[7,9]</sup>

For recycling of oxidized nicotinamide cofactors either glutamate dehydrogenase or nicotinamide oxidase can be utilized.<sup>[9]</sup> Electrochemical and photochemical regeneration methods have been proven to work too, but are not as efficient as enzymatic methods.<sup>[7,9]</sup>

### 1.3.3. Whole Cells vs. Isolated Enzymes

The choice of the appropriate biocatalyst form (whole cells or isolated enzyme) to produce the desired product depends on the most economic operation mode of the manufacturing process.

Herein, the two options whole cells and isolated enzyme have distinct advantages and disadvantages, which will be discussed in the next paragraph.

Generally, whole cells have the big advantage that they are easy to produce and that tedious and expensive enzyme purification is not necessary.<sup>[26a]</sup> For an efficient process the biocatalytic activity may be enhanced by overexpression of the enzyme of interest. The type of reaction treated here requires nicotinamide cofactors; whole cells provide this expensive component from their intrinsic cofactor pool and can even regenerate it effectively *in situ*. Compared to isolated enzymes whole cell catalysts exhibit considerably higher process stability since the enzymes are operated in a native-like environment. A disadvantage of whole cells is that other host enzymes may cause side reactions and reduce the final yield and especially enantiomeric excess of the product. Furthermore, substrates and products have to cross the membrane barrier, which constitutes a mass-transfer barrier.

Recently, so-called “*designer bugs*” have been generated to overcome limitations of whole cell biocatalysis such as side-reactions and insufficient cofactor regeneration. Side products were eliminated by knocking out genes coding for competing enzymes and cofactor regeneration was enhanced by overexpression of cofactor regenerating enzymes in the same microorganism.<sup>[14b]</sup> Additionally, efficient “*cell factories*” might be generated by metabolic engineering to carry out highly optimized biotransformations or multi-enzyme synthesis of high value product.<sup>[26a]</sup>

The application of isolated enzymes bears the advantage of higher productivity and less side reactions. The major drawback is; however, that the cofactor has to be added externally to drive the reaction. The cofactor as well as the enzymes may exhibit limited stabilities under process conditions. Immobilization of both was shown to improve stabilities, but reduce enzyme activity. Additionally, the enzymes have to be purified, which is tedious and costly. Nowadays, commercial enzyme preparations consist mostly of crude cell lysate containing the desired enzyme in an enriched, sometimes partially purified form, which reduces the production costs. Nevertheless, in such semi-pure preparations side reactions may occur caused by protein impurities.

#### **1.3.4. Large-Scale Production of Chiral Alcohols**

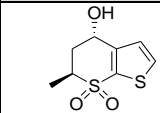
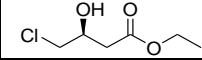
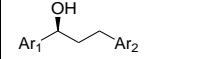
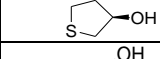
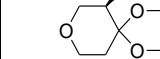
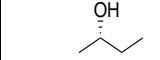
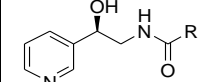
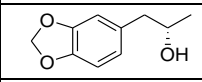
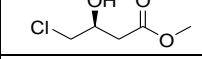
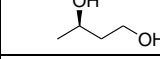
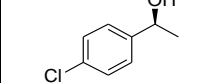
Implementation of an enzymatic process is determined by certain performance parameters in order to be competitive to chemical processes. Herein, an optimal biocatalyst converts >99 % of substrate at a concentration >100 g L<sup>-1</sup> in less than 24 h with the product having >99.5 % *ee* and a catalyst load of <5 g L<sup>-1</sup>.<sup>[17, 29]</sup> In 134 industrial-scale biotransformations (>100 kg) for fine chemicals (not pharmaceuticals) average performance parameters were found to be 78 % yield, 108 g L<sup>-1</sup> product concentration and 372 g L<sup>-1</sup> d volumetric productivity.<sup>[2]</sup> These parameters indicate how challenging industrial biocatalysis is and where to go when new processes or biocatalysts are designed for industrial applications. In general, the biocatalyst itself has to be optimized to meet these

requirements and/or the process has to be adapted by process engineering. The methods for enzyme optimization will be outlined in chapter 1.6.

In Table 2, large-scale industrial processes for the asymmetric production of chiral alcohols are summarized together with important performance parameters such as substrate concentration, conversion, yield and reaction scale. Entries in Table 2 are sorted on the basis of reaction scale starting with a multi-ton process down to few kilograms. It may be noted that substrate loading is mostly higher than  $100 \text{ g L}^{-1}$ , enantiomeric excess (*ee*) is higher than 94 % and yields are higher than 80 %, which is close to the above mentioned parameters for industrial processes.

Interestingly, non-recombinant whole cell microorganisms are employed for multi-kg (see Table 2, entries 7-9) as well as multi-ton (see Table 2, entries 1) preparation of highly pure enantiomeric alcohols. Herein, the molecular identity of the enzyme or enzymes performing the reaction is generally not known.

**Table 2 Biocatalytic asymmetric reduction of C=O compounds in industrial scale (>1kg).**

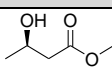
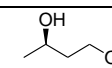
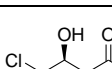
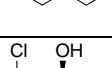
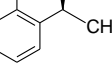
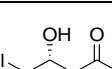
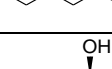
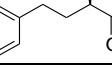
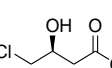
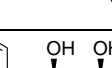
Entry	Catalyst	Product	Substrate ( $\text{g L}^{-1}$ )	<i>ee</i> (%)	Conversion/ Yield (%)	Reaction Scale [kg]	Source
1	<i>Neospora crassa</i>		-	>98	-/>85	multi ton	[21]
2	Engineered CR		160	>99.5	-/92	1104	[30]
3	Engineered CR		100	99.9	-/85-90	>200	[31]
4	Engineered CR		150	>99	>95	200	[32]
5	CR from screening		100	>99	-/>96	80	[33]
6	CR from <i>Candida parapsilosis</i>		100	98.4	68/-	10	[34]
7	<i>Candida sorbophila</i>		60	>99.8	>99/82.5	13.9	[21]
8	<i>Zygosaccharomyces rouxii</i>		40	>99.9	-/96	11.5	[21]
9	<i>Geotrichium candium</i>		10	99	-/95	7.1	[21]
10	CR from <i>Candida parapsilosis</i>		100	94	-/15.5	3.1	[35]
11	ADH from <i>Rhodococcus erythropolis</i>		156	>99.8	94/91	1.56	[36]

The product of the largest scale is manufactured by Zeneca Life Sciences Molecules with several tons serving as an intermediate in the synthesis of a carbonic anhydrase inhibitor Trusopt® (see Table 2, entry 1).<sup>[21]</sup> Very important building blocks are (*S*)-4-chloro-3-hydroxybutanoic acid esters (see Table 2

entries 2 & 9) produced in scales >1000 kg. This chiral alcohol is the key intermediate for an anticholesterol agent. The final drug inhibits hydroxymethyl glutaryl (HMG) CoA.<sup>[15b]</sup> Another multi kg process performs asymmetric reduction of a bulky ketone via an engineered carbonyl reductase providing a chiral intermediate for Montelukast sodium (Singulair®) a leukotriene receptor antagonist developed by Merck (see Table 2, entry 3).<sup>[31]</sup> (*R*)-Tetrahydrothiophene-3-ol (see Table 2, entry 4) is a key component in Sulopenem®, a potent antibacterial, a prodrug, which is being developed by Pfizer.<sup>[32]</sup>

Carbonyl reductases are developed on academic and industrial level to match the requirements for efficient manufacturing. Such enzyme candidates are investigated in preparative scale under process-like conditions. Table 3 demonstrates selected examples for asymmetric reduction of prochiral ketones for important chiral products on preparative scale (<1 kg). Some of these enzymatic processes exhibit interesting features making them attractive for industrial use. Especially high substrate loads were enhanced to values higher than 600 g L<sup>-1</sup> (see Table 3, entries 6 & 7). As benchmark substrates important chiral intermediates like the 4-chloro-3-hydroxybutanoic acid esters are used to validate these processes (see Table 3, entries 3, 5 & 7).

**Table 3 Biocatalytic asymmetric reduction in preparative scale (<1 kg).**

Entry	Catalyst	Product	Substrate (g L <sup>-1</sup> )	ee (%)	Conversion/Yield (%)	Reaction Scale [g]	Source
1	ADH from <i>Lactobacillus kefir</i>		290	99	78/-	797	[37]
2	ADH from <i>Leifsonia sp.</i>		50	99	99/99	250	[38]
3	ADH from <i>Candida magnoliae</i>		450	>99	-/89	22.5	[39]
4	CR from <i>Saccharomyces cerevisiae</i>		178	>99	99/89	15	[40]
5	ADH from <i>Sporobolomyces salmonicolor</i>		300	91.7	94.1/-	14.1	[41]
6	FabG from <i>Bacillus sp.</i> ECU0013		620	>99	99/91	5.6	[42]
7	CR from <i>Streptomyces coelicolor</i>		600	>99	-/93	grams	[43]
8	<i>Acinetobacter calcoaceus</i>		10	99	-/92	-	[21]
9	<i>Staphylococcus epidermis</i>		35.6	99	91/-	-	[21]
10	ADH-A from <i>Rhodococcus ruber</i>		120	>99	90/-	-	[44]



Also difficult substrates like the small prochiral ketone 4-hydroxy-2-butanone (see Table 3, entry 2) or bulky ketones like 6-benzyloxy-3,5-dioxo-hexanoic acid ethyl ester (see Table 3, entry 8) are converted in enantioselective manner. The latter reduction yields two stereocenters applying a whole cell catalyst and this enantiopure diol produced by Bristol-Myers Squibb serves as an intermediate for the synthesis of an anticholesterol drug.<sup>[21]</sup> Inhibitors of angiotensin-converting enzyme (ACE) all require a (*S*)-homophenylalanine moiety, which can efficiently be provided by reduction of the corresponding ketones as shown in Table 3 (entries 6 and 9). The ACE inhibitors such as Enalapril, Lisinopril, Cilapril and Benazepril are widely used as antihypertensive drugs and in the therapy for congestive heart failure. Another interesting product is methyl (*R*)-*o*-chloromandelate (see Table 3, entry 8), which is a key compound for the manufacture of Clopidogrel a platelet aggregation inhibiting drug.<sup>[40]</sup> The process parameters look very promising for large-scale production.

Taken together, almost all processes on industrial or preparative scale produce intermediates for pharmaceuticals rendering this market as most important driving force for the development of new processes involving carbonyl reductases.

### 1.3.5. Alcohol Dehydrogenases in Non-conventional Media

Biocatalysts are naturally designed to work in dilute aqueous solutions; however, it is known since the pioneering work of Klibanov *et al.* that enzymes can also perform in nearly anhydrous environments such as pure organic solvent.<sup>[45]</sup> The term non-conventional media summarizes all reaction media different from pure aqueous buffers including mono- or biphasic mixtures of organic solvents, ionic liquids, gas and solid phases or supercritical fluids.<sup>[46]</sup> Under certain circumstances enzymes are active in all of these media, which drastically increases the scope of their application in organic synthesis.

For ADHs the use of organic solvents as reaction medium is advantageous since organic substrate molecules can be dissolved in higher amounts in comparison to aqueous buffers. Additionally, water-labile compounds can be converted in anhydrous environments. Herein, aqueous organic biphasic systems using water-immiscible solvents as second phase are useful since the organic phase serves as substrate reservoir and facilitates product extraction from the aqueous phase simplifying downstream processing. Furthermore, the enzyme and the cofactor remain in the aqueous phase, where they are protected from possible inhibition or inactivation of organic molecules.

Also monophasic mixtures of water-miscible organic solvents with buffer is advantageous, since high concentrations of an auxiliary alcohol or ketone may be used to achieve efficient substrate-coupled cofactor regeneration (see Figure 3, left). Taking organic solvents as the only reaction medium for

asymmetric reduction a process can be envisaged wherein the ketone substrate is solubilized in pure isopropanol as auxiliary substrate omitting any other solvent.

In 1986, the ADH from horse liver (HLADH) was the first ADH operated in pure organic solvent. The enzyme was suspended in isopropyl ether co-precipitated with NAD<sup>+</sup> on glass beads.<sup>[47]</sup> The dry enzyme showed 25 % of its activity in the organic solvent when compared to the activity in aqueous buffer.<sup>[47]</sup> Later on, the HLADH performance was studied in different organic solvents and different pretreatments. It was found that the pH in the solution prior to freeze drying plays an important role and that catalytic activity in organic solvent, which increased with the amount of water added.<sup>[48]</sup> From this and other studies the conclusion was drawn that the absence of water reduced conformational flexibility and hence reduced activity.<sup>[48-49]</sup> On the other hand, stability was increase and bioimprinting was promoted.<sup>[48-49]</sup> Other ADHs also exhibit catalytic activity in water-immiscible organic solvents, like ADH from *Thermoanaerobacter brockii* (TbADH) and *Rhodococcus erythropolis* (ReADH), whereas the ADH from bakers' yeast (YADH) was not active in any of the tested solvents.<sup>[50]</sup>

Operation of ADHs in aqueous organic biphasic systems was also realized with HLADH, TbADH and *Lactobacillus brevis* (LbADH) and all three enzymes showed good stabilities in the system tested depending on the functionality of the organic solvent applied.<sup>[51]</sup> Gröger *et al.* demonstrated that ReADH can perform asymmetric reduction of ketones in biphasic systems composed of heptane or hexane with enzyme-coupled cofactor regeneration.<sup>[52]</sup> Interestingly, electrochemical cofactor regeneration applying a rhodium complex was achieved in a buffer-octane biphasic system employing an ADH from *Thermus sp.*<sup>[53]</sup>

High tolerance to 80 % (v/v) isopropanol and 50 % (v/v) acetone was demonstrated for ADH-A from *Rhodococcus ruber* rendering this enzyme valuable for application with substrate-coupled cofactor regeneration for both, the reduction and the oxidation direction.<sup>[27b]</sup> Investigation of the crystal structure showed the presence of ten salt bridges at the dimer interface, possibly being responsible for the high stability in the tested solvents.<sup>[54]</sup> Similarly, *Thermoanaerobacter ethanolicus* secondary ADH showed low inactivation when mixed with 30 % (v/v) isopropanol or 10 % (v/v) acetone.<sup>[55]</sup> Activation upon addition of water-miscible organic solvents was observed for ADH from *Aeropyrum pernix* depending on the kind and concentration of solvent.<sup>[56]</sup> The same was observed for ADH from *Paracoccus pantotrophus* DSM 11072 where operation in 15 % (v/v) DMSO increased conversion by twofold.<sup>[57]</sup>

The application of organic solvents with alcohol dehydrogenases has effects on stability and activity depending on the nature of organic solvent employed. Additionally, it was observed that stereoselectivity is affected in monophasic mixtures of buffer and organic solvent. For TbADH it was

found that increasing amounts of organic solvent decrease the stereoselectivity, whereas the opposite effect was observed for ADH from *Thermoanaerobacter sp.* Ket4B1.<sup>[58]</sup> For ADH from *Thermoanaerobacter ethanolicus* stereoselectivity seemed to be even tunable dependent on the solvent applied; however, there was no correlation found between the physicochemical properties of the solvent and *ee*.<sup>[55]</sup> Similar observations were made for carbonyl reductase from *Sporobolomyces salmonicolor* and ADH from *Lactobacillus brevis*.<sup>[59]</sup>

Another prominent non-conventional medium for biocatalysis are ionic liquids (ILs), which are salts in the liquid state with low melting points and virtually no vapor pressure. ILs applied in biocatalysis are liquid at room temperature and feature reusability, non-flammability and compatibility with enzymes and microorganisms.<sup>[60]</sup>

LbADH was the first ADH operated in ionic liquids in 2004.<sup>[51b]</sup> The biphasic system composed of IL and buffer was superior to a MTBE-buffer system due to more favorable partition coefficients of substrates and products. Application of water-immiscible ILs with ReADH substantially increased productivity and simplified product isolation.<sup>[61]</sup> In this work, the same ADH was used together with a glucose dehydrogenase for cofactor regenerating with a large number of water-miscible and immiscible ILs.<sup>[61]</sup> Also whole cells were employed for asymmetric ketone reduction in ILs. For example, *E. coli* whole cells with overexpressed LbADH and formate dehydrogenase from *Candida boidinii* were tested with various water-immiscible ILs giving up to 180 g L<sup>-1</sup> d<sup>-1</sup> (*R*)-octanone in a continuous process.<sup>[62]</sup> An effect on stereoselectivity for ketone reduction with cells of bakers' yeast was observed wherein the (*R*)-alcohol was obtained (70.4 % *ee*) with benzene or ethyl ether but addition of an IL yielded the (*S*)-alcohol, however with moderate selectivity (27.7 % *ee*).<sup>[63]</sup>

The concept using a gaseous phase as substrate carrier and a solid phase as catalyst carrier was employed for ADHs as well. The main arguments to use such gas-solid system are the increased catalyst stabilities as well as easy supply with hardly water-soluble substrates. In 1986, HLADH was used, co-immobilized with NADH, as solid phase converting several aldehydes supplied via the gas phase.<sup>[64]</sup> The same group also showed applicability of thermostable ADH from *Sulfolobus solfataricus* in this system.<sup>[65]</sup> For LbADH a 40-fold stabilization in gas-solid system could be achieved by adding sucrose to the enzyme preparation after discovering that process stability is governed by enzyme rather than cofactor inactivation.<sup>[66]</sup> It was found that dried whole cells of *Saccharomyces cerevisiae* can be used in gas-solid systems to transform ethanol and hexanal and that the relative humidity, expressed as water activity ( $a_w$ ) triggers activity and stability.<sup>[67]</sup>

Asymmetric reduction of several ketones with a crude enzyme preparation of *Geotrichium candidum* was performed in buffer overlaid with supercritical carbon dioxide (CO<sub>2</sub>).<sup>[68]</sup> Herein, enzyme inactivation caused by pH drop upon CO<sub>2</sub> dissolution in the aqueous phase was overcome by

buffering with bicarbonate. This system is characterized by a simple workup since the alcohol product could be recovered from the supercritical fluid by lowering the pressure to ambient conditions.

Taken together, a huge number of ADHs have been employed in various non-conventional media showing reasonable performance by taking advantage of the various benefits like increased substrate and cosubstrate concentrations, catalyst stabilization, simple product work-up or tunable selectivities. However, usually activity is decreased when non-conventional media are used and selectivity might be negatively affected. Many of the observed effects are not easy to rationalize; hence more research has to be carried out to address the open questions.

## 1.4. Biochemical Properties of Alcohol Dehydrogenases

### 1.4.1. Classification of NAD(P)H-dependent Alcohol Dehydrogenases

The enzyme class 1 according to the nomenclature of the Enzyme Commission (EC) is termed oxidoreductases, which contains enzymes enhancing the rate of electron transfer reactions. Class EC 1.1.1.1, in particular, targets electron transfer to carbon atoms with hydroxyl functions (alcohols) with NAD(P)<sup>+</sup> as electron acceptor; the last number refers to the serial number of the enzyme name in its class.<sup>[69]</sup> The members of this class catalyze the reversible oxidation of alcohols to the corresponding aldehydes or ketones (see Scheme 1). Alcohol dehydrogenases (ADHs) or synonymously ketoreductases have been classified EC 1.1.1.1 and are part of a large and diverse protein superfamily. Herein, medium-chain (MDR) and short-chain dehydrogenase/reductase (SDR) superfamilies have the most members. A third superfamily is the family of “*iron-activated*” long chain dehydrogenases/reductases (LDR).<sup>[50]</sup>

ADHs may also be categorized according to their stereoselectivity using the delivery of the two diastereotopic hydrogens of the cofactor as criterion (see Figure 4, right). If the *pro-S* hydride is transferred, the enzyme is classified group A if the *pro-R* is delivered it is denoted group B enzyme.

ADHs are ubiquitous in all kingdoms of life and play various roles in detoxification and metabolism, among them most famously ethanol fermentation. They can accept a wide variety of substrates like branched and non-branched as well as cyclic alcohols. Many organisms comprise several very similar ADH isoenzymes each adapted to its physiological function. Historically, the ADH1 from bakers' yeast (YADH1) was the first enzyme of this class described in 1937.<sup>[70]</sup> In the early sixties, the ADH from horse liver (HLADH) was isolated and characterized structurally as well as biochemically.<sup>[71]</sup> Additionally, many aspects about ADH enzyme kinetics as well as structure function relationships were elucidated with HLADH or YADH1 serving as a general model enzymes for ADHs.<sup>[72]</sup>

These two famous enzymes belong to the MDR superfamily with 10888 members, wherein the enzymes are categorized according to the amino acid chain length of ~350 residues.<sup>[73]</sup> Furthermore, this superfamily consists of homodimeric (like HLADH) or homotetrameric (like YADH1) proteins, which mostly contain zinc in the active center.<sup>[73]</sup>

### 1.4.2. Catalytic Mechanism and Enantioselectivity

The catalytic mechanism of alcohol dehydrogenase is characterized by a two electron process, wherein these get transferred in form of a hydride (H<sup>-</sup>). In the suggested ordered bi-bi mechanism, first NAD(P)<sup>+</sup> binds tightly to a specific binding site followed by the substrate. The alcohol substrate is coordinated by a divalent zinc atom in the active site stabilizing the alcohol oxygen and concurrently acidifying the hydroxyl proton. A catalytic histidine is activated by protonation via a base to withdraw

a proton from the nicotine amide ribose. The proton relay system involves also a negatively charged threonine (or serine), which abstracts the proton from the actual substrate after it got deprotonated by itself through  $\text{NAD}^+$  (see Figure 4, left). Finally, a hydride is transferred from the alkoxide ion to the  $\text{NAD}^+$  leading to a  $\text{NADH}$  and a carboxyl compound.<sup>[74]</sup> However, the final mechanism with detailed insights of structure-function relationships and protein dynamics is still not fully elucidated even though studies using advanced quantum mechanics were undertaken.<sup>[75]</sup> Recently, a comprehensive model for a "tunneling ready state" was developed to explain the hydrogen transfer.<sup>[76]</sup>

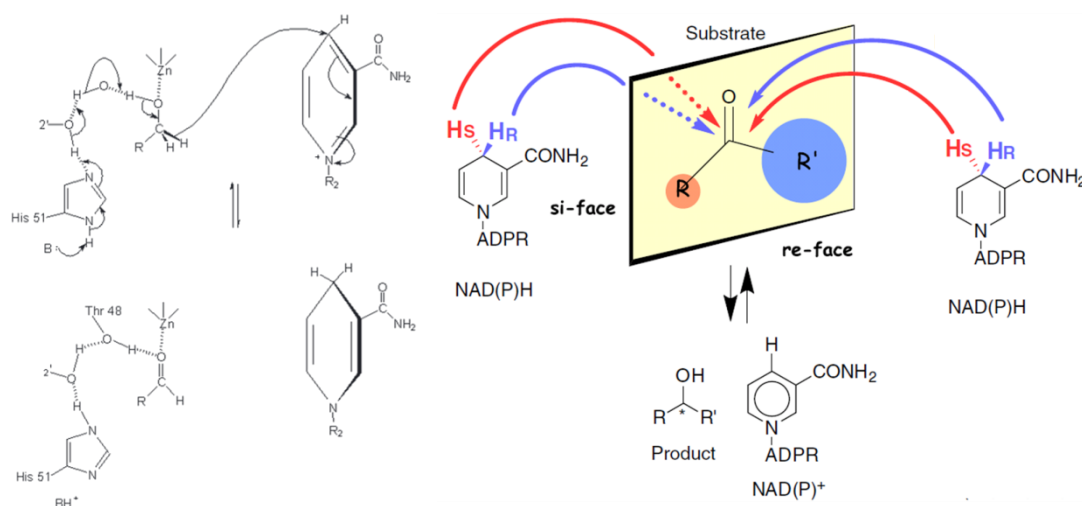


**Figure 4** Mechanism and enantioselectivity of alcohol dehydrogenases. Left: Mechanistic hydride transfer from an alcohol substrate to  $\text{NAD}^+$  in horse liver ADH.<sup>[77]</sup> Right: The four possibilities to generate chiral alcohol from a prochiral ketone in ADHs; the *pro-R* ( $\text{H}_R$ ) or *pro-S* ( $\text{H}_S$ ) hydride attacks from *si*- or *re*-face of the ketone. Adapted from<sup>[7]</sup>.

The stereoselectivity is determined by the transfer of the hydride and the orientation of the substrate. For the reduction reaction the hydride from the  $\text{NAD(P)H}$  attacks either the *si*-face or the *re*-face of the planar carbonyl substrate. On the other hand, the enzyme transfers the *pro-R* ( $\text{H}_R$ ) or the ( $\text{H}_S$ ) hydride from the cofactor to the substrate, which is enzyme-dependent (see Figure 4, right). This results in four stereochemical patterns for a possible outcome of this reaction.<sup>[7]</sup> For example, when the *pro-R* hydride is transferred to the *si*-face of the substrate the (*R*)-product results (*Prelog's* rule). So far, an ADH performing *pro-S* hydride transfer to the *re*-face of the substrate has not been reported.

Most commercially available ADHs deliver the *pro-R* hydride to the *si*-face and are so-called *Prelog*-ADHs yielding usually (*S*)-alcohol from the corresponding ketones.<sup>[9, 78]</sup> Conversely, *anti-Prelog* ADH deliver mostly (*R*)-alcohols. Generally, ADHs are classified due to the chiral configuration of the products using (*R*)- and (*S*)-nomenclature according to the Cahn-Ingold-Prelog rules. However, in some cases a so-called (*S*)-specific ADH may yield the (*R*)-alcohols, since the substituents at the chiral center can reverse the assignment of the priorities. For example, an ADH reduces acetophenone to (*S*)-1-phenylethanol but a chlorine substitution at the  $\alpha$ -position ( $\alpha$ -chloro acetophenone) will yield

2-chloro (*R*)-1-phenylethanol. Therefore, it is more accurate to designate the specificity of an alcohol dehydrogenase according to *Prelogs'* specificity rules in Fig. 4 rather than to the nomenclature of the products.

In principle, the substrate could bind in the opposite manner (exchange of *R* and *R'* in Fig. 4) into the active site of an ADH. By this, the outcome of the reduction would yield the opposite stereoselectivity. This is often observed for almost symmetrical ketone substrates, such as 2-butanone, as these fit in both orientations into the active site. Hence, both enantiomers results as products and the *ee* is low. In some rare cases, the enantiopreference of some ADHs strongly be influenced by the substrate geometry.<sup>[9]</sup>

### 1.4.3. Structural Motifs & Substrate Specificity

The overall sequence identity of ADHs is often not very high (<30 %); however, they exhibit an overall conserved fold with characteristic structural motifs. Generally, the polypeptide chain is divided in the N-terminal catalytic and the C-terminal cofactor-binding domain.<sup>[79]</sup> In the following, horse liver alcohol dehydrogenase (HLADH) is taken as model enzyme and amino acid numbering is according to this enzyme (structural model see Figure 5, left).

Since all ADHs are dependent on NAD(P) cofactors a conserved fold for cofactor binding is present called Rossmann-fold (see Figure 5, right).<sup>[80]</sup> It consists of five to six  $\beta$ -strands in parallel arrangement, flanked by  $\alpha$ -helices. In this fold, three  $\beta\alpha$ -pairs make up one of the two motifs ( $\beta_1$ - $\alpha_1$ - $\beta_2$ - $\alpha_2$ - $\beta_3$ ,  $\beta_4$ - $\alpha_4$ - $\beta_5$ - $\alpha_5$ - $\beta_6$ ), which are connected by a  $\alpha$ -helix ( $\alpha_3$ ).<sup>[81]</sup> Each of the two ( $\beta\alpha$ )<sub>3</sub> motifs binds one mononucleotide of the cofactor. Within this secondary structure motif, a conserved glycine-rich region is found (GX<sub>1-2</sub>GXXG) necessary to bind the phosphate of the cofactor. Other amino acid residues (Phe-319, Ala-317, His-51, Ile-269 and Val-292) make hydrogen bonds to stabilize the cofactor.

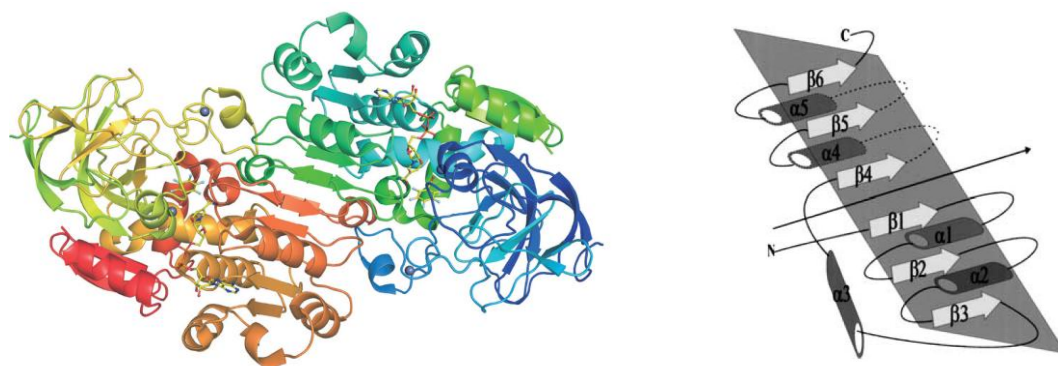


**Figure 5** Overall structure of a dimeric alcohol dehydrogenase and the Rossmann-fold. Left: Structural model of HLADH as a dimer in complex with NADH and pentafluorobenzylalcohol. The zinc ions are dark blue spheres and the dimer interface is between the green and the brown strands and helices.<sup>[79]</sup> Right: Topology diagram of the Rossmann-fold; cylinders represent  $\alpha$ -helices and arrows denote  $\beta$ -strands. Dashed lines indicate elements of secondary fold below the plane of fold.<sup>[81]</sup>

In HLADH, a catalytic  $Zn^{2+}$  is coordinated in tetrahedral fashion by two cysteine residues (Cys46, Cys174) and a histidine (His67). One coordination site is occupied by a water molecule and can be replaced for the oxygen of the substrate molecule (see Figure 6, left).<sup>[79]</sup> This coordination promotes catalysis and is therefore termed *catalytic zinc*. A second  $Zn^{2+}$  may be found in mammalian (or eukaryotic) ADHs as *structural zinc* coordinated by four cysteines (Cys97, Cys100, Cys103 & Cys111) (see Figure 6, right). The role of this zinc is attributed mainly to maintain the tertiary/quaternary structure of the enzyme.<sup>[82]</sup>

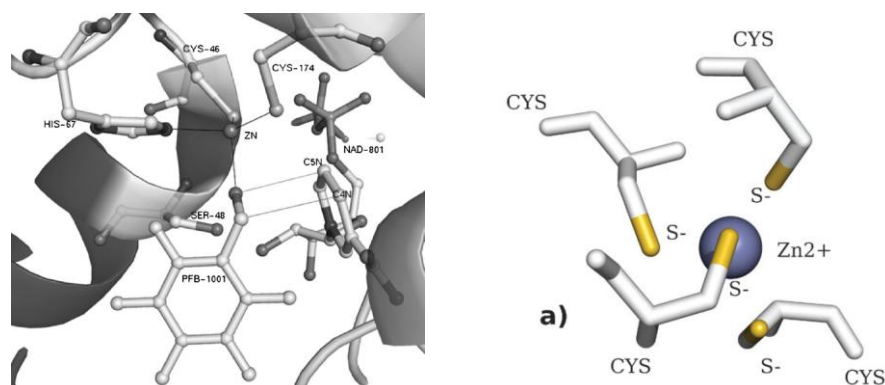


**Figure 6** Catalytic and structural zinc in HLADH. Left: Binding of pentafluorobenzylalcohol and NADH in an active conformation with coordinated zinc ion.<sup>[79]</sup> Right: Geometry of the structural zinc site from simulations, all cysteines are considered to be deprotonated.<sup>[83]</sup>

Substrate recognition and binding is facilitated by many amino acids in the active site from the catalytic as well as from the cofactor-binding domain. Most importantly, a serine (Ser48) in HLADH is in hydrogen-bonding distance to the oxygen atom of the substrate. The flanking parts of the substrate are protruding into the binding pocket of the enzyme lined by several non-conserved amino acids, which shape the architecture with respect to available space and affinity.<sup>[84]</sup> For zinc-containing MDRs generally two separate substrate binding pockets of different size are found (see Figure 7, left). The available space determines the orientation how a prochiral substrate can bind and the orientation defines the enantioference of the conversion.<sup>[84]</sup>

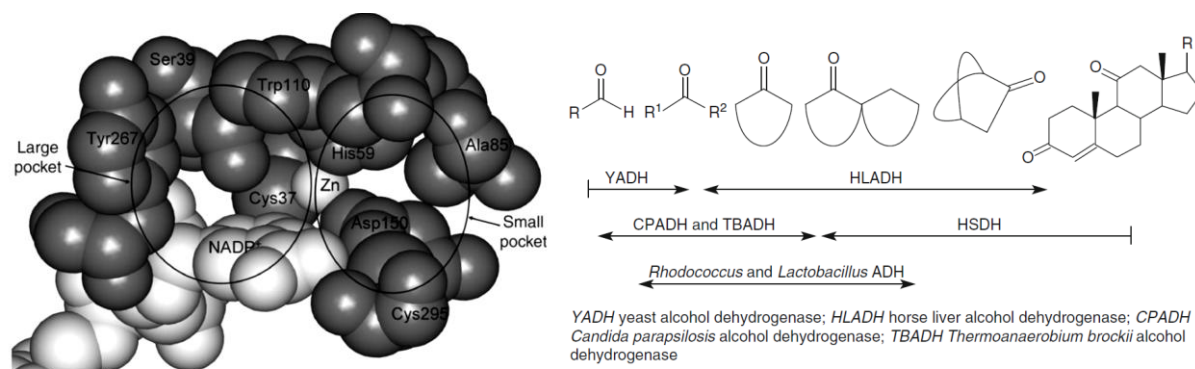


**Figure 7** General architecture of an alcohol dehydrogenase and overview of substrate spectrum of commonly used alcohol dehydrogenases. Left: Active site of alcohol dehydrogenase from *Thermoanaerobacter ethanolicus* in space-filling representation based on PDB#1YKF. NADP<sup>+</sup> and Zn<sup>2+</sup> are in white, amino acid residues are in gray.<sup>[85]</sup> Right: Preferred sizes of ketone and aldehyde structures accepted by alcohol dehydrogenases.<sup>[9]</sup>



The substrate spectrum is a very important feature for the synthetic applicability of alcohol dehydrogenases. From the most commonly used alcohol dehydrogenases YADH exhibits a very narrow substrate spectrum accepting only aldehydes and methyl ketones.<sup>[9]</sup> In contrast, HLADH has a very broad substrate range, especially suited for cyclic moieties; however, only weakly accepting open-chain ketones.<sup>[9]</sup> This gap is filled by a variety of ADHs from mesophilic and thermophilic microorganisms (see Figure 7, right).<sup>[9]</sup>

#### 1.4.4. Limitations of Using Alcohol Dehydrogenases in Industrial Applications

Industrial applications aim at stable processes with robust, simple and sustainable operation and product recovery as well as an efficient use of the resources.<sup>[8]</sup> This holds also true for biocatalytic ketone reduction for chiral alcohol manufacture. The question arises what prevents this route to become the standard method of choice in organic synthesis.

The drawback of the cofactor dependency of ADHs is largely solved by recycling and applied on industrial scale with methods outlined in 1.3.2. The availability of ADHs was much improved in the last years by screening and protein engineering campaigns.<sup>[7]</sup> However, the known ADHs are not suitable for every application due to limitations in activity, selectivity and very often stability.

Good basal activity and selectivity on non-natural substrates are important to reach high space-time yields but more important is process or operational stability.<sup>[2]</sup> These critical parameters might be approached by reaction engineering to provide an optimal environment for the catalyst. Nowadays, the advancements in molecular biology, protein chemistry and screening methods make it possible to tailor the enzyme to the process requirements by applying enzyme engineering methods. The latter will be described in more detail in chapter 1.6.

The engineering of activity and specificity is studied since a long time applying model enzymes such as YADH.<sup>[86]</sup> General concepts how substrate acceptance is triggered are developed due to the “localized” nature. However, very large substrate molecules with two bulky substituents flanking the carbonyl function remain challenging targets. The same holds true for very small ketones such as 2-butanone, since many enzyme cannot distinguish between methyl and ethyl-group, which results in low stereoselectivity (compare 1.4.2). Furthermore, the stereoselective reduction of more than one carbonyl group leading to  $2^n$  possible stereoisomers is difficult ( $n$  = number of carbonyl groups).

The engineering of stability on the protein level comprises a more demanding problem, because stabilization mechanisms are only poorly understood on the molecular level and many amino acids may be involved. Hence, rational single amino acid exchanges do usually not result in fundamental stabilization rendering this issue a “non-localized” engineering problem. Here, mostly traditional immobilization methods are applied or whole cells are used in industrial processes. Nevertheless, engineering of protein stability is still emerging due to the ever growing progress in protein engineering techniques.

## 1.5. Carbonyl Reductase from *Candida parapsilosis*, a Powerful Catalyst with a Moving History

### 1.5.1. Discovery and Impact

The carbonyl reductase from *Candida parapsilosis* DSM 70125 (CPCR) is regarded as a very valuable tool in synthetic applications. Since the discovery in 1992 by Peters *et al.* this enzyme attracted much attention due to its enzymatic features and is labeled with an exciting development.<sup>[87]</sup>

Back in 1992, exploitation of strain collections and environmental samples were the major sources for new biocatalytic activities. During a screening campaign with four ketoesters and two ketoacids with 36 bacterial and 29 yeast strains, *Candida parapsilosis* DSM 70125 cell free extract exhibited highest activities with NADH on ketoesters.<sup>[88]</sup> Nowadays, two enzyme preparations labeled “CPCR” are traded by Codexis® and X-zyme® underlining the importance of the enzyme. Nevertheless, the molecular identity of the original CPCR discovered by Peters was never fully clarified. This will be done in this thesis.

### 1.5.2. Substrate Scope and Selectivity

In the following, the enzyme responsible for this activity was purified from *Candida* crude cell extract and biochemically characterized.<sup>[89]</sup> The preparation showed conversion of a broad variety of ketone compounds, especially ketoesters, aliphatic, cyclic and aromatic ketones as well as aliphatic aldehydes and ketoacetals (compare Table 7).<sup>[89b]</sup> Also propargylic alcohols were shown in a later work to be produced effectively.<sup>[90]</sup> Most interestingly, also the small 2-butanone was reduced to (*S*)-2-butanol with highest selectivity.<sup>[91]</sup> This large substrate scope together with the generally high enantioselectivity (*ee* >95 % *Prelog* product) and tolerance towards 10 % (v/v) isopropanol rendered the CPCR a promising catalyst for synthetic applications (see 1.5.5).<sup>[89b]</sup>

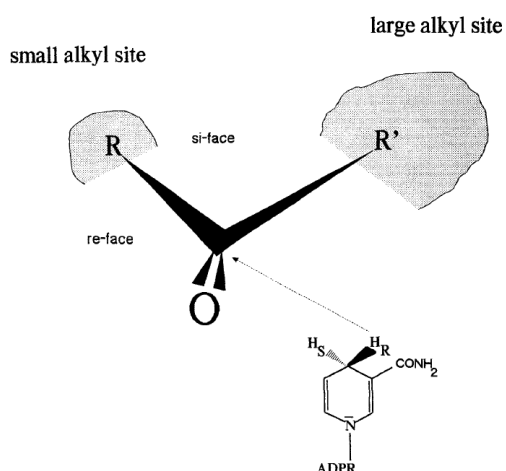


Figure 8 Proposed model of the substrate binding pocket of *Candida parapsilosis* carbonyl reductase and stereochemical pattern of hydride transfer (*pro-R* to *re-face*) indicating *Prelog*'s specificity. Taken from <sup>[89a]</sup>.

These promising features were the reason for further investigation of the mechanism and kinetics, herein the first model of the architecture of the substrate binding pocket was proposed.<sup>[89a]</sup> A screening of many structurally different substrates allowed deducing the shape of the active site. It was suggested that a small pocket accommodating mostly methyl and ethyl groups is located next to a large pocket fitting larger groups such as aromatic or branched alkyl groups (see Figure 8).<sup>[89a]</sup> In the same study, an ordered bi-bi-mechanism and evidence for *Prelog's* specificity (*pro-R* hydride transferred to *re*-face, Figure 8) were described as known for many other ADHs (see 1.4.2 and 1.4.3).<sup>[78, 89a]</sup> Stereoselectivity for CPCR was tested for many substrates and turned out to obey *Prelog's* rule as proposed with *ee*-values always exceeding 94 % (compare Table 7, entries 1-10). However, CPCR was found to have also some limitations in substrate scope as ketoacids in general, formaldehyde,  $\alpha$ -chloroacetophenone and propiophenone were no substrates for CPCR.<sup>[89b]</sup> Furthermore, stereoselectivity for reduction of 3-butyne-2-one was only 49 % *ee*.<sup>[90]</sup>

### 1.5.3. Temperature, pH Optimum and Stability

The purified enzyme prepared from *Candida* lysate was fully characterized and the optimal conditions for reduction and oxidation were determined.<sup>[89b]</sup> The values for temperature optimum are in a range typical for enzymes from mesophilic microorganisms (see Table 4).<sup>[50]</sup> Also pH optimum for oxidation is expected to be more in the alkaline regime as the one for reduction (see Table 4).

**Table 4** Temperature and pH optimum for CPCR preparation.

Temperature Optimum		pH Optimum		Source
Reduction	Oxidation	Reduction	Oxidation	
39-40°C	50-52°C	7.5-8.5	9-10	[89b]

CPCR is fairly stable at ambient temperature when stored in buffer (see Table 5, entry 3) and remains stable for several weeks at lower temperatures and long-term storage conditions (see Table 5, entry 1 & 2). Operation of non-immobilized Codexis®-CPCR in an emulsion membrane reactor exhibited extraordinary high half-life time of 1488 hours, which is explained by the low concentrations of substrate and production promoting operational enzyme stability (Table 5, entry 4).<sup>[92]</sup> This demonstrates well how reaction engineering can assist the stabilization of biocatalysts in generating more appropriate operation conditions. Furthermore, a recombinant CPCR in purified form was operated in an aqueous-organic biphasic system with varying organic phases. In this, CPCR was severely inactivated by the presence of the interphase (see Table 5, entries 5-6). This feature limits the applicability of free CPCR in two-phase systems, which are frequently applied for asymmetric ketones reductions.<sup>[93]</sup> However, CPCR purified from *Candida* lysate encapsulated in poly vinyl alcohol beads showed reasonable stability in pure hexane proving that immobilization is an efficient tool for CPCR stabilization (see Table 5, entry 7).<sup>[94]</sup>

**Table 5 Stability of CPCR preparations under different conditions.**

Entry	Condition	Half life time [h]	Source
1	25 % glycerol, -20°C	>984	[89b]
2	temperature (4°C)	990	[95]
3	temperature (25°C)	115.5	[96]
4	emulsion membrane reactor (25°C)	1488	[92]
5	cyclohexane interphase (25°C)	4.0	[97]
6	heptane interphase (25°C)	17.7	[97]
7	immobilized in hexane (25°C)	63.7	[94]

As mentioned before, the stability of a catalyst under operation conditions is one of the most important parameters for process development. Therefore, characteristics like thermostability and solvent stability can be valuable measures for possible application in a process since they may correlate with operational stability.

#### 1.5.4. Comparison to Other Carbonyl Reductases from *Candida spp.*

The *Candida* genus is exploited since a long time as a source for oxidoreductases and provides a biocatalytic platform for practical applications and academic insights.<sup>[98]</sup> Especially, strains categorized as *parapsilosis* species show interesting reducing activities. For instance, whole cells perform selective imine reduction<sup>[99]</sup> or effective stereoinversion of racemic 2-octanol<sup>[100]</sup> indicating the presence of several alcohol dehydrogenases/carbonyl reductases. With this knowledge, it is not surprising that in the literature many entries about carbonyl reductases isolated from *Candida* type strains are found.

**Table 6 Recombinant carbonyl reductases from various *Candida parapsilosis* type strains compared to CPCR.**

Entry	Type strain	Enzyme name	Uniprot accession	Protein length	Cofactor	Stereo-specificity	Source
1	DSM 70125	CPCR	-	-	NADH	<i>Prelog</i>	[89b]
2	IFO 1396	CpSADH	BAA24528.1	336	NADH	<i>Prelog</i>	[101]
3	CCTCC M203011	rCR	ABP38340.1	336	NADH	<i>Prelog</i>	[102]
4	CCTCC M203011	CpADH	ABG57118.1	279	NADPH	<i>anti-Prelog</i>	[103]
5	IFO 0708	CPR-C1	BAD01652.1	299	NADPH	<i>Prelog</i>	[104]
6	IFO 0708	CPR-C2	BAD01653.1	307	NADPH	<i>Prelog</i>	[104]

A carbonyl reductase from *Candida parapsilosis* IFO1396 was described by the Japanese company Daciel and denoted CpSADH.<sup>[105]</sup> The according nucleotide sequence was described and the enzyme was expressed in *E. coli* (see Table 6, entry 2).<sup>[101]</sup> Furthermore, recombinant alcohol dehydrogenase from *Candida parapsilosis* CCTCC M203011 was shown to resolve racemate of 1-phenyl-1,2-ethanediol (see Table 6, entry 3).<sup>[102, 106]</sup> Analysis of the latter two carbonyl reductases revealed that they are identical except one amino acid. Structural information is not available and only low sequence identity (<35 %) is found in the protein data bank (PDB) with ADHs mainly from thermophilic hosts or the archaea kingdom.

The DNA sequence of CpSADH is also present in the genome of *Candida parapsilosis* strain CDC317. The transcriptome was fully sequenced and translated proteins were automatically annotated.<sup>[107]</sup> Within the fully sequenced genome automated annotation revealed 20 members of the zinc-binding dehydrogenases family (PF00107), which are vastly overlapping with the 21 members found belonging to the alcohol dehydrogenase GroES-like protein family (PF08240).<sup>[107]</sup> Partial coding sequences identical to CPCR (42-274) were discovered in *Candida parapsilosis* strains T30451, 452 and 480.<sup>[107]</sup> However, activity of the according enzymes was never reported.

Additionally, also a short-chain alcohol dehydrogenase has been isolated from *Candida parapsilosis* CCTCC M203011 exhibiting anti-*Prelog* specificity (see Table 6, entry 3).<sup>[103]</sup> For this enzyme, a crystal structure is available (PDB: 3CTM).<sup>[108]</sup> Furthermore, two polyketone reductases were simultaneously found in *Candida parapsilosis* IFO 0708 converting ketopantoyl lactone to D-(–)-Pantoyl lactone with NADPH as cofactor (see Table 6, entries 5 & 6).<sup>[104]</sup>

**Table 7 Applications of CPCR in preparative scale and in different reaction setups. FDH is formate dehydrogenase from *Candida boidinii* for regeneration of the NADH cofactor. EMR is enzyme membrane reactor for retention of the biocatalyst. PVA stands for polyvinyl alcohol.**

Entry	Biocatalyst	Product	Yield [%]	ee [%]	Reactor, scale	Cofactor recycling	Substrate [mmol L <sup>-1</sup> ]	Source
1	Purified from <i>Candida</i> extract	Ethyl-( <i>S</i> )-3-hydroxybutanote	-	98.5 <i>S</i>	5 mL aqueous	FDH	100	[89b]
2	Purified from <i>Candida</i> extract	( <i>S</i> )-1-(2-naphtyl)-ethanol	70	99.5 <i>S</i>	30-200 mL aqueous, cyclodextrin	FDH	50	[109]
3	<i>Candida</i> extract	Lactate aldehyde dimethyl acetal	92	100 <i>S</i>	100 mL aqueous	FDH	200	[110]
4	<i>Candida</i> extract	Various hydroxyl ester	>83	>95 <i>S</i>	100 mL aqueous	FDH	30–200	[91a]
5	<i>Candida</i> extract	( <i>S</i> )-1-phenylethanol	61	94 <i>S</i>	100 mL aqueous	5 % (v/v) 2-propanol	50	[91a]
6	Commercial CPCR ( <i>X-Zyme</i> )	( <i>S</i> )-2-octanol	99.5	97 <i>S</i>	EMR, continuous	FDH	7 (21 g L <sup>-1</sup> d <sup>-1</sup> )	[92]
7	Commercial CPCR ( <i>X-Zyme</i> )	( <i>S</i> )-2-octanol	99.5	97 <i>S</i>	Emulsion reactor, continuous	FDH	68 (11 g L <sup>-1</sup> d <sup>-1</sup> )	[92]
8	Purified from <i>Candida</i> extract	( <i>S</i> )-2-butanol	60	100 <i>S</i>	Micro-emulsion	FDH	670	[91b]
9	Purified from recombinant <i>E. coli</i>	( <i>S</i> )-1-phenylethanol	25	99 <i>S</i>	Biphasic, continuous	10 % (v/v) isopropanol	100	[96]
10	recombinant <i>E. coli</i> whole cells	( <i>S</i> )-2-butanol	-	-	Encapsulated cells	2.8 % (v/v) isopropanol	40	[111]
11	Purified from <i>Candida</i> extract	( <i>S</i> )-1-phenylethanol	-	-	PVA beads, hexane	FDH, 5 % (v/v) isopropanol	150	[94]

### 1.5.5. Synthetic and Preparative Applications of CPR Preparations

Due to afore the mentioned features of CPR, the enzyme was used for several synthetic applications in preparative scale and also for validation of reactor concepts for asymmetric ketone reduction involving strategies to increase the substrates load and cofactor regeneration (see Table 7). Table 7 demonstrates the versatility of CPR with respect to applicability in various reactor types and operation modes (see Table7, entries 6-9) as well as tolerance to additives (see Table 7, entry 2, 5, 9 and 10) and immobilization (see Table 7, entry 11). However, *E. coli* whole cells with CPR overexpressed do not withstand encapsulation in polyelectrolyte multilayer systems (see Table 7, entry 10).<sup>[111]</sup>

For all applications stereoselectivity exceeded 94 % and yields were generally high, which speaks for the robustness of the catalyst under operation conditions and indicates the absence of inhibition phenomena.

### 1.5.6. Patent Situation

The detected carbonyl reducing activity in cell-free lysate of *Candida parapsilosis* DSM 70125 discovered by Peters *et al.* was filed for patenting in 1992 (see Table 8, entry 1-2). The responsible carbonyl reductase protein was purified and characterized but the amino acid or nucleotide sequence was not identified.<sup>[87]</sup> Most interestingly, a work group from the company Daciel patented the DNA and amino acid sequence of a carbonyl reductase recovered from *Candida parapsilosis* type strain IFO1396 exhibiting similar reducing activities (see Table 8, entry 3-5).<sup>[112]</sup> However, biochemical data from the enzyme described by Peters *et al.* were at odds with data reported in the patent and corresponding publications.<sup>[89b, 101]</sup> In Table 8 only patents covering the activity or amino acid sequence of the protein are covered.

**Table 8 Patents published for reductive activities of *Candida parapsilosis*.**

Entry	Inventors	Date (priority)	Date (published)	Application	Patent no.	Source
1	Kula, Peters	1992/03/12	1993/09/16	New ketonic ester reductase, its preparation and use for enzymatic redox reactions	WO 93/18138	[87]
2	Kula, Peters	1993/03/05	1996/06/04	Ketoester reductase for conversion of keto acids esters to optically active hydroxy esters	US 5,523,223	[113]
3	Kojima, Yamamoto, Kawada, Matsuyama	1996/09/12	1998/06/09	Method for producing ketone or aldehyde using an alcohol dehydrogenase of <i>Candida parapsilosis</i>	US 5,763,236	[105]
4	Kojima, Yamamoto, Kawada, Matsuyama	1993/09/24	2004/11/24	ADH, DNA encoding its, preparation & method of preparing optically active alcohols	EP 0645453	[112]
5	Kojima, Yamamoto, Kawada, Matsuyama	1997/06/11	2001/06/03	Stereospecific ADH isolated from <i>Candida parapsilosis</i> , amino acid and DNA sequences thereof, and method of preparation thereof	US 6,255,092	[114]

## 1.6. Enzyme Engineering for Improving Enzyme Performance

### 1.6.1. General Concepts for Enzyme Improvement

Enzymes with interesting activity do rarely match all requirements for application in commercially viable processes such as sufficient specific activity and selectivity on the desired substrates as well as reasonable operational stability and absence of inhibition phenomena.<sup>[2, 115]</sup> However, advancements in enzyme engineering and screening technologies demonstrate many astonishing examples where enzyme properties were improved up to several thousand folds (see Table 9, entries 3, 6, 7 & 10). These success stories also increased the understanding of structure-function relationships in biocatalysts.

There are two different strategies of enzyme engineering *Rational Protein Design & Directed Evolution* both exhibiting advantages and disadvantages. Recent developments enforce the combination of both techniques as well as more data-driven approaches due to the accumulation of sophisticated information in extensive data bases.<sup>[6, 115]</sup> The general methodology in protein engineering involves the selection of changes (rational or random), the introduction of these changes (mutagenesis) and their evaluation (screening or selection).

**Table 9 Selected examples of recent achievements in protein engineering towards improvement of various properties with random, rational and combined methods.**

Entry	Protein	Property	Improvement	Mutations	Method	Source
1	gluco corticoid receptor	stability & solubility	$\Delta T_m = 8^\circ\text{C}$ , 26x more soluble protein	4	random	[116]
2	glucose dehydrogenase ketoreductase	activity & stability	7-13x more active, higher substrate resistance	-	random	[30, 117]
3	ketoreductase	activity	>3000x	19	random	[31]
4	imidazoleglycerol-phosphate synthase	<i>de novo</i> function	Kemp elimination, $k_{\text{cat}} = 1.375 \text{ s}^{-1}$	>9	rational	[118]
5	ketosteroid isomerase	<i>de novo</i> function	Diels-Alderase $k_{\text{cat}} = 0.036 \text{ s}^{-1}$	14	rational	[119]
6	glucose dehydrogenases	half-life	> $10^6$	2-3	rational	[120]
7	transaminase	substrate specificity	27000x higher activity	27	combined	[121]
8	enoate reductase	enantioselectivity	>98 (S) & (R)-selectivity	2	combined	[122]
9	ketoreductases	enantioselectivity	63 to 99.4 % ee	10	combined	[32]
10	cyanohydrin dehalogenase	activity	4000x	35	combined	[123]

### 1.6.2. Rational Protein Design & Computational Methods

In rational protein design amino acid changes are introduced on the basis of structural information such as X-ray structures, NMR data or homology models of the enzyme of interest. With this methodology problems of well understood enzyme properties like substrate acceptance or selectivity can be targeted and *a priori* hypotheses on the expected effects have to be made. Here, only few amino acid exchanges are generated resulting in small number of possible variants to test for an improvement in the targeted property. The necessity of structural information and a basic understanding of the property to improve clearly constitute a drawback but the small screening effort exhibits the major advantage. Moreover, with this approach it is rather unlikely to find the best possible variant since the understanding of protein function and dynamics is only limited and synergistic effects are poorly understood and often cannot be predicted. For example, substitutions affecting activity may be scattered throughout the whole protein and not only located at the active site. The reasons for that are in general hard to rationalize.

For single amino acid exchanges simple methods based on polymerase chain reaction (PCR) are applied using a primer pair containing the nucleotide triplet coding for the desired amino acid. Semi-rational approaches would be performed similarly by site-saturation, where all nineteen possible amino acids are substituted to identify the most appropriate by screening. Larger library sizes are obtained by simultaneous multiple site-saturation giving access to possible synergistic effects. A powerful tool for probing the sequence space is the *combinatorial active-site saturation test* (CAST) after careful selection of target residues. With CAST the substrate specificity of a lipase was changed saturating 3 amino acids.<sup>[124]</sup> In principle, the size of (multiple) site-saturation libraries can be reduced by using reduced sets of codon like NNK (32 codons for 20 amino acids) or NDT (12 codons for 12 amino acids). These libraries are referred to as “*smart libraries*” since they exhibit a desired amino acid diversity with a significantly smaller diversity on the DNA level compared to completely degenerated codons with NNN (64 codons for 20 amino acids).

Lately, tremendous advances in protein engineering have emerged through computational methods. Rational computational design greatly decreases the need for probing randomized sequence space, rendering the route to novel biocatalyst much more efficient. Herein, SCHEMA, ProSAR and ROSETTA are the most prominent tools.<sup>[115]</sup> SCHEMA is a computational methodology, wherein the amount of protein disruption upon DNA recombination is scored. Screening is focused on the chimeras with less structural disruption resulting in functionality enriched diversity. ProSAR stands for *Protein Sequence Activity Relationships* a statistical approach, which finds the contribution of amino acid substitutions to an improvement out of a large number of variants.<sup>[123]</sup> Previously collected DNA sequence and enzyme activity data from different mutants is applied to ProSAR as a training set and beneficial



mutations are fixed for subsequent rounds of mutation. Variants contain an average of ten mutations and the final candidate may contain even more substitutions. An impressive example is a halohydrin dehalogenase with 35 substitutions with 4000-fold improved activity (see Table 9, entry 10).<sup>[123]</sup>

ROSETTA represents a fully rational approach creating novel biocatalysts by fitting a theoretically designed active site ("*theozyme*") in to stable protein backbone. Herein, different active site designs, are suggested and composed on the basis of quantum mechanics for a desired reaction.<sup>[125]</sup> ROSETTA in conjunction with the *theozyme* approach has been proven to be very successful in design of *de novo* catalysts with new functions (see Table 9, entries 4 & 5).

### 1.6.3. Directed Evolution

In contrast to rational protein design, directed evolution does not require structural information since nucleotide substitutions are incorporated randomly into a targeted DNA sequence. Multiple rounds of genetic diversity generation and gene recombination (step 1) combined with functional screening or selection are carried out to identify improved variants (step 2, see Figure 9). Improved variants are used for the next cycle of mutagenesis and screening/selection mimicking the natural process of Darwinian evolution (step 3). The iterative nature of this approach results in stepwise improvements and may lead to substantial overall improvements of the desired enzyme property after several rounds. This strategy produces a vast number of possible variants in diversity generation. For example, a ten amino acid peptide can yield theoretically  $20^{10}$  (ca.  $10^{13}$ ) combinations for a complete randomization. Consequently, screening or selecting all possible variants of an average enzyme is impossible, which constitutes the main limitation of this strategy.

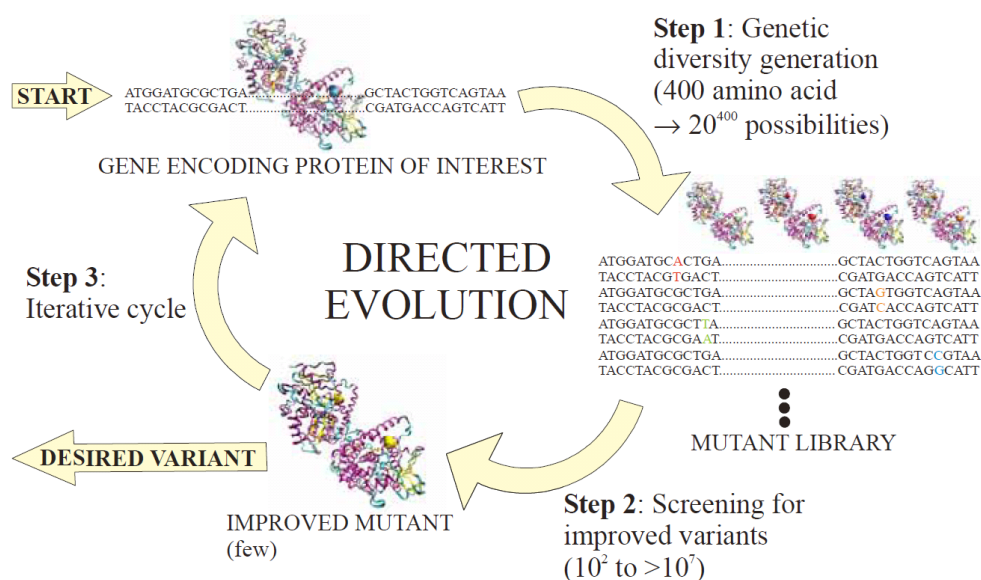


Figure 9 Scheme of the three steps in a directed evolution experiment. Taken from <sup>[126]</sup>.

The strategy of stepwise accumulation of random beneficial mutations is powerful to elucidate new positions and substitutions for improving enzyme properties, also referred to as “*hot spots*”. This methodology can lead to tremendous improvement of enzyme properties like stability and solubility (see Table 9, entry 1 & 3) as well as catalytic activity (see Table 9, entry 2 & 3). Incorporation of random mutations can lead to enzyme destabilization or complete loss of activity due to misfolding. Therefore, the choice of the template, which can bear many mutations is desired. Evolving for stability first to make the enzyme fit for subsequent mutations is an approved strategy as well as exploiting neutrally drifted mutations or starting from a consensus sequence.<sup>[115, 127]</sup>

The probably most applied and robust method for random mutagenesis is error-prone (ep) PCR, in which usually one to three nucleotides are altered per gene. Besides, high-error rate epPCR with 27 nucleotide exchanges on the average also yielded functional enzymes with novel properties.<sup>[128]</sup> However, epPCR is strongly biased in the mutational pattern since transition mutations (A↔G, C↔T) are highly favored and only single nucleotide exchanges are performed.<sup>[129]</sup> This results in only an average of 6 of the 20 possible amino acid substitutions on the protein level because transversions and/or consecutive mutations are rare events.<sup>[127]</sup> However, there are developments to circumvent these limitations by advanced techniques such as Sequence Saturation Mutagenesis (SeSaM).<sup>[130]</sup>

Another frequently used method to generate genetic diversity is gene shuffling, where DNA fragments from different parent genes are recombined *in vitro*.<sup>[131]</sup> Herein, a certain degree of minimum homology is required, which limits applicability only to related genes. The main advantage; however, is that only functional parts are shuffled yielding a higher fraction of active variants in contrast to epPCR.

#### **1.6.4. Selection and Screening for Improved Variants**

The experimental test system for evaluation of improved variants generated in rational or random fashion is the most vital part for a protein engineering campaign. Most appropriately, these systems should at best mimic the final operation conditions or properties of improvement, because “*You get what you screen for*”.<sup>[132]</sup> Moreover, a physical connection between the gene (genotype), the protein it encodes (phenotype) and the test signal has always to be maintained. Basically, a test system should be as sensitive and reproducible as possible, otherwise positive variants might get lost due to high variations in the assay. Hence, an activity related standard deviation established with wild type activity under test conditions is an important quality parameter for assay validation; usually numbers <15 % are regarded as suitable. The number of false positives and false negative should be negligibly low.

Herein, two main routes can be described; one is (*in vivo* & *in vitro*) selection and the other is screening. Unlike screening, where individual (also the *inactive*) clones are analyzed, selection targets the whole gene pool and only *active* clones are selected. Applying a selection setup very large libraries ( $10^{12-13}$  variants) may be tested.<sup>[127]</sup> However, *in vivo* selection is limited by transformation efficiencies, which generally do not exceed  $10^{10}$  transformants.<sup>[133]</sup> In *in vivo* selection the establishment of a reliable, low noise complementation system is difficult. The latter systems mostly dependent on the survival or growth of host organisms and the selection pressure may surpassed leading to many false positives. Furthermore, reduced membrane permeability constitutes a mass transfer barrier for assay compounds, which can be challenging.<sup>[134]</sup> *In vitro* selection is not dependent on transformation or mass transfer limitations; additionally, harsher non-physiological selection pressures can be applied than for living cells. Powerful systems like phage display, ribosome display, cell surface display and *in vitro* compartmentalization have been developed and validated to find improved proteins.<sup>[134]</sup>

High-throughput screening (HTS) is generally more tedious than selection and library sizes of only  $10^{5-7}$  are the average because each clone, also inactive ones, are tested.<sup>[115]</sup> In screening, theoretically every enzymatic reaction can be used as long the substrate or product can be directly or indirectly detected. Simple, qualitative assays with high throughput rely on color, fluorescence or halo formation on agar plates. Other more advanced methods to separate active from inactive clones in a HTS manner use microfluidics or flow cytometry, wherein  $>10^{10}$  variants can be tested.<sup>[135]</sup> The latter techniques can be exploited as *pre-screen* to consider only the active portion of clones for closer examination. Quantitative assays like UV-Vis and fluorescent spectroscopy or gas and high performance liquid chromatography are more appropriate to screen in detail for improved properties. Commonly, multiter plates in 96-well- or 384-well-formates are applied for spectrophotometric assays.

Further developments of efficient selection and screening methods are emerging rapidly. The rather philosophical question whether it is the better strategy to go for higher sample throughput to test larger libraries or to design smarter libraries, which can be screened with much less effort remains to be answered.

### 1.6.5. Enzyme Engineering of Alcohol Dehydrogenases

Since horse liver alcohol dehydrogenase (HLADH) was one of the first oligomeric enzymes in 1973 with amino acid sequence and crystal structure available, many structure-guided mutagenesis studies were performed to alter the properties of this enzyme.<sup>[136]</sup> From the late 1980s' onwards, ADH1 from bakers' yeast (YADH) was also mutated intensively because it was one of the most employed catalysts for synthetic applications. For this, a structural model of YADH was derived from

HLADH, since the crystal structure of YADH was solved first in 1994; however, at low resolution of 3.2 Å.<sup>[137]</sup> Advances on the field of protein structure determination resulted in a rapid increase in available highly accurate ADH crystal structures for mutational analyses. Hence, a structure at 2.44 Å resolution is available now for YADH in the protein data bank with the ID 2HCY. Additionally, computational simulations such as molecular modeling gave insights into the mechanisms of catalysis, cofactor specificity, stability, selectivity and substrate acceptance promoting rational approaches to tailor enzyme properties.<sup>[76, 79, 83, 138]</sup>

### Substrate Specificity and Activity

Site-directed mutagenesis experiments targeting the substrate binding pocket broadened the narrow substrate range of YADH (compare Figure 7, right) by exchanges from large to small amino acids.<sup>[86, 139]</sup> The same approach was followed for ADH from *Thermoanaerobacter ethanolicus*<sup>[140]</sup> and human liver ADH isoenzyme  $\beta_1\beta_1$ <sup>[141]</sup> leading to the general hypothesis, that the acceptance of substrates is largely dependent on the architecture of the substrate binding pocket. If the pocket is widened, larger substrates fit better and *vice versa*.

Furthermore, apart from rational also random mutagenesis or combined approaches succeed in altering the activity profile of ADHs. For example, activity of a carbonyl reductase and glucose dehydrogenase was increased 7- and 13-fold, respectively by several generations of DNA shuffling (see Table 9, entry 2).<sup>[30]</sup> For the (*R*)-selective ADH from *Lactobacillus kefir* a platform technology has been developed by Codexis to tailor activity and selectivity to the desired needs and several patents have been filed for the evolved variants used in various synthetic applications.<sup>[13a]</sup>

For AdhA from *Pyrococcus furiosus* random exchanges of amino acids, which are not in direct contact with the substrate, showed acceptance of larger substrates.<sup>[142]</sup> Furthermore, a glyceraldehyde dehydrogenase was engineered to convert 2-hydroxybutanone 26-fold more efficient than the wild type after DNA shuffling and site-directed mutagenesis.<sup>[143]</sup>

### Enantioselectivity

High enantioselectivity is a very important feature of ADHs and enantiomeric excesses found are usually >95 % for natural substrates. Most known ADHs exhibit *Prelogs'* specificity (see chapter 1.4.2). In order to increase or invert the stereoselectivity mostly rational approaches are used, since the orientation of the substrate has to be carefully tuned to give the desired product. Site-directed single point mutations showed inversion of stereoselectivity for substituted aromatic ketones of ADHs from *Sporobolomyces salmonicolor*<sup>[59a, 144]</sup> and *Thermoanaerobacter ethanolicus*<sup>[140b]</sup>. Short-chain carbonyl reductase from *Candida parapsilosis* showed reversed enantioselectivity with 1 – 3 site-directed substitutions<sup>[145]</sup>, whereas an aldo-keto reductase from *Penicillium citrium* was evolved via epPCR and saturation mutagenesis to increase enantioselectivity.<sup>[146]</sup> The most astonishing example

for engineering this enantioselectivity is reported for a carbonyl reductase developed by Codexis where the *ee* of a non-natural substrate was increased from 63 to 93 %.<sup>[32]</sup> In eight rounds of random mutagenesis and application of ProSAR (see chapter 1.6.2) also activity and stability could be improved substantially by introducing 10 mutations.<sup>[32]</sup>

### Cofactor Preference

ADHs are dependent on either NADH or NADPH, wherein NADPH is more expensive and less stable rendering this cofactor less attractive for application.<sup>[147]</sup> Therefore, it is desired to change the cofactor preference from NADPH to NADH by rational protein engineering. Generally, the cofactor binding site is altered in a way that the adenylyl ribose 2'-phosphate group of NADP, which is not present in NADH, cannot bind anymore. This has been achieved for ADH from *Lactobacillus brevis*, wherein an exchange from glycine to aspartate led to steric hindrance and charge repulsion of NADPH in the cofactor binding domain.<sup>[148]</sup> However, this change compromised activity but further engineering yielded fourfold increase activity with NADH with an additional point mutation.<sup>[149]</sup> An ADH from *Saccharomyces cerevisiae* was mutated in the cofactor binding site, which resulted in mixed cofactor acceptance.<sup>[150]</sup> Site-directed mutagenesis has been used to introduce eight amino acid substitutions into *Candida magnolia* reductase S1 to completely overcome NADPH dependency and switch to NADH as preferred cofactor.<sup>[151]</sup> A substitution to the negatively charged asparagine in the cofactor binding site has a repulsive effect for the adenosine 2'-phosphate anion of NADPH.

Notably, cofactor preference of glucose dehydrogenase from *Haloferax mediterranei* was switched from NADPH to NADH by a single amino acid substitution broadening its applicability for cofactor regeneration.<sup>[152]</sup>

Conversely, cofactor preference of formate dehydrogenases was converted to NADPH rather than NADH rendering it a suitable catalyst for enzyme-coupled regeneration of both cofactors in industrial applications (see chapter 1.3.2.).<sup>[153]</sup>

### Stability

Catalyst stability can be measured in different ways like thermo-, pH- or solvent stability, but for synthetic application the overall process stability under operational conditions is most important.<sup>[2]</sup> Nevertheless, protein stability is most commonly connected to a rigid protein fold and stabilization against thermal inactivation oftentimes also protects against denaturants like organic solvents or detergents. Rigidification by removal of flexible loops as well as introduction of stabilizing molecular connections such as hydrogen bonds, disulfide bonds and salt bridges can be achieved by rational protein design. However, the effects of the latter alterations are generally not so easy to predict since exact spatially arrangement of the interaction partners is required.

Another rational approach follows the strategy of *rigidification* by reducing the entropy of the unfolded state by introduction of prolines or removal of glycines.<sup>[154]</sup> By this, a thermostable alcohol dehydrogenase from *Clostridium beijerinckii* has been generated by introducing a proline. This single substitution gained substantial increase in thermal resistance.<sup>[155]</sup> (*R*)-selective ADH from *Lactobacillus kefir* was engineered by Codexis to meet certain characteristics predetermined by the process.<sup>[31]</sup> In *Penicillium citrium*  $\beta$ -ketoester reductase a single amino acid substitution identified by combination of random followed by saturation mutagenesis increased thermostability.<sup>[146]</sup> A similar approach was followed for phenylacetaldehyde reductase from *Rhodococcus sp.* ST-10 where increase resistance in the presence of isopropanol was achieved, which is advantageous for substrate-coupled cofactor regeneration.<sup>[156]</sup> Conversely, Adha from *Pyrococcus furiosus* partly lost its inherent thermostability upon directed evolution towards acceptance of new substrates.<sup>[142]</sup> The same effect was observed with amino acid exchange W95L in ADH from thermophile *Solfolobus solfataricus* disrupting an aromatic cluster responsible for stability.<sup>[157]</sup>

### **Other Properties & Recent Developments**

Alcohol dehydrogenases and carbonyl reductases are distinguished by their directional preference in catalysis. The underlying reasons were elucidated for a mannitol-2-dehydrogenase and a “one-way” carbonyl reductase was generated by active-site redesign.<sup>[158]</sup>

Recent achievements in engineering of alcohol dehydrogenases are inferring multi-parameter optimization to meet all requirements for an economic relevant industrial process. In this, factors like substrate loading, reaction time, biocatalyst loading as well activity and selectivity are considered.<sup>[30, 159]</sup> Implications on process engineering are occurring for example when reduced catalyst load facilitates easier downstream processing. In turn, biocatalyst improvements are measured as overall gain in process productivity and not as increase in a single property.

## 1.7. Aim of This Thesis

Biocatalysis became a well-established alternative to classical chemical routes to manufacture a huge variety of products in economical and sustainable manner. However, it is far from being the standard choice. Therefore, the development towards greener production processes applying biocatalysts has to be promoted by meeting the requirements for industrial applications. To achieve this, engineering of the reaction or the biocatalyst has to be performed to optimize the overall system. From the gained results, fundamental knowledge can be extracted to create a basic understanding to meet upcoming challenges in optimization procedures.

In this thesis, the model enzyme carbonyl reductase *Candida parapsilosis* (CPCR) is employed for asymmetric reduction of ketones. The resulting chiral alcohols comprise key intermediates in the synthesis of diverse important drugs and fine chemicals. CPCR was found previously to exhibit interesting reducing activity; however, the activity could not be assigned to a definite enzyme. The *Candida* native host contains two isoenzymes of CPCR, which appeared to have very similar biochemical properties. The identity of CPCR1 and CPCR2 is clarified here by combining tools of classical biochemical and modern computational chemistry. The broad substrate spectrum observed is now allocated to CPCR2.

With this promising enzyme at hand, a reaction system for efficient ketone reduction is strived for. So far, the current biocatalytic reduction systems suffer from low substrate loadings, limited process stability of the catalyst or tedious work up procedures. These constraints are addressed in this thesis. Furthermore, it is aimed to characterize the reaction system with respect to its limitations and broaden the applicability to other ketone reducing enzymes.

CPCR2 is particularly powerful with regard to substrate spectrum and stereoselectivity; however, some substrates are only poorly accepted. Moreover, the CPCR2 undergoes fast inactivation at aqueous-organic interphases in biphasic reaction systems. These drawbacks are tackled by means of protein engineering, wherein the enzyme is altered by introduction of mutations. The findings deduced from broadening the substrate scope and interfacial stabilization build the basis for further improvement of CPCR2 and other enzymes of this class.

To this end, this work is supposed to provide a new powerful reaction system for efficient biocatalytic ketone reduction as well as a CPCR2 enzyme with substantially improved properties.

## 1.8. References

- [1] P. Grunwald, *Biocata. Biochem. I Fund. App.*, Imperial College Press, London, **2009**.
- [2] A. S. Bommarius, B. R. Riebel, *Biocatalysis: Fundamentals & Applications*, John Wiley & Sons Inc, Weinheim, **2004**.
- [3] R. Bachmann, in *Bio-Conference* (Ed.: McKinsey), New York, **2003**.
- [4] G. Festel, C. Detzel, R. Maas, *J. Comm. Biotechnol.* **2010**, 118.
- [5] S. Panke, M. Wubbolts, *Curr. Opin. Chem. Biol.* **2005**, 9, 188-194.
- [6] D. Böttcher, U. T. Bornscheuer, *Curr. Opin. Micob.* **2010**, 13, 274-282.
- [7] T. Matsuda, R. Yamanaka, K. Nakamura, *Tetrahedron: Asymmetry* **2009**, 20, 513-557.
- [8] R. Wohlgemuth, *Curr. Opin. Biotechnol.* **2010**, 21, 713-724.
- [9] K. Faber, *Biotransformations in organic chemistry: a textbook*, 6 ed., Springer-Verlag, **2011**.
- [10] M. Breuer, K. Ditrich, T. Habicher, B. Hauer, M. Kessler, R. Sturmer, T. Zelinski, *Angew. Chem. Int. Ed.* **2004**, 43, 788-824.
- [11] R. Wohlgemuth, *Curr. Opin. Micob.* **2010**, 13, 283-292.
- [12] B. M. Nestl, B. A. Nebel, B. Hauer, *Curr. Opin. Chem. Biol.* **2011**, 15, 187-193.
- [13] a) G. A. Strohmeier, H. Pichler, O. May, M. Gruber-Khadjawi, *Chem. Rev.* **2011**, 111, 4141-4164; b) G. W. Zheng, J. H. Xu, *Curr. Opin. Biotechnol.* **2011**, 22, 784-792.
- [14] a) W. Liu, P. Wang, *Biotechnol. Adv.* **2007**, 25, 369-384; b) A. Weckbecker, H. Gröger, W. Hummel, *Adv. Biochem. Eng./Biotechnol.* **2010**, 120, 195-242.
- [15] a) D. J. Pollard, J. M. Woodley, *Trends Biotechnol.* **2007**, 25, 66-73; b) R. N. Patel, *Coord. Chem. Rev.* **2008**, 252, 659-701.
- [16] S. Panke, M. Held, M. Wubbolts, *Curr. Opin. Biotechnol.* **2004**, 15, 272-279.
- [17] G. W. Huisman, J. Liang, A. Krebber, *Curr. Opin. Chem. Biol.* **2010**, 14, 122-129.
- [18] W. Kroutil, H. Mang, K. Edegger, K. Faber, *Curr. Opin. Chem. Biol.* **2004**, 8, 120-126.
- [19] R. Noyori, T. Ohkuma, *Angew. Chem. Int. Ed.* **2001**, 40, 40-73.
- [20] K. Goldberg, K. Schroer, S. Lutz, A. Liese, *Appl. Microbiol Biotechnol.* **2007**, 76, 237-248.
- [21] A. Liese, K. Seelbach, C. Wandrey, *Industrial Biotransformations*, Wiley-VCH, Weinheim, **2000**.
- [22] K. Bogar, B. Martin-Matute, J. E. Backvall, *Beilstein J. Org. Chem.* **2007**, 3, 50.
- [23] R. A. Sheldon, *Pure Appl. Chem.* **2000**, 72, 1233-1246.
- [24] C. V. Voss, C. C. Gruber, K. Faber, T. Knaus, P. Macheroux, W. Kroutil, *JACS* **2008**, 130, 13969-13972.
- [25] J. B. van Beilen, W. A. Duetz, A. Schmid, B. Witholt, *Trends Biotechnol.* **2003**, 21, 170-177.
- [26] a) J. D. Carballeira, M. A. Quezada, P. Hoyos, Y. Simeo, M. J. Hernaiz, A. R. Alcantara, J. V. Sinisterra, *Biotechnol. Adv.* **2009**, 27, 686-714; b) W. Kroutil, H. Mang, K. Edegger, K. Faber, *Adv. Synth. Catal.* **2004**, 346, 125-142.
- [27] a) W. Stampfer, B. Kosjek, C. Moitzi, W. Kroutil, K. Faber, *Angew. Chem. Int. Ed.* **2002**, 41, 1014-1017; b) B. Kosjek, W. Stampfer, M. Pogorevc, W. Goessler, K. Faber, W. Kroutil, *Biotechnol. Bioeng.* **2004**, 86, 55-62.
- [28] W. Stampfer, B. Kosjek, W. Kroutil, K. Faber, *Biotechnol. Bioeng.* **2003**, 81, 865-869.
- [29] S. Lütz, L. Giver, J. Lalonde, *Biotechnol. Bioeng.* **2008**, 101, 647-653.
- [30] S. K. Ma, J. Gruber, C. Davis, L. Newman, D. Gray, A. Wang, J. Grate, G. Huisman, R. A. Sheldon, *Green Chem.* **2010**, 12, 81-86.
- [31] J. Liang, J. Lalonde, B. Borup, V. Mitchell, E. Mundorff, N. Trinh, D. A. Kochre, R. N. Cherat, G. P. Ganesh, *Org. Proc. Res. Dev.* **2010**, 14, 193-198.
- [32] J. Liang, E. Mundorff, R. Voladri, S. J. Jenne, L. Gilson, A. Conway, A. Krebber, J. Wong, S. Truesdell, J. Lalonde, *Org. Proc. Res. Dev.* **2010**, 14, 188-192.
- [33] B. Kosjek, J. Nti-Gyabaah, K. Telari, L. Dunne, J. C. Moore, *Org. Proc. Res. Dev.* **2008**, 12, 584-588.
- [34] A. Gupta, A. Tschentscher, M. Bobkova, (US patent US7371903) IEP GmbH Wiesbaden, **2005**.
- [35] A. Matsuyama, H. Yamamoto, N. Kawada, Y. Kobayashi, *J. Mol. Catal. B: Enzymatic* **2001**, 11, 513-521.



- [36] H. Gröger, F. Chamouleau, N. Orogas, C. Rollmann, K. Drauz, W. Hummel, A. Weckbecker, O. May, *Angew. Chem. Int. Ed.* **2006**, *45*, 5677-5681.
- [37] K. Schroer, U. Mackfeld, I. A. Tan, C. Wandrey, F. Heuser, S. Bringer-Meyer, A. Weckbecker, W. Hummel, T. Dausmann, R. Pfaller, A. Liese, S. Lutz, *J. Biotechnol.* **2007**, *132*, 438-444.
- [38] N. Itoh, M. Nakamura, K. Inoue, Y. Makino, *Appl. Microbiol. Biotechnol.* **2007**, *75*, 1249-1256.
- [39] N. Kizaki, Y. Yasohara, J. Hasegawa, M. Wada, M. Kataoka, S. Shimizu, *Appl. Microbiol. Biotechnol.* **2001**, *55*, 590-595.
- [40] T. Ema, T. Ide, N. Okita, T. Sakai, *Adv. Synth. Catal.* **2008**, *350*, 2039-2044.
- [41] M. Kataoka, K. Yamamoto, H. Kawabata, M. Wada, K. Kita, H. Yanase, S. Shimizu, *Appl. Microbiol. Biotechnol.* **1999**, *51*, 486-490.
- [42] Y. Ni, C.-H. Chun-Xiu Li, J. Jie Zhang, N.-D. Shen, U. T. Bornscheuer, J.-H. Xu, *Adv. Synth. Catal.* **2011**, *353*, 1213.
- [43] L. J. Wang, C. X. Li, Y. Ni, J. Zhang, X. Liu, J. H. Xu, *Biores. Technol.* **2011**, *102*, 7023-7028.
- [44] G. de Gonzalo, I. Lavandera, K. Faber, W. Kroutil, *Org. Lett.* **2007**, *9*, 2163-2166.
- [45] A. Zaks, A. M. Klibanov, *Science* **1984**, *224*, 1249-1251.
- [46] a) A. Ballesteros, U. Bornscheuer, A. Capewell, D. Combes, J.-S. Condoret, K. Koenig, F. N. Kolisis, A. Marty, U. Menge, T. Scheper, H. Stamatis, A. Xenakis, *Biocatal. Biotrans.* **1995**, *13*, 1-42; b) M. H. Vermue, J. Tramper, *Pure Appl. Chem.* **1995**, *67*, 345-373.
- [47] J. Grunwald, B. Wirz, M. P. Scollar, A. M. Klibanov, *JACS* **1986**, *108*, 6732-6734.
- [48] R. M. Guinn, P. S. Skerker, P. Kavanaugh, D. S. Clark, *Biotechnol. Bioeng.* **1991**, *37*, 303-308.
- [49] A. Johansson, K. Mosbach, M. O. Mansson, *Eur. J. Biochem. / FEBS* **1995**, *227*, 551-555.
- [50] W. Hummel, in *Advances in biochemical engineering/biotechnology, Vol. 58* (Ed.: T. Scheper), Springer-Verlag, Berlin Heidelberg, **1997**.
- [51] a) M. V. Filho, T. Stillger, M. Müller, A. Liese, C. Wandrey, *Angew. Chem. Int. Ed.* **2003**, *42*, 2993-2996; b) M. Eckstein, M. V. Filho, A. Liese, U. Kragl, *Chem. Commun.* **2004**, 1084-1085.
- [52] H. Groger, W. Hummel, S. Buchholz, K. Drauz, T. V. Nguyen, C. Rollmann, H. Husken, K. Abokitse, *Org. Lett.* **2003**, *5*, 173-176.
- [53] V. Höllrigl, K. Otto, A. Schmid, *Adv. Synth. Catal.* **2007**, *349*.
- [54] M. Karabec, A. Lyskowski, K. C. Tauber, G. Steinkellner, W. Kroutil, G. Grogan, K. Gruber, *Chem. Commun.* **2010**, *46*, 6314-6316.
- [55] M. Musa Musa, R. S. Phillips, *Catal. Sci. Technol.* **2011**, *1*, 1311-1323.
- [56] H. Hirakawa, N. Kamiya, Y. Kawarabayashi, T. Nagamune, *Biochi. Biophys. Act.* **2005**, *1748*, 94-99.
- [57] I. Lavandera, A. Kern, M. Schaffenberger, J. Gross, A. Glieder, S. de Wildeman, W. Kroutil, *ChemSusChem* **2008**, *1*, 431-436.
- [58] D. L. Graham, H. D. Simpson, D. Cowan, *Annal. New York Acad. Sci.* **1996**, 799.
- [59] a) H. Li, D. Zhu, L. Hua, E. R. Biehl, *Adv. Synth. Catal.* **2009**, *351*, 583-588; b) J. Schumacher, M. Eckstein, U. Kragl, *Biotechnol. J.* **2006**, *1*, 574-581.
- [60] C. Christoph Roosen, P. Müller, L. Greiner, *Appl. Microbiol. Biotechnol.* **2008**, *81*, 607-614.
- [61] W. Hussain, D. J. Pollard, M. Truppo, G. L. Lye, *J. Mol. Catal. B: Enzymatic* **2008**, *55*, 19-29.
- [62] a) S. Bräutigam, S. Bringer-Meyer, D. Weuster-Botz, *Tetrahedron: Asymmetry* **2007**, *18*, 1883-1887; b) S. Bräutigam, D. Dennewald, M. Schürmann, J. Lutje-Spelberg, W.-R. Pitner, D. Weuster-Botz, *Enz. Microb. Technol.* **2009**, *45*, 310-316.
- [63] Y. G. Shi, Y. Fang, Y. P. Ren, H. P. Wu, H. L. Guan, *J. Ind. Microb. Biotechnol.* **2008**, *35*, 1419-1424.
- [64] S. Pulvin, M. D. Legoy, R. Lortie, M. Pensa, D. Thomas, *Biotechnol. Lett.* **1986**, *8*, 783-784.
- [65] S. Pulvin, F. Parvaresh, D. Thomas, M. D. Legoy, *Annals of the New York academy of sciences* **1988**, *542*, 434-439.
- [66] C. Ferloni, M. Heinemann, W. Hummel, T. Dausmann, J. Buchs, *Biotechnology progress* **2004**, *20*, 975-978.
- [67] T. Goubet, T. Maugard, S. Lamare, M. D. Legoy, *Enz. Microb. Technol.* **2001**, *31*, 425-430.

- [68] T. Harada, Y. Kubota, T. Kamitanaka, K. Nakamura, T. Matsuda, *Tetrahedron Letters* **2009**, *50*, 4934-4936.
- [69] E. C. Webb, *Enzyme nomenclature 1992: recommendations of the Nomenclature Committee of the International Union of Biochemistry and Molecular Biology on the nomenclature and classification of enzymes.*, Academic press, San Diego, **1992**.
- [70] N. E., H. J. Wulff, *Biochemie Z.* **1937**, *293*, 351-389.
- [71] H. Eklund, J. P. Samma, L. Wallen, C. I. Branden, A. Akeson, T. A. Jones, *J. Mol. Biol.* **1981**, *146*, 561-587.
- [72] H. Theorell, K. J. Mc, *Nature* **1961**, *192*, 47-50.
- [73] B. Persson, J. Hedlund, H. Jornvall, *Cell molecular life science* **2008**, *65*, 3879-3894.
- [74] S. Hammes-Schiffer, S. J. Benkovic, *Annual reviews in biochemisrty* **2006**, *75*, 519-541.
- [75] C. Alhambra, J. C. Corchado, M. L. Sánchez, J. Gao, D. G. Truhlar, *Jouranl of the American chemical society* **2000**, *122*, 8197-8203.
- [76] D. Roston, A. Kohen, *Proceedings of the national academy of sciences of the United States of America* **2010**, *107*, 9572-9577.
- [77] S. E. Suadi, Santa Barbara, **2000**. web page (12/04/07):  
[http://mcdb-webarchive.mcdb.ucsb.edu/sears/biochemistry/presentations/f00\\_student\\_presentations/SuhairSuadi/buttons.htm#rec](http://mcdb-webarchive.mcdb.ucsb.edu/sears/biochemistry/presentations/f00_student_presentations/SuhairSuadi/buttons.htm#rec)
- [78] V. Prelog, *Pure applied chemistry* **1964**, *9*, 119-130.
- [79] H. Eklund, S. Ramaswamy, *Cell Mol Life Sci* **2008**, *65*, 3907-3917.
- [80] M. G. Rossmann, D. Moras, K. W. Olsen, *Nature* **1974**, *250*, 194-199.
- [81] O. Dym, D. Eisenberg, *Protein science* **2001**, *10*, 1712-1728.
- [82] D. S. Auld, T. Bergman, *Cell molecular life science* **2008**, *65*, 3961-3970.
- [83] E. G. Brandt, M. Hellgren, T. Brinck, T. Bergman, O. Edholm, *Physical chemistry chemical physics* **2009**, *11*, 975-983.
- [84] M. Knoll, J. Pleiss, *Protein Science* **2008**, *17*, 1689-1697.
- [85] K. I. Ziegelmann-Fjeld, M. M. Musa, R. S. Phillips, J. G. Zeikus, C. Vieille, *Protein engineering design & selection* **2007**, *20*, 47-55.
- [86] E. H. Creaser, C. Murali, K. A. Britt, *Protein engineering* **1990**, *3*, 523-526.
- [87] M. R. Kula, J. Peters, (*Int. patent WO/9318138*) Forschungszentrum Jülich, **1993**.
- [88] J. Peters, T. Zelinski, M. R. Kula, *Applied mircobiology and biotechnology* **1992**, *38*, 334-340.
- [89] a J. Peters, T. Minuth, M. R. Kula, *Biocatal. Biotrans.* **1993**, *8*, 31-46; b J. Peters, T. Minuth, M. R. Kula, *Enz. Microb. Technol.* **1993**, *15*, 950-958.
- [90] T. Schubert, W. Hummel, M. R. Kula, M. Muller, *European journal of organic chemistry* **2001**, 4181-4187.
- [91] a J. Peters, T. Zelinski, T. Minuth, M.-R. Kula, *Tetrahedron: Asymmerty* **1993**, *4*, 1683-1692; b B. Orlich, R. Schomaecker, *Biotechnol. Bioeng.* **1999**, *65*, 357-362.
- [92] A. Liese, T. Zelinski, M. R. Kula, H. Kierkels, M. Karutz, U. Kragl, C. Wandrey, *J. Mol. Catal. B: Enzymatic* **1998**, *4*, 91-99.
- [93] a M. Eckstein, T. Daußmann, U. Kragl, *Biocatal. Biotrans.* **2004**, *22*, 89-96; b H. Gröger, W. Hummel, C. Rollmann, F. Chamouleau, H. Hüsken, H. Werner, C. Wunderlich, K. Abokitse, K. Drauz, S. Buchholz, *Tetrahedron* **2004**, *60*.
- [94] T. Hischer, S. Steinsiek, M. B. Ansorge-Schumacher, *Biocatal. Biotrans.* **2006**, *24*, 437-442.
- [95] M. Bhattacharjee, *Doctoral thesis*, RWTH Aachen **2006**.
- [96] A. van den Wittenboer, *Doctoral thesis*, RWTH Aachen **2009**.
- [97] A. van den Wittenboer, T. Schmidt, P. Muller, M. B. Ansorge-Schumacher, L. Greiner, *Biotechnol. J.* **2009**, *4*, 44-50.
- [98] D. Gamemara, P. Dominguez de Maria, *Biotechnology advances* **2009**, *27*, 278-285.
- [99] T. Vaijayanthia, A. Chadha, *Tetrahedron: Asymmetry* **2008**, *19*, 93-96.
- [100] Y. Nie, Y. Xu, X. Qing Mu, Y. Tang, J. Jiang, Z. Hao Sun, *Biotechnol. Lett.* **2005**, *27*, 23-26.
- [101] H. Yamamoto, N. Kawada, A. Matsuyama, Y. Kobayashi, *Biosci. Biotechnol. Biochem.* **1999**, *63*, 1051-1055.

- [102] N. Xu, H. Wang, Y. Nie, Y. Xu, R. Xiao, *Front. Biol. China* **2008**, *3*, 19-25.
- [103] Y. Nie, Y. Xu, X. Q. Mu, H. Y. Wang, M. Yang, R. Xiao, *Appl. Environ. Microb.* **2007**, *73*, 3759-3764.
- [104] M. Kataoka, A. R. Delacruz-Hidalgo, M. A. Akond, E. Sakuradani, K. Kita, S. Shimizu, *Appl. Microbiol. Biotechnol.* **2004**, *64*, 359-366.
- [105] T. Kojima, H. Yamamoto, N. Kawada, A. Matsuyama, (*US patent US5,763,236*), Daciel Chemical Industries Ltd., **1998**.
- [106] Y. Nie, Y. Xu, H. Y. Wang, N. Xu, R. Xiao, Z. H. Sun, *Biocatal. Biotrans.* **2008**, *26*, 210-219.
- [107] A. Guida, C. Lindstaedt, S. L. Maguire, C. Ding, D. G. Higgins, D. Harris, M. Berriman, G. Butler, *unpublished work* **2011**.
- [108] R. Zhang, G. Zhu, W. Zhang, S. Cao, X. Ou, X. Li, M. Bartlam, Y. Xu, X. C. Zhang, Z. Rao, *Protein Sci.* **2008**, *17*, 1412-1423.
- [109] T. Zelinski, M. R. Kula, *Biocatal. Biotrans.* **1997**, *15*, 57-74.
- [110] J. Peters, H. P. Brockamp, T. Minuth, M. Grothus, A. Steigel, M. R. Kula, L. Elling, *Tetrahedron: Asymmetry* **1993**, *4*, 1173-1182.
- [111] L. O. Wiemann, A. Buthe, M. Klein, A. van den Wittenboer, L. Dahne, M. B. Ansorge-Schumacher, *Langmuir* **2009**, *25*, 618-623.
- [112] T. Kojima, H. Yamamoto, N. Kawada, A. Matsuyama, *Eur. patent 0645453 B1*, **1995**.
- [113] M. R. Kula, J. Peters, *US patent. 5,523,223*, Research Center Jülich, **1996**.
- [114] T. Kojima, H. Yamamoto, N. Kawada, A. Matsuyama, *US patent 6,255,092*, Daciel Chemical Industries Ltd., **2001**.
- [115] A. S. Bommarius, J. K. Blum, M. J. Abrahamson, *Curr. Opin. Chem. Biol.* **2011**, *15*, 194-200.
- [116] T. Seitz, R. Thoma, G. A. Schoch, M. Stihle, J. Benz, B. D'Arcy, A. Wiget, A. Ruf, M. Hennig, R. Sterner, *J. Mol. Biol.* **2010**, *403*, 562-577.
- [117] C. Davis, J. Grate, D. Gray, J. M. Gruber, G. W. Huisman, S. K. Ma, L. M. Newman, R. A. Sheldon, L. A. Wang, *Int. patent WO04015132*, Codexis Inc., **2005**.
- [118] A. N. Alexandrova, D. Rothlisberger, D. Baker, W. L. Jorgensen, *JACS* **2008**, *130*, 15907-15915.
- [119] J. B. Siegel, A. Zanghellini, H. M. Lovick, G. Kiss, A. R. Lambert, J. L. St Clair, J. L. Gallaher, D. Hilvert, M. H. Gelb, B. L. Stoddard, K. N. Houk, F. E. Michael, D. Baker, *Science* **2010**, *329*, 309-313.
- [120] E. Vazquez-Figueroa, J. Chaparro-Riggers, A. S. Bommarius, *Chembiochem* **2007**, *8*, 2295-2301.
- [121] C. K. Savile, J. M. Janey, E. C. Mundorff, J. C. Moore, S. Tam, W. R. Jarvis, J. C. Colbeck, A. Krebber, F. J. Fleitz, J. Brands, P. N. Devine, G. W. Huisman, G. J. Hughes, *Science* **2010**, *329*, 305-309.
- [122] D. J. Bougioukou, S. Kille, A. Taglieber, M. T. Reetz, *Adv. Synth. Catal.* **2009**, *351*, 3287 – 3305.
- [123] R. J. Fox, S. C. Davis, E. C. Mundorff, L. M. Newman, V. Gavrilovic, S. K. Ma, L. M. Chung, C. Ching, S. Tam, S. Muley, J. Grate, J. Gruber, J. C. Whitman, R. A. Sheldon, G. W. Huisman, *Nature Biotechnol.* **2007**, *25*, 338-344.
- [124] M. T. Reetz, M. Bocola, J. D. Carballeira, D. Zha, A. Vogel, *Angew. Chem. Int. Ed.* **2005**, *44*, 4192-4196.
- [125] X. Zhang, J. DeChancie, H. Gunaydin, A. B. Chowdry, F. R. Clemente, A. J. Smith, T. M. Handel, K. N. Houk, *J. Org. Chem.* **2008**, *73*, 889-899.
- [126] K. L. Tee, U. Schwaneberg, *Com. Chem. High T. Scr.* **2007**, *10*, 197-217.
- [127] R. J. Kazlauskas, U. T. Bornscheuer, *Nature Chem. Biol.* **2009**, *5*, 526-529.
- [128] D. A. Drummond, B. L. Iverson, G. Georgiou, F. H. Arnold, *J. Mol. Biol.* **2005**, *350*, 806-816.
- [129] T. S. Wong, D. Zhurina, U. Schwaneberg, *Com. Chem. High T. Scr.* **2006**, *9*, 271-288.
- [130] H. Mundhada, J. Marienhagen, A. Scacioc, A. Schenk, D. Roccatano, U. Schwaneberg, *Chembiochem* **2011**, *12*, 1595-1601.
- [131] W. P. Stemmer, *Nature* **1994**, *370*, 389-391.
- [132] C. Schmidt-Dannert, F. H. Arnold, *Trends Biotechnol.* **1999**, *17*, 135-136.
- [133] A. Aharoni, A. D. Griffiths, D. S. Tawfik, *Curr. Opin. Chem. Biol.* **2005**, *9*, 210-216.

- [134] Y. L. Boersma, M. J. Droge, W. J. Quax, *The FEBS journal* **2007**, *274*, 2181-2195.
- [135] A. D. Griffiths, D. S. Tawfik, *Trends Biotechnol.* **2006**, *24*, 395-402.
- [136] C.-I. Braenden, H. Eklund, B. Nordstrom, T. Boiwe, G. Soderlund, E. Zeppezauer, I. Ohlsson, A. Akesson, *Proc. Nat. Aacad. Sci.* **1973**, *70*, 2439-2442.
- [137] S. Ramaswamy, D. A. Kratzer, A. D. Hershey, P. H. Rogers, A. Arnone, H. Eklund, B. V. Plapp, *J. Mol. Biol.* **1994**, *235*, 777-779.
- [138] a) B. V. Plapp, *Arch. Biochem. Biophys.* **2010**, *493*, 3-12; b) L. Esposito, I. Bruno, F. Sica, C. A. Raia, A. Giordano, M. Rossi, L. Mazzarella, A. Zagari, *Biochemistry* **2003**, *42*, 14397-14407.
- [139] A. J. Ganzhorn, D. W. Green, A. D. Hershey, R. M. Gould, B. V. Plapp, *J. Biol. Chem.* **1987**, *262*, 3754-3761.
- [140] a) M. M. Musa, K. I. Ziegelmann-Fjeld, C. Vieille, R. S. Phillips, *Org. Biomol. Chem.* **2008**, *6*, 887-892; b) M. M. Musa, N. Lott, M. Laivenieks, L. Watanabe, C. Vieille, R. S. Phillips, *ChemCatChem* **2009**, *1*, 89. **2009**.
- [141] T. D. Hurley, W. F. Bosron, *Biochem. Bioph. Res. Commun.* **1992**, *183*, 93-99.
- [142] R. Machielsen, N. G. Leferink, A. Hendriks, S. J. Brouns, H. G. Hennemann, T. Dausmann, J. van der Oost, *Extremophiles* **2008**, *12*, 587-594.
- [143] H. Zhang, G. T. Lountos, C. B. Ching, R. Jiang, *Appl. Microbiol. Biotechnol.* **2010**, *88*, 117-124.
- [144] D. Zhu, H. Ling, *Pure Appl. Chem.* **2010**.
- [145] R. Zhang, Y. Xu, Y. Sun, W. Zhang, R. Xiao, *Appl. Environ. Microb.* **2009**, *75*, 2176-2183.
- [146] H. Asako, M. Shimizu, N. Itoh, *Appl. Microbiol. Biotechnol.* **2008**, *80*, 805-812.
- [147] L. Kulishova, *Doctoral thesis*, Heinrich-Heine Universität Düsseldorf, **2010**.
- [148] N. H. Schlieben, K. Niefind, J. Muller, B. Riebel, W. Hummel, D. Schomburg, *J. Mol. Biol.* **2005**, *349*, 801-813.
- [149] R. Machielsen, L. L. Looger, J. Raedts, S. Dijkhuizen, W. Hummel, H.-G. Hennemann, T. Dausmann, J. van der Oost, *Eng. Life Sci.* **2009**, *9*, 38-44.
- [150] M. Katzberg, N. Skorupa-Parachin, M. F. Gorwa-Grauslund, M. Bertau, *Int. J. Mol. Sci.* **2010**, *11*, 1735-1758.
- [151] S. Morikawa, T. Nakai, Y. Yasohara, H. Nanba, N. Kizaki, J. Hasegawa, *Biosci. Biotechnol. Biochem.* **2005**, *69*, 544-552.
- [152] C. Pire, J. Esclapez, S. Diaz, F. Perez-Pomares, J. Ferrer, M. J. Bonete, *J. Mol. Catal. B: Enzymatic* **2009**, *59*, 261-265.
- [153] V. I. Tishkov, A. G. Galkin, V. V. Fedorchuk, P. A. Savitsky, A. M. Rojkova, H. Gieren, M. R. Kula, *Biotechnol. Bioeng.* **1999**, *64*, 187-193.
- [154] V. G. Eijsink, A. Bjork, S. Gaseidnes, R. Sirevag, B. Synstad, B. van den Burg, G. Vriend, *J. Biotechnol.* **2004**, *113*, 105-120.
- [155] E. Goihberg, O. Dym, S. Tel-Or, I. Levin, M. Peretz, Y. Burstein, *Proteins* **2007**, *66*, 196-204.
- [156] Y. Makino, T. Dairi, N. Itoh, *Appl. Microbiol. Biotechnol.* **2007**, *77*, 833-843.
- [157] A. Pennacchio, L. Esposito, A. Zagari, M. Rossi, C. A. Raia, *Extremophiles* **2009**, *13*, 751-761.
- [158] M. Klimacek, B. Nidetzky, *J. Biol. Chem.* **2010**, *285*, 30644-30653.
- [159] O. W. Gooding, R. Voladri, A. Bautista, T. Hopkins, G. Huisman, S. Jenne, S. Ma, E. C. Mundorff, M. M. Savile, *Org. Proc. Res. Dev.* **2010**, *14*, 119-126.

## 2. Experimental

### 2.1. Molecular Biology Techniques

#### 2.1.1. Used Strains and Plasmids

<i>E. coli</i> DH5 $\alpha$ or 10G	<i>[(supE44 <math>\Delta</math>lacU169 <math>\Phi</math>80 lacZ<math>\Delta</math>M15) hsdR17 recA1 gyrA96 thi-1 relA1]]</i>
<i>E. coli</i> BL21(DE3)	<i>[F- ompT gal dcm lon hsdSB (rB- mB-) <math>\lambda</math>(DE3 [lacI lacUV5-T7 gege 1 ind1 sam7 nin5])]</i>
pET-22b(+)	Novagen (Cat. No. 69744-3)

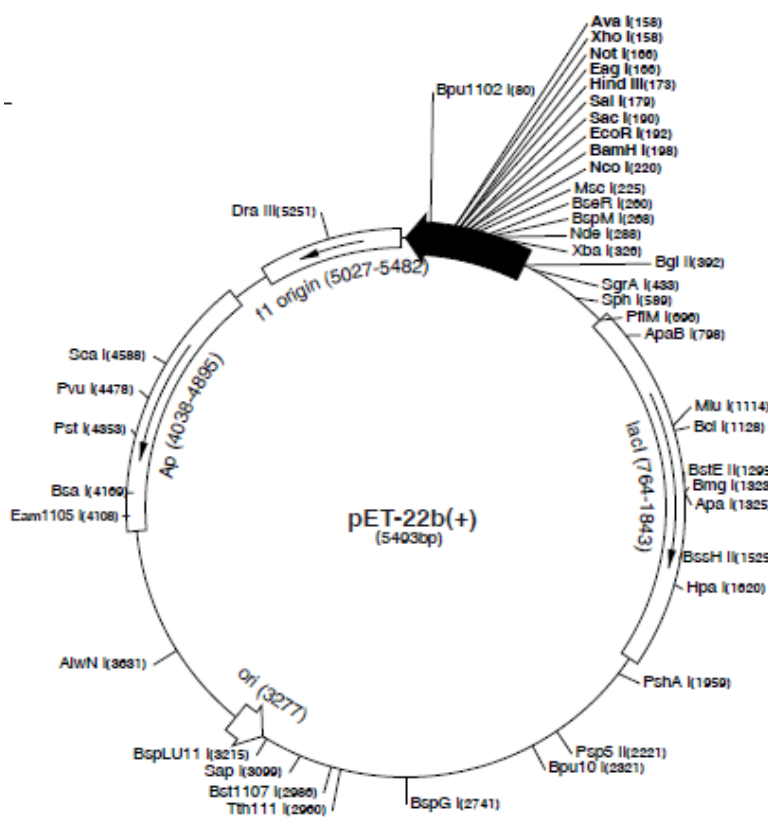


Figure 1 Vector map of pET22b(+) vector from Novagen (Cat. No. 69744-3)

### 2.1.2. Design of CPCR2 Gene Construct

For protein engineering of carbonyl reductase from *Candida parapsilosis* DSM 70125 (CPCR2), the gene with Genbank accession number AB010636 was taken as a template. A DNA construct was newly designed and synthesized with *E. coli* codon usage by GeneArt (Invitrogen, Darmstadt) using the provided standard algorithm. Adaption of codon usage was carried out to minimize the probability of expression mutants. For example, when codons commonly used by *Candida* are rare in *E. coli* expression might be reduced or even terminated. In the newly designed recombinant CPCR2 gene construct, rare codons are replaced by codons frequently used in *E. coli*. These may account for optimal expression and silent mutations introduced by protein engineering techniques will not lead to increased expression levels. Higher expression levels of the identical protein are directly reflected in activity-based screening assays yielding false positives.

For efficient cloning, recognition sites for endonucleases NdeI at the C-terminus and NotI at the N-terminus were incorporated (see black boxes in Figure 2). Two stop codons are positioned right in front of the NotI restriction site to terminate protein synthesis (see Figure 2, grey box). For possible subcloning, HindIII and BamHI sites were introduced between functional elements of the DNA constructs. The resulting gene fragments are compatible with pET22b(+) vector (Novagen) and can be cloned in frame using DNA ligation (see Figure 1).

Three elements were attached to the C-terminal end of the 336 amino acid sequence of CPCR2 (see Figure 2). C-terminal extensions are preferred over N-terminal ones, since protein folding starts from the N-terminus. Hence, C-terminal extensions interfere less with native folding of the target protein.



**Figure 2** Design of the wtCPCR2 construct.

For convenient and mild purification of the protein, an affinity tag of eight amino acids was fused (see Figure 2, ocher box). The motif WSHQPQFEK binds with high selectivity to the column matrix, and facilitates one-step purification by elution with desthiobiotin (IBA BioTAGnology, Göttingen) (see also 2.2.4). A decamer of alanines is placed upstream of the strep tag (see Figure 2, green box), which is prone to form a stiff  $\alpha$ -helix and serves a spacer peptide. The structural motif provides mobility to the strep-tag thereby reducing the probability that it is inaccessible for purification. Furthermore, a recognition site for the commercially available protease from tobacco etch virus (TEV) is positioned subsequent to the terminal amino acid of CPCR2 (see Figure 2, red box). The protease recognizes the peptide sequence ENLYFQG and cleaves between Q and G. In case, the C-terminal extension negatively affects CPCR2 properties, the extension could be eliminated upon TEV protease treatment.

### 2.1.3. Generation of Site-specific CPCR2 Mutants

In this work, amino acid exchanges were introduced at specific sites in the protein using a method based on polymerase chain reaction (PCR). In this, the primer contains the nucleotides coding for the desired mutation whereas the flanking parts of the primer sequence are fully complementary to the template DNA. A high-fidelity DNA polymerase amplifies the whole plasmid construct and the final PCR product contains the mutation(s) at the desired position since the synthetic primer was integrated. The principle is known and commercialized as QuikChange® method (Stratagene).

The example in Figure 3 depicts an exchange from leucine (Leu, green box) to asparagine (Asn, red box) with a primer carrying an AAC nucleotide codon, whereas the template DNA exhibits a CTG-codon.

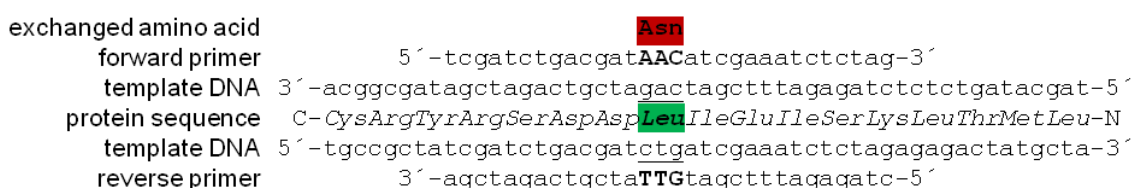


**Figure 3 Principle of a single amino acid exchange using the QuikChange® method.**

To obtain only mutated DNA from PCR, template DNA with wild type codon has to be removed efficiently. For this, the DNA restriction enzyme DpnI is applied, since it cleaves only template DNA from microbial origin. For instance, DNA from *E. coli* is specifically methylated to mark it as host DNA and DpnI works only on the template DNA leaving non-methylated PCR-products intact.

The design of the primer results in two oligonucleotides, which are fully complementary to each other and are prone to annealing, which gives primer dimers. Thus, PCR will result in reduced yield since the primer dimers cannot be used for elongation. Hence, a two-step protocol was applied wherein at first the two primers are elongated separately and are mixed afterwards.<sup>[1]</sup>

### 2.1.4. Construction of CPCR2 Site-saturation Libraries

For protein engineering not only site-specific single amino acid exchanges are performed but also site-saturation in, which all 19 alternative amino acids occur. For this semi-rational approach the QuikChange® method with primers having degenerated codons are employed. The maximum degeneracy for an amino acid would be NNN, where N stands for all four nucleotides giving  $4^3 = 64$  possible triplet codons. The NNN codons cover all 20 amino acids as well as the three stop codons. However, reduced codon degeneracy *e.g.* NNS (S stands for G & C) also covers the full set of amino acids but only one stop codon with 32 variations. It has been shown that a minimal set of twelve chemically different amino acids encoded by NDT codon (D = G, A & T) can lead to similar results than using NNN codon but with screening much less variants.<sup>[2]</sup> For a site-saturation experiment the codon degeneracy strongly affects the effort in screening.

The quality of a library may be analyzed with respect to the wild type gene unintentionally present. This is usually done by DNA sequencing of few clones to check efficient mutagenesis and removal of wild type DNA after PCR. High content of wild type DNA lowers the quality of the library and more clones have to be analyzed to cover all possible variants.

To assure that all possible variants are present in the library after PCR and transformation, a library of certain size has to be generated. With a set completeness (usually >95 %), the library size depends on the number of codons and the degeneracy applied in the experiment. For example, a site-saturation library for a single amino acid with codon degeneracy NNN comprises 64 possible variants. For a library with desired 100 % completeness, statistically a three times excess of variants ( $64 \times 3 = 192$  clones) represents the full set of variants with 95 % probability.<sup>[2]</sup>

Codon degeneracy NNS (32 possible codons) requires only 96 clones to match the same statistical parameters. When the number of codons increases the number of possible variations rise exponentially, e.g. two amino acids with NNS codon,  $32^2 = 1024$  variants are possible and at least 3066 variants have to be screened. Hence, addition of only one amino acid increases the screening effort by the factor of 33. Therefore, the design of a site-saturation experiment has to be carried out with care. A comprehensive online-tool provides the possible codon degeneracies as well as the statistics and minimum number of variants to screen for.<sup>[3]</sup>

#### **2.1.5. Transformation of Plasmid Constructs to *E. coli***

To introduce recombinant plasmid DNA generated by restriction and ligation (compare 2.1.2) or QuikChange® (compare 2.1.3 & 2.1.4) to the expression host *E. coli* two methods were applied.

Heat shock transformation was carried out with *E. coli* previously made competent according to Inoue<sup>[4]</sup> or Sambrook & Russell<sup>[5]</sup>. After conferring competence, *E. coli* was able to take up plasmid DNA upon heat treatment.

For higher transformation efficiencies, e.g. for library construction, usually electroporation was applied with commercial *E. coli* cells (E. cloni® BL21(DE3) Express, Lucigen). Transformation was done according to the manufacturers' manual. If the number of transformants was too low, commercial "ultra-competent" cells were used (E. cloni® 10G, Lucigen). Then plasmids were recovered and re-transformed to the expression host. In all cases ampicillin at  $100 \mu\text{g mL}^{-1}$  was used as antibiotic as the gene for ampicillin resistance is provided by pET22b(+) (see Figure 1).



## 2.2. Protein Chemistry Techniques

### 2.2.1. CPCR2 Protein Expression in Flask Scale

CPCR2 was cloned into pET22b(+)-vector and transformed to *E. coli* BL21(DE3). The vector contains a promoter for a RNA-polymerase from the phage T7. The gene for T7-RNA polymerase is encoded in the genome of *E. coli* (DE3)-strains and is under the control of the lac-promotor. Upon induction with isopropylthiogalactoside (IPTG), T7-RNA polymerase is expressed by the *E. coli* protein synthesis machinery. The polymerase binds to its promoter on the plasmid and generates mRNA of the gene encoded downstream. The repressor of the lac-promotor (lac I) is encoded not only on the *E. coli* genome but also on the plasmid, ensuring a minimum basal expression of the recombinant gene since the T7-promotor also contains a binding site for lac I (lac o). The tight control of expression together with the high expression levels induced by the strong T7 promoter render this system very powerful for heterologous protein expression.

A CPCR2 construct used in former projects consisted of the gene with original *Candida* codon usage cloned in to pET26 vector.<sup>[6]</sup> This construct was successfully applied in *E. coli* JM109(DE3) at 30 °C expression temperature and 1 mol L<sup>-1</sup> IPTG to produce soluble and active CPCR2. For the newly designed CPCR2 construct; however, expression conditions were changed. To obtain soluble CPCR2, the expression temperature had to be lowered to 15 °C and 0.1 mol L<sup>-1</sup> IPTG were added. It can be assumed that higher expression temperatures led to excessive production of CPCR2 beyond the folding capacities of the *E. coli* resulting in formation of inclusion bodies. Reduced expression temperatures slow down the whole metabolism as well as protein expression allowing CPCR2 to fold properly.

CPCR2 expression in flask scale was carried out in TB medium (24 g L<sup>-1</sup> yeast extract, 12 g L<sup>-1</sup> tryptone, 4 g L<sup>-1</sup> glycerol, 0.1 mol L<sup>-1</sup> M KPi pH 7.0) with a ratio of medium to flask volume of at least 1:5. As inoculum, 2 % (v/v) of an overnight culture in LB medium (5 g L<sup>-1</sup> yeast extract, 10 g L<sup>-1</sup> tryptone, 10 g L<sup>-1</sup> NaCl) were added. The culture was incubated at 37 °C and 250 rpm until an optical density at 600 nm of 0.6 was reached indicating the early exponential growth phase. Then, 0.1 mol L<sup>-1</sup> IPTG was put in and the temperature was shifted down to 15 °C. CPCR2 expression was usually carried out overnight but never longer than 18 hours.

### 2.2.2. CPCR2 Protein Expression in Fermenter

For production of larger amounts of CPCR2, high-cell density fermentation in 2 liter was carried out. For this a BIOSTAT®Bplus (Sartorius) was applied. In principle, all parameters such as medium, temperature and IPTG concentration were identical to flask expressions. Though, TB medium was supplemented with 30 g L<sup>-1</sup> glycerol to serve as carbon source and promote cell growth to high

densities. Ammonia (30 % (w/v)) had the function of pH regulation agent as well as nitrogen source. Oxygen saturation was set to 30 %, relative to air.

Fermentation was initiated by inoculation with 5-6 % (v/v) of a pre-culture and cell proliferation was assessed by measuring optical cell density at regular time intervals. A stable fermentation was achieved by keeping the oxygen saturation level constant by controlling stirrer speed. In the early exponential phase (usually  $OD_{600}$  8-10) expression was induced with  $0.1 \text{ mol L}^{-1}$  IPTG. After the temperature shift to  $15 \text{ }^{\circ}\text{C}$ , cell growth was further monitored and activity of CPC2R was determined (for activity assay see section 2.2.6). After 8-10 hours, fermentation was terminated and cells were harvested.

### 2.2.3. CPC2R Protein Expression in 96-well Multititer Plates

As for flask and fermenter expression, the principle parameters for expression in  $150 \text{ }\mu\text{L}$  scale in 96-well plates were similar. The standard procedure is depicted in Figure 4.

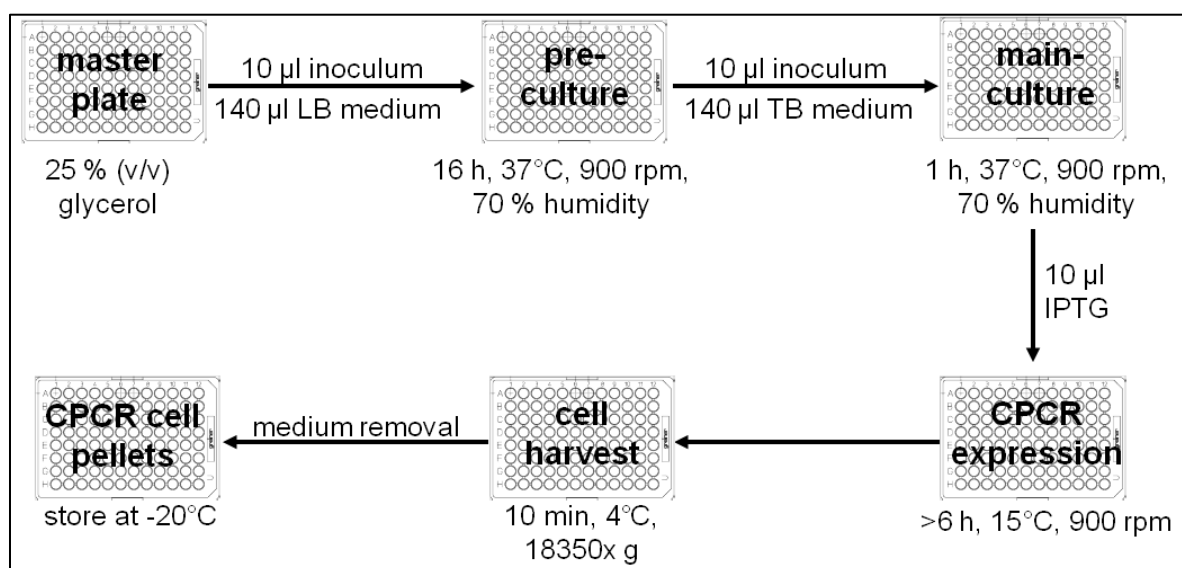


Figure 4 Standard operation procedure for CPC2R expression in multititer plate

The starting point is the master plate, a storage culture in a microtiter plate, containing the library of clones mixed with 25 % (v/v) glycerol. From this, a pre-culture was inoculated and grown overnight at  $37 \text{ }^{\circ}\text{C}$  in a flat bottom plate. The main culture was inoculated with  $10 \text{ }\mu\text{L}$  of the pre-culture in a V-bottom plate. Ideally, this culture has only little deviation in growth across the plate ( $<10 \%$ ) since stationary growth phase should be reached. The initial growth phase in TB medium at  $37 \text{ }^{\circ}\text{C}$  takes one hour and was followed by the expression phase of 6-8 hours at  $15 \text{ }^{\circ}\text{C}$  after addition of  $0.1 \text{ mol L}^{-1}$  IPTG. Expression was terminated by harvest of the cells through centrifugation. Cell pellets with overexpressed CPC2R were stored at  $-20 \text{ }^{\circ}\text{C}$  after medium removal.

To obtain lowest growth deviation throughout the microtiter plate, inoculation was carried out using a multichannel pipet. Furthermore, plates were tightly sealed with tape to prohibit influx of oxygen

promoting bacterial growth on the edges of the plate. For accurate evaluation of screening results controls were added to each plate. One control was the parent protein (e.g. wild type CPCR2) to compare the features of the variants with the basal values. Furthermore, a negative control usually carrying empty vector was integrated to check whether *E. coli* lysate interferes with detection assay. These controls appeared at least three times per plate and at best equally distributed across the plate (e.g. 2x corner, 1x center of the plate) to have an estimate on the significance of the values.

#### 2.2.4. Cell Lysis & CPCR2 Protein Purification

Fresh or frozen cell pellets from flask culture or fermentation were lysed enzymatically and mechanically by adding lysis buffer (0.05 mol L<sup>-1</sup> NaP<sub>i</sub>, 0.3 mol L<sup>-1</sup> NaCl, 1 g L<sup>-1</sup> lysozyme) in a ratio 1:4. At first cells were resuspended in lysis buffer and incubated for 1 h at 37 °C to weaken the *E. coli* cells walls by lysozyme. Afterwards, the slurry was subjected to ultra-sonication to break the cells and release CPCR2 into the medium. Here, an ultrasonic homogenizator (MS73/UW 200 with generator Sonopuls HD 200, Bandelin) at 40 % amplitude and 40 cycles was used. The treatment was done for 1 minute for three times with intermittent cooling steps on ice. Cell debris was collected by centrifuging with 2820x g for 10 minutes at 4 °C. The cleared lysate was applied for strep-tag protein purification.

For strep-tag purification in small scale (up to 5 mL lysate), gravity columns with 1 mL bed volume were applied, whereas for larger scales high-capacity columns for fast liquid protein chromatography (FPLC) were utilized. For all purifications commercial columns and chemicals were used supplied by IBA BioTAGnology (IBA BioTAGnology GmbH, Göttingen). Proteins comprising a strep-tag bind with high selectivity ( $K_d = 1 \mu\text{mol L}^{-1}$ ) to immobilized *Strep-Tactin*, an engineered streptavidin and can be eluted efficiently by addition of 2.5 mmol L<sup>-1</sup> desthiobiotin. Up to 100 nmol L<sup>-1</sup> highly pure protein can be recovered. Conveniently, no gradient of eluent has to be applied and eluent concentration in the final sample is fairly low. Hence, this method is easy to handle, mild and the purified protein is readily usable.

For FPLC strep-tag purification, parameters for appropriate CPCR2 purification were established. Here, an ÄKTA Prime (GE Healthcare) was applied equipped with a *Strep-Tactin*<sup>®</sup>Superflow<sup>®</sup> cartridge with 5 mL capacity (IBA BioTAGnology GmbH, Göttingen). For purification procedure, wash buffer (0.3 mol L<sup>-1</sup> NaCl, 0.1 mol L<sup>-1</sup> Tris pH 8.0) and elution buffer (0.025 mol L<sup>-1</sup> desthiobiotin, 0.3 mol L<sup>-1</sup> NaCl, 0.1 mol L<sup>-1</sup> Tris pH 8.0) were prepared, degassed and chilled to 4 °C. Prior application of cleared cell lysate, the system was equilibrated with wash buffer until a stable baseline was reached. Cell lysate was pumped with 4 mL min<sup>-1</sup> and the column was rinsed with wash buffer until the original baseline value was obtained (usually 4-5 column volumes). After washing, elution buffer was pumped by the FPLC device and fractions were collected. Pure CPCR2 protein was eluted

after one column volume plus dead volume of the system (ca. 1-2 mL). Flow rates and fraction sizes were adjusted according to back pressure requirements and grade of separation desired.

### 2.2.5. Cell Lysis in 96-well Plate-scale

For cell lysis in 96-well plate, a new protocol was established since ultra-sonication could not be carried out. The standard operation procedure for effective cell lysis in microtiter scale to release CPCR2 is Figure 5.

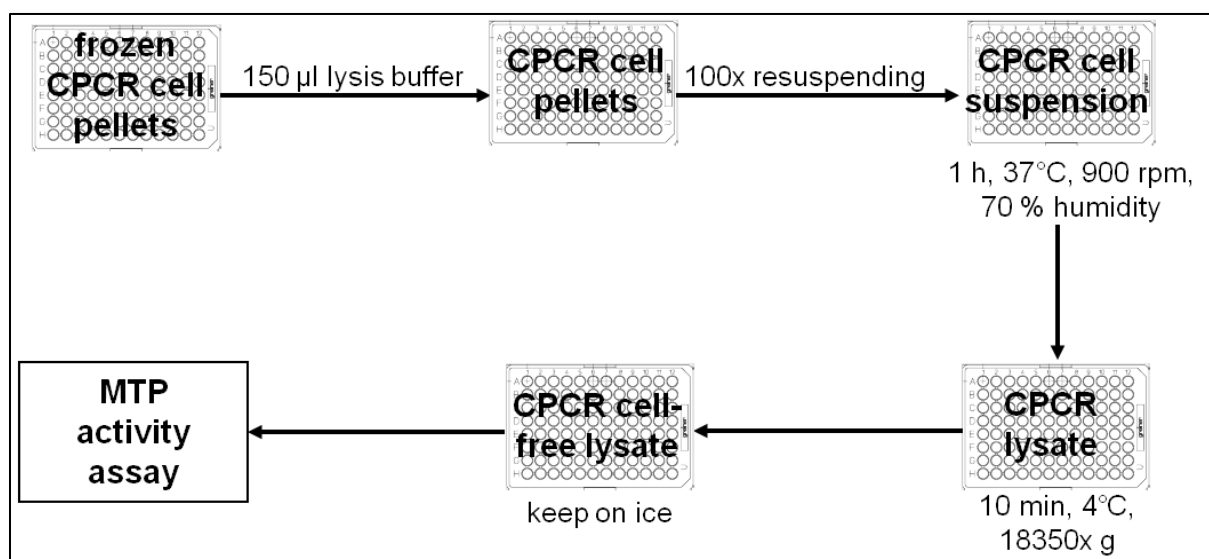


Figure 5 Standard operation procedure for cell lysis of CPCR2 in microtiter plate scale

Wells with frozen pellets were filled with 150  $\mu\text{L}$  lysis buffer (0.3 mol  $\text{L}^{-1}$  NaCl, 0.05 mol  $\text{L}^{-1}$  NaP<sub>i</sub>, pH 8.0) containing 5 g  $\text{L}^{-1}$  lysozyme for enzymatic rupture of the outer *E. coli* membrane. Resuspending and additional mechanical lysis was facilitated by pipetting 100 times 100  $\mu\text{L}$  volume with a pipetting tool specially designed to aspire 96 times with one action (liquidator96®, Steinbrenner GmbH, Wiesbaden). After incubation of one hour at 37 °C cell lysis was completed and cell debris was collected by centrifugation. The cleared lysate was kept on ice and applied to microtiter plate screening.

### 2.2.6. NADH-depletion Assay for Activity Determination in Cuvette-scale

Volumetric activity of CPCR2 was determined by initial rate measurements using an NADH depletion assay. During reduction of a ketone substrate the cofactor NADH is converted in an equimolar fashion wherein NADH absorbs light at 340 nm and NAD<sup>+</sup> does not. Consequently, the consumption of NADH is proportional to the accumulation of product accessible through the molar extinction coefficient of cofactor  $\epsilon_{\text{NADH}}$ . Hence, NADH depletion over time can directly be linked to the enzymatic unit [U], which is defined as the amount of enzyme generating 1  $\mu\text{mol}$  of product produced per minute. The relation of decrease in absorbance and enzymatic activity is given in Equation 1 known as Lambert-Beer Law.

$$A_{vol} = \frac{\frac{\Delta Abs}{\Delta t} \cdot V_{total} \cdot F}{\epsilon_{NADH} \cdot d \cdot V_{enzyme}}$$

$A_{vol}$ =	volumetric enzyme activity	[U mL <sup>-1</sup> ]
$\Delta Abs/\Delta t$ =	linear slope of absorption over time	[min <sup>-1</sup> ]
$V_{total}$ =	total assay volume	[mL]
$F$ =	dilution factor	[-]
$\epsilon_{NADH}$ =	molar extinction coefficient	[mol <sup>-1</sup> L cm <sup>-1</sup> ]
$d$ =	path length	[cm]
$V_{enzyme}$ =	volume of enzyme solution	[mL]

**Equation 1: Calculation of volumetric activity of CPCR2 in NADH depletion assay.**

In a standard NADH depletion assay for CPCR2 in 1mL scale, acetophenone served as a model substrate for ketone reduction and was used in 5 mmol L<sup>-1</sup> concentration in assay buffer (0.1 mol L<sup>-1</sup> triethanolamine (TEA), pH 8.0). Generally, 10  $\mu$ L enzyme solution was added and the reaction was initiated by 10  $\mu$ L 30 mmol L<sup>-1</sup> NADH (final concentration 0.3 mmol L<sup>-1</sup> NADH). The decrease in absorption at 340 nm was monitored over 2 minutes. CPCR2 solution has to be diluted appropriately to give a linear decrease in initial rate measurement. Most reliable values are obtained when  $\Delta Abs/\Delta t$  are ranging between 0.5-0.05 min<sup>-1</sup>. The coefficient for linear regression R<sup>2</sup> was always >0.95 indicating a high probability of linear correlation of the measured values.

In this setup, volumetric CPCR2 activity was calculated by combining the constant factors ( $V_{total} = 1$  mL,  $V_{enzyme} = 10 \mu$ L,  $d = 1$  cm,  $\epsilon_{NADH} = 6,220$  mol<sup>-1</sup> L cm<sup>-1</sup>) to one value of 16.078  $\mu$ mol. This value was simply multiplied with the obtained slope and corrected for the dilution giving the volumetric activity of CPCR2 in enzymatic units. Reference measurements were carried out omitting substrate to evaluate whether NADH is consumed by mechanisms except ketone reduction by CPCR2.

For normalization to specific CPCR2 activity, total protein concentrations of purified CPCR2 preparations were determined using Bradford assay. In this colorimetric assay, the dye Coomassie Brilliant blue G250 interacts with proteins and shifts the absorption maximum of the dye to 595 nm. Here, calibration curves using 20  $\mu$ L of bovine albumin serum standard from 0-1 mg mL<sup>-1</sup> in 980  $\mu$ L Bradford reagent were prepared fresh. CPCR2 enzyme solutions were diluted accordingly to fit in the linear range of the standard curve. To obtain specific CPCR2 activity, volumetric activity [U mL<sup>-1</sup>] was divided by measured protein concentration of the sample mg<sub>Protein</sub> mL<sup>-1</sup> giving U mg<sub>Protein</sub><sup>-1</sup>. Since in the Bradford assay, the total protein concentration is determined, purity of CPCR2 has been checked carefully by sodium dodecyl sulfate polyacrylamide gel electrophoresis (SDS-PAGE) described elsewhere.<sup>[5]</sup>

### 2.2.7. NADH-depletion Assay for Activity Determination in Microtiter Plate

The principle of activity determination of CPCR2 in multiter plate formate remains the same as outlined in section 2.2.6; however, the assay had to be down-scaled for 250  $\mu$ L volume, smaller path length and CPCR2 activities found after expression and cell lysis in microtiter plate.

For library screening, 50  $\mu\text{L}$  of enzyme solution was mixed with 150  $\mu\text{L}$  substrate in assay buffer (8.33  $\text{mmol L}^{-1}$  acetophenone, 0.1  $\text{mol L}^{-1}$  TEA, pH 8.0) in a flat bottom plate made of polystyrene. The reaction was initiated by addition of 50  $\mu\text{L}$  5  $\text{mmol L}^{-1}$  NADH in assay buffer and proper mixing. Bubbles occurring during mixing were burst applying a heat gun.

Absorption at 340 nm was recorded for 5 minutes using a multiter plate reader Infinite<sup>®</sup> M1000 equipped with the according software i-control 1.6 (Tecan Ltd.). The assay was validated using a plate containing wild type CPCR2 and empty vector controls. This analysis revealed that virtually no background activity from *E. coli* proteins consuming NADH was present. Furthermore, standard deviation in activity for the whole procedure starting from the master plate via CPCR2 expression and cell lysis was <15 %, which is considered sufficient to screen libraries for improved variants.<sup>[7]</sup>

### 2.2.8. Inactivation Assays for CPCR2

CPCR2 is prone to inactivation in the presence of aqueous-organic interphases as reported earlier.<sup>[8]</sup> Hence, there is a demand for improvement of CPCR2 stability to make the enzyme more suitable for possible industrial applications. Therefore, one goal of this thesis was the general stabilization of CPCR2 using methods of protein engineering. To analyze stability improvement of CPCR2 variants, appropriate inactivation assays had to be developed and transferred to microtiter plate format for screening.

For library screening, CPCR2 in *E. coli* cell-free lysate was exposed to elevated temperature and detergent for inactivation to identify variants with higher residual activity than wtCPCR2. These variants are, in turn, supposed to be more stable. For this, suitable conditions with respect to incubation time, applied temperature and detergent, as well as concentrations and volumes of assay components have to be discovered. Generally, parameters found suitable for screening can also be useful for subsequent characterization of improved purified CPCR2 variants.

#### 2.2.8.1. Inactivation by Temperature

Since thermostability often correlates with organic solvent stability, the behavior of wtCPCR2 at elevated temperatures was investigated. More precisely, the  $T_{50}$ -value was determined as the temperature at, which 50 % of the initial enzyme activity is lost upon thermal incubation at constant time. Inactivation of CPCR2 lysates was tested after 20 minutes incubation in a range of 30-70 °C. A typical inactivation profile for an enzyme is depicted in Figure 6. In this profile the  $T_{50}$ -value is the transition midpoint of the curve. Equation 2 shows the underlying mathematical model describing thermal enzyme inactivation.

$$\text{residual activity [\%]} = \frac{100}{1 + e^{a(T-T_{50})}}$$

**Equation 2** Mathematical model for determination of the  $T_{50}$ -value. Letter  $a$  is a fitting parameter.

A temperature close to  $T_{50}$  can be applied for thermal inactivation in screening, because changes in thermal resistance are most prominent in this regime of the curve (see Figure 6). Hence, subtle improvements in  $T_{50}$  will be reflected in strong changes in residual activity, which can be identified by screening.

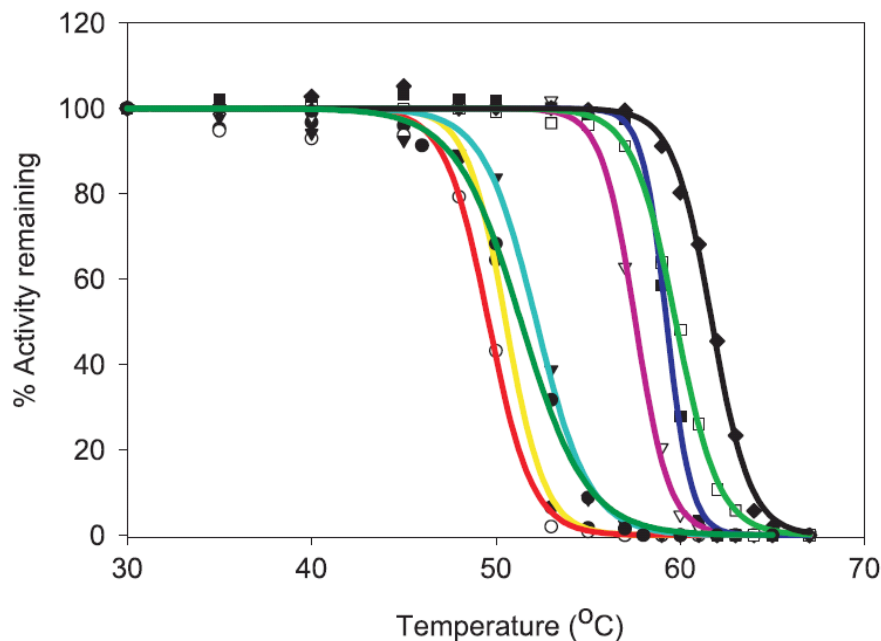


**Figure 6** Typical inactivation profile of an enzyme to determine  $T_{50}$ -value. Taken from <sup>[9]</sup>.

For CPC2 variants identified by screening,  $T_{50}$ -values were determined for purified enzyme and compared to wtCPC2 as a stability parameter.

#### 2.2.8.2. Inactivation by Detergents

As potent inactivating agents for enzymes, detergents are well known. That is why four different detergent classes were tested to identify the most appropriate candidate for inactivation of CPC2 for screening. TritonX100 as non-ionic, sodium dodecyl sulfate (SDS) as negatively charged, cetyl trimethyl ammonium bromide (CTAB) as positively charged and 3-[(3-Cholamidopropyl)dimethylammonio]-1-propanesulfonate (CHAPS) as zwitterionic detergent were tested with crude lysate of wtCPC2. Properties and applied concentrations are listed in Table 1.

**Table 1 Properties and applied concentrations of selected detergents for CPCR22 inactivation. Critical micelle concentrations (cmc) were retrieved from booklet Calbiochem® Detergents.**

Entry	Detergent	Type	cmc [mmol L <sup>-1</sup> ]	Tested concentrations [mmol L <sup>-1</sup> ]	
1	TritonX100	non-ionic	0.2-0.9	0.5	1
2	SDS	anionic	7-10	0.5	2
3	CTAB	cationic	1	0.5	5
4	CHAPS	zwitterionic	6-10	2	20

For the inactivation assay, 10 units of CPCR2 in crude *E. coli* extract were mixed in final volume of 2 mL with detergent in assay buffer (0.1 mol L<sup>-1</sup> TEA, pH 8.0) at 30 °C and 100 rpm stirring. Enzymatic activity was assayed at regular time intervals using the cuvette-scale activity assay. Measurements were carried out in duplicates.

SDS was found to inactivate CPCR2 within minutes for CPCR2 concentrations >1 mmol L<sup>-1</sup>. Hence, for the inactivation assay in multiter plate SDS was selected. Convenient SDS concentration and incubation time were established to inactivate wtCPCR2 activity in 96-well plates by 50 %. Library screening for improved detergent stability was performed under these conditions.

### 2.2.8.3. Inactivation by Organic Solvents

As fundamental drawback of CPCR2, low interfacial was identified previously.<sup>[8]</sup> To alleviate this disadvantage, stabilization of CPCR2 towards elevated temperature and a detergent is undertaken, since stabilities were shown to correlate. Screening with water-immiscible solvents directly would be an adequate approach to find variants with improved interfacial stability; however, this was not perused due to practical reasons. For instance, inactivation of CPCR2 at an interface in crude *E. coli* is not convenient due to evaporation of solvent, dissolution of plastic equipment and extended incubation times. Therefore, temperature and detergent incubation were selected due to better handling in screening.

Nevertheless, purified CPCR2 variants were tested in the presence of an aqueous-organic interphase. For the analysis of interfacial stability, cyclohexanone as second was applied. Herein, 2-3 mL of solvent-saturated buffer (0.1 mol L<sup>-1</sup> TEA, pH 8.0) was mixed with purified CPCR2 enzyme at 100 mg mL<sup>-1</sup> in standard glass vials. The aqueous phase was overlaid with the same amount of buffer-saturated cyclohexanone. The setup was incubated at room temperature and 100 rpm stirring. Residual activity was assayed at regular time intervals by application of the cuvette-scale activity assay.

In this, a first order decay of enzyme activity was assumed to describe the decrease in CPCR2 activity. The mathematical model describing the decrease of CPCR2 activity is presented in Equation 3. Usually, enzyme stabilities are compared by the half-life time ( $t_{1/2}$ ). This is the time, when 50 % of the initial enzyme activity ( $A_t = 0.5$ ) is lost and can be derived from Equation 3:  $t_{1/2} = 0.693/k$ .



$$A_t = A_0 e^{-k t}$$

**Equation 3** Mathematical model to describe the decrease of CPCR2 activity.  $A_0$  is initial activity,  $A_t$  is residual activity after the time  $t$ ,  $k$  is the deactivation constant.

Improved CPCR2 variants identified by screening were purified and tested in this system to elucidate whether interfacial stability and thermostability correlate.

### 2.2.9. Screening Strategy for Identification of More Stable CPCR2 Variants

Improved variants of CPCR2, generated by protein engineering, can be identified by comparing initial activity with residual activities after treatment with SDS and temperature. However, for libraries containing various CPCR2 variants growth behavior and expression levels may vary, which results in high deviation in the activity assay wherein volumetric activity is detected. To eliminate false negatives and false positives, activity ratios rather than absolute values are considered for comparison. The overall screening strategy is depicted in Figure 7.

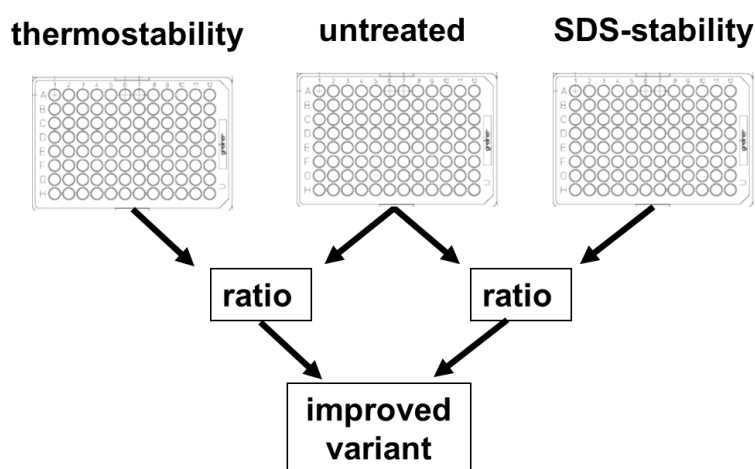


**Figure 7** Screening strategy to find CPCR2 variants with increased activity and stability.

## 2.3. CPCR2 Biotransformations

### 2.3.1. Biotransformation with Purified CPCR2 Enzyme

Biotransformations with purified CPCR2 enzyme were carried out to obtain chiral in alcohol in analytical amounts to determine conversion and enantiomeric excess. For this, CPCR2 was purified as described in 2.2.4 and used with up to 30 U in the experimental setups in 25-50 mL scale. Usually, 1 mmol L<sup>-1</sup> dithiothreitol as reducing agent and 1-5 mmol L<sup>-1</sup> NADH as cofactor were added. Organic substrates were solubilized in isopropanol, the latter serving as cosubstrate for enzyme-coupled

cofactor regeneration. This mixture was added to assay buffer (0.1 mol L<sup>-1</sup> TEA, pH 8.0) with final concentration of 2.5-5 % (v/v) isopropanol. The setup was stirred at 200 rpm for 24 hours at 30 °C.

Conversion was monitored by taking regular samples and extracting organic compounds with dichloromethane or ethylacetate. The dried organic portion was analyzed by gas chromatography. Identification of compound peaks was performed with authentic commercial standards. For some compounds, derivatization was necessary to obtain reasonable separation. Conversions were calculated by taking the peak areas of substrate and product into account (see Equation 4).

$$conversion[\%] = \frac{area_{Product}}{area_{Product} + area_{Substrate}}$$

**Equation 4 Calculation of conversion on the basis of peak areas deduced from gas chromatography**

Enantiomeric as well as diastereomeric excess (*ee* & *de*) was determined by comparing the peak areas obtained for the products. The *ee* & *de* is always calculated for the stereoisomer in excess (see Equation 5).

$$ee / de [\%] = \frac{area_{excess\ stereoisomer}}{area_{excess\ stereoisomer} + area_{non-excess\ stereoisomer}}$$

**Equation 5 Calculation of enantiomeric and diastereomeric excess on the basis of peak areas deduced from gas chromatography**

### 2.3.2. Biotransformation with Whole Cells with CPCR2-overexpressed

For analytical scale, *E. coli* cells with overexpressed CPCR2 were used for asymmetric reduction in aqueous buffer. In this, 1 g wet *E. coli* whole cells were resuspended in 25 mL buffer (0.1 mol L<sup>-1</sup> KPi, pH 6.8). As second phase methyl tert-butyl ether (MTBE) was used containing the organic substrates and serving as extraction phase for the products. For cofactor regeneration, isopropanol (5 % (v/v) or glucose (5 g L<sup>-1</sup>) were used. Samples of the organic phase were directly applied to gas chromatography to calculate conversion and *ee* with Equation 4 and Equation 5, respectively.

### 2.3.3. Biotransformation in Neat Substrates

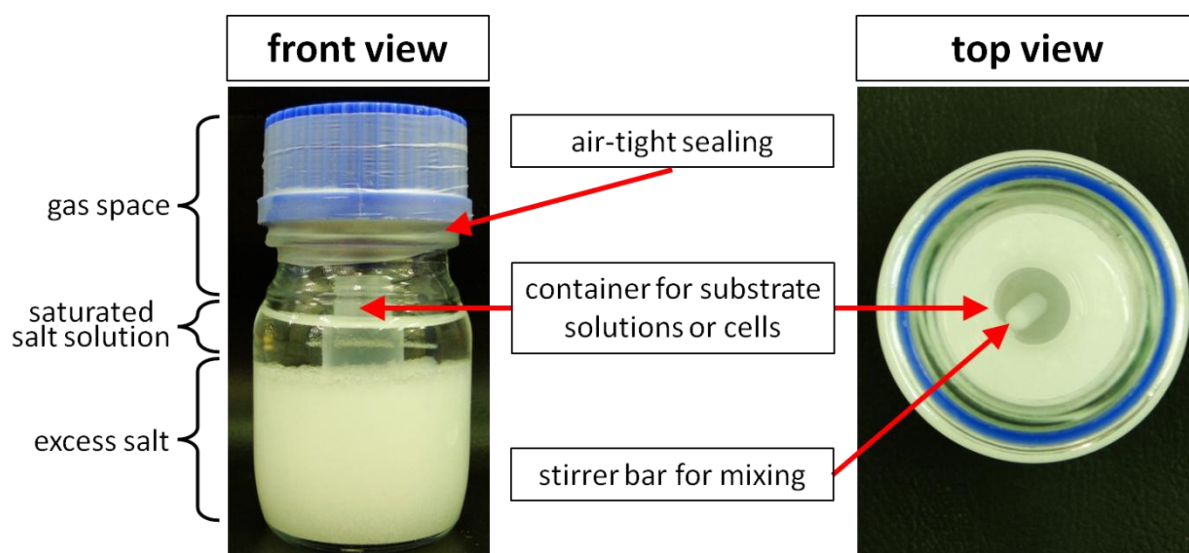
Asymmetric ketone reduction was carried out with *E. coli* cells containing overexpressed CPCR2 in neat organic substrates. Additionally, alcohol dehydrogenases from *Lactobacillus brevis* (LbADH) and *Rhodococcus erythropolis* (ReADH) overexpressed in *E. coli* were investigated in this system. For this, the cells have to be completely dried, which is facilitated by lyophilization. This was carried out for at least 48 hours in a lyophilizer (Alpha 1-2 LD plus, Christ ) at default settings. The organic substrates for biotransformation were dried with molecular sieves for at least 48 hours.

**Table 2** Composition of saturated salt solutions and water activity at 30 °C, taken from <sup>[10]</sup>.

salt		Salt amount [g]	Water [mL]	$a_w$ [%]
Potassium Acetate	$K(CH_3COO)$	200	65	22.4
Magnesium Nitrate	$Mg(NO_3)_2$	200	30	51.4
Sodium Chloride	NaCl	200	60	75.4
Potassium Chloride	KCl	200	80	83.6
Potassium Nitrate	$KNO_3$	200	75	92.3

Water activity ( $a_w$ ) was established by equilibrating dry substrates and dry *E. coli* whole cells in the presence of saturated salt solutions via the vapor phase. Certain salts with fixed humidity points ( $a_w$ -values) at a certain temperature according to Greenspan were used.<sup>[10]</sup> Saturated salt solutions of fixed  $a_w$  were composed according to Table 2.

For equilibration to fixed  $a_w$ -values portions of the compositions from Table 2 were placed in a 100 mL screw cap bottle and a container plus stirrer bar with dry substrates or cells was pressed into the excess solid salt (see Figure 8). The sealing was air-tight to prevent evaporation of the substrate solutions or influx of humidity from the environment.

**Figure 8** Setup for equilibration to fixed  $a_w$ -values of substrate solutions and cells with saturated salt solutions

For complete equilibration, substrate solutions and cells were incubated in this setup for at least 48 hours at 30 °C. Liquid substrates were stirred at 200 rpm and solid cells were mixed applying a spatula.

## 2.4. Computational Methods

### 2.4.1. DNA & Protein Design and Sequence Analysis

For design of DNA constructs and primers as well as analysis of DNA-sequencing results, the software packages ApE<sup>®</sup> plasmid editor version 2.0.15 (by M. Wayne Davis) and BioEdit version 7.0.9 (by Tom Hall) were applied. Structural analysis of enzymes was done with PyMol software version 0.99rc6 (DeLano Scientific).

### 2.4.2. DNA & Protein Alignments

For comparison of DNA and protein sequences, alignments were generated using the standard multiple sequence alignment tool CLUSTAL W imbedded in BioEdit.<sup>[11]</sup> Searching DNA and protein sequences in online databases was performed using basic local alignment search tool (BLAST) with default settings.<sup>[12]</sup> Structural alignments were performed using PyMol version 0.99rc6 (DeLano Scientific).

### 2.4.3. Data Analysis and Fitting

Data analysis was performed using Microsoft Professional Plus 2010 Excel<sup>®</sup> with a built-in software Solver. Additionally, data fitting software SimFit (version 6.2, release 2) was utilized.<sup>[13]</sup>

## 2.5. References

- [1] W. Wang, B. A. Malcolm, *Biotechniques* **1999**, *26*, 680-682.
- [2] M. T. Reetz, D. Kahakeaw, R. Lohmer, *Chembiochem* **2008**, *9*, 1797-1804.
- [3] a) W. M. Patrick, A. E. Firth, J. M. Blackburn, *Prot. Eng.* **2003**, *16*, 451-457; b) A. E. Firth, W. M. Patrick, *Nuc. Ac. Res.* **2008**, *36*, W281-285.
- [4] H. Inoue, H. Nojima, H. Okayama, *Gene* **1990**, *96*, 23-28.
- [5] J. Sambrook, D. Russell, W., *Molecular Biology: A Laboratory Manual, Vol. 1-3*, 3 ed., CSH Press, Cold Spring Harbor, **2000**.
- [6] M. Bhattacharjee, *Doctoral thesis*, RWTH Aachen, **2006**.
- [7] K. L. Tee, U. Schwaneberg, *Angew. Chem. Int. Ed.* **2006**, *45*, 5380-5383.
- [8] A. van den Wittenboer, T. Schmidt, P. Muller, M. B. Ansorge-Schumacher, L. Greiner, *Biotechnol. J.* **2009**, *4*, 44-50.
- [9] J. Hao, A. Berry, *Protein Eng. Des. Sel.* **2004**, *17*, 689-697.
- [10] L. Greenspan, *J. Res. Nat. Bureau Stand. - A. Phys. Chem.* **1977**, *81A*, 89-96.
- [11] Larkin M.A., Blackshields G., Brown N.P., Chenna R., McGettigan P.A., McWilliam H., Valentin F., Wallace I.M., Wilm A., Lopez R., Thompson J.D., G. T.J., H. D.G., *Bioinformatics* **2007**, *23*, 2947-2948.
- [12] S. F. Altschul, T. L. Madden, A. A. Schaffer, J. Zhang, Z. Zhang, W. Miller, D. J. Lipman, *Nuc. Ac. Res.* **1997**, *25*, 3389-3402.
- [13] H. G. Holzhutter, A. Colosimo, *Comput. Appl. Biosci.* **1990**, *6*, 23-28.

## 3 Results & Discussion

### 3.1 Who's who? – Allocation of Carbonyl Reductase Isoenzymes from *Candida parapsilosis* by Combination of Bio- and Computational Chemistry

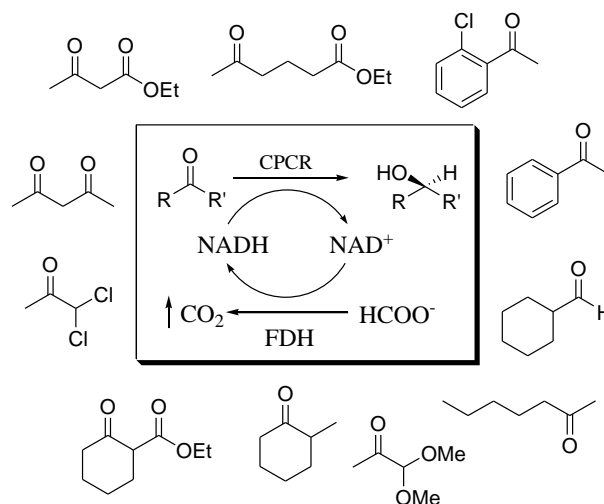
#### 3.1.1 Abstract

The identification of a single enzyme responsible for an interesting catalytic property remains challenging especially when isoenzymes are present in the host organism. In this work, we show the allocation of two carbonyl reductase isoenzymes from *Candida parapsilosis* (CPCR1 & CPCR2) by a rational combination of classical biochemical methods and computational chemistry. By building homology models and comparison of the substrate binding pockets, distinctive indicator substrates were predicted and tested with the single enzyme candidates. Herein, a previously described carbonyl reducing activity on structurally diverse substrates detected in *Candida parapsilosis* lysate could be undoubtedly assigned to only one of the enzymes (CPCR2). Likewise, a complementary substrate scope of the two carbonyl reductases could be excluded

#### 3.1.2 Introduction

Years ago, carbonyl reductase from *Candida parapsilosis* (CPCR; E.C.1.1.1.1) was described as a suitable catalyst for the asymmetric reduction of various carbonyl compounds, such as aliphatic and aromatic ketones and diketones, keto acids, esters, and amides (see Scheme 1).<sup>[1]</sup> Apart from the large substrate range and high stereoselectivity, it is characterized by high stability in the presence of low molecular weight alcohols, such as isopropanol<sup>[2]</sup>, and a preference for NADH as cofactor instead of the more expensive and less stable NADPH associated with many other alcohol dehydrogenases.<sup>[1a]</sup> As a result, regeneration of the essential cofactor can be achieved either by providing isopropanol as co-substrate<sup>[1a, 1b, 3]</sup> or by use of established co-catalysts such as formate dehydrogenase (FDH; 1.2.1.2) from *C. boidinii*.<sup>[4]</sup> All these features imply a special utility of CPCR for organic synthesis.

Nevertheless, application in research as well as industrial production is only limited today. This can probably be explained by the uncertainties regarding the biocatalyst's identity and thus its precise and reproducible synthetic use: Two preparations are currently commercially available, isolated either from the native production strain *C. parapsilosis* (Codexis, USA), or from *Escherichia coli* as recombinant host organism (X-zyme, Germany). However, the preparations reveal clear differences in their biochemical features and do not match those of the data defining the original target enzyme.<sup>[1a, 5]</sup>



**Scheme 1** Sample compounds from the substrate range of carbonyl reductase from *Candida parapsilosis* DSMZ 70125

This study describes the elucidation of the molecular identity of CPR isoenzymes by the interdisciplinary approach of combining classical biochemical methods and methods from computational chemistry. It involves a stepwise identification of two possible enzyme candidates with their amino acid sequences, the establishment of active site molecular models with subsequent application to the prediction of substrate binding patterns and a final discrimination of enzymes by experimental investigation of activity towards selected indicator substrates.

### 3.1.3 Experimental

If not stated otherwise all buffer salts, media ingredients, and chemicals were of highest available quality and used without further purification.

#### 3.1.3.1 Preparation of CPR from *C. parapsilosis*

According to the protocol of Peters *et al.*<sup>[1a]</sup> *C. parapsilosis* DSMZ 70125 was cultivated in shake flasks (2 L, 30 °C) using yeast extract (0.3 % (w/v) ), malt extract (0.3 % (w/v) ), peptone (0.5 % (w/v) ), and glucose (1.0 % (w/v) ) for preculture, and glycerol (2 % (w/v) ), yeast extract (1 % (w/v) ),  $\text{KH}_2\text{PO}_4$  (0.1 % (w/v) ),  $\text{Na}_2\text{HPO}_4$  (0.1 % (w/v) ), and  $(\text{NH}_4)_2\text{SO}_4$  (0.12 % (w/v) ) for main culture (pH 4.5).<sup>[1a]</sup> Cells were harvested by centrifugation and disintegrated in a wet bead mill (4 °C, 30-40 % (w/v) cells in aqueous buffer (0.1 mol  $\text{L}^{-1}$  TEA, 0.1 mmol  $\text{L}^{-1}$  dithiothreitol (DTT), 0.1 mmol  $\text{L}^{-1}$  phenylmethanesulfonylfluorid (PMSF, AppliChem, Darmstadt, Germany), pH 7.5), bead diameter 0.5 mm [ratio bead/cell suspension 2 : 1]. Cell debris was removed by centrifugation (4 °C) and the resulting crude extract was purified as described by Peters *et al.*<sup>[1a]</sup> This included precipitation (4 °C) by adding an aqueous solution of PEG 4,000 (50 % (w/v) ), 0.1 mol  $\text{L}^{-1}$  TEA, 0.1 mmol  $\text{L}^{-1}$  DTT, 0.1 mmol  $\text{L}^{-1}$  PMSF, pH 7.5) to the cell debris to a final concentration of 2.5 % (w/v), centrifugation (4 °C), and subsequent increase of the PEG concentration in the supernatant to 17 % (w/v). The precipitated protein was collected by centrifugation (4 °C), dissolved in aqueous buffer (0.1 mol  $\text{L}^{-1}$  TEA, pH 7.5) and separated on an anion exchanger (Macro-Prep High Q, Bio-Rad, München,

Germany; 4 °C; 0.1 mol L<sup>-1</sup> TEA, pH 7.5, 0.1 mmol L<sup>-1</sup> DTT, 5 % (v/v) isopropanol, 1 mol L<sup>-1</sup> NaCl, pH 7.5). CPCR eluted at a NaCl concentration of 260 mol L<sup>-1</sup> (pH 7.5), and was concentrated by ultrafiltration (size exclusion 30 kDa, 4 °C, 3 bar). Protein for sequencing was additionally subjected to affinity chromatography (5'AMP-Sepharose 4B; Sigma-Aldrich, 0.01 mol L<sup>-1</sup> TEA, pH 7.0, 1 mmol L<sup>-1</sup> DTT, 3 mmol L<sup>-1</sup> NAD<sup>+</sup>) and gel filtration (Sephadex G 75, Amersham Pharmacia-Biotech, Freiburg, Germany). Protein concentration was measured in a spectrophotometer (Beckmann DU, Fullerton, CA) by use of Bio-Rad protein assay according to the manufacturers' advice.

### 3.1.3.2 Biochemical Characterization of CPCR1

Purity of enzyme preparations and protein size were determined by SDS-PAGE according to Laemmli<sup>[6]</sup> (1.5 mol L<sup>-1</sup> Tris-HCl, pH 8.8, 10 % ((w/v) ) bisacrylamide, 10 % (w/v) SDS) using Mark12 wide-range protein standard (Novex, San Diego, CA), bovine serum albumin (BSA, 66 kDa), and white egg albumin (WEA, 40 kDa) as size standards. The proteins were stained with an aqueous solution of Coomassie brilliant blue (0.05 % (w/v) Coomassie R250, 30 % (v/v) methanol, 10 % (w/v) acetic acid). For sequence analysis, the separated, unstained proteins were blotted on a PVDF membrane and stained with an aqueous solution of Amidoblack (40 % (v/v) ethanol, 10 % (v/v) acetic acid, 0.1 % (w/v) amidoblack). In that case, the pre-stained "low range" marker (Bio-Rad) was used as size standard for SDS-PAGE. The target proteins were cut out, partly digested with the endoproteases Lys-C and Glu-C (Roche Diagnostics), and sequenced by Edman degradation using an Automated Sequencer 477A with on-line HPLC 120A (Applied Biosystems, München).<sup>[7]</sup> The sequences were aligned by using MAFFT with default settings.<sup>[8]</sup>

The activity of CPCR was determined by measuring cofactor or substrate consumption in a UV/Vis spectrophotometer (340 nm; Microplate reader Spectramax Plus 340, Molecular Devices, Ismaning, Germany), with HPLC [Beckmann Coulter System Gold (Beckmann, München, Germany), NUCLEOSIL 100-5 C<sub>18</sub> (250 x 4 mm), 40 °C, 60 % H<sub>2</sub>SO<sub>4</sub> (pH 3), 40 % acetonitrile at 0.6 mL min<sup>-1</sup> as mobile phase], or GC [HP 5890 Series II (Walbronn, Germany) equipped with FS-FFAP capillary column (25 m, 250 µm; CS-Chromatographie Service GmbH, Langerwehe, Germany), N<sub>2</sub> 3.8 mL min<sup>-1</sup>, injector 220 °C, split 1:50, 40 °C (4 min), 100 °C (20K min<sup>-1</sup>), 180 °C (30K min<sup>-1</sup>), 180 °C (7 min); internal standard decane; typical t<sub>R</sub> values: acetone = 1.6 min, isopropanol = 2.2 min, decane = 2.9 min, acetophenone = 10.1 min, and phenylethanol = 11.0 min], respectively. 1 U is defined as the amount of enzyme that catalyzes the reduction of 1 µmol ethyl 5-oxohexanoate per min in aqueous solution (0.1 mol L<sup>-1</sup> TEA, pH 7.0, 2.5 mmol L<sup>-1</sup> NADH+H<sup>+</sup>, 10 mmol L<sup>-1</sup> substrate, 37 °C). To measure substrate consumption, NADH+H<sup>+</sup> regeneration was performed by addition of isopropanol.

To determine  $T_{opt}$  and  $pH_{opt}$  (activity optima for reduction), buffered CPCR solutions (0.1 mol L<sup>-1</sup> TEA, pH 7.0) were added to solutions of ethyl 5-oxohexanoate at different temperatures (25-52 °C, pH 7.0)

or pHs (6-8, T = 37 °C) and measured for initial NADH+H<sup>+</sup> consumption, as described in the previous paragraph.

### 3.1.3.3 Cloning and Sequencing of CpSADH and CPCR1

Genomic DNA was extracted from *C. parapsilosis* DSMZ 70125 cells by dissolving cell walls with Zymolase 100T (37 °C, 1 h, 0.9 mol L<sup>-1</sup> sorbitol, 0.1 mol L<sup>-1</sup> EDTA, 0.05 % (v/v) mercaptoethanol), the cell membranes with SDS (1 % (w/v) ) and the proteins with protease K (10 mg mL<sup>-1</sup>, 60 °C, 30 min, reaction stopped by addition of 0.5 mol L<sup>-1</sup> potassium acetate). The DNA was precipitated with ethanol (100 %, 2 volumes, -20 °C, 1-2 days). RNA was digested in the resuspended DNA (10 mmol L<sup>-1</sup> Tris-HCl, pH 7.5, 1 mmol L<sup>-1</sup> EDTA, pH 8.0), with RNase (30 min, 37 °C), and the DNA was finally precipitated with isopropanol (100 %). The gDNA was twice washed with ethanol (70 %), dried, resuspended in buffer (10 mmol L<sup>-1</sup> Tris-HCl, pH 7.5, 1 mmol L<sup>-1</sup> EDTA, pH 8.0), and stored at -20 °C.

The genomic DNA libraries of *C. parapsilosis* were prepared as described in the user's manual of the Universal Genome Walker kit (BD Biosciences, Clontech, Heidelberg, Germany). Four libraries were constructed with the genomic DNA of *C. parapsilosis* by digesting with EcoRV, DraI, StuI and PvuII. The kit also provides human genomic DNA as positive control library that has to be digested with PvuII, and a pre-constructed human genome-walker library. Each of the digested DNA libraries was ligated to the genome walker adaptor. The digested and ligated libraries were stored at -20 °C until use. For long-term storage, the libraries may also be kept at -80 °C.

The gene coding for CpSADH was amplified by conventional PCR from the DraI-digested genomic DNA library of *C. parapsilosis* DSMZ 70125 strain according to the instruction manual of (BD Biosciences). Primers were deduced from published sequences.<sup>[6b]</sup> An N-terminal His<sub>6</sub>-tag was introduced into the forward primer in order to facilitate easy purification. The fragment was ligated into the multiple cloning site of pET26b+ (Novagen) and the resultant expression vector pET26b+CpSADH28his was transformed into *E. coli* BL21(DE3).

### 3.1.3.4 Measurement of Activity on Indicator Substrates

Comparative activity measurements of CPCR preparations were performed on a Cary 300 UV/Vis-spectrophotometer (340 nm; Varian). All substrates were used in 5 mmol L<sup>-1</sup> in triethanolamine buffer (0.1 mol L<sup>-1</sup>, pH 8.0). Absorption was monitored at room temperature for 2 min. CPCR1 was provided from commercial source (X-zyme, Düsseldorf, Germany). CpSADH was recombinantly expressed in *E. coli* and used as crude extract. All measurements were performed in triplicate.



### 3.1.3.5 Computational Analysis

Homology modeling of the structure of two CpCR isoenzymes was performed using YASARA Structure Version 11.6.16 with default settings (PSI-BLAST iterations:<sup>[10]</sup> 6, E value cutoff: 0.5, templates: 5, OligoState: 4).<sup>[11]</sup> A position-specific scoring matrix (PSSM)<sup>[12]</sup> was used to score the obtained template structures. Four X-ray templates were selected for modeling the CpCR1 structure (349aa): Yeast ADH I from *S. cerevisiae* with bound trifluoroethanol (347 residues with quality score 0.522, PDB ID 2HCY), ADH from *Brucella melitensis* (341 residues with quality score 0.590, PDB ID 3MEQ), ADH from *Bacillus stearothermophilus* Strain Lld-R (339 residues with quality score 0.560, PDB ID 1RJW), ADH from *Pseudomonas aeruginosa* with bound ethylene glycol (341 residues with quality score 0.555, PDB ID 1LLU). The best scoring model (Z score -0.73) was a hybrid model built on X-ray structure 2HCY and 1RJW and consisted of a dimer of dimers with two bound Zinc ions, one NAD(H) and one trifluoroethanol per monomer.

Five X-ray templates were selected for the modeling of CpSADH structure (336aa): N249Y Mutant of ADH from *Sulfolobus tokodaii* Strain7 (347 residues with quality score 0.550, PDB ID 2EER), SsADH from *Sulfolobus solfataricus* (347 residues with quality score 0.547, PDB ID 1NTO), SsADH N249Y/W95I (340 residues with quality score 0.541, PDB ID 3I4C), SsADH (347 residues with quality score 0.534, PDB ID 1JVB) and SsADH complexed with NAD(H) and 2-ethoxyethanol (347 residues with quality score 0.524, PDB ID 1R37). The best scoring model (Z score -1.96) was built on X-ray structure 1R37 consisting of a dimer of dimers with two bound Zinc-ions, NAD(H) and 2-ethoxyethanol per monomer.

For the docking studies, one close dimer of the modeled structures was used, all energy calculations were performed using AMBER03<sup>[13]</sup> for the protein and GAFF<sup>[14]</sup> with AM1/BCC charges<sup>[15]</sup> for the substrates. All residues within 15 Å radius of the bound alcohol were free to move. The active site above the bound NAD(H) is located at the interface of the two Rossmann-fold monomers. The Zn-bound alcohol-ligand in the active site of the homology models was manually replaced by the respective substrates in their keto form and relaxed using cycles of steepest-descent minimization and simulated annealing MD<sup>[5b]</sup> from 298K to 5K. Reference calculations for binding energies were performed using the substrates in a water box and the apo-enzyme with water coordinated to the catalytic Zn<sup>2+</sup>. The stabilization energies of the substrates in a catalytic orientation were calculated by subtracting the solvation energy for the substrate from the energy in the Zn<sup>2+</sup> bound state and the energy difference of an active-site subset consisting of 10 residues lining the binding pocket in the substrate-bound state versus the apo-structure with bound water. (CpCR1: Thr 101, Ala 105, Trp 110, Trp 148, Tyr 175, Leu 326, Tyr 350, Val 351, Phe B337, Val B341 ; CpCR2: Ser 46, Val 50, Leu 55, Trp 116, Leu 119, Leu 262, Phe 285, Trp 286, Gly B272, Leu B276)

### 3.1.4 Results and Discussion

#### 3.1.4.1 Biochemical and Molecular Characteristics of CPCR Preparations

For systematic investigation, the native host *C. parapsilosis* DSMZ 70125 was cultivated under the same conditions as in the original work on CPCR.<sup>[1a]</sup> Accordingly, partially purified lysate from this culture revealed a substrate spectrum and relative enzymatic activities similar to the reported data (see Table S1, 3.1.6), thus indicating the presence of the desired enzyme. A NADH-dependent protein with distinct carbonyl reducing activity could be purified to homogeneity.

**Table 1 Measured and published biochemical features of carbonyl reductase from *Candida parapsilosis*.**

Feature	CPCR this work*	Codexis-CPCR	CPCR published	CpSADH
Weight/subunit [kDa]	≈40	≈40	67.5	36
pH opt. (reduction)	6.0	5-5.5	7.8-8.0	5.5-6.5
Temp. opt. (reduction) [°C]	48	43-47	36-40	50

\*Data was measured by M. Bhattacharjee (PhD thesis 2006, RWTH Aachen University)

Nevertheless, molecular weight, pH optimum and temperature optimum of the isolated protein were at odds with the published biochemical data of original CPCR (Table1). The molecular weight of one subunit of the homodimeric CPCR was originally reported as 67.5 kDa,<sup>[1a]</sup> whereas the purified protein found in this study was only 40 kDa. Proteins at both sizes, 67.5 kDa and 40 kDa, respectively, were found in a SDS-PAGE analysis of partly purified *Candida* lysate and a comparable commercial CPCR preparation (Codexis, USA, Figure S1, 3.1.6), but a direct allocation of any of these proteins to carbonyl reduction activity was not possible. The temperature and pH optima for ethyl 5-oxo-hexanoate reduction of both partially purified CPCR and the dialyzed commercial preparation from Codexis were found at 43-47 °C and 5.5, respectively, not at 36-40 °C and 7.8-8.0 as reported by Peters *et al.*<sup>[1a, 5a]</sup> This cannot be related to a failure in purification since both preparations revealed distinct CPCR activity.

The obtained biochemical data indicate that, despite the identical expression, purification and very similar substrate range, the carbonyl reducing protein investigated in this study was not identical to the CPCR preparation described by Peters *et al.*<sup>[1a]</sup> However, it was similar to the CPCR preparation traded by Codexis. Surprisingly, the biochemical properties also complied with a recombinantly expressed NADH-dependent secondary alcohol dehydrogenase (CpSADH) isolated from *C. parapsilosis* type strain IFO 1396 (Table 1).<sup>[16]</sup> The reported substrate range of this enzyme lies within the substrate range of CPCR preparations, but as the authors investigated only a few compounds, it could not be deduced whether it covers the complete range.

In order to elucidate the relation between the here purified carbonyl-reducing protein and CpSADH, the genes coding for the isolated enzymes were identified and compared to each other.

```

CPCR1+preseq 1  MPIGSTHFFHFKSFIRSIAVNKVTTIPIKAFTTTTTKT
ADH1-CanAl 1  MS-----
ADH2-CanAl 1  M-----
ADH1_Yeast 1  M-----

39  KTKITTTTNSFISTMPEIPKTKAVVFETSGGKLEYKDIPVVPKPKSNET
3  -----EQIPKTKAVVFDTNGGQLVYKDYPVPTPKPNEL
2  -----SVPTTQKAVIFETNGGKLEYKDIPVVPKPKANEL
2  -----SIPETQKGVIFYESHGKLEYKDIPVVPKPKANEL

90  LINVKYSGVCHTDLHAWKGDWPLDTKLPLVGGHEGAGVVVMGDNVKGWEI
37  LIHVKYSGVCHTDLHARKGDWPLATKLPLVGGHEGAGVVVMGENVKGWKI
35  LINVKYSGVCHTDLHAWKGDWPLATKLPLVGGHEGAGVVVALGENVKGWV
35  LINVKYSGVCHTDLHAWHGDWPLPVKLPLVGGHEGAGVVVMGENVKGWKI

141  GDYAGIKWLNSGCLNCFCEQGAEPNCPQADLSGYTHDGSFEQYATADAVQ
88  GDFAGIKWLNSGCMSCFEQQGAEPNCGEADLSGYTHDGSFEQYATADAVQ
86  GDYAGIKWLNSGCLNCEYCQSGAEPNCAEADLSGYTHDGSFQYATADAVQ
86  GDYAGIKWLNSGCMACEYCELGNESNCPHADLSGYTHDGSFQYATADAVQ

192  AARIPKNADLAKAAPILCAGVTVYKALKTAQLKAGEWVCISGAGGGLGSLA
139  AAKIPAGTDLANVAPILCAGVTVYKALKTADLAAGQWVAISGAGGGLGSLA
137  AARIPAGTDLANVAPILCAGVTVYKALKTAELEAGQWVAISGAGGGLGSLA
137  AAHIPQGTDLAQVAPILCAGITVYKALKSANLMAGHWVAISGAGGGLGSLA

243  IQYAIAMGYRVIGIDGGAEKGEYLKSLGAEAYIDFTKEKDIVEAVKKATNG
190  VQYARAMGLRVVAIDGGDEKGEFVKSLGAEAYVDFTKDKDIVEAVKKATDG
188  VQYAKAMGYRVLAIDGGEDKGEFVKSLGAETFIDFTKEKDIVEAVKKATNG
188  VQYAKAMGYRVLGIDGGEKEELFRSIGGEVFIDFTKEKDIVGAVLKATDG

294  GPHGVINVSVSEKAINQSVEYVRPLGKVVLVGLPAGSKVVAPVFDAVVKSI
241  GPHGAINVSVSEKAIDQSVEYVRPLGKVVLVGLPAHAKVTAPVFDAVVKSI
239  GPHGVINVSVSERAIGQSTEYVRTLGKVVLVGLPAGAKISTPVFDAVIKTI
239  GANGVINVSVSEAAIEASTRYVRANGTTVLVGMPAGAKCCSDVFNQVVKSI

345  EIKGSYVGNRKDTQEALDFFARGVNCOIKIVGLSELPEVFKLMEEGKILG
292  EIKGSYVGNRKDTAEALDFSRGLIKCPIKIVGLSDLPEVFKLMEEGKILG
290  QIKGSYVGNRKDTAEALDFTRGLIKCPIKIVGLSELPEVYKLMEEGKILG
290  SIVGSYVGNRADTREALDFFARGLVKSPIKVVGLSTLPEIYEKMEKQIVG

396  RYVLDTSK 403
343  RYVLDTSK 350; MAFFT alignment score: 238
341  RYVLDNDK 348; MAFFT alignment score: 261
341  RYVVDTSK 348; MAFFT alignment score: 233

```

**Figure 1** Alignment of the complete amino acid sequence from the purified carbonyl reductase protein (CPCR1) with the amino acid sequences of ADH 1 and ADH 2 from *C. albicans* and ADH1 from bakers' yeast. Partial sequences derived by Edman degradation are highlighted in grey and the N-terminal presequence is underlined. Bold letters indicate identical amino acids. Edman degradation and retrieval of the CPCR1-DNA sequence was performed and published by M. Bönitz-Dulat (PhD thesis, 2001, RWTH Aachen University).

### 3.1.4.2 Identification and Analysis of the Amino Acid Sequence

The homogeneously purified carbonyl-reducing protein was digested and separated into six distinct pieces. In order to identify the N-terminal amino acid sequences, the resulting fragments and the complete protein were submitted to Edman degradation<sup>[17]</sup> on an Automated Sequencer 477A with online HPLC according to Baumann.<sup>[7]</sup> All fragments revealed an overall sequential homology of 82 % to the known alcohol dehydrogenase 2 and 81 % to alcohol dehydrogenase 1 from *Candida albicans*. According to this homology, the fragments were aligned in their natural order (Figure 1) and used to design degenerate primers for gene amplification.

Starting from a primer aligning within the internal nucleic acid sequence coding fragment 3, the complete open reading frame (*orf*) for expression of the 40 kDa protein was identified in a two-step molecular walking process. The *orf* consists of 1212 nucleic acid bases and codes for 403 amino acids (Figure 1). Surprisingly, the N-terminal sequence determined by Edman degradation revealed that the active enzyme is 55 amino acids shorter than deduced from the coding sequence and starts with a proline instead of methionine.

This implies that a processing of the protein takes place in the host organism, although typical sequential cleaving signals could not be identified. As expected from the sequencing of protein fragments, the protein was highly homologous to ADH 1 from *C. albicans* (73 %), and also revealed a strong homology to ADH 2 from the same organism (71 %). However, these homologies exclusively lay in the protein part coding the active enzyme; while no homologies with any known alcohol dehydrogenase could be found for the N-terminal extension. In accordance with that observation, difficulties experienced with the heterologous expression of carbonyl reductase when only the partial sequence coding the active protein was used (data not shown) imply that the function of the N-terminal extension sequence lies in protein folding rather than in activity. Recently, shotgun sequencing followed by expression profiling of *Candida parapsilosis* CDC317 revealed the presence an almost identical nucleotide sequence as retrieved in this work (gene bank accession: HE605207.1 contig 006139).<sup>[18]</sup> Automated annotation yielded the CPCR protein sequence (gene bank accession: CCE44033.1). The coding sequence for CpSADH was also found in the same strain (gene bank accession: HE605205.1 contig 005807).<sup>[18]</sup>

The protein coded by the complete nucleic acid sequence has a calculated molecular weight of  $\approx 43.1$  kDa, the calculated weight of the active part of that protein is  $\approx 37.0$  kDa. Both do not comply with the molecular weight of 67.5 kDa reported for CPCR by Peters *et al.*<sup>[1a]</sup>, but they are in good accordance with the findings on the molecular weight of CpSADH ( $\approx 36$  kDa) and the carbonyl reducing protein purified here. This last protein will hence be designated CPCR1 ( $\approx 40$  kDa).

However, despite the compliance between the biochemical data determined for CPCR1 and CpSADH, only little homology (31.5 %) was found between the amino acid sequences of these enzymes. Instead, the active part of the amino acid sequence of CPCR1 is largely identical with the sequence of a commercial recombinant CPCR (personal communication, Shukrallah Na'amnieh, X-zyme). Differences can only be found at the N-terminus, since the commercial CPCR is expressed as an N-terminal fusion protein.

Nevertheless, running a PCR with primers generated from the amino acid sequence of CpSADH on the genomic DNA of *C. parapsilosis* DSMZ 70125 revealed that CpSADH is present in this host organism as well. It is known from *Saccharomyces cerevisiae* that yeast organisms can be hosts of

alcohol dehydrogenase isoenzymes.<sup>[19]</sup> The expression of these isoenzymes strongly depends on O<sub>2</sub> availability, ethanol content, and cell age.<sup>[20]</sup> For example, under anaerobic conditions, four NADH-dependent alcohol dehydrogenases and a NADPH-dependent one are expressed in parallel.<sup>[21]</sup> Also for *Candida maltose*, different ADH isoenzymes expression levels could be detected depending on the carbon source used.<sup>[22]</sup> Against this background, a contribution of two distinct enzymes to the reported CPCR activity would be possible.<sup>[1a]</sup>

In order to allocate CPCR activity either to CPCR1 or to CpSADH or rule both of them out, a novel strategy involving computational chemistry was applied. Homology modeling and modeling of substrate binding patterns were used to identify differences in the substrate range of both enzymes. Various CPCR preparations were then subjected to experimental verification.

**Table 2 Results from sequence alignment and modeling parameters.**

Enzyme	CPCR1	CpSADH
X-ray template	2HCY (2.44 Å)	1R37 (2.3 Å)
Organism	<i>S. cerevisiae</i> ADH1	<i>S. solfataricus</i> ADH
Cofactor	NADH	NADH
Ligand	2,2,2-trifluoroethanol	2-ethoxyethanol
alignment score	1383 (99 %)	441 (97 %)
sequence identity [%]	74.9	34.3
sequence similarity [%]	84.1	53.5
overall Z score	-0.729 (good)	-1.961 (satisfactory)

### 3.1.4.3 Computational analysis of CPCR Structure and Binding of Substrates

Based on the sequences of CPCR1 and CpSADH, two homology models were constructed applying YASARA Structure Version 11.6.16 software<sup>[11]</sup> (see Figure S2, 3.1.6). Details on chosen templates, sequence identities and similarities are given in Table 2. According to the 3D-quality assessment (Z score) of the modeled structures (see Table 2) the models are rated “good” in the case of CPCR1 and “satisfactory” for CpSADH.

A look into the substrate binding pocket of the two models reveals that the volume available for substrate binding is much larger in CpSADH than in CPCR1 (525 Å<sup>3</sup>) and in CPCR1 (300 Å<sup>3</sup>, see Figure 2 C & D).<sup>[23]</sup> Having more space to accommodate bulky substrates hints to a broader substrate range of CpSADH. Furthermore, most of the active-site residues in CPCR1 are identical to the X-ray template 2HCY (ADH1 from bakers’ yeast); this suggests a similar substrate range of both enzymes (see Figure S3).

The clear assignment of a molecular identity to any of the carbonyl reductases found in *C. parapsilosis*, as intended in this work, required the identification of substrates that are able to discriminate one from the other. This was facilitated by the observed high similarity of CPCR1 to ADH1 from bakers’ yeast, as the known substrate scope of the latter could easily be compared with the reported substrate scope of the original CPCR. Earlier studies on ADH1 from bakers’ yeast reveal

that cyclohexanone and benzaldehyde are not substrates<sup>[24]</sup>, whereas, in the original paper about CPR, structurally similar substrates such as 4-methyl-cyclohexanone or acetophenone were well converted.<sup>[1a]</sup> Hence, cyclohexanone and acetophenone were used as indicator substrates for the in silico substrate screening. Additionally, ethyl 5-oxohexanoate and methyl-3-oxovalerate were included as reference substrates because these are known to be converted by both enzymes.

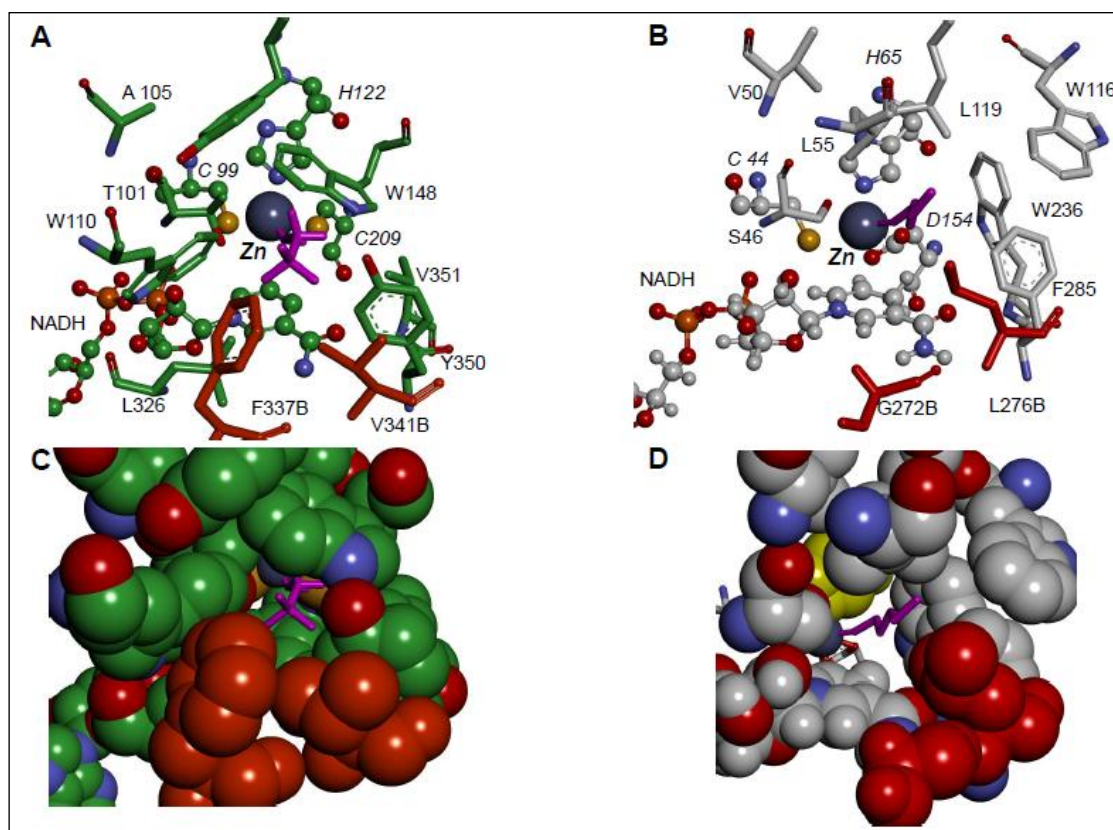


**Figure 2** A) Binding site of the CPR1 model with bound 2,2,2-trifluoroethanol (magenta) and B) binding site of the CpSADH-model with bound ethoxyethanol (magenta). Catalytic residues around  $Zn^{2+}$  and NADH are represented in ball and stick, all other residues in stick representation. Residues from the monomer B are colored red. Binding sites of C) CPR1 model and D) CpSADH model in van der Waals representation.

Molecular docking of these selected indicator substrates in a reactive conformation bound to the catalytic zinc was performed, and the relative stabilization energy in the active site was calculated by using the general AMBER force field (see Tables S3 & S4, 3.1.6).<sup>[13]</sup> Only the reference substrate 5-oxohexanoate shows favorable stabilization energy for CPR1; the other three indicator substrates reveal unfavorable relative energy values (Figure 3B). In contrast, CpSADH showed even better relative energy values for cyclohexanone compared to the reference substrate. Methyl-3-oxovalerate shows modest and acetophenone shows medium stabilization energies bound to CpSADH in a reactive conformation according to the energy calculations.

When comparing the calculated relative stabilization energy data to the relative activities measured with the recombinant enzymes CPR1 and CpSADH, a clear similarity of the substrate pattern can be observed (Figure 3A). Strikingly, cyclohexanone is very well accepted by CpSADH but not by CPR1 as

predicted by the *in silico* modeling. As methyl-3-oxovalerate and acetophenone are converted by CpSADH but are only weakly accepted by CPCR1, the broad substrate spectrum can now evidently be assigned to CpSADH. The commercial CPCR preparation traded by Codexis was found to have an intermediate relative activity profile, thus indicating that a mixture of at least the two identified CPCR isoenzymes is present.

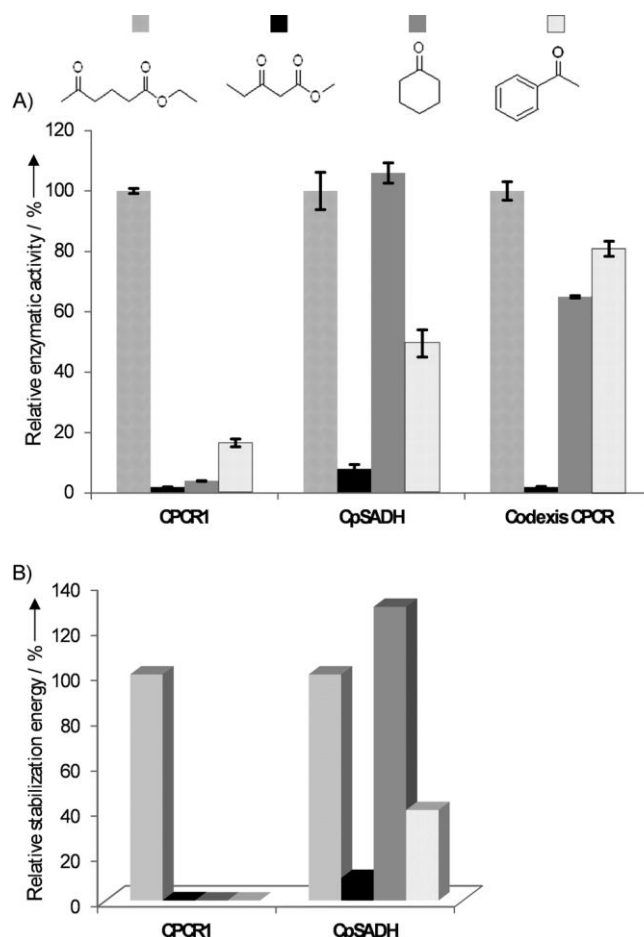


**Figure 3** A) The bar diagram represents relative volumetric enzyme activities of three different CPCR preparations for ethyl 5-oxohexanoate, methyl-3-oxovalerate cyclohexanone and acetophenone. B) The bar diagram depicts the calculated relative activation energies ( $\Delta E$ ) for the same substrates for the two CpCR homology models.

### 3.1.5 Conclusion

The activity of the synthetically potent CPCR described by Peters *et al.* in 1993<sup>[1a]</sup> can be allocated to at least two distinct carbonyl reductases (E.C.1.1.1.1). These enzymes show low homology in amino acid sequence, but high similarity in the overall fold. Monomers of both have a molecular weight lower than reported by Peters *et al.* It might well be, however, that this is an artifact resulting from problems with protein denaturation in the reported study because the molecular weight observed by Peters *et al.* is in good accordance with the weight of the homodimeric complexes forming the active structures of both CPCR1 and CpSADH.

Interestingly, the wide substrate range reported for CPCR does not result from a complementary combination of both substrate spectra. Rather, the enzymes can rather be classified as a minor and

major CPR, which we suggest calling CPR1 and CPR2. CPR2, which is identical with CpSADH described by Kojima *et al.*<sup>[9, 16]</sup> converts all compounds so far described for CPR, whereas CPR1 fails to convert of a couple of bulky substrates. Both isoenzymes are probably present in CPR preparations from the native source (*C. parapsilosis*), although they have not yet been experimentally verified in parallel. It can be assumed that enzyme expression in *C. parapsilosis* reacts extremely sensitively to small changes in cultivation conditions, that is, even if data from fermentation indicates comparability of the physiological state of the organism, the composition of carbonyl reductases can considerably vary.

The molecular identity of CPR was elucidated by the rational combination of classical biochemical methods and computational chemistry; in consideration of the extremely broad range of compounds converted by CPR, this turned out to be a fast and most efficient method of identifying differences in substrate conversion. In future it might contribute to improving of the investigation of sequence-function relationships in similar systems.

### 3.1.6 Supplementary Information

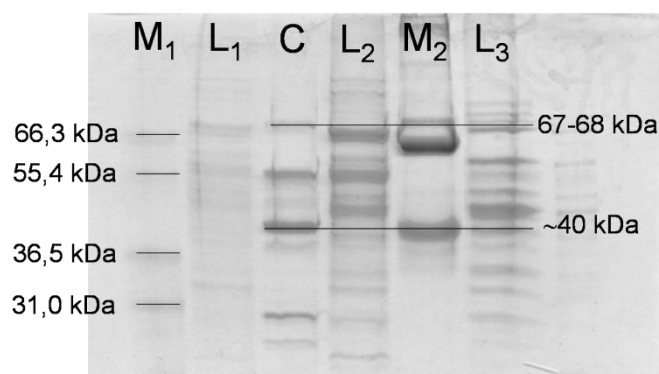


**Figure S1** Coomassie stained SDS-PAGE of differently concentrated CPR preparations and commercial CPR (Codexis, USA). M<sub>1</sub>/M<sub>2</sub>: Size markers; L<sub>1</sub>, L<sub>2</sub>, L<sub>3</sub>: lyophilized CPR purified from a batch fermentation, a shake flask culture, and a concentrated shake flask culture; C: Commercial CPR. The gel was prepared and published by S. Steinsiek (PhD thesis, 2006, RWTH Aachen University)



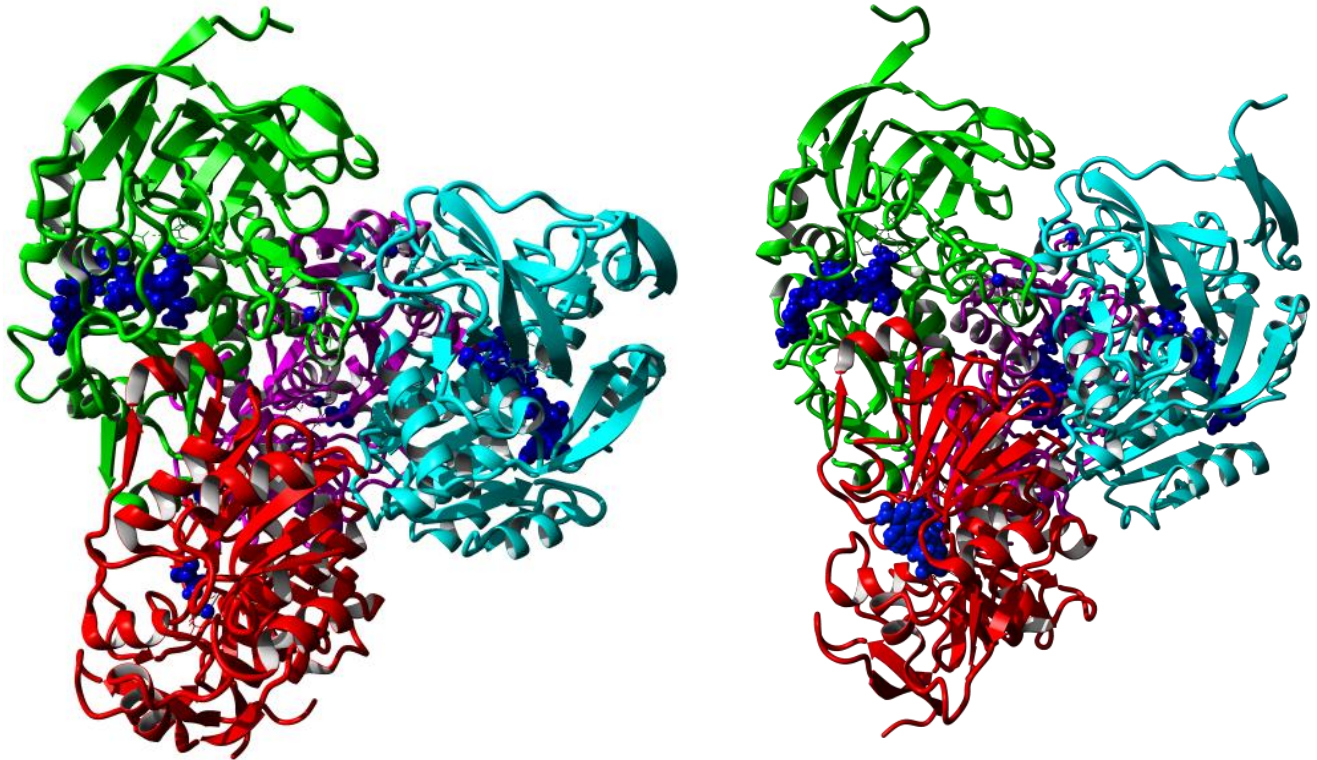


Figure S 2 PCR1 (left) and CpSADH (right) quaternary structures are modelled as tetramers (dimer of dimers). The first dimer contains Chain A (green) and Chain B (red), second dimer is formed by Chain C (cyan) and D (magenta). Cofactor NADH and two bound Zn-ions are coloured blue.

```

CPCR1/1-349      1 MPEIPKTKQKAVVFETSGGKLEYKDI PVPKPKSNELLINVKYSGVCHTDLHAWKGDW56
ADH1_YEAST/1-347 1 --SIPETQKGVIIFYESHGKLEYKDI PVPKPKANELLINVKYSGVCHTDLHAWHGDW54
ADH_SULSO/1-312 1 - - - - - MRVRLVEIGKPLSLQEI GVPKPKGPQVLI KVEAAGVCHSDVHMRGRRF 49
CPSADH/1-336    1 - MIPSSQYGFVFNKQSGLNLRNDLPVHKKPKAGQLLLKVDVAVGLCHSDLHVVIYEG 55

CPCR1/1-349      57 PLDTKPLPLVGGHEGAGVVVGMGDNVKGWEIGDYAGIKWLNGLSCLNCFCEQGAEPN 112
ADH1_YEAST/1-347 55 PLPVKLPLVGGHEGAGVVVGMGENVKGWKIGDYAGIKWLNGLSCMACCEYCELGNESN 110
ADH_SULSO/1-312 50 - - - - - VTLGHEIAGKIEEVGDEVVGYSKGDLVAVNFWQG-EGNCYYCRIGEEHL 97
CPSADH/1-336    56 DCGDN--YVMGHEIAGTVAAVGDDVIN YKVGDRVACVGPNG-CGGCKYCRGAIDNV 108

CPCR1/1-349      113 CPGADLS--GYTHDGSFEQYATADAVQAARIPKNADLAKAAPILCAGVTVYKALKT 166
ADH1_YEAST/1-347 111 CPHADLS--GYTHDGSFQQYATADAVQAAHIPPQGLAQVAPILCAGITVYKALKS 164
ADH_SULSO/1-312 98 CD--RWLGINFDGAYAEYVIVPHYKMYK--NAVEAAPLTCSGITTYRAVR 144
CPSADH/1-336    109 CKNAFGDFWGLGYDGGYDQYLLVTRPRNLSRIPDNVSDVAAASTDVAVLTPYHAIK 164

CPCR1/1-349      167 AQLKAGEWVCI SGAGGGLGSLAIQYAIAMGYRVIIGDGAEKGEYIKSLGAEAYID 222
ADH1_YEAST/1-347 165 ANLMAGHWVAISGAAGGLGLAVQYAKAMGYRVLGIDGEGEKEELFRSIGGEVFI 220
ADH_SULSO/1-312 146 KASLDPTKTLVVG--GGLGTMAVQIAKAV-ATIGVVRVEEAVEAAKRAGADYVIA 198
CPSADH/1-336    165 MAQVSPSTNILLIGAGGLGNAIQVAKAFGAKVTVLDKKKEARDQAKKLGADAVYE 220

CPCR1/1-349      223 FTKEKDIVAVKKAATNGGPHGVINVSVSEKAINQSVYVVRPLGKVVVLVGLPAGSKV 278
ADH1_YEAST/1-347 221 FTKEKDIVGAVLKAATDGGAHGVINVSVSEAAIEASTRYVRANGITVVLVGMPPAGAKC 276
ADH_SULSO/1-312 199 EIRRI TESKGVDAVIDLNNSEKTL SVYPKALAKQGGKYVMVGLFGADLHYHAPLITL 254
CPSADH/1-336    221 TLPESISP6SFSACDFVSVQATFDVCCQKYVEPKGVIMPVGLGAPNLSFNLGDLAL 276

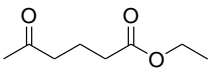
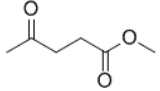
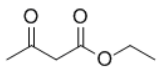
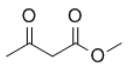
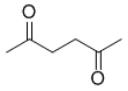
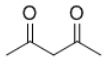
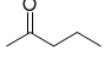
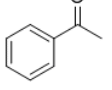
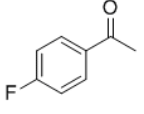
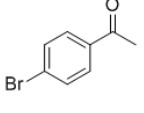
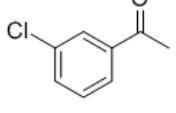
CPCR1/1-349      279 VAPVFDVAVKSVIEIKG SYVGNRDKDTQ EALDFFARGKVNCCQIKIVGLSELPEVFKLM 334
ADH1_YEAST/1-347 277 CSQVFNQVVKSI SIVGSYVGNRADTREALDFFARGLVKSPKVVGLSTLPEIYK 332
ADH_SULSO/1-312 255 SEIQFVGLVGNQSDFLGIMRLAEAGKVKPMITKTM--SANEAIQNLNFKAIGR 308
CPSADH/1-336    277 REIRILGSLFWGTTNDLDDVLLKLVSEGVKVPVVRSAKLLKELPEYIEKLRNNAYEGRV 332

CPCR1/1-349      335 EEGKILGRYVLDTSK 349
ADH1_YEAST/1-347 333 EKGQIVGRYVVDTSK 347
ADH_SULSO/1-312 309 VLI F 312
CPSADH/1-336    333 VFN P 336

```

Figure S 1 Sequence Alignment of PCR1 and CpSADH with the homologous X-ray templates ADH1 from yeast *S. cerevisiae* (2HCY) and ADH from *Sulfolobus solfataricus* (1R37), respectively. Figure is created using JalView, colours are according to the Zappo.code for indication of chemical similar amino acids

**Table S1.** Conversion by partially purified CPCR preparation of selected substrates related to the conversion of ethyl 5-oxohexanoate as standard substrate. Measurements were done photometrically using equation 1 for analysis. Equation 1:  $\text{Vol.act.} = V_{\text{tot}} \cdot dA/dt \cdot V_{\text{CPCR}}^{-1} \cdot \epsilon \cdot d$  (Vol.act: volumetric activity [ $\text{U mL}^{-1}$ ];  $V_{\text{tot}}$ : total volume [ $\mu\text{L}$ ];  $V_{\text{CPCR}}$ : volume of dissolved enzyme [ $\mu\text{L}$ ];  $dA$ : change in absorption [ $\text{min}^{-1}$ ];  $\epsilon$ : extinction coefficient of NADH [ $6.22 \text{ mL} \mu\text{mol}^{-1} \text{cm}^{-1}$ ];  $d$ : cuvette width)

Substrate	Conversion [%] by CPCR Measured*	Conversion [%] by CPCR Published <sup>[x]</sup>
 Ethyl 5-oxohexanoate	100	100
 Laevulinic acid ethyl ester	63	76
 Ethylacetoacetate	81	71
 Methyl-3-oxovalerate	71	67
 2,5-Hexadione	54	46
 2,4-Pentadione	18	15
 2-Pentanone	17	40
 Acetophenone	75	34
 4'-Fluoroacetophenone	75	40
 4'-Bromoacetophenone	103	40
 3'-Chloroacetophenone	38	35

\*The data was generated and published by S. Steinsiek (PhD thesis, 2006, RWTH Aachen University)

**Table S2** Comparison of active site residues of CPCr1 and CpSADH with according X-templates. Bold letters indicate differences between X-ray template and CPCr-model. Shaded residues indicate the larger active site residue when comparing CpCr1 and CpSADH. Active site volume was calculated by <http://www.modelling.leeds.ac.uk/pocketfinder/>.

2HCY	CpCr-I	1R37	CpCr-II
Thr45	Thr101	Ser40	Ser46
Trp54	Trp110	<b>Phe49</b>	<b>Leu55</b>
Trp92	Trp148	<b>Trp95</b>	<b>Gly91</b>
Asn110	Asn166	<b>Leu111</b>	<b>Val108</b>
Leu116	<b>Leu172</b>	Trp117	Trp116
Tyr119	Tyr175	<b>Ile120</b>	<b>Leu119</b>
Thr120	Thr176	<b>Asn121</b>	<b>Gly120</b>
<b>Met270</b>	<b>Leu326</b>	Leu272	Leu262
Val295	<b>Val351</b>	<b>Val296</b>	<b>Trp286</b>
Tyr294	Tyr350	<b>Leu295</b>	<b>Phe285</b>
<b>Ile156</b>	<b>Val212</b>	<b>Ile157</b>	<b>Leu157</b>
Phe281B	Phe337B	<b>Pro282B</b>	<b>Gly272B</b>
Val285B	Val341B	Leu286B	Leu276B
Active site sequence identity [%]			
84.6		23.1	
Active site volume [ $\text{\AA}^3$ ]			
300	312	525	544

**Table S3** CPCr1: Calculated energy-values given in kJ/mol using AMBER03/GAFF within Yasara. Active site residues are Thr 101, Ala 105, Trp110, Trp 148, Tyr 175, Leu 326, Tyr 350, Val 351, Phe 337B, Val 341B.

Compound	Solvation energy	compound energy bound to Zn	active site apo-energy difference	reactive complex energy	relative reactive complex energy
Ethyl 5-oxohexanoate	-162,68	-371,37	109,8	-98,89	0
Methyl-3-oxovalerate	-297,62	-501,88	122,23	-82,03	16,86
Cyclohexanone	-57,42	-279,33	150,94	-70,97	27,92
Acetophenone	-54,68	-250,22	124,21	-71,33	27,56

**Table S4** CpSADH: Calculated energy-values given in kJ/mol using AMBER03/GAFF within Yasara. Active site residues are Ser 46, Val 50, Leu 55, Trp 116, Leu 119, Leu 162, Phe 285, Trp 286, Gly 272B, Leu 276B .

Compound	Solvation energy	compound energy bound to Zn	active site apo-energy difference	reactive complex energy	relative reactive complex energy
Ethyl 5-oxohexanoate	-162,68	-375,54	124,25	-88,61	0
Methyl-3-oxovalerate	-297,62	-505,24	123,31	-84,31	4,3
Cyclohexanone	-57,42	-273,43	124,77	-91,24	-2,63
Acetophenone	-54,68	-258,65	117,48	-86,49	2,12

### 3.1.7 References

- [1] a J. Peters, T. Minuth, M. R. Kula, *Enz. Microb. Technol.* **1993**, *15*, 950-958; b J. Peters, T. Minuth, M. R. Kula, *Biocatal. Biotransform.* **1993**, *8*, 3146; c J. Peters, T. Zelinski, T. Minuth, M.-R. Kula, *Tetrahedron: Asymmetry* **1993**, *4*, 1683-1692; d S. Rissom, *Doctoral thesis*, Rheinische-Friedrichs-Wilhelm-Universität, Bonn (Germany), **1999**.
- [2] J. Peters, in *Biotechnology : biotransformations I, Vol. 8a*, 2nd ed. (Eds.: H.-J. Rehm, G. Reed), Wiley-VCH, Weinheim, **1998**, pp. 391-474.
- [3] T. Zelinski, A. Liese, C. Wandrey, M. R. Kula, *Tetrahedron: Asymmetry* **1999**, *10*, 1681-1687.
- [4] W. A. van der Donk, H. Zhao, *Curr. Opin. Biotechnol.* **2003**, *14*, 421-426.
- [5] a M. R. Kula, J. Peters (*US patent* US. 5,523,223), Forschungszentrum Jülich **1996**  
b A. Liese, T. Zelinski, M. R. Kula, H. Kierkels, M. Karutz, U. Kragl, C. Wandrey, *J. Mol. Catal. B: Enzymatic* **1998**, *4*, 91-99.
- [6] U. K. Laemmli, *Nature* **1970**, *227*, 680-685.
- [7] M. Baumann, *Anal. Biochem.* **1990**, *190*, 198-208.
- [8] K. Katoh, K. Misawa, K. Kuma, T. Miyata, *Nuc. Ac. Res.* **2002**, *30*, 3059-3066.
- [9] T. Kojima, H. Yamamoto, N. Kawada, A. Matsuyama (*European patent* EP 0645453) Daciel Chemical Industries Ltd., **2004**
- [10] S. F. Altschul, T. L. Madden, A. A. Schaffer, J. Zhang, Z. Zhang, W. Miller, D. J. Lipman, *Nuc. Ac. Res.* **1997**, *25*, 3389-3402.
- [11] E. Krieger, G. Koraimann, G. Vriend, *Proteins* **2002**, *47*, 393-402.
- [12] a) D. T. Jones, *J. Mol. Biol.* **1999**, *292*, 195-202; b) J. Qiu, R. Elber, *Proteins structure function & bioinformatics* **2006**, *62*, 881-891.
- [13] Y. Duan, C. Wu, S. Chowdhury, M. C. Lee, G. Xiong, W. Zhang, R. Yang, P. Cieplak, R. Luo, T. Lee, J. Caldwell, J. Wang, P. Kollman, *J. Comput. Chem.* **2003**, *24*, 1999-2012.
- [14] J. Wang, R. M. Wolf, J. W. Caldwell, P. A. Kollman, D. A. Case, *J. Comput. Chem.* **2004**, *25*, 1157-1174.
- [15] A. Jakalian, D. B. Jack, C. I. Bayly, *J. Comput. Chem.* **2002**, *23*, 1623-1641.
- [16] a T. Kojima, H. Yamamoto, N. Kawada, A. Matsuyama, (*US patent* US 6,255,092) Daciel Chemical Industries, Ltd., **2001**  
b H. Yamamoto, N. Kawada, A. Matsuyama, Y. Kobayashi, *Biosci. Biotechnol. Biochem.* **1999**, *63*, 1051-1055.
- [17] P. Edman, *Arch. Biochem. Biophys.* **1949**, *22*, 475.
- [18] A. Guida, C. Lindstaedt, S. L. Maguire, C. Ding, D. G. Higgins, D. Harris, M. Berriman, G. Butler, *unpublished work* **2011**.
- [19] a) V. Leskovac, S. Trivic, D. Pericin, *FEMS Yeast Res.* **2002**, *2*, 481-494; b) C. S. Chen, B. N. Zhou, G. Girdaukas, W. R. Shieh, F. Vanmiddlesworth, A. S. Gopalan, C. J. Sih, *Bioorg. Chem.* **1984**, *12*, 98-117.
- [20] P. W. Fowler, A. J. Ball, D. E. Griffiths, *Can. J. Biochem.* **1972**, *50*, 35-43.
- [21] M. F. van Iersel, M. H. Eppink, W. J. van Berkel, F. M. Rombouts, T. Abee, *Appl. Environ. Microb.* **1997**, *63*, 4079-4082.
- [22] Y. Lin, P. He, Q. Wang, D. Lu, Z. Li, C. Wu, N. Jiang, *PLoS One* **2010**, *5*, 11752.
- [23] A. T. Laurie, R. M. Jackson, *Bioinformatics* **2005**, *21*, 1908-1916.
- [24] E. H. Creaser, C. Murali, K. A. Britt, *Prot. Eng.* **1990**, *3*, 523-526.

**This chapter was reprinted from the publication “Who’s who? – Allocation of Carbonyl Reductase Isoenzymes from *Candida parapsilosis* by Combination of Bio- and Computational Chemistry”**  
Jakoblinnert, A.; Bocola, M.; Bhattacharjee, M.; Steinsiek, S.; Bonitz-Dulat, M.; Schwaneberg, U.; Ansorge-Schumacher, M. B.\**Chembiochem* **13**: 803-809, 2012 **with permission from Wiley**

## 3.2 Asymmetric Reduction of Ketones with Recombinant *E. coli* Whole Cells in Neat Substrates

### 3.2.1 Abstract

The asymmetric reduction of ketones is performed by using lyophilized whole cells in neat substrates with defined water activity ( $a_w$ ). Ketones and alcohols prone to be unstable in aqueous media can now be converted *via* biocatalysis.

### 3.2.2 Introduction

Biocatalysis is receiving increasing attention as a powerful synthetic tool providing environmentally-friendly reaction conditions with high regio- and stereoselectivities.<sup>[1]</sup> However, a broader extension of industrial biocatalysis is still hampered due to several reasons, *e.g.* restricted enzyme availabilities, in-sufficient productivities and stabilities, time- and material-intensive work-ups in aqueous media – often leading to waste production, as well as costs related to catalysts and cofactors.<sup>[2]</sup> Low product concentrations resulting from a limited water solubility of many organic compounds can be, to some extent, enhanced by reaction engineering using, organic co-solvents or water-organic biphasic systems.<sup>[3]</sup> On the other hand, process stability of biocatalysts can be increased and costs for catalysts and cofactors can be reduced by use of whole cells rather than isolated enzymes.<sup>[4]</sup>

For the industrial performance of the asymmetric reduction of prochiral ketones by alcohol dehydrogenases the demand for expensive nicotinamide cofactors plays a particular role in cell-free systems.<sup>[5]</sup> Hence, the use of whole cells exhibits the major advantage that cofactors can be intrinsically recycled *via* the coupling of a second substrate or by a second enzyme.<sup>[6]</sup> Few reduction reactions have been reported which work in water-organic mixtures showing exceedingly high substrate loads and no or only little demand for external cofactor.<sup>[5, 7]</sup> However, in such water-based systems emulsions may be formed, decreasing isolated yields and requiring tedious product separation. Moreover, the general applicability of the latter method is restricted when substrates and products with low stability in aqueous environments are involved.

Herein we show that *E. coli* whole cells, overexpressing a NADH-dependent carbonyl reductase, are able to perform enantioselective carbonyl reduction in quantitative yields in a solvent-free system without external co-factor addition (Figure 1).

### 3.2.3 Results and Discussion

The reaction setup only requires substrate, co-substrate, and the biocatalyst at a defined water activity (see below). Despite its potentiality, there are only few examples using dried yeast cells in organic solvents,<sup>[8]</sup> as well as lyophilized *E. coli* overexpressing an alcohol dehydrogenase from *Rhodococcus ruber* in 99 % (v/v) isopropanol.<sup>[9]</sup> In that latter example, however, cells displayed little catalytic activity, presumably due to cell rehydration before using them in the micro-aqueous system.<sup>[9]</sup>

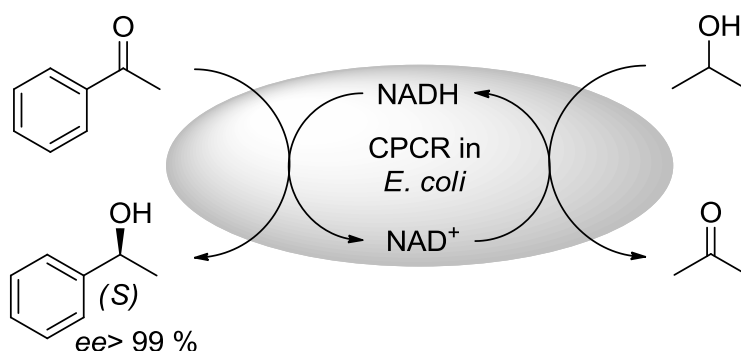


**Figure 1** Biocatalytic reduction of acetophenone using lyophilized *E. coli* cells overexpressing carbonyl reductase in a solvent-free system with isopropanol-coupled cofactor regeneration.

As a model reaction, acetophenone as substrate and isopropanol as ancillary co-substrate for cofactor regeneration were used (Figure 1). The catalyst was a NADH-dependent carbonyl reductase from *Candida parapsilosis* (CPCR)<sup>[10]</sup> overexpressed and directly applied in *E. coli* whole cells. In this highly non-natural environment the biocatalyst was able to effectively produce *S*-phenylethanol (*ee* >99 %; >98 % conversion) with high productivities (300-500 g L<sup>-1</sup>) (Figure 2).<sup>[11]</sup> Compared to existing production processes, the developed reaction system has advantage in simplicity, economics (cheap starting material, no NADH addition, very limited waste production, high added value), scalability and high yields.<sup>[5, 7, 9]</sup> Moreover, a key feature is the straightforward work-up as the whole cells can easily be separated and product downstream requires only evaporating co-substrate and co-product.

Further studying the whole-cell-catalyzed reduction of acetophenone demonstrated a dependence of the initial reaction rate on the volumetric substrate to co-substrate ratio, indicating the underlying equilibrium conditions (Figure 2).

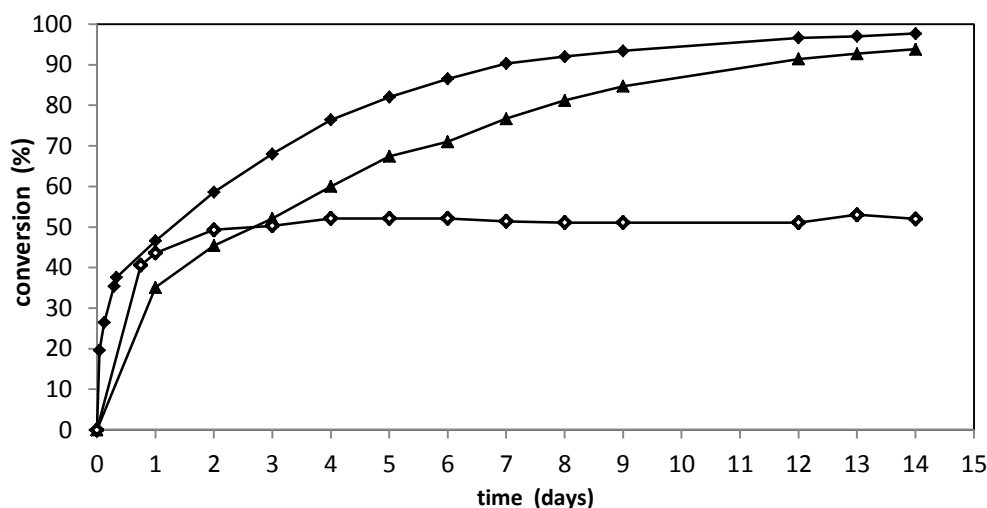


**Figure 2** Conversion of acetophenone by *E. coli* whole cells overexpressing CPCR in solvent-free conditions. Different volumetric ratios of isopropanol to acetophenone were set (50:50 ▲, 70:30 ■ □). Closed symbols: daily removed acetone; open symbol: No acetone removal.

Nevertheless, the conversion of acetophenone was always driven to completion, when acetone was intermittently removed from the reaction, and the enantioselectivity was always at maximum ( $ee > 99\%$ ).<sup>[12]</sup> Obviously, with a highly optimized process development these full conversions could be achieved in much shorter reaction times. Remarkably, after 14 days of operation in the system cells still displayed activity rendering this biocatalyst extremely stable.<sup>[13]</sup> This is consistent with the reported stable operation of *E. coli* cells harboring an alcohol dehydrogenase at high concentrations of isopropanol in aqueous media,<sup>[14]</sup> and can mainly be attributed to the enzyme preserving microenvironment of the host cell.<sup>[4a]</sup> Inhibition or inactivation of the catalyst at elevated co-substrate concentrations could not be observed. Consequently, with this system it was possible to produce up to  $500 \text{ g L}^{-1}$  optically pure (*S*)-phenylethanol.

The role of the water on the activity of the biocatalyst was analyzed in depth, since it is widely accepted that water plays a crucial role for biocatalysis in non-conventional media,<sup>[15]</sup> for lyophilized whole cells in gas-solid reactor systems,<sup>[16]</sup> and for whole cell biocatalysis in transesterification and trans-glucosylation reactions.<sup>[17]</sup> Lyophilized cells were exposed to seven different  $a_w$  values ranging from dry ( $a_w = 0$ ) to wet ( $a_w = 1$ ) and used under solvent-free conditions (see Figure 3).<sup>[18]</sup> For low  $a_w$  values biocatalytic activity is increasing with water activity, which is in agreement with former findings.<sup>[16]</sup> The optimum water activity is around  $a_w$  value of 0.84 (see Figure 3). Additionally, non-equilibrated wet cells were active but rapidly deactivated within few hours, whereas lyophilized cells remained stable for several days (data not shown).

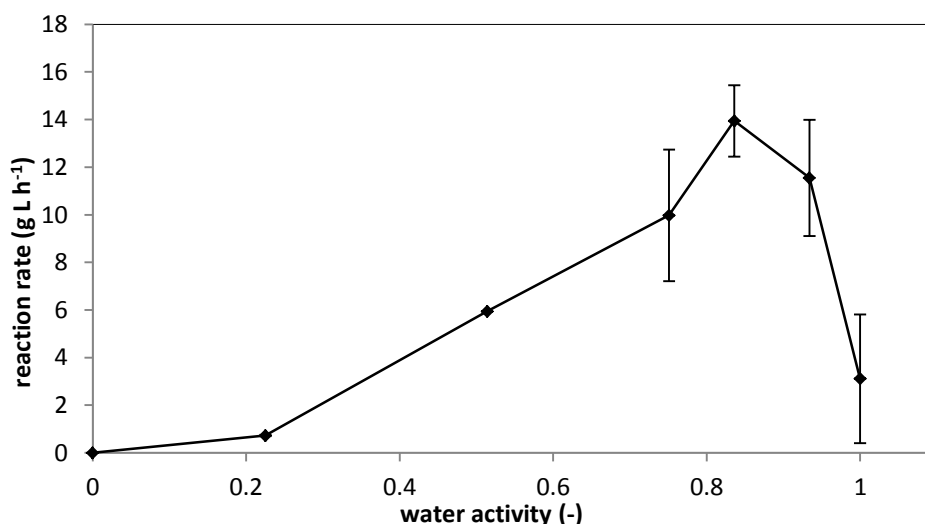


**Figure 3** Initial reaction rate of acetophenone in neat substrates employing *E. coli* whole cells with overexpressed CPR. Dried cells and reaction mixtures were previously equilibrated to different water activities. <sup>[18a, 19]</sup>

As indicated previously, application of the here described solvent-free reaction system may be particularly beneficial for the asymmetric reduction of compounds exhibiting low stabilities in aqueous environments. For instance, propargylic ketone 3-butyn-2-one is instable in aqueous media, shows thermal decomposition and, moreover, has been reported to deactivate enzymes and cells.<sup>[20]</sup> Notably, the corresponding (*S*)-3-butyn-2-ol is an important building block for anti-asthma drugs like 5-lipoxygenase inhibitors<sup>[20c]</sup>, the potent  $\beta_2$ -adrenergic stimulant broxaterol<sup>[21]</sup> or the protease inhibiting hydroxyethylene dipeptide isosteres.<sup>[22]</sup> In virtue of this importance, the enzymatic production of (*S*)-3-butyn-2-ol has already been attempted *via* the asymmetric reduction of 3-butyn-2-one with alcohol dehydrogenases or *via* the enantioselective hydrolysis of the corresponding esters. To overcome substrate and product instability in aqueous media, either biphasic systems were applied, or derivatized trimethylsilan-based compound was used as substrate, albeit at the cost of adding further synthetic steps.<sup>[20b, 20c, 21, 23]</sup>

So far, the alcohol dehydrogenases displayed moderate to low enantioselectivities in monophasic systems (5-86 %<sup>[20-21]</sup>), whereas the hydrolase-catalyzed ester hydrolysis led to high *ee*'s, but with limited conversions at 50 %.<sup>[24]</sup> To date, there is only one multi gram-scale preparation of *S*-3-butyn-2-ol using an alcohol dehydrogenase from *Pseudomonas aeruginosa* in a biphasic system with *ee* >99 %, though at low conversion (45.5 %).<sup>[20a]</sup>

In the herein developed solvent-free whole-cell system high enantioselectivities were achieved (*ee* = 99.9 %; Figure 4).<sup>[11]</sup> Data are at odds with the value reported by Schubert for CPR for 3-butyn-2-one (*ee* = 49 %).<sup>[20c]</sup> However, in the mentioned work, CPR was used not in recombinant form but as a crude extract from the *Candida* host. Hence, discrepancies may be explained by the acceptance



of butynone by yeast oxidoreductases other than CPCR which in turn may lower the *ee*, as it has been reported for other yeast systems like baker's yeast.<sup>[25]</sup>

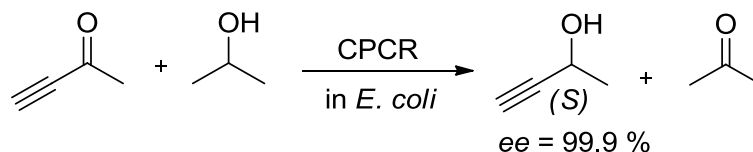


**Figure 4** Biocatalytic reduction of 3-butyn-2-one using lyophilized *E. coli* cells overexpressing CPCR in the developed solvent-free system with isopropanol-coupled co-factor regeneration.

According to the above-described findings that increasing the co-substrate concentration favors the product formation, a volumetric ratio 90:10 (isopropanol to 3-butyn-2-one) at optimum *a<sub>w</sub>* was set up in this case. As proof-of-concept 67.6 % conversion was achieved in 24 h, corresponding to 57.4 g L<sup>-1</sup> of optically pure *S*-3-butyn-2-ol. This product concentration is already 2-fold higher than the so far reported maximum value (24.7 g L<sup>-1</sup>).<sup>[20a]</sup> Without acetone removal (hence, under non-optimized conditions), full conversion could be obtained within 120 h, yielding a product concentration of 87 g L<sup>-1</sup>. This example notably points out that this solvent-free reduction system, while lacking bulk water, is very powerful in accessing optically pure alcohols, even if substrates and/or products are instable in aqueous solutions. It can be expected that this will open new biocatalytic routes to the production of so far non- or hardly accessible building blocks.

### 3.2.4 Summary and Outlook

In summary, lyophilized *E. coli* whole-cells overexpressing carbonyl reductase are able to perform enantioselective reductions of ketones in neat substrates conditions, leading to the production of enantiomerically pure alcohols in large amounts. The approach of lyophilized *E. coli* whole-cells in solvent-free conversions is characterized by a high cost-effectiveness (high added-value, no cofactor addition, simple work-up) and by an environmentally-friendly operation mode (largely diminished waste production, bio-based catalyst). A further notable point is use of compounds in the reaction system that unstable in aqueous environments. Together with the further inherent advantages of biocatalysis (high selectivity, high activity), the described solvent-free system may represent a competitive alternative to classical chemical production of optically pure alcohols.

### 3.2.5 References & Notes

- [1] R. Wohlgemuth, *Curr. Opin. Microb.* **2010**, *13*, 283-292.
- [2] S. M. De Wildeman, T. Sonke, H. E. Schoemaker, O. May, *Acc. Chem. Res.* **2007**, *40*, 1260-1266.
- [3] a) A. M. Klibanov, *Acc. Chem. Res.* **1990**, *23*, 114-120; b) P. Adlercreutz, in *Organic synthesis with enzymes in non-aqueous media* (Eds.: G. Carrea, S. Riva), **2008**, pp. 3-24.
- [4] a) C. C. de Carvalho, *Biotechnol. Adv.* **2011**, *29*, 75-83; b) K. Goldberg, K. Schroer, S. Lutz, A. Liese, *Appl. Microb. Biotechnol.* **2007**, *76*, 249-255.
- [5] H. Groger, F. Chamouveau, N. Orolagas, C. Rollmann, K. Drauz, W. Hummel, A. Weckbecker, O. May, *Angew. Chem. Int. Ed.* **2006**, *45*, 5677-5681.
- [6] W. Stampfer, B. Kosjek, C. Moitzi, W. Kroutil, K. Faber, *Angew. Chem. Int. Ed.* **2002**, *41*, 1014-1017.
- [7] a) A. Weckbecker, H. Groger, W. Hummel, *Adv. Biochem. Eng. Biotechnol.* **2010**, *120*, 195-242; b) Y. Ni, C.-H. Chun-Xiu Li, J. Jie Zhang, N.-D. Shen, U. T. Bornscheuer, J.-H. Xu, *Adv. Syn. Catal.* **2011**, *353*, 1213.
- [8] a) K. Nakamura, S.-I. Kondo, Y. Kawai, A. Ohno, *Tetrahedron Lett.* **1991**, *32*, 7075-7078; b) P. Nikolova, O. P. Ward, *Biocatal.* **1994**, *9*, 329-341; c) P. Hoyos, G. Sansottera, M. Fernandez, F. Molinari, J. F. Sinisterra, A. R. Alcantara, *Tetrahedron* **2008**, *64*, 7929-7936; d) F. Molinari, R. Gandolfi, R. Villa, E. G. Occhiato, *Tetrahedron: Asymmetry* **1999**, *10*, 3515-3520
- [9] G. de Gonzalo, I. Lavandera, K. Faber, W. Kroutil, *Org. Lett.* **2007**, *9*, 2163-2166.
- [10] a) H. Yamamoto, N. Kawada, A. Matsuyama, Y. Kobayashi, *Biosci. Biotechnol. Biochem.* **1999**, *63*, 1051-1055; b) D. Gamenara, P. Dominguez de Maria, *Biotechnol Adv* **2009**, *27*, 278-285; c) J. Peters, T. Minuth, M. R. Kula, *Enz. Microb. Technol.* **1993**, *15*, 950-958.
- [11] *Conversion and enantiomeric excess were calculated from the peak areas observed in chiral GC analysis. Assignment of peaks was done with commercial authentic standards.*
- [12] a) *Cells were removed by centrifugation. The cleared reaction mixtures was applied to evaporation under reduced to remove the co-product acetone alongside with isopropanol. The remaining mixture of acetophenone and phenyl was replenished with isopropanol and the old cell were added;*  
b) K. Goldberg, K. Edegger, W. Kroutil, A. Liese, *Biotechnol. Bioeng.* **2006**, *95*, 192-198.
- [13] *Residual activity of cells after operation in solvent-free conditions was assessed in aqueous system. For this, cells were washed in buffer (100 mmol L<sup>-1</sup> K<sub>2</sub>HPO<sub>4</sub>/KH<sub>2</sub>PO<sub>4</sub>, pH 6.5) and used in the same buffer for bioconversion of acetophenone (50 mmol L<sup>-1</sup> acetophenone, 5 % v/v isopropanol, 10 mmol L<sup>-1</sup> NADH, 200 g L<sup>-1</sup> cells). The biocatalyst was able to convert the substrate almost quantitatively in one day, proven by GC analysis.*
- [14] K. Schroer, U. Mackfeld, I. A. Tan, C. Wandrey, F. Heuser, S. Bringer-Meyer, A. Weckbecker, W. Hummel, T. Dausmann, R. Pfaller, A. Liese, S. Lutz, *J. Biotechnol.* **2007**, *132*, 438-444.
- [15] P. J. Halling, *Enz. Microb. Technol.* **1984**, *6*, 513-516.
- [16] a) B. Erable, T. Maugard, I. Goubet, S. Lamare, M. D. Legoy, *Proc. Biochem.* **2005**, *40*, 45-51; b) T. Goubet, T. Maugard, S. Lamare, M. D. Legoy, *Enz. Microb. Technol.* **2001**, *31*, 425-430.
- [17] a) D. Huang, S. Han, Z. a. Han, Y. Lin, *Biochem. Eng. J.* **2011**, *63*, 10-14.  
b) M. Y. Rather, S. Mishra, S. Chand, *J. Biotechnol.* **2010**, *150*, 490-496.
- [18] a) L. Greenspan, *Journal of Res. Nat. Bureau Stand. - A. Physics and Chemistry* **1977**, *81A*, 89-96; b) *Water activities of dry substrate solution and cells were established by equilibration for least 48 h with saturated salt solutions.*

- [19] Initial reaction rate was calculated from substrate conversion after 4 hours of operation in solvent-free system. The data set was collected from two independent experiments.
- [20] a) S. M. De Wildeman, (*Int. patent WO2008074506*), DSM **2009**; b) C. Heiss, R. S. Phillips, *J. Chem. Soc., Perkin Transactions 1* **2000**, 2821-2825; c) T. Schubert, W. Hummel, M. R. Kula, M. Muller, *Eur. J. Org. Chem.* **2001**, 4181-4187.
- [21] M. De Amici, C. De Micheli, G. Carrea, S. Spezia, *J. Org. Chem.* **1989**, *54*, 2646-2650.
- [22] A. K. Ghosh, N. Kumaragurubaran, C. Liu, T. Devasamudram, H. Lei, L. M. Swanson, S. V. Ankala, J. J. N. Tang, G. M. Bilcer, (*European patent EP 1871739*), CoMentis **2009**.
- [23] W. Y. Lou, L. Chen, B. B. Zhang, T. J. Smith, M. H. Zong, *BMC Biotechnol.* **2009**, *9*, 90.
- [24] a) M. Schmidt, D. Hasenpusch, M. Kahler, U. Kirchner, K. Wiggenghorn, W. Langel, U. T. Bornscheuer, *Chembiochem* **2006**, *7*, 805-809;  
b) K. Nakamura, K. Takenaka, A. Ohno, *Tetrahedron: Asymmetry* **1998**, *9*, 4429-4439
- [25] S. Rodriguez, M. Kayser, J. D. Stewart, *Org. Lett.* **1999**, *1*, 1153-1155.

**This chapter was reprinted from the publication "Asymmetric reduction of ketones with recombinant *E. coli* whole cells in neat substrates."** Jakoblinnert, A.; Mladenov, R.; Paul, A.; Sibilla, F.; Schwaneberg, U.; Ansorge-Schumacher, M. B.\*; de Maria, P. D.\* *Chemical Communications* **47**: 12230-12232, 2011 **with permission of The Royal Society of Chemistry**  
<http://pubs.rsc.org/en/Content/ArticleLanding/2011/CC/c1cc14097c>

### 3.3 Synthetic Toolbox to Chiral Alcohols via Asymmetric Ketone Reduction with Recombinant *E. coli* Cells in Neat Substrates

#### 3.3.1 Introduction

Biocatalytic asymmetric reduction of prochiral ketones to manufacture enantiopure alcohols is nowadays considered as fully complementary to classical chemical routes.<sup>[1]</sup> Asymmetric reduction is rendered by high atom efficiency and cost-effectiveness since 100 % theoretical yield is possible and cheap ketonic starting material is converted to high value-added products.<sup>[1-2]</sup> The chiral alcohols serve as key building blocks in pharmaceutical, food, fragrance and agricultural industries.<sup>[3]</sup> As biocatalysts, alcohol dehydrogenases (ADHs), also called carbonyl or keto reductases (CRs), are used herein as isolated enzymes or in whole cells to convert ketones to the corresponding alcohols with supreme stereoselectivities unmatched by chemical catalysis.

These enzymes are dependent on costly nicotinamide cofactors such as NADH and NADPH, which deliver the required oxidation ( $\text{NAD(P)}^+$ ) or reduction ( $\text{NAD(P)H}$ ) equivalents in stoichiometric amounts. The latter drawback was addressed by effective methods to regenerate the cofactor by enzyme- or substrate coupled approaches as well as other biocatalytic or chemical routes.<sup>[4]</sup> The cofactor regeneration in an enzyme-coupled approach by the application of formiate dehydrogenase or glucose dehydrogenase on industrial scale has recently been reported.<sup>[4b]</sup> Furthermore, isolated enzymes suffer from low process stabilities since they are not suited for conditions usually present in industrial processes such as elevated temperatures or high concentrations of organic molecules.<sup>[5]</sup> For this, either the process has to be optimized for the catalyst or the enzymes have to be improved to match process requirements. Protein engineering has lately been demonstrated to be a suitable strategy to improve an ADH for industrial-scale applications.<sup>[6]</sup>

The two problems of cofactor regeneration and enzyme stabilities can also be addressed by the application of whole cells as biocatalysts. In this case the enzyme stays inside the production host (e.g. *E. coli*) and the cofactors are provided by the microorganism.<sup>[7]</sup> Regeneration of the cofactor takes place intracellularly by a second enzyme or the same enzyme.<sup>[7]</sup> Additionally, whole cells are more robust towards hazardous conditions and protect the enzymes they contain.<sup>[8]</sup>

A general weakness of biocatalysis, regardless if cells or enzymes are used, is the dependency on aqueous environment for optimal performance, which results in low productivities due to low solubility of organic substrate and product molecules. To alleviate this drawback, various reactor concepts for reduction of hydrophobic ketones were developed, which are relying on membrane separation of the biocatalyst containing aqueous phase and substrate containing organic phase.<sup>[9]</sup> Additionally, medium engineering is undertaken to find suitable reaction conditions providing high a

biocatalyst stability and selectivity accompanied by substrate loadings exceeding  $100 \text{ g L}^{-1}$ .<sup>[10]</sup> Species isolated from extreme environments can withstand very high temperatures or co-solvent concentrations (>80 % (v/v)) and effectively carry out ketone reduction.<sup>[11]</sup> However, due to host enzymes in whole cells also accepting the substrate molecules, stereoselectivity can be reduced, thus limiting the general applicability of this approach.<sup>[12]</sup>

In the previous chapter 3.2, the concept of ketone reduction in a medium composed of only the substrate acetophenone and the cosubstrate isopropanol was demonstrated to work with lyophilized *E. coli* whole cells containing the carbonyl reductase from *Candida parapsilosis* (CPCR2).<sup>[13]</sup> This reaction mode provides substrate loads up to  $500 \text{ g L}^{-1}$  with stereoselectivity at maximum (>99 % *ee*). Furthermore, the water-labile compound 3-butyn-2-one was converted to the (*S*)-alcohol with *ee* >99 % in this system; whereas, biotransformation in aqueous medium showed *ee* of only 49 % *ee*.<sup>[13a, 14]</sup> The system showed strong dependency on water activity ( $a_w$ ) as well as limitation of the reaction rate by the thermodynamic equilibrium of the reaction. However, conversion could be completed by intermittent removal of the coproduct acetone by simple evaporation and replenishing of isopropanol.<sup>[13]</sup>

### 3.3.1.1 Selection of Biocatalysts

To examine whether this system is restricted to CPCR2, ADHs from *Rhodococcus erythropolis* (ReADH) and *Lactobacillus brevis* (LbADH) were applied in the same system in recombinant form overexpressed in *E. coli*.<sup>[15]</sup> Both enzymes are reported to exhibit a broad substrate spectrum and high stereoselectivity and are used in preparative or industrial scale.<sup>[15b, 16]</sup> ReADH resembles CPCR2 with respect to stereoselectivity, cofactor dependency and biochemical properties (see Table 1). In contrast, LbADH is complementary to CPCR2 and ReADH since it exhibits *anti-Prelog* specificity and depends on NADPH as cofactor.

**Table 1 Comparison of enzymes selected for application in the neat substrate system**

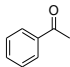
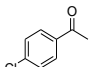
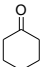
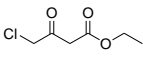
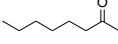
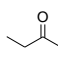
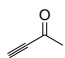
Source	Enzyme name	Enantioselectivity	Cofactor	Source
<i>Candida parapsilosis</i>	CPCR2	<i>Prelog</i>	NADH	[13b, 13c, 17]
<i>Rhodococcus erythropolis</i>	ReADH	<i>Prelog</i>	NADH	[15a, 18]
<i>Lactobacillus brevis</i>	LbADH	<i>anti-Prelog</i>	NADPH	[15b, 19]

### 3.3.1.2 Selection of Benchmark Substrates

Furthermore, the versatility of the reaction system was investigated by reduction of various structurally different benchmark substrates (see Table 2). Herein, the substrate class of aromatic ketones is covered by acetophenone and 4-chloroacetophenone. The corresponding alcohols are useful building blocks for chiral high value-added products and are often applied as model substrates.<sup>[20]</sup> Alcohols with cyclohexanone moiety are found in many natural products and

cyclohexanone is chosen as substrate for this class.<sup>[21]</sup> A key intermediate for manufacture of statin drugs is ethyl (*S*)-4-chloro-3-hydroxybutanoate, which is produced on industrial scale via reduction of the corresponding ketoester; thus 4-chloroacetoacetate represents the substrate class of keto esters.<sup>[3a, 22]</sup> Also the (*R*)-alcohol is valuable in the synthesis of *L*-carnitin.<sup>[3a, 23]</sup> Moreover, aliphatic alcohols constitute interesting building blocks.<sup>[24]</sup> As long chain aliphatic ketone, 2-octanone is selected due to the versatile application field of (*S*)- and (*R*)-2-octanol as building blocks in organic synthesis or production of liquid crystals.<sup>[23, 25]</sup> Especially, manufacturing enantiomerically pure 2-butanol from 2-butanone is difficult since many enzymes cannot differentiate between the methyl- and the ethyl-substitution at the carbonyl carbon.<sup>[1]</sup> At last, 3-buten-2-one as small propargylic ketone, is applied, which is prone to degradation in aqueous buffers.<sup>[14, 26]</sup> The corresponding alcohols have several functions as outlined in 3.2.<sup>[13a]</sup>

**Table 2 Benchmark substrates selected for reduction in the neat substrate system**

Substrate structures							
Substrate class	aromatic	substituted, aromatic	cyclic	keto ester	long, aliphatic	short, aliphatic	small, propargylic

### 3.3.1.3 Mass Transfer Limitation, Cofactor Availability & Process Stability

Whole cell biotransformation is a powerful tool in biocatalysis but limited mass transfer across the membrane or cell wall can prevent potential catalysts from application in industrial processes.<sup>[27]</sup> In gram-negative bacteria such as *E. coli* the outer membrane, composed of an amphiphilic lipopolysaccharide layer (LPS), constitutes an effective barrier for small hydrophobic molecules.<sup>[28]</sup> Thus, uptake of hydrophobic substrates like acetophenone may account for a major limitation in the overall reaction rate. Therefore, the influence of different permeabilizers on reaction rate was tested. Furthermore, the effect of cofactor addition and increased temperatures was analyzed. The intracellular level of NADH in *E. coli* cells was estimated to be around 1 mmol L<sup>-1</sup><sup>[29]</sup>; however, in the system applied here substrates are present in molar concentrations. Hence, the availability of cofactor in neat substrates might limit the reaction speed.

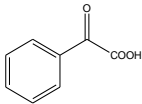
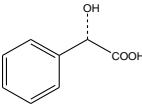
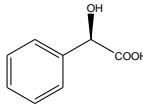
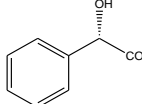
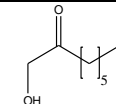
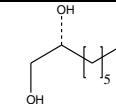
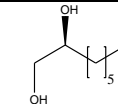
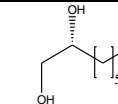
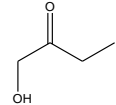
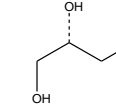
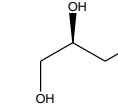
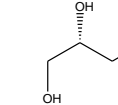
Catalyst stability is besides activity and selectivity the most important feature for the development of an economic viable biocatalytic process.<sup>[5a, 30]</sup> Thus, the performance of the whole cells in neat substrates was tested in repeated batch mode reusing the catalyst.

### 3.3.1.4 Deracemization for Production of Chiral Alcohols

Asymmetric reduction of prochiral ketones is a direct and efficient way to access chiral alcohols. However, in some cases the ketonic starting material can be more expensive or less stable than the corresponding racemic alcohol.<sup>[3b]</sup> In Table 3, three examples are demonstrated wherein the

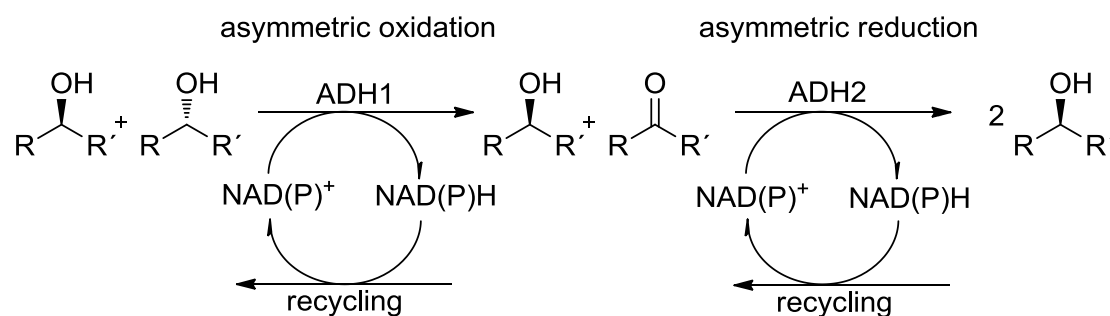
prochiral ketone is much more expensive than the racemic alcohol. The most striking case is for the pair 4-hydroxybutanone and 1,3-butanediol where the ketone is 67.5x more expensive than the racemic alcohol (1215 € kg<sup>-1</sup> vs. 18 € kg<sup>-1</sup>, see Table 3, entry 3). From an economical point of view it makes more sense to use the racemate as starting material. In this example, the added-value for production of (*S*)-1,3-propanediol would be only 4.6x for the ketone but 311x for full conversion of the racemate as substrate.

**Table 3** Price comparison of ketones with their corresponding alcohols in racemic and enantiopure form. All prices are deduced from Sigma-Aldrich online catalogue taking the largest quantity and comparably purities.

Entry	Ketone	Racemic alcohol	( <i>R</i> )-alcohol	( <i>S</i> )-alcohol	Source
1	 2930 € kg <sup>-1</sup>	 134 € kg <sup>-1</sup>	 2580 € kg <sup>-1</sup>	 1190 € kg <sup>-1</sup>	[31]
2	 62,200 € kg <sup>-1</sup>	 1830 € kg <sup>-1</sup>	 437,000€ kg <sup>-1</sup>	 -	[32]
3	 1215 € kg <sup>-1</sup>	 18 € kg <sup>-1</sup>	 5040 € kg <sup>-1</sup>	 5590 € kg <sup>-1</sup>	[33]

In such cases, racemate resolution presents an attractive route to obtain the desired enantiomer by asymmetric oxidation of the undesired enantiomer to the corresponding ketone. This is indeed possible with enzymes, since the asymmetric ketone reduction catalyzed by ADHs is fully reversible. The alcohol oxidation is promoted by NAD<sup>+</sup>, which can be regenerated by providing acetone as auxiliary cosubstrate instead of isopropanol. Racemate resolution by asymmetric oxidation holds the drawbacks that the yield is limited to 50 % and high *ee* requires high conversions.

The maximum yield with a racemate as starting material can be boosted to 100 % when the oxidation is followed by reduction of the produced ketone. This can be achieved with an ADH accepting the produced ketone exhibiting an opposing stereoselectivity than the ADH used for oxidation. The overall process is called deracemization, since the racemate is completely resolved to one enantiomer. Deracemization can be achieved by concurrent or consecutive combination of asymmetric oxidation of one enantiomer to the prochiral ketone using one ADH and the asymmetric reduction using an ADH showing the opposite enantioselectivity (see Scheme 1).



**Scheme 1 Deracemization:** Racemic starting material is subjected to asymmetric oxidation where only one enantiomer is converted by ADH1 to the ketone. In the second step, the produced ketone is asymmetrically reduced by ADH2 to produce the desired enantiomer. ADH1 and ADH2 have opposing stereoselectivities.

Here, an exemplary approach to deracemized 1-phenylethanol to pure (*R*)-1-phenylethanol by consecutive application of the neat substrate system running first the oxidation reaction with (*S*)-selective CPCR2 and then the reduction reaction with (*R*)-selective LbADH is undertaken.

Generally, the versatility of the neat substrate system with respect to the biocatalysts, substrates and reaction direction will be demonstrated. Additionally, the limitations like mass transfer, cofactor availability, temperature and operational stability will be investigated.

### 3.3.2 Materials and Methods

#### 3.3.2.1 Supply of Biocatalysts

Whole cells of *E. coli* with overexpressed CPCR2 or ReADH were produced in-house by flasks cultivation or high-cell density fermentation. LbADH was provided from an external source as ready-to-use cell pellet. For protein expression of CPCR2, conditions as stated in 2.2.1 and 2.2.2 were applied. For production of ReADH cell pellet, the expression conditions were generally the same as for CPCR2, but temperature after induction was shifted to 25 °C according to Abokitse et al.<sup>[15a]</sup> Carbonyl reducing activity of the cells was monitored using the NADH-depletion assay described in 2.2.6.

After production of cell mass, the pellets were washed in ice cold  $\text{KP}_i$ -buffer (0.1 mol L<sup>-1</sup>, pH 6.8). If not processed immediately, pellets were flash frozen in liquid nitrogen and stored at -20 °C. For self-contained experiments, only cells from one production batch were applied to keep the comparability.

#### 3.3.2.2 Pre-treatment of Whole Cells & Liquid Substrates

For operation in the neat substrate system, cells were dried by lyophilization according to 2.3.3 and water was removed from liquid substrates by molecular sieves. Cells and substrates were equilibrated to certain water activity ( $a_w$ ) values by exposing the dry material to the vapor phase of saturated salt solutions. The composition of the applied salt solutions and the corresponding  $a_w$



values are shown in Table 2 in chapter 2.3.3. Additionally, the experimental setup for establishment of different  $a_w$  values is depicted in Figure 8 in the same chapter.

### 3.3.2.3 General Setup of the Neat Substrate System

The standard system used for evaluation of the neat substrate system was composed of substrate and cosubstrate in a volumetric ratio of 1:9, if not indicated differently. Usually, acetophenone as model substrate and isopropanol as model cosubstrate were employed. Whole cells and liquid substrates were equilibrated to optimal  $a_w$ , which were determined for the individual catalysts as described in 2.3.3. Catalyst load was established according to the cell-specific activity of the individual catalysts (CPCR2: 120-200 g L<sup>-1</sup>, ReADH: 300 g L<sup>-1</sup>, LbADH: 200 g L<sup>-1</sup>). Standard reactions were carried out at 30 °C in an over-head shaker at 50 rpm, if not indicated differently.

Samples volumes of 250 µL were withdrawn and directly analyzed by chiral gas chromatography according to 3.3.2.7.

### 3.3.2.4 Permeabilization of Whole Cells & Cofactor Addition

An amount of 500 mg CPCR2 cell pellet of one batch was resuspended in 2 mL KP<sub>i</sub> buffer (0.1 mol L<sup>-1</sup>, pH 6.8) containing different permeabilizing agents as listed in Table 4. After incubation (1 h, 30 °C, 50 rpm overhead shaking), cells were pelleted by centrifugation and washed with KP<sub>i</sub> buffer. The supernatant was removed after another centrifugation step and the pellets were flash frozen in liquid nitrogen. Finally, the frozen cells were pre-treated as described in 3.3.2.2 and operated in the standard reaction system as outlined in 3.3.2.3. For cofactor addition, cell pellets were treated in the same way applying KP<sub>i</sub> buffer supplemented with varying concentrations of NAD<sup>+</sup> (0, 10, 20 & 30 mmol L<sup>-1</sup>).

**Table 4 Concentrations of agents used for permeabilization of *E. coli* whole cells**

Agent	Concentration [%] (w/v)	
	0.1	1
toluene	0.1	1
Cetyltrimethylammoniumbromid (CTAB)	1	
polymyxin B sulfate	0.08	

### 3.3.2.5 Repeated Batch Operation

For investigation of operational catalyst stability, the standard reaction batch according to 3.3.2.3 was carried out applying CPCR2 whole cells in 4 mL scale. After 24 h operation, cells were pelleted and washed in 4 mL isopropanol of  $a_w = 83.6\%$ . Washed cells were pelleted again and replenished with fresh substrate solution for the next batch reaction. This procedure was repeated four times always using the same cells.

### 3.3.2.6 Deracemization of 1-phenylethanol

For deracemization of 1-phenylethanol to yield pure (*R*)-1-phenylethanol first asymmetric oxidation with (*S*)-selective CPR2 whole cells was performed followed by reduction using the (*R*)-selective LbADH catalyst. Herein, the standard reaction as described in 3.3.2.3 was carried out in 4 mL scale. For oxidation, 1-phenylethanol as substrate and acetone as cosubstrate were mixed with CPR2 whole cell catalyst. For the reduction, the final mixture from the oxidation reaction was supplemented with isopropanol as cosubstrate and LbADH whole cells according to 3.3.2.3. At certain time points, additional cosubstrate (acetone in oxidation mode and isopropanol in reduction mode) was added or completely removed by evaporation. After evaporation (150 rpm, 40 °C, 100 mbar in IKA® RV10 evaporator), the remaining mixture was replenished with the appropriate cosubstrate to continue the reaction.

**Table 5** Conditions for gas chromatographic separation of ketone/alcohol pairs and typical retention times. AcPh stands for acetophenone and PhEt for phenylethanol. AcAc is short for acetoacetate and But is an abbreviation for butyrate.

substrate/product pair	column	N <sub>2</sub> pressure [kPa]	temperature profile	retention time [min]
3-butyln-2-one / 3-butyln-2-ol	ChiraSil-DEX CB	50	initial: 80 °C, 11 min gradient: 70 °C min <sup>-1</sup> hold: 150 °C, 4 min	3-butyln-2-one 4.5 ( <i>R</i> )-3-butyln-2-ol 8.3 ( <i>S</i> )-3-butyln-2-ol 8.6
2-butanone / 2-butanol	ChiraSil-DEX CB	40	Initial: 60 °C, 14 min gradient: 70 °C min <sup>-1</sup> hold: 180 °C, 4 min	2-butanone 7.8 ( <i>R</i> )-2-butanol 13.6 ( <i>S</i> )-2-butanol 13.9
Cyclohexanone / cyclohexanol	FS-Cyclo DEX beta I/P	50	Initial: 70 °C, 4 min gradient: 70 °C min <sup>-1</sup> hold: 120 °C, 0 min	cyclohexanone 7.0 cyclohexanol 7.7
2-octanone / 2-octanol	ChiraSil-DEX CB	55	Initial: 90 °C, 25 min	2-octanone 16.6 ( <i>R</i> )-2-octanol 21.8 ( <i>S</i> )-2-octanol 22.4
p-Cl-AcPh / p-Cl-PhEt	ChiraSil-DEX CB	70	Initial: 140 °C, 0 min gradient: 1 °C min <sup>-1</sup> hold: 65 °C, 0 min	p-ClAcPh 10.7 ( <i>R</i> )-p-ClPhEt 17.5 ( <i>S</i> )-p-ClPhEt 18.5
Et-4-Cl-AcAc / Et-4-Cl-3-OH-But	ChiraSil-DEX CB	70	Initial: 100 °C, 4 min gradient: 70 °C min <sup>-1</sup> hold: 120 °C, 15 min	Et-4-Cl-AcAc - ( <i>S</i> )-Et-4-Cl-3-OH-but 19.6 ( <i>R</i> )-Et-4-Cl-3-OH-but 18.0
AcPh / 1-PhEt	ChiraSil-DEX CB	70	Initial: 120 °C, 10 min	AcPh 4.7 ( <i>R</i> )-1-PhEt 6.4 ( <i>S</i> )-1-PhEt 6.8
AcPh / 1-PhEt	FS-Cyclo DEX beta I/P	70	Initial: 120 °C, 22 min	AcPh 10.5 ( <i>R</i> )-1-PhEt 19.5 ( <i>S</i> )-1-PhEt 205

### 3.3.2.7 Chiral Gas Chromatography

Determination of conversion and selectivity of all substrates and products after operation the neat substrate system were performed by gas chromatography using a Hewlett Packard 5890 series II chromatograph equipped with chiral columns (FS-CycloDEX beta-I/P, CP-ChiraSil-DEX CB) and nitrogen as carrier gas. Protocols were developed to separate substrates from cosubstrate and

products. Special emphasis was laid on separation and assignment of the two enantiomers utilizing authentic commercial standards. Temperature profiles, pressures and typical retention times are listed in Table 5. The compounds 2-octanol and ethyl-4-chloro-3-hydroxy-butyrate (Et-4-Cl-3-OH-But) had to be derivatized to achieve satisfactory separation of the enantiomers. Derivatization was done using N-methyl-N-trimethylsilyl-trifluoroacetamide (MSTFA, Merck) in 10x molar excess and heating to 80 °C for 20 min.

Conversion and enantiomeric excess were calculated by comparison of the corresponding peak areas obtained from the chromatograms according to the equations in 2.3.1.

### 3.3.3 Results and Discussion

3.3.3.1 Application of Three Different ADHs in Neat Substrates and Effect of Water Activity ( $a_w$ ) Together with CPCR2, here, also alcohol dehydrogenases from *Lactobacillus brevis* (LbADH) as well as *Rhodococcus erythropolis* (ReADH) both overexpressed in *E. coli*, were applied in pure acetophenone and isopropanol in 1:9 volumetric ratio. The different whole cell catalysts were equilibrated via vapour phase to different water activities ( $a_w$ ) according to Greenspan.<sup>[34]</sup>

Relative reactions rates were monitored for seven different  $a_w$ -values ranging from dry cells ( $a_w = 0\%$ ) to wet cells ( $a_w = 100\%$ ). Herein, for whole cell catalysts no initial reduction of acetophenone was detected when cells were dry, but reaction rates increased rapidly with increasing  $a_w$ . LbADH reached maximal reaction rate at  $a_w = 93.2\%$ ; whereas CPCR2 has highest reaction rate at  $a_w = 83.6\%$  and ReADH at  $a_w = 75.1\%$  (see Figure 1). With increasing  $a_w$ , reaction rate drops significantly for all three catalysts. The effect was less pronounced for LbADH since the relative reaction rate is still at 72 % for wet cells ( $a_w = 100\%$ ); whereas it is only 28 % for ReADH and 12 % for CPCR2, respectively.

It can be deduced that reduction of acetophenone with *E. coli* containing overexpressed ADHs in neat substrates is not limited to CPCR2, but that the concept is rather applicable to at least two additional, if not more, ADHs. Herein, LbADH is most different from CPCR2 and ReADH since it is NADPH-dependent and exhibits *anti*-Prelogs' specificity.<sup>[15b]</sup>

The increase in catalytic activity with increasing  $a_w$  is most likely linked to overexpressed enzyme, which needs a critical amount of water to become active in organic medium as reported for many other enzymes<sup>[35]</sup> or whole cell catalysts at low water concentrations.<sup>[36]</sup>

The decrease in reaction rate at higher  $a_w$ -values is possibly due to catalyst inactivation, since the progression curves indicate that the reaction stopped within the first 7 hours for higher  $a_w$ -values of 93 % and 100 % for ReADH and CPCR2 (data not shown). Also for *E. coli* swelling of cells was reported for  $a_w > 90\%$  possibly leading also to influx of isopropanol and acetophenone inactivating the enzyme inside the cell.<sup>[37]</sup>

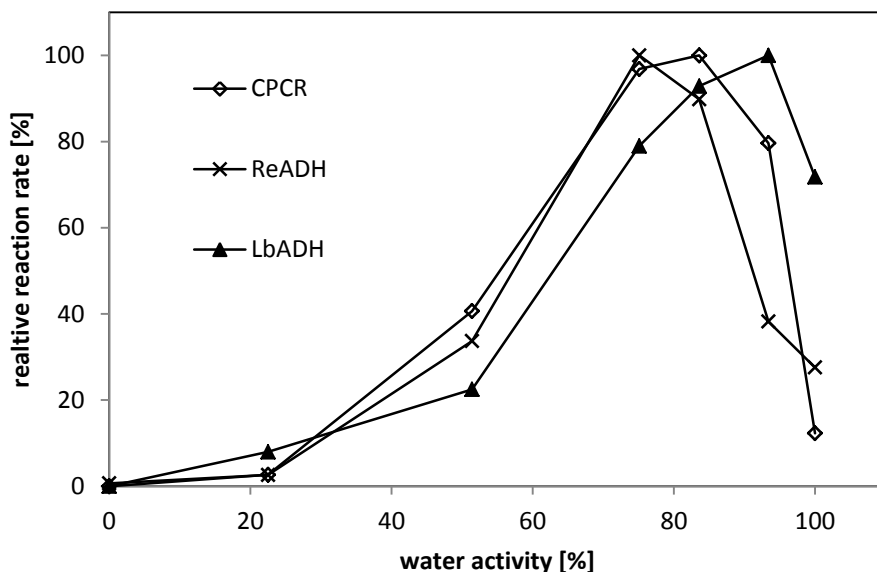


**Figure 1** Dependence on water activity of the three different ADH whole cell catalysts in neat substrates.

Lyophilized *E. coli* in isooctane showed a similar response for transesterification activity versus  $a_w$  with a recombinant lipase.<sup>[38]</sup> Herein, the decrease in conversion at high water concentration was explained by induction of diffusional limitations of the substrate and also preference for hydrolysis. Furthermore, optimal  $a_w$ -values were also identified in gas-solid reactions with *Saccharomyces cerevisiae* and *Rhodococcus erythropolis* as reductive whole cell catalysts.<sup>[36a, 36c]</sup> Viability of *E. coli* cells was not examined in this system; however, in gas-solid reactor lyophilized cells of *Rhodococcus erythropolis* did not survive but retained reducing activity.<sup>[36c]</sup>

### 3.3.3.2 Conversion of Structurally Diverse Ketones & Stereoselectivity of the Alcohols

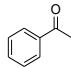
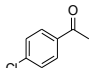
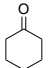
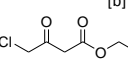
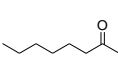
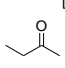
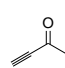
To demonstrate the broad applicability of asymmetric reduction in neat substrates, structurally diverse ketones were selected and used with the three whole cell catalysts. In Table 6 conversions of all substrates and the enantiomeric excess of the corresponding alcohols are listed. Biotransformations were carried out in the standard reaction conditions at optimum  $a_w$  as previously identified for the three individual whole cell catalysts (see Figure 1).

All tested substrates were accepted and converted in most cases to more than 80 % giving product concentrations of 50-100 g L<sup>-1</sup> (see Table 6). Differences in final conversion may be due to varying position of equilibrium or differences in activity of the individual enzymes towards the substrates. In principle, it is possible to obtain 100 % conversion by removal of the co-product acetone and replenishment of cosubstrate as reported previously (see 3.2.3, Figure 2).<sup>[13a]</sup> Conversion of cyclohexanone was described for the first time for CPR2 and ReADH (see Table 6). Additionally, for ReADH asymmetric reduction 3-butyne-2-one was not reported previously but showed high conversion. For 2-butanone reduction, 2-pentanol was successfully applied instead of isopropanol for

cofactor regeneration, demonstrating the variability of the system with respect to the ancillary cosubstrate. Inhibition phenomena like substrate or product inhibition were never observed.

Taken together, Table 6 illustrates that the newly developed reaction system is capable of reducing a whole array of structurally diverse ketones. Hence, it can be expected that the substrate scope determined for the three employed ADHs, can be fully exploited in this system.

**Table 6 Conversion & enantioselectivity (*ee* meas.) of structurally different substrates by LbADH, ReADH and CPR2 whole cell catalysts in neat substrates. Literature values of enantiomeric excess (*ee* lit.) for asymmetric reduction of the substrates in aqueous systems are presented as well.**

Substrates <sup>[a]</sup>								
LbADH <sup>[d]</sup>	conversion [%]	61	88	99	>80	97	85	80
	<i>ee</i> meas. [%]	>99 <i>R</i>	97.5 <i>R</i>	-	>99 <i>S</i>	>99 <i>R</i>	>1.4 <i>R</i>	46.6 <i>R</i>
	<i>ee</i> lit. [%]	>99 <i>R</i> <sup>[39]</sup>	>99 <i>R</i> <sup>[40]</sup>	- <sup>[41]</sup>	>99 <i>S</i> <sup>[40]</sup>	>99 <i>R</i> <sup>[42]</sup>	35 <i>R</i> <sup>[43][g]</sup>	60 <i>R</i> <sup>[14]</sup>
ReADH <sup>[e]</sup>	conversion [%]	50	86	99	>80	97	84	79
	<i>ee</i> meas. [%]	>99 <i>S</i>	>99 <i>S</i>	-	>99 <i>R</i>	>99 <i>S</i>	>0.4 <i>S</i>	42.8 <i>R</i>
	<i>ee</i> lit. [%]	>99 <i>S</i> <sup>[44]</sup>	>99 <i>S</i> <sup>[20]</sup>	-	>99 <i>R</i> <sup>[45]</sup>	>99 <i>S</i> <sup>[44]</sup>	- <sup>[45b]</sup>	-
CPCR2 <sup>[f]</sup>	conversion [%]	50	64	90 (-)	>80	83	79	64
	<i>ee</i> meas. [%]	>99 <i>S</i>	>99 <i>S</i>	-	>99 <i>R</i>	>98 <i>S</i>	>62 <i>S</i>	>99 <i>S</i>
	<i>ee</i> lit. [%]	>99 <i>S</i> <sup>[46]</sup>	-	-	>99 <i>R</i> <sup>[47]</sup>	>99 <i>S</i> <sup>[48]</sup>	>99 <i>S</i> <sup>[49][h]</sup>	49 <i>S</i> <sup>[14][i]</sup>

<sup>[a]</sup>ratio of substrate to isopropanol 1:9, reaction times 48-144h <sup>[b]</sup>nomenclature reversed due to CIP rules

<sup>[c]</sup>2-pentanol was used instead of isopropanol <sup>[d]</sup>*a<sub>w</sub>* = 92.3 %, <sup>[e]</sup>*a<sub>w</sub>* = 75.1 %, <sup>[f]</sup>*a<sub>w</sub>* = 83.6 %

<sup>[g]</sup>measured with *E. coli* whole cells <sup>[h]</sup>*ee* determined in microemulsion system <sup>[i]</sup>measured with *Candida* lysate

In general, enantiomeric excess of the aromatic alcohols as well as for ethyl 4-chloro-3-hydroxybutanoate and 2-octanol observed in this system are >98 % and hence, as good as reported for isolated enzymes in aqueous systems (see *ee* lit. in Table 6). This supports the assumption that the whole cell catalysts performed in neat substrates at defined low water concentration in the same way as the isolated enzymes in dilute buffer. It can be speculated that the host ADHs are inhibited by the high concentration initial of isopropanol and are therefore not affecting *ee*.

For small substrate such as 2-butanone and 3-butyn-2-one; however, *ee*-values deviate from values reported in literature (see Table 6). For 2-butanone all *ee*-values found in neat substrates are significantly smaller than obtained in buffer systems. Stereoselectivity for (*R*)-3-butyn-2-ol was slightly reduced for LbADH but significantly increased for CPR2 and reverted for ReADH. These findings indicate that for small substrates the presence of high amounts of substrates and cosubstrates as well as the low water concentration greatly influence stereoselectivity.

It has been reported for other ADHs in non-conventional media that stereoselectivity can be affected by the reaction medium as well as by the water activity of the system. For example, ADH from *Thermoanaerobium* KET4B1 changed *ee* in a range of 23-65 % depending on type and concentration of co-solvents for 2-butanone reduction.<sup>[50]</sup> Furthermore, stereoselectivity of ADHs from *Thermoanaerobacter ethanolicus* and *Sporobolomyces salmonicolor* were reported to be dependent

on the co-solvents.<sup>[51]</sup> A strong increase in enantioselectivity was detected with increasing  $a_w$ -values for an ADH from *Thermoanaerobium brockii* in hexane, converting 2-pentanone with 2-butanol as cosubstrate.<sup>[35c]</sup> However, when approaching  $a_w = 83.6\%$  at 25 °C enantioselectivity dropped again. For LbADH, in particular, racemization was reported for 2-butanol in aqueous buffer depending on the enzyme preparation, substrate and cosubstrate concentration as well as on reaction time.<sup>[52]</sup> Nevertheless, *ee*-values for (*R*)-2-butanol of 95 % with LbADH could be obtained by application of a biphasic system and optimization of reaction conditions.<sup>[15b, 52-53]</sup> The same enzyme showed varying *ee*-values (33-43 % *R*) for reduction of 600 mmol L<sup>-1</sup> 2-butanone depending on the type and amount of co-solvent used.<sup>[43]</sup> LbADH employed in the here developed system produces almost racemic 2-butanol (see Table 6) indicating that reaction conditions are not appropriate for selective reduction. The *ee* might be influenced by  $a_w$  or substrate concentration. Hence, performance of the whole cell catalyst at different  $a_w$ -values has to be investigated as well as the impact of the cosubstrate and substrate concentrations, for instance by substrate dosing. If the *ee* is time-dependent, a tighter sampling has to be carried out to resolve this. Here, only the end conversion after 48h was recorded.

The effect on *ee* with 2-butanone as substrate was examined more closely for the model enzyme CPCR2. Herein, the *ee*-value of whole cells with overexpressed CPCR2 was determined in aqueous buffer (see Table 7, entry 2) and compared to the *ee* obtained in neat substrates (see Table 7, entry 1). Additionally, CPCR2 was purified and used in aqueous buffer and 50 mmol L<sup>-1</sup> 2-butanone according to 2.3.1 (see Table 7, entry 4).

**Table 7 Enantiomeric excess of 2-butanone with CPCR2 in different reaction systems after 48h.**

entry	catalyst	substrate	medium	<i>ee</i> -value
1	<i>E. coli</i> whole cells with overexpressed CPCR2	1.12 mol L <sup>-1</sup>	isopropanol, 2-butanone, ratio 9:1 (v/v)	62 % <i>S</i>
2	<i>E. coli</i> whole cells with overexpressed CPCR2	0.45 mol L <sup>-1</sup>	0.1 mol L <sup>-1</sup> KP <sub>i</sub> (pH 6.8), 5 % (v/v) isopropanol	37 % <i>S</i>
3	<i>E. coli</i> whole cells with empty vector	0.45 mol L <sup>-1</sup>	0.1 mol L <sup>-1</sup> KP <sub>i</sub> (pH 6.8), 5 % (v/v) isopropanol	no reaction
4	purified enzyme	0.05 mol L <sup>-1</sup>	0.1 mol L <sup>-1</sup> triethanolamine (pH 8.0), 2.5 % (v/v) isopropanol, 1 mmol L <sup>-1</sup> NADH	>99 % <i>S</i>

Purified CPCR2 was able to convert 2-butanone with high enantioselectivity (*ee* >99 % *S*, see Table 7, entry 4), which is consistent with values found in literature.<sup>[49, 54]</sup> When overexpressed in whole cells of *E. coli*; however, *ee*-values are significantly lower; whereas cells containing only empty vector did not show 2-butanone conversion under the tested conditions as displayed in Table 7 in entry 3. These results imply that host ADHs do not interfere with the reaction but that the CPCR2 enzyme cannot perform optimal in conditions present in the whole cell approaches. As reported for LbADH, stereoselectivity may also be dependent on substrate concentration, which was 1.12 mol L<sup>-1</sup> in the

neat substrate system (see Table 7, entry 1) and 0.45 mol L<sup>-1</sup> in aqueous buffer (see Table 7, entry 2), respectively. High *ee*-values; however, were obtained with comparably low substrate concentrations like 0.05 mol L<sup>-1</sup> as applied with purified CPCR2 (see Table 7, entry 4) or 0.001 mol L<sup>-1</sup> as reported previously.<sup>[49]</sup> Hence, for obtaining high *ee* for 2-butanol, reaction conditions might be optimized towards lower substrate loads for instance by setup of a continuous reaction system with constant low 2-butanone concentration but high productivities. Otherwise, influences of water activity, reaction time and cosubstrate on *ee* might be investigated as well.

For reduction of 3-butyn-2-one, CPCR2 exhibits excellent stereoselectivity (>99 % *S*) in the neat substrate system (see Table 6 and <sup>[13a]</sup>); whereas crude *Candida* lysate exhibits an *ee* of only 49 % *S* (see Table 6). This finding was already discussed in chapter 3.2.2. For LbADH, selectivity was moderate in aqueous buffer and in neat substrates with 60 % *R* and 46 % *R*, respectively. However, selectivity is higher in buffer systems. For ReADH, a reversion of stereoselectivity was observed, since it was expected that (*S*)-3-butyn-2-ol would be produced but (*R*)-3-butyn-2-ol was detected with *ee* of 42.8 % (see Table 6). Inversion of stereoselectivity was, as yet, not observed for ReADH in any reaction medium. However, it is the first time that conversion of this compound was reported for ReADH, and hence, a substrate-size induced reversion of stereospecificity is possible as found for ADH from *Thermoanaerobium Brockii*.<sup>[55]</sup>

Some effects on stereoselectivity in non-conventional media have been reported for yeasts used as reductive whole cell catalyst. When operated in pure benzene, bakers' yeast showed reverse selectivity, which was explained by variation of the *K<sub>m</sub>*-values by the solvent of two or more concurrently active enzymes.<sup>[24]</sup> Furthermore, lyophilization of the yeasts *Zygosaccharomyces rouxii* and *Debaryomyces hansenii* affected stereoselectivity after reduction of ketones in comparison to non-lyophilized cells wherein inactivation of substrate-competing oxidoreductases were thought to account for the detected differences.<sup>[56]</sup> However, these effects can be ruled out here, since *E. coli* enzymes seem not to convert 2-butanone under the conditions in neat substrates (see Table 7, entry 3).

In sum, the newly developed reaction system comprised of just substrates and lyophilized whole cell catalyst, exhibit high conversions for all tested ketones and retained high stereoselectivity for most of the tested substrates. These findings make this method for ketone reduction a valuable tool for production of chiral alcohols in high concentrations. However, especially for small ketones enantioselectivity was not sufficiently high for industrial demands (*ee* >95 %). From literature, it turns out that for CPCR2 and LbADH stereoselectivity for production of 2-butanol might be dependent on the substrate load or time.<sup>[17, 49, 53-54]</sup> Thus, *ee* can be optimized by reaction engineering for instance by establishment of a continuous operation mode or substrate dosing.

### 3.3.3.3 Mass Transfer Limitations of the Reaction System

Asymmetric ketone reduction is preferably carried out in whole cells since the expensive nicotinamide cofactors are supplied and recycled by the cell. This advantage is economically most relevant, but the cell as “reaction vessel” can inhibit effective mass transfer of products and substrates.<sup>[27a, 57]</sup> The cell membrane provides a natural barrier for mass transfer and leads to decreased space time yields in whole cell biocatalysis. For *E. coli* used as whole cell biocatalyst for oxidation of cyclic ketones, mass transfer of cyclohexanone across the membrane was identified as the major rate limiting step and not enzyme performance or NADH availability.<sup>[29]</sup> However, for the neat substrate system used here, *E. coli* whole cells are lyophilized prior use and lyophilization was found to make the cytoplasmic membrane permeable.<sup>[58]</sup> This would reduce mass transfer limitations. Nevertheless, the cell envelope seems to be still intact enough to protect cofactors and enzyme from leaching, as the catalyst is active in the system for more than 14 days (see 3.2.3 Figure 2).

The problem of mass transfer limitation can be alleviated by permeabilization of the *E. coli* cells using different agents. Herein, organic solvents are used since decades to promote mass transfer.<sup>[57b, 59]</sup> Also detergents<sup>[38, 60]</sup> and antibiotics<sup>[61]</sup> have been applied for this purpose as well as mechanical methods.<sup>[62]</sup> Interestingly, isopropanol, applied here as cosubstrate, was shown to have a permeabilizing effect on the yeast *Trichosporon brassicae* increasing biocatalytic activity.<sup>[62]</sup>

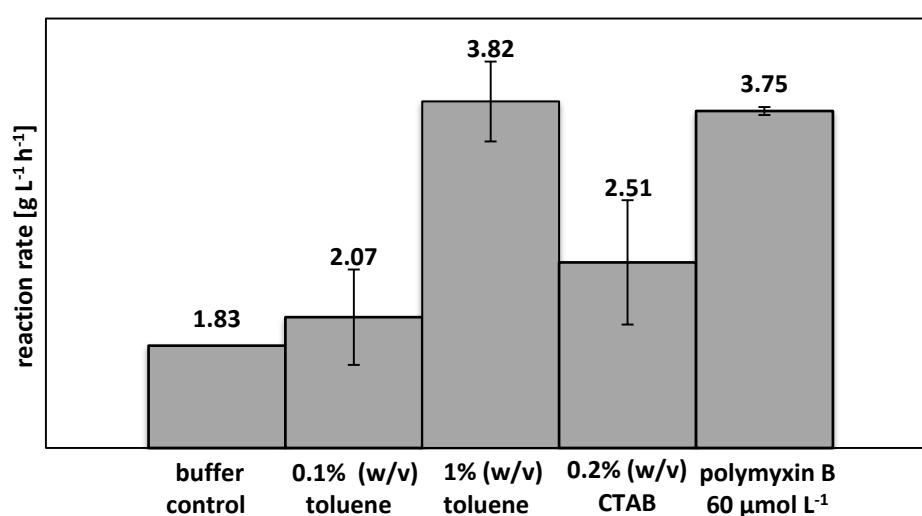
Herein, two rather low concentrations of toluene (0.1 % & 1 % (w/v)) were chosen since it was reported that *E. coli* whole cells treated with this organic solvents significantly increased reaction rate in asymmetric ketone reduction.<sup>[63]</sup> Furthermore, the cationic detergent cetyl trimethylammonium bromide (CTAB) was applied at 0.2 % (w/v)<sup>[60b]</sup>, since treatment with this agent dramatically increased initial rate and final conversion in setup with horse liver ADH and NADH-dependent hydrogenase in gram-negative bacteria.<sup>[60a]</sup> Rate enhancement was also observed for other biotransformations using CTAB-permeabilized *E. coli* whole cells.<sup>[38, 64]</sup> At last, the antibiotic polymyxin B sulfate targeting the cell wall of gram-negative microorganisms was used. This agent is reported to act like a detergent by making the cell wall more permeable.<sup>[65]</sup> The compound was used with *E. coli* whole cells to facilitate mass transfer of substrates across the membrane in reduction of aromatic ketones<sup>[61b]</sup> and a whole-cell screening assay.<sup>[61a]</sup>

Figure 2 displays the influence of cell permeabilization on the initial reaction rate in acetophenone reduction in the neat substrate system. Notably, permeabilization in general resulted in an increase of reaction rates; hence, no substantial enzyme or cofactor leaching took place as a consequence of membrane perforation. Alteration in stereoselectivity was not detected for any additive.



Toluene at 1 % (w/v) and polymyxin B sulfate represent effective permeabilizers, since reaction rates could be improved by more than twofold. The cationic detergent CTAB was shown to slightly increase reaction rate; however, deviation is high. No significant increase was detected for 0.1 % (w/v) toluene addition.

The outer membrane is the most effective mass transfer barrier for small hydrophobic molecules such as acetophenone.<sup>[28]</sup> As toluene, CTAB and polymyxin B sulfate mainly target the LPS layer of the outer membrane of gram negative bacteria a positive effect on initial reaction rates is not surprising.<sup>[59, 60b, 66]</sup> However, especially the treatment with toluene may have some negative effects such as cofactor leaching.<sup>[63a, 63c, 67]</sup>



**Figure 2** Reaction rate in pure isopropanol and acetophenone (ratio 9:1) with *E. coli* whole cells overexpressing CPCR2 after treatment with different permeabilizing agents.

These findings indicate that the system is limited by mass transfer phenomena and that cell permeabilization with 1 % (w/v) toluene or 60 μmol L<sup>-1</sup> polymyxin B constitutes an effective method to improve initial reaction rates. Twofold improvement of reaction rate is significant; though, further increase might be achieved by optimizing the permeabilizing process.

#### 3.3.3.4 Cofactor Limitations of the Reaction System

To examine, whether the reaction system is limited by the amount of cofactor available, cells were resuspended in NAD<sup>+</sup> containing solution prior to lyophilization. The effect of NAD<sup>+</sup> addition was interpreted on the basis of initial reaction rates in the reaction system with acetophenone and isopropanol and results are depicted in Figure 3.

Resuspension of the whole cell biocatalyst in NAD<sup>+</sup>-solution displayed a clear positive response as reaction rate almost linearly increased upon cofactor addition (see Figure 3). The reaction rate could

be improved 2.7-fold for 30 mmol L<sup>-1</sup> NAD<sup>+</sup> relative to the system with untreated cells. The trend observed for further cofactor addition tends to saturation. Stereoselectivity was not affected.

This observation supports the idea that cofactor concentration limits the performance of the system. Intracellular cofactor levels were not determined and it is also not clear how much of the supplied NAD<sup>+</sup> was imported to the cells. However, one possible explanation for the observed trend is that basal cofactor levels are beyond  $K_m$  of CPCR2 and addition lead to an increase in reaction velocity according to Michealis-Menten kinetics (see Figure 3).<sup>[68]</sup>

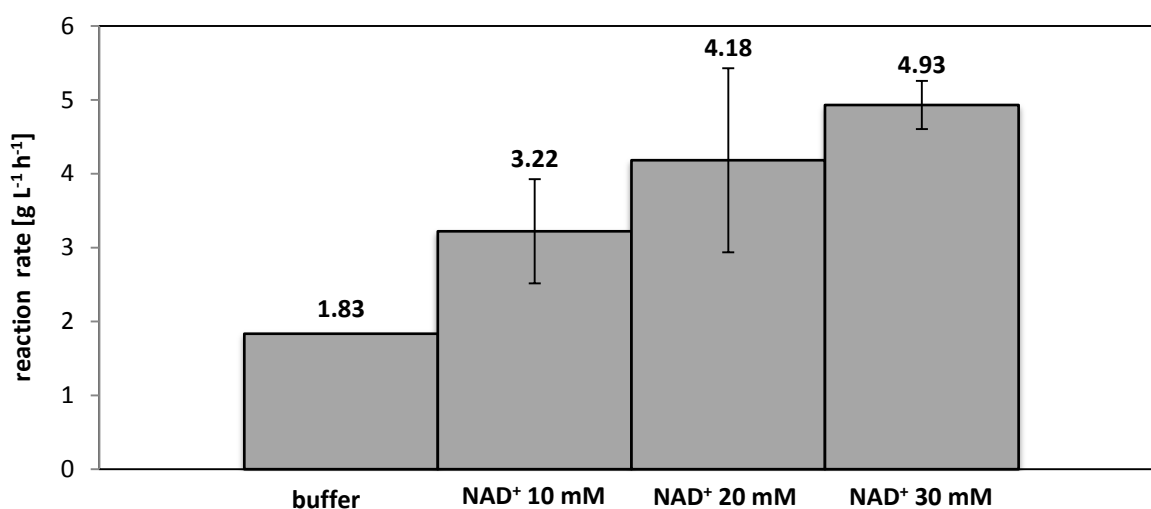


**Figure 3** Reaction rate in pure isopropanol and acetophenone (ratio 9:1) with *E. coli* whole cells overexpressing CPCR2 after resuspension in NAD<sup>+</sup>-solutions.

The basal level of NADH in resting *E. coli* cells was reported to be around 1000 μmol L<sup>-1</sup><sup>[29]</sup> and  $K_m$  of free CPCR2 being 38 μmol L<sup>-1</sup> for NADH and 77 μmol L<sup>-1</sup> for NAD<sup>+</sup>, respectively.<sup>[17]</sup> Hence, the free enzyme would be most likely saturated with cofactor and exhibit maximum velocity. However, for ketone reduction with *E. coli* whole cells, addition of 1 mmol L<sup>-1</sup> cofactors resulted in significant rate acceleration as reported by Weckbecker *et al.*<sup>[67]</sup> Herein, an NADPH-dependent ADH and an NADH-dependent formiate dehydrogenase (FDH) for cofactor recycling were employed exhibiting  $K_m$  (NADPH) = 140 μmol L<sup>-1</sup> for the ADH and  $K_m$  (NAD<sup>+</sup>) = 90 μmol L<sup>-1</sup> for FDH, respectively. Hence, local concentration of cofactors at the enzymes might be different from the determined values of the whole cells and the apparent  $K_m$  of the whole cell catalyst might also be increased. The latter phenomenon has been reported for *E. coli* cells overexpressing a tryptophanase, wherein the  $K_m$  of the whole cell was about ten times higher than  $K_m$  of the isolated enzyme.<sup>[69]</sup>

Nevertheless, cofactor in the neat substrate system is recycled by the same enzyme, which is also carrying out the reduction of the prochiral ketone employing ancillary cosubstrate. For further increasing productivity of the reaction system, enzyme-coupled cofactor regeneration might be

established. For this, a “designer cells” can be developed expressing a synthetic-ADH with reduction preference and a regeneration-ADH utilized to reduce the NAD(P)<sup>+</sup> cofactor.<sup>[4b]</sup> Such systems have already been shown to be superior to other cofactor regenerating approach.<sup>[61b, 67, 70]</sup>

### 3.3.3.5 Influence of Temperature on the Reaction System

The influence of reaction temperature on the reaction rate of the neat substrate system was analyzed by conducting the standard reaction setup with *E. coli* overexpressing CPCR2. Here, three temperatures 30 °C, 40 °C and 50 °C were chosen and relative reaction rates are plotted in Figure 4.

So far, for a standard setup 30 °C was chosen as reaction temperature and among the selected temperatures, it displayed the highest reactions rate (see Figure 4). Running the reaction at 40 °C resulted in slightly reduced reaction rate but at 50 °C productivity was decreased by 90%. Stereoselectivity was again not affected.

Biocatalysis at elevated temperatures is usually a tradeoff between catalyst stability and activity. Like most chemical reactions, the rate of an enzyme-catalyzed reaction increases as the temperature is raised. The rate rises up to a catalyst-specific temperature optimum, which is 36-40 °C for reduction by CPCR2<sup>[13c]</sup>, and declines due to catalyst degradation or enzyme denaturation. Most enzymes from mesophilic hosts, like the yeast *Candida*, denature at temperatures >40 °C as seen for the temperature profile for purified CPCR2.<sup>[13c]</sup> Hence, one reason for the observed trend is the thermal denaturation of CPCR2 in the *E. coli* whole cells; however, after 24h reaction catalyst activity was still detectable at 50 °C.

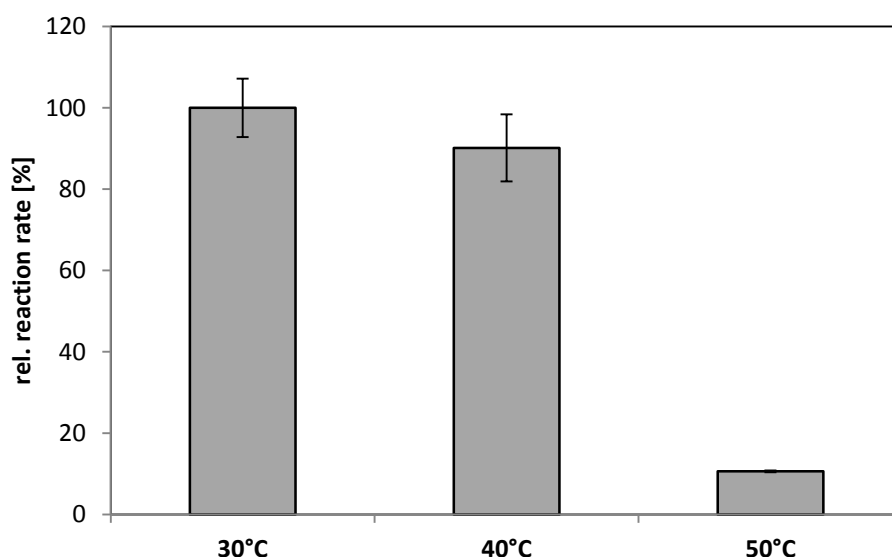


**Figure 4** Relative reaction rates in pure isopropanol and acetophenone (ratio 9:1) with *E. coli* whole cells overexpressing CPCR2 operated at different temperatures for 24h.

As the CPCR2 is enclosed in the cell and protected against hazardous conditions in the exterior, also the cell stability at elevated temperatures has to be taken into account. Furthermore, the response to temperature of a whole cell catalyst compared to the isolated enzyme may be different as shown for ADH from *Rhodococcus ruber* in *E. coli*. In this work, ketone reduction with previously lyophilized *E. coli* cells was carried out at 19 % (v/v) isopropanol and a sharp drop in activity was observed at reaction temperatures just above 40 °C.<sup>[71]</sup> However, optimal temperature of the isolated ADH was determined to be 65 °C indicating that the microbial host dictates stability.<sup>[71]</sup> These results are in accordance with the temperature profile observed in neat substrates (see Figure 4).

The loss of enzymatic activity of *E. coli* at temperatures higher than 40 °C can be explained by melting of the cell membranes, which was investigated previously by differential scanning calorimetry.<sup>[72]</sup> The cell membrane comprises an effective protective barrier against uptake of organic molecules, such as isopropanol or acetophenone.<sup>[28]</sup> Thus, thermal destruction of the membrane integrity may lead to influx of these compounds into the cell finally resulting in enzyme deactivation. In contrast, optimum temperature for an *E. coli* whole cell catalyst harboring a mesophilic hydantoinase was found to be 55 °C; however, they did not state reaction times.<sup>[73]</sup>

### 3.3.3.6 Operational Stability of the Catalyst in the Reaction System

Catalyst stability under process conditions is one of most important parameters for implementation of a biocatalytic synthesis route in industrial scale.<sup>[5a, 30]</sup> Therefore, catalyst stability was assayed in the standard reaction system by performing five consecutive reactions and recycling the cells, which is also known as repeated batch operation mode.

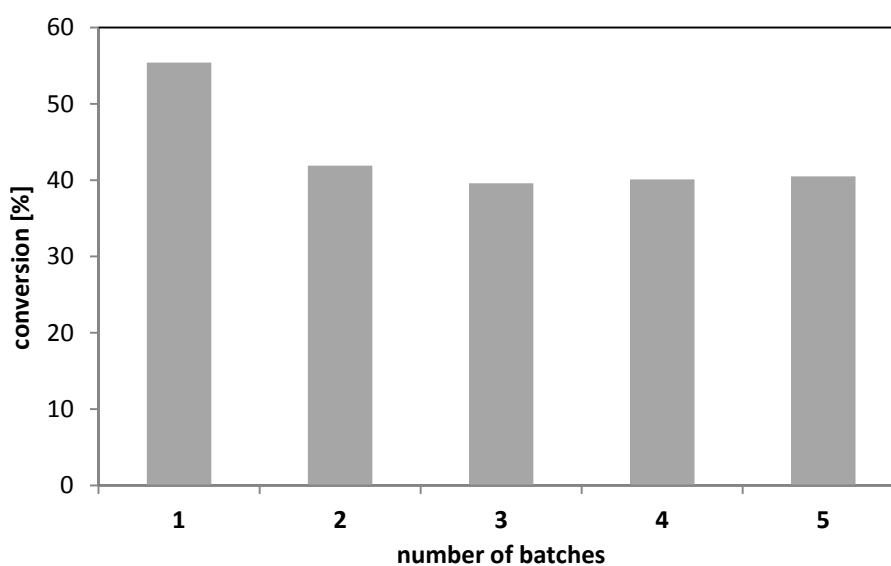


**Figure 5** Operational stability of the whole catalyst in the standard reaction system in repeated batch mode. Reactions were terminated after 24h and cells were washed with isopropanol prior to addition of fresh reaction solution.

As Figure 5 depicts, final conversion is decreasing only after the first batch and remains constant for the following batches. From this result an excellent operational stability can be inferred, since final conversion dropped only from 55.4 % to 40.5 % in five days. The initial loss in catalytic activity after the first day of operation may be explained by inactivation of cells, which were not optimally conditioned by lyophilization and  $a_w$ -equilibration. These cells were then inactivated within the first 24 h and did not contribute to conversion in the following batches. High stability was already implied previously when cells were operated in the system for 14 days still showing activity (see 3.2.3 Figure 2).

Gratifyingly, catalyst stability is high; however, for catalyst loads in the neat substrate system were rather high (50-200 g cell dry weight L<sup>-1</sup>), depending on activity and expression level of the ADHs applied. For industrial processes, a ratio of substrate to catalyst of >20 (better >50<sup>[1]</sup>) is demanded to reduce costs and promote downstream processing.<sup>[74]</sup> For the neat substrate system, substrate loading up to 500 g L<sup>-1</sup> was demonstrated (see 3.2.3) leading to substrate to catalyst ratios ranging from 2.5 to 10, is close to the benchmark. By demonstration of high operational stability, it is possible to reuse the cells, thereby drastically reducing catalyst costs. Furthermore, expression levels can be increased as well as pre-treatment of the cells to preserve as much biocatalytic activity as possible.

### 3.3.3.7 Sequential Deracemization in Neat Substrates

The complete resolution of racemic alcohol or deracemization was carried out in the neat substrate system by applying (*S*)-selective CPCR2 and (*R*)-selective LbADH for production of (*R*)-1-phenylethanol from the racemate in sequential fashion. The first part of the reaction was the asymmetric oxidation of (*S*)-1-phenylethanol to acetophenone by driving the NAD<sup>+</sup>-regeneration by acetone. In this case, the (*R*)-enantiomer remains untouched since CPCR2 is strictly (*S*)-selective. This reaction can only result in a maximum yield of 50 % of the desired enantiomer, as it is typical for racemic resolution reactions. At high conversions the reaction mixture contains 50 % (*R*)-1-phenylethanol at high *ee* and nearly 50 % prochiral acetophenone. Hence, the reaction mixture can be subjected to an asymmetric reduction with (*R*)-selective LbADH and isopropanol for NADH regeneration. The biocatalyst converts acetophenone to (*R*)-1-phenylethanol leading to an overall maximum yield of 100 % with high *ee*. The concept is outlined in Figure 6.

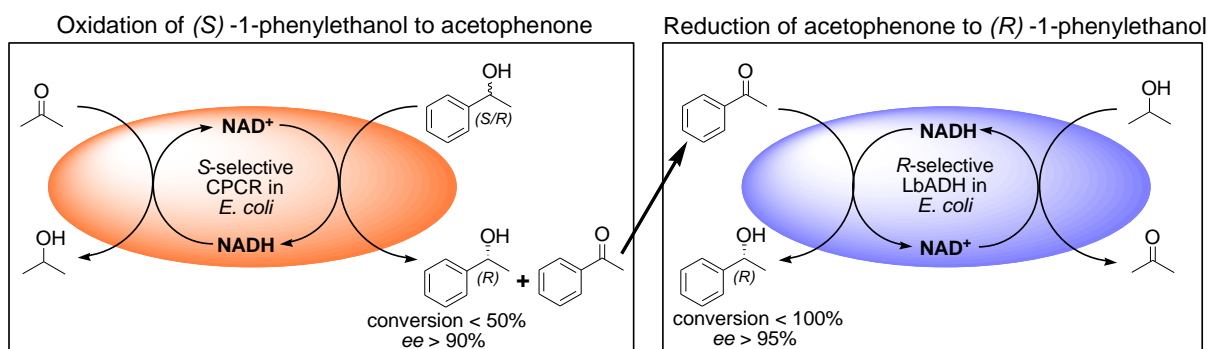


**Figure 6** Sequential deracemization of 1-phenylethanol by consecutive use of two whole cell catalysts with opposing stereoselectivity. Here, oxidation was performed first with (*S*)-selective CPR2 and afterwards reduction was carried out with (*R*)-selective LbADH

As displayed in Figure 7, oxidation of (*S*)-1-phenylethanol by the CPR2 whole cell biocatalyst progressed well within the first five days but approached equilibrium conditions after accumulation of ~40 % acetophenone. Fresh pre-equilibrated acetone was replenished after 5 and 9 days (see Fig. 7, evaporation steps #1 and #2). Thereby, a new driving force was established to achieve high conversions. After 13 and 18 days the substrate to cosubstrate ratio was increased from 1:9 to 1:18 for the same reason (see Fig. 7, evaporation steps #3 and #4). After 21 days, only 1.54 % of the unwanted (*S*) enantiomer was left and *ee* of 94.1 % for (*R*)-1-phenylethanol was achieved. The thermodynamic driving force at the end of the reaction is very weak and in ten days of operation only 1.44 % of the unwanted Oxidation with CPR2 converts Reduction with LbADH te that all remaining (*S*)-1-phenylethanol, which is not oxidized to acetophenone, will lower the final *ee* after reduction in sequential deracemization. Hence, highest conversion in the first oxidation step is demanded.

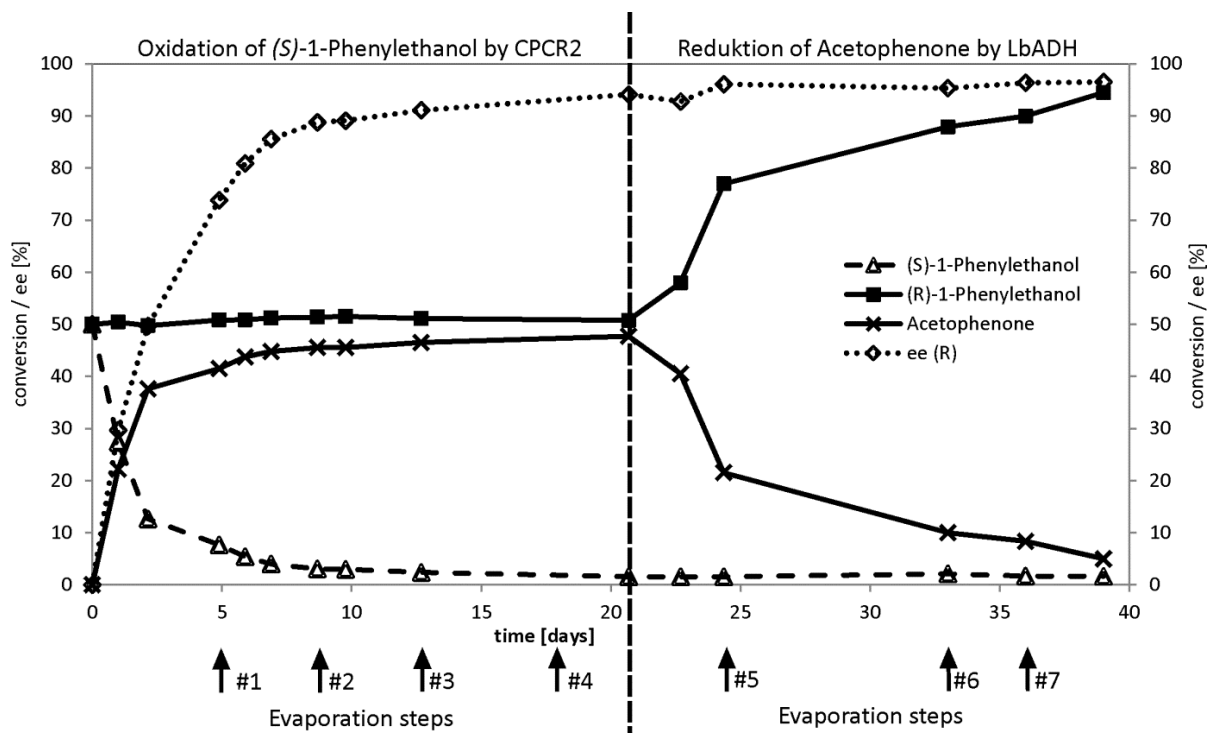


**Figure 7** Conversion and enantioselectivity of sequential deracemization of 1-phenylethanol. The arrows indicate removal of coproduct and replenishment with fresh cosubstrate.

For the reduction step, remaining acetone and isopropanol were removed by evaporation and the resulting mixture of acetophenone and (*R*)-1-phenylethanol was replenished with fresh pre-equilibrated isopropanol as cosubstrate. As whole cell catalyst, *E. coli* with overexpressed (*R*)-selective LbADH was applied. Figure 7 depicts fast initial reduction of acetophenone and further increase of *ee* within the first days. As for the oxidation, the reaction speed slowed down due to attainment of equilibrium conditions. Therefore, acetone as co-product was removed alongside with isopropanol by evaporation on day 24, 33 and 36 and fresh isopropanol was added (see Fig. 7, evaporation steps #5, #6 and #7). After 39 days of operation, 96.1 % of (*R*)-1-phenylethanol (96 g L<sup>-1</sup>) was yielded with *ee* = 96.5 %. Successful operation of each catalyst for about 20 days in neat substrates again illustrates the high process stability as previously shown in the repeated batch experiment (see Figure 5).

The results demonstrate that complete deracemization is possible by application of the neat substrate system with different catalysts of opposing stereoselectivity. Final conversion and *ee* are >95 % and hence, satisfying since they exceed the benchmarks regarded as relevant for industrial application. Furthermore, deracemization illustrates the versatility of the developed reaction system since the complete set of products can be obtained by smart combination of the biocatalysts, substrates and cosubstrates. As long as the catalysts exhibit reasonable activity and high, but opposing, stereoselectivity on a common substrate; a desired enantiomer can be manufactured from the ketone or the racemate.

As a concept, deracemization of 1-phenylethanol is a valid approach but the operation last 39 days, which is far too long to be attractive for industrial application. Hence, optimization is required and reaction engineering such *in-situ* product removal to retain a thermodynamic driving force might be applied. Furthermore, initial reaction rates may be increased by minimizing limitations like mass transfer or cofactor availability as identified previously in this work.

Deracemization of alcohols by was carried out before in versatile setups like *in vivo* deracemization employing two or only one microorganisms as native and recombinant host or *in vitro* deracemization using combinations of different isolated enzymes also together with chemical catalysts.<sup>[2b, 75]</sup>

Recently, combination of two microorganisms to deracemize alcohols was performed in one pot with *Microbacterium oxydans* ECU2010 and *Rhodotorula sp.* AS2.2241 or *Aspergillus niger* CCT 1435 and *Candida albicans* CCT 0776.<sup>[32, 76]</sup> Herein, one species carries out the oxidation whereas the other takes care of the stereoselective reduction. However, the enzymes responsible for the reactions are unknown and not overexpressed unlike the ADHs used in the here presented system. The knowledge about the identity of the active enzyme is very beneficial, since substrate scope as well as

stereoselectivity and possible limitations in application are already reported for the enzymes utilized here. Furthermore, since the enzymes are present in *E. coli* in recombinant form they can be produced easily on a large scale and high cell-specific activity with leads to high volumetric productivity.

So far, the reaction is performed in two steps, since if the two whole cell biocatalysts would be operated at the same time the net driving force of the reaction would be zero. However, a reaction setup with four enzymes able to perform one-pot one-step deracemization of alcohols was reported.<sup>[77]</sup> Herein, the different cofactor preference of the ADHs is exploited and regeneration of NADH and NADPH was driven by two separate enzymatic processes. In principle, this could also be achieved with the neat substrate system if the two ADHs exhibit strict preference for only one cosubstrate but accept the racemic alcohols to be deracemized. By driving the oxidation with only one ketonic cosubstrate and the reduction at the same time by the alcoholic cosubstrate the two reactions are decoupled. Such one-step one-pot approach would shorten reaction time; however, for high conversions fresh coproducts have to be removed to retain reasonable reaction rates.

### 3.3.4 Conclusion

The closer investigation of the neat substrate system first described in chapter 3.2 demonstrates that the principle of asymmetric ketone reduction with CPCR2 in *E. coli* whole cells can be transferred to other ADHs. The enzymes ReADH and LbADH performed in a similar way as CPCR2 and did not show inactivation or inhibition under the conditions tested. This opens the road to apply additional ADHs in this system like ADH from *Lactobacillus kefir*, horse liver ADH or ADH1 from bakers' yeast to broaden the scope to manufacture various enantiopure alcohols. Also different enzymes classes may be tested in this system since *E. coli* as lyophilized whole cell seems to be compatible with pure isopropanol, which can aid as effective solvent for organic molecules.

As the conversion of various benchmark substrates in the neat substrate system suggests, the full scope of the applied ADHs can be exploited. However, a severe limitation seems to be reduced stereoselectivity at elevated substrate concentrations as implied for the small ketones 2-butanone and 3-butanone. This problem might be addressed by to convey the neat substrate system to continuously operated reaction mode wherein the substrate concentration is kept low.

As several reaction parameters for the neat substrate were investigated, an optimized process can be envisaged wherein the reaction rate is increased by cell permeabilization and cofactor addition the optimal reaction temperature. For this, a substrate with high value-added corresponding product can be selected from the benchmark substrates exhibiting high conversion and selectivity such as 2-



octanone or 4-chloroacetoacetate. The ultimate goal would be to run a process at preparative kg-scale with substrate loads  $>100 \text{ g L}^{-1}$ , conversion and *ee*  $>99 \%$  in less than a day.

At last, the versatility of the neat substrate system by means of deracemization was demonstrated. The direction of reaction could be steered by the selection of cosubstrate to either promote oxidation with acetone or reduction with isopropanol. By smart combination of the catalyst and the reaction medium both enantiomers from ketone or racemate are accessible. However, reaction times are still too long and have to be optimized.

### 3.3.5 References

- [1] G. W. Huisman, J. Liang, A. Krebber, *Curr. Opin. Chem. Biol.* **2010**, *14*, 122-129.
- [2] a) R. A. Sheldon, *Pure Appl. Chem.* **2000**, *72*, 1233-1246; b) T. Matsuda, R. Yamanaka, K. Nakamura, *Tetrahedron: Asymmetry* **2009**, *20*, 513-557; c) M. Musa Musa, R. S. Phillips, *Catal. Sci. Technol.* **2011**, *1*, 1311-1323.
- [3] a) R. N. Patel, *Coord. Chem. Rev.* **2008**, *252*, 659-701; b) K. Faber, *Biotransformations in organic chemistry: a textbook*, 6 ed., Springer-Verlag, **2011**.
- [4] a) W. A. van der Donk, H. Zhao, *Curr. Opin. Biotechnol.* **2003**, *14*, 421-426; b) A. Weckbecker, H. Groger, W. Hummel, *Adv. Biochem. Eng./Biotechnol.* **2010**, *120*, 195-242; c) W. Liu, P. Wang, *Biotechnol. Adv.* **2007**, *25*, 369-384.
- [5] a) K. M. Polizzi, A. S. Bommarius, J. M. Broering, J. F. Chaparro-Riggers, *Curr. Opin. Chem. Biol.* **2007**, *11*, 220-225; b) A. S. Bommarius, J. K. Blum, M. J. Abrahamson, *Curr. Opin. Chem. Biol.* **2011**, *15*, 194-200.
- [6] a) V. G. Eijsink, A. Bjork, S. Gaseidnes, R. Sirevag, B. Synstad, B. van den Burg, G. Vriend, *J. Biotechnol.* **2004**, *113*, 105-120; b) V. G. Eijsink, S. Gaseidnes, T. V. Borchert, B. van den Burg, *Biomol. Eng.* **2005**, *22*, 21-30; c) J. Liang, J. Lalonde, B. Borup, V. Mitchell, E. Mundorff, N. Trinh, D. A. Kochre, R. N. Cherat, G. P. Ganesh, *Org. Proc. Res. & Dev.* **2010**, *14*, 193-198; d) J. Liang, E. Mundorff, R. Voladri, S. J. Jenne, L. Gilson, A. Conway, A. Krebber, J. Wong, S. Truesdell, J. Lalonde, *Org. Proc. Res. Dev.* **2010**, *14*, 188-192.
- [7] K. Goldberg, K. Schroer, S. Lutz, A. Liese, *App. Microbiol. & Biotechnol.* **2007**, *76*, 249-255.
- [8] C. C. de Carvalho, *Biotechnol. Adv.* **2011**, *29*, 75-83.
- [9] S. Lütz, N. Rao, N., C. Wandrey, *Chem. Eng. Technol.* **2006**, *29*, 1404-1415.
- [10] a) M. H. Vermue, J. Tramper, *Pure Appl. Chem.* **1995**, *67*, 345-373; b) M. N. Gupta, I. Roy, *Eur. J. Biochem. / FEBS* **2004**, *271*, 2575-2583.
- [11] W. Stampfer, B. Kosjek, W. Kroutil, K. Faber, *Biotechnol. Bioeng.* **2003**, *81*, 865-869.
- [12] I. A. Kaluzna, T. Matsuda, A. K. Sewell, J. D. Stewart, *JACS* **2004**, *126*, 12827-12832.
- [13] a) A. Jakoblinnert, R. Mladenov, A. Paul, F. Sibilla, U. Schwaneberg, M. B. Ansorge-Schumacher, P. D. de Maria, *Chem. Commun.* **2011**, *47*, 12230-12232; b) A. Jakoblinnert, M. Bocola, M. Bhattacharjee, S. Steinsiek, M. Bonitz-Dulat, U. Schwaneberg, M. B. Ansorge-Schumacher, *Chembiochem* **2012**; c) J. Peters, T. Minuth, M. R. Kula, *Enz. Microbial Technol.* **1993**, *15*, 950-958.
- [14] T. Schubert, W. Hummel, M. R. Kula, M. Muller, *Eur. J. Org. Chem.* **2001**, 4181-4187.
- [15] a) K. Abokitse, W. Hummel, *Appl. Microbiol. Biotechnol.* **2003**, *62*, 380-386; b) S. Leuchs, L. Greiner, *Chem. Biochem. Eng. Q.* **2011**, *25*, 267-281.

- [16] H. Gröger, W. Hummel, C. Rollmann, F. Chamouveau, H. Hüsken, H. Werner, C. Wunderlich, K. Abokitse, K. Drauz, S. Buchholz, *Tetrahedron* **2004**, *60*.
- [17] J. Peters, T. Minuth, M. R. Kula, *Biocatal. Biotrans.* **1993**, *8*, 31-46.
- [18] K. Abokitse, Heinrich-Heine-Universität Düsseldorf (Jülich), **2004**.
- [19] N. H. Schlieben, K. Niefind, J. Muller, B. Riebel, W. Hummel, D. Schomburg, *J. Mol. Biol.* **2005**, *349*, 801-813.
- [20] H. Groger, W. Hummel, S. Buchholz, K. Drauz, T. V. Nguyen, C. Rollmann, H. Husken, K. Abokitse, *Org. Lett.* **2003**, *5*, 173-176.
- [21] R. M. De Conti, A. L. M. Porto, J. Augusto, R. Rodrigues, P. J. S. Moran, G. P. Manfio, A. J. Marsaioli, *J. Mol. Catal. B: Enzymatic* **2001**, *11*, 233-236.
- [22] a) Q. Ye, P. Ouyang, H. Ying, *Appl. Microbiol. Biotechnol.* **2011**, *89*, 513-522; b) S. K. Ma, J. Gruber, C. Davis, L. Newman, D. Gray, A. Wang, J. Grate, G. Huisman, R. A. Sheldon, *Green Chem.* **2010**, *12*, 81-86.
- [23] K. Honda, T. Ishige, M. Katatoka, S. Shimizu, in *Biocatalysis in the Pharmaceutical and Biotechnology Industries* (Ed.: R. N. Patel), Francis & Taylor, New York, **2007**.
- [24] K. Nakamura, R. Yamanaka, T. Matsuda, T. Harada, *Tetrahedron: Asymmetry* **2003**, *14*, 2659 - 2681.
- [25] a) H. Yang, S. G. Cao, S. P. Han, N. N. Guo, X. G. Gao, Z. L. Huang, H. Dong, N. X. Zhang, T. S. Yang, Y. Chu, J. L. Xu, *Annal. New York Acad. Sci.* **1996**, *799*, 358-363; b) D.-Z. Dai, L.-M. Xia, *Proc. Biochem.* **2006**, *41*, 1455-1460.
- [26] S. M. De Wildeman, (*int. patent*) *WO2008074506*, **2009**.
- [27] a) T. Ishige, K. Honda, S. Shimizu, *Curr. Opin. Chem. Biol.* **2005**, *9*, 174-180; b) Y. Ni, R. R. Chen, *Biotechnol. Bioeng.* **2004**, *87*, 804-811.
- [28] R. R. Chen, *Appl. Microbiol. Biotechnol.* **2007**, *74*, 730-738.
- [29] A. Z. Walton, J. D. Stewart, *Biotechnol. Prog.* **2004**, *20*, 403-411.
- [30] A. S. Bommarius, B. R. Riebel, *Biocatalysis: Fundamentals & Applications*, John Wiley & Sons Inc, Weinheim, **2004**.
- [31] R.-H. Huang, J.-H. Xu, *Biochem. Eng. J.* **2006**, *30*, 11-15
- [32] L. S. Chen, S. M. Mantovani, L. G. de Oliveira, M. C. T. Duarte, A. J. Marsaioli, *J. Mol. Catal. B: Enzymatic* **2008**, *54*, 50-54.
- [33] a) A. Matsuyama, H. Yamamoto, N. Kawada, Y. Kobayashi, *J. Mol. Catal. B: Enzymatic* **2001**, *11*, 513-521; b) H. Yamamoto, A. Matsuyama, Y. Kobayashi, *Biosci. Biotechnol. Biochem.* **2002**, *66*, 925-927.
- [34] L. Greenspan, *J. Res. Nat. Bureau of Stand. - A. Physics and Chemistry* **1977**, *81A*, 89-96.
- [35] a) R. H. Valivety, P. J. Halling, A. D. Peilow, A. R. Macrae, *Eur. J. Biochem. / FEBS* **1994**, *222*, 461-466; b) K. Hwang, S. Lee, K. Lee, *Biotechnol. Lett.* **1995**, *17*; c) A. Jonsson, W. van Breukelen, E. Wehtje, P. Adlercreutz, B. Mattiasson, *J. Mol. Catal. B: Enzymatic* **1998**, *5*, 273-276; d) S. Lamare, M. D. Legoy, *Biotechnol. Bioeng.* **1995**, *45*, 387-397; e) R. Mikolajek, A. C. Spiess, M. Pohl, S. Lamare, J. Buchs, *ChemBiochem* **2007**, *8*, 1063-1070.
- [36] a) T. Goubet, T. Maugard, S. Lamare, M. D. Legoy, *Enz. Microb. Tech.* **2001**, *31*, 425-430; b) B. Erable, T. Maugard, I. Goubet, S. Lamare, M. D. Legoy, *Process Biochem.* **2005**, *40*, 45-51; c) P. Marchand, E. Rosenfeld, B. Erable, T. Maugard, S. Lamare, I. Goubet, *Enz. Micro. Techn.* **2008**, *43*, 423-430.
- [37] J. B. Bateman, C. L. Stevens, W. B. Mercer, E. L. Carstensen, *J. Gen. Microbiol.* **1962**, *29*, 207-219.
- [38] B. Gao, E. Su, J. Lin, Z. Jiang, Y. Ma, D. Wei, *J. Biotechnol.* **2009**, *139*, 169-175.

- [39] F. Hildebrand, S. Lütz, *Tetrahedron: Asymmetry* **2007**, *18*, 1187-1193.
- [40] S. Bräutigam, S. Bringer-Meyer, D. Weuster-Botz, *Tetrahedron: Asymmetry* **2007**, *18*, 1883–1887
- [41] L. Kulishova, *Docotrla thesis*, Heinrich-Heine Universität Düsseldorf, **2010**.
- [42] S. Bräutigam, D. Dennewald, M. Schürmann, J. Lutje-Spelberg, W.-R. Pitner, D. Weuster-Botz, *Enz. Microb. Technol.* **2009**, *45*, 310–316.
- [43] J. Schumacher, M. Eckstein, U. Kragl, *Biotechnol. J.* **2006**, *1*, 574-581.
- [44] W. Hummel, K. Abokitse, K. Drauz, C. Rollmann, H. Gröger, *Adv. Syn. Catal.* **2003**, *345*.
- [45] a) J. Peters, T. Zelinski, T. Minuth, M.-R. Kula, *Tetrahedron Asymmerty* **1993**, *4*, 1683-1692; b) T. Zelinski, M. R. Kula, *Bioorg. Med. Chem.* **1994**, *2*, 421-428.
- [46] A. van den Wittenboer, *Doctaoral thesis*, RWTH Aachen, **2009**.
- [47] H. Yamamoto, A. Matsuyama, Y. Kobayashi, *Biosci. Biotechnol. Biochem.* **2002**, *66*, 481-483.
- [48] A. Liese, T. Zelinski, M. R. Kula, H. Kierkels, M. Karutz, U. Kragl, C. Wandrey, *J. Mol. Catal. B: Enzymatic* **1998**, *4*, 91-99.
- [49] B. Orlich, H. Berger, M. Lade, R. Schomacker, *Biotechnol. Bioeng.* **2000**, *70*, 638-646.
- [50] H. D. Simpson, D. A. Cowan, *Prot. Pep. Lett.* **1997**, *4*, 25-32.
- [51] a) M. M. Musa, K. I. Ziegelmann-Fjeld, C. Vieille, R. S. Phillips, *Org. Biomol. Chem.* **2008**, *6*, 887-892; b) M. V. Filho, T. Stillger, M. Muller, A. Liese, C. Wandrey, *Angew. Chem. Int. Ed.* **2003**, *42*, 2993-2996; c) H. Li, D. Zhu, L. Hua, E. R. Biehl, *Adv. Syn. Catal.* **2009**, *351*, 583-588.
- [52] P. Müller, *Doctoral thesis*, RWTH Aachen, **2010**.
- [53] A. van den Wittenboer, T. Schmidt, P. Muller, M. B. Ansorge-Schumacher, L. Greiner, *Biotechnol. J.* **2009**, *4*, 44-50.
- [54] A. Gupta, Tschentscher, A., M. Bobkova, (*US patent US7371903*), **2008**.
- [55] E. Keinan, E. K. Hafeli, K. K. Seth, R. Lamed, *JACS* **1986**, *108*, 162 - 169.
- [56] E. Erdélyi, A. Szabó, G. Seres, L. Birincsik, J. Ivanics, G. Sztatzke, L. Poppe, *Tetrahedron: Asymmetry* **2006**, *17*, 268-274.
- [57] a) M. J. Hernaiz, A. R. Alcantara, J. I. Garcia, J. V. Sinisterra, *Chemistry (Weinheim an der Bergstrasse, Germany)* **2010**, *16*, 9422-9437; b) R. Leon, P. Fernandes, H. M. Pinheiro, J. M. S. Cabral, *Enz. Microb. Technol.* **1998**, *23*, 483-500.
- [58] E. Israeli, E. Giberman, A. Kohn, *Cryobiology* **1974**, *11*, 473-477.
- [59] L. M. McMurry, M. Hendricks, S. B. Levy, *Antimicrob. Agents Chemother.* **1986**, *29*, 681-686.
- [60] a) M. Andersson, H. Holmberg, P. Adlercreutz, *Biotechnol. Bioeng.* **1998**, *57*, 79-86; b) V. Nagalakshmi, J. S. Pai, *Biotechnol. Tech.* **1994**, *8*, 431-434.
- [61] a) U. Schwaneberg, C. Otey, P. C. Cirino, E. Farinas, F. H. Arnold, *J. Biomol. Screen.* **2001**, *6*, 111-117; b) R. Kratzer, M. Pukl, S. Egger, B. Nidetzky, *Microb. Cell Fact.* **2008**, *7*.
- [62] D. Shen, J.-H. He Xu, H.-Y. Wu, Y.-Y. Liu, *J. Mol. Catal. B: Enzymatic* **2002**, *18*, 2119-2244.
- [63] a) J. Zhang, B. Witholt, Z. Li, *Chem. Commun. (Camb)* **2006**, 398-400; b) G. J. Salter, D. B. Kell, *Crit. Rev. Biotechnol.* **1995**, *15*, 139-177; c) W. Zhang, K. O'Connor, D. I. Wang, Z. Li, *Appl. Environ. Microb.* **2009**, *75*, 687-694.
- [64] F. Tao, Y. Zhang, C. Ma, P. Xu, *Sci. Rep.* **2011**, *1*, 142.
- [65] H. Tsubery, I. Ofek, S. Cohen, M. Fridkin, *J. Med. Chem.* **2000**, *43*, 3085-3092.
- [66] a) W. J. Sulling, W. M. O'Leary, *Antimicrob. Agents Chemother.* **1975**, *8*; b) M. Eriksson, P. E. Nielsen, L. Good, *J. Biol. Chem.* **2002**, *277*, 7144-7147.
- [67] A. Weckbecker, W. Hummel, *Biotechnol. Lett.* **2004**, *26*, 1739-1744.
- [68] L. Michaelis, M. L. Menten, K. A. Johnson, R. S. Goody, *Biochem.* **2011**, *50*, 8264-8269.
- [69] D. M. Mateus, S. S. Alves, M. M. Da Fonseca, *J. Biosci. Bioeng.* **2004**, *97*, 289-293.

- [70] H. Groger, F. Chamouleau, N. Orogas, C. Rollmann, K. Drauz, W. Hummel, A. Weckbecker, O. May, *Angew. Chem. Int. Ed.* **2006**, *45*, 5677-5681.
- [71] K. Edegger, C. C. Gruber, K. Faber, A. Hafner, W. Kroutil, *Eng. Life Sci.* **2006**, *6*, 149-154.
- [72] B. M. Mackey, C. A. Miles, S. E. Parsons, D. A. Seymour, *J. Gen. Microbiol.* **1991**, *137*, 2361-2374.
- [73] A. I. Martinez-Gomez, S. Martinez-Rodriguez, J. M. Clemente-Jimenez, J. Pozo-Dengra, F. Rodriguez-Vico, F. J. Las Heras-Vazquez, *Appl. Environ. Microb.* **2007**, *73*, 1525-1531.
- [74] S. Lütz, L. Giver, J. Lalonde, *Biotechnol. Bioeng.* **2008**, *101*, 647-653.
- [75] a) F. Hollmann, I. W. C. E. Arends, D. Holtmann, *Green Chem.* **2011**, *13*, 2285; b) N. J. Turner, *Curr. Opi. Chem. Biol.* **2010**, *14*, 115-121; c) J. H. Schrittwieser, J. Sattler, V. Resch, F. G. Mutti, W. Kroutil, *Curr. Opi. Chem. Biol.* **2011**, *15*, 249-256.
- [76] Y.-L. Li, J.-H. Xu, Y. Xu, *J. Mol. Catal. B: Enzymatic* **2010**, *64*, 48-52.
- [77] a) C. V. Voss, C. C. Gruber, W. Kroutil, *Angew. Chem. Int. Ed.* **2008**, *47*, 741-745; b) C. V. Voss, C. C. Gruber, K. Faber, T. Knaus, P. Macheroux, W. Kroutil, *JACS* **2008**, *130*, 13969-13972.

## 3.4 Reengineered Carbonyl Reductase for Reducing Methyl-substituted Cyclohexanones

### 3.4.1 Abstract

The carbonyl reductase 2 from *Candida parapsilosis* (CPCR2) is a versatile biocatalyst for production of optically pure alcohols from ketones. Prochiral ketones like 2-methyl cyclohexanone are; however, only poorly accepted, despite CPCR2's large substrate spectrum. The substrate spectrum of CPCR2 was investigated by selecting five amino positions (55, 92, 118, 119 and 262) and exploring them by single site-saturation mutagenesis. Screening of CPCR2 libraries with poor (14 compounds) and well-accepted (2 compounds) substrates showed that only position 55 and position 119 showed an influence on activity. Saturation of positions 92, 118 and 262 yielded only wild-type sequences for the two well-accepted substrates and no variant converted one of the 14 other compounds. Only the variant (L119M) showed a significantly improved activity (7-fold on 2-methyl cyclohexanone;  $v_{\max} = 33.6 \text{ U mg}^{-1}$ ,  $K_m = 9.7 \text{ mmol L}^{-1}$ ). The L119M substitution exhibited also significantly increased activity towards reduction of 3-methyl (>2-fold), 4-methyl (>5-fold) and non-substituted cyclohexanone (>4-fold). After docking 2-methyl cyclohexanone into the substrate binding pocket of a CPCR2 homology model, we hypothesized that the flexible side chain of M119 provides more space for 2-methyl cyclohexanone than branched L119. This report represents the first study on CPCR2 engineering and provides first insights how to redesign CPCR2 towards a broadened substrate spectrum.

### 3.4.2 Introduction

Biocatalysis enables novel and innovative production of chemicals with high regio- and stereoselectivity under often environmentally-friendly conditions.<sup>[1]</sup> Especially, the asymmetric reduction of prochiral ketones to the corresponding enantiomerically pure alcohols by carbonyl reductases (CR) or alcohol dehydrogenases (ADH; EC 1.1.1.1) display a very attractive synthesis route to these important building blocks used in chemical and pharmaceutical industries.<sup>[2]</sup>

The particularly versatile NADH dependent carbonyl reductase CPCR2<sup>[3]</sup> from *Candida parapsilosis* was first isolated from the strain DSM 70125 and characterized by Peters *et al.*<sup>[4]</sup> The identical enzyme was later isolated from a related strain IFO 0369 and expressed in *E. coli* by Yamamoto *et al.*<sup>[5]</sup> The homodimeric CPCR2 consists of two subunits (each 36 kDa) and belongs to the medium-chain and zinc-containing alcohol dehydrogenase family. The wild type enzyme was recombinantly expressed in *E. coli* and employed in several synthetic setups to produce high value-added chiral alcohols like (*R*)-1,3-butanediol by racemic resolution.<sup>[6]</sup> and ethyl (*R*)-4-chloro-3-hydroxybutanoate by asymmetric reduction of the corresponding ketone.<sup>[7]</sup> Furthermore, CPCR2 preparations were

utilized to obtain (*S*)-ethyl-hydroxyesters<sup>[4]</sup> and propargylic alcohols.<sup>[8]</sup> Additionally, wtCPCR2 was used to validate an enzyme-membrane reactor<sup>[9]</sup>, an enzyme emulsion reactor<sup>[10]</sup> and a biphasic mini-reactor.<sup>[11]</sup> Recently, we have employed CPCR2 in *E. coli* whole cells in neat organic substrates and in absence of any additional solvent with yields up to 500 g L<sup>-1</sup> enantiopure alcohol.<sup>[12]</sup>

CPCR2 has a broad substrate spectrum and exhibits generally high enantiomeric excess (*ee* >95 %).<sup>[4-5, 8, 13]</sup> It was only recently distinguished from the isoenzyme CPCR1, which has a narrow substrate spectrum.<sup>[3]</sup>

Key for substrate acceptance is the general shape of the binding pocket. CPCR2's binding pocket was proposed to be composed of a small pocket with high affinity to small alkyl groups and a larger pocket accommodating small methyl and ethyl groups but preferably aromatic groups.<sup>[13b]</sup> The latter architecture is in agreement with the common fold of the substrate binding pocket of zinc-dependent medium-chain ADHs.<sup>[14]</sup>

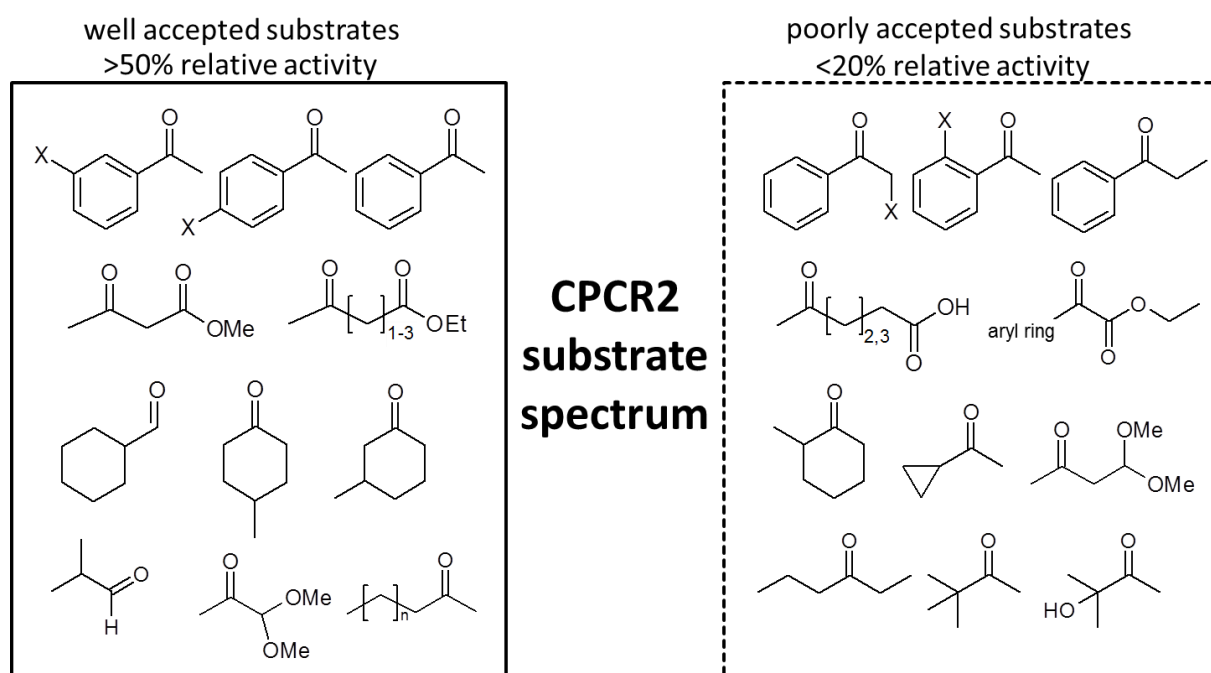


Figure 1 Substrates reported for CPCR2 and normalized to ethyl 5-oxo-hexanoate reduction.<sup>[4]</sup> Substrates, which are well accepted (> 50 % relative activity), are grouped in the left box, substrates, which are poorly accepted (< 20 % relative activity), are displayed in the right box. The relative activities were determined using ethyl-5-oxohexanoate as reference substrate. X: hydroxyl group, or halide (-Cl, -Br, -F) and n indicates the number of carbons in the chain (n: 1 to 4).

Despite the broad substrate spectrum of CPCR2, there are classes of prochiral ketones which are only poorly converted, like *ortho*-substituted acetophenones, 2-methyl cyclohexanone (2-MCHone) or ketones carrying bulky side chains neighboring the carbonyl function (see Figure 1; dashed line).<sup>[13b]</sup> These substrates are generally difficult to be accepted by ADHs.<sup>[15]</sup> The corresponding (*S*)-alcohols of the poorly accepted substrates represent; however, industrially valuable synthons like (*S*)-2-chlorophenylethanol derivatives, which serve as key intermediates for anticancer drugs.<sup>[2c]</sup>

Consequently, there is a demand to enlarge the substrate scope of CPCR2 towards substrates as depicted in Figure 1 (right box).

Tailoring of substrate scope can be achieved by rational design of the substrate binding pocket, random mutagenesis or combinations thereof. Structurally guided exchanges of amino acids that affect substrate- and stereospecificity require a crystal structure or a reliable homology model. For example Green and co-workers could increase activity of ADH1 from bakers' yeast up to 10-fold for hexanol oxidation by enlarging the substrate binding pocket.<sup>[16]</sup> Unlike rational design, random mutagenesis allows to discover mutations, which are located more distantly from the active site as shown for AdhA from *Pyrococcus furiosus*.<sup>[17]</sup> Recently, the activity of a carbonyl reductase for an unnatural substrate was increased by 3000-fold after including 19 substitutions in a directed evolution campaign.<sup>[18]</sup>

In this study, we used a semi-rational approach targeting five amino acid residues to improve CPCR2 activity towards 14 poorly accepted substrates. Widening the substrate spectrum will make CPCR2 an attractive catalyst in organic synthesis and will possibly provide a deeper understanding about the underlying structure-function relationships that govern acceptance of cyclic ketones.

### 3.4.3 Materials & Methods

#### 3.4.3.1 Preparation of Chiral Standards

Preparation of the four stereoisomers of 2-methylcyclohexanol (2-MCHol) was done by stereoselective reduction of 2-MCHone with carrot root as described previously.<sup>[19]</sup> The conversion was monitored by gas chromatography (GC) and compared with commercial standards *cis*- and *trans*-2-MCHol. The major peaks were assigned to the (*S*)-alcohol.

#### 3.4.3.2 Molecular Modeling

Homology modeling of the structure of CPCR2 (wtCPCR2) was performed previously.<sup>[3]</sup> Docking studies were performed on a close dimer of the modeled CPCR2 structure and relaxed models of wtCPCR2, CPCR2-L119M with zinc-bound 2-MCHone in a reactive conformation were constructed. All energy calculations were performed using the modeling suite YASARA<sup>[20]</sup> employing AMBER03 force field<sup>[21]</sup> for the protein and GAFF<sup>[22]</sup> with AM1/BCC charges<sup>[23]</sup> for the substrates.

All residues within 15 Å radius of the bound alcohol were free to move. The active site above the bound NAD(H) is located at the interface between the two monomers possessing Rossmann-fold. The Zn-bound alcohol-ligand in the active site of the homology models was manually replaced by the respective substrates in their keto form and relaxed using cycles of steepest descent energy minimization and simulated annealing molecular dynamics (MD) simulations from 298 °K to 5 °K. Reference calculations for binding energies were performed using the respective substrates in a

water box and the apo-enzyme with water coordinated to the catalytic  $Zn^{2+}$ . The stabilization energies of the substrates in a catalytic orientation were calculated by subtracting the solvation energy for the substrate from the energy in the  $Zn^{2+}$  bound state and the energy difference of an active site subset consisting of ten residues lining the binding pocket in the substrate bound state versus the apo-structure with bound water (Ser46, Val50, Leu55, Trp116, Leu119, Leu262, Phe285, Trp286, GlyB272, LeuB276, B denote amino acid of the other monomer).

### 3.4.3.3 Cloning of CPC2 into pET22

The CPC2 gene construct was newly designed with an N-terminal extension consisting of a protease recognition site for tobacco etch virus (TEV) protease, an alanine decamer as spacer helix and a streptavidin affinity tag for convenient purification. The gene sequence was retrieved from Genbank accession number AB010636. The CPC2 DNA construct was synthetically produced applying codon optimization for *E. coli* (GeneArt, Invitrogen, Darmstadt, Germany). The gene construct was cloned into pET22b+ vector (Invitrogen, Darmstadt, Germany) with NdeI and NotI restriction enzymes and T4 ligase. The attachment of the N-terminal extension had no influence on activity with acetophenone when compared to the originally cloned CPC2 (data not shown).

### 3.4.3.4 Site Saturation Mutagenesis

Degeneracy at five selected sites (Leu55, Pro92, Gly118, Leu119 & Leu262) was introduced by site-saturation mutagenesis using degenerated primer sets and a two-step protocol for polymerase chain reaction (PCR) adapted from Wang & Malcom.<sup>[24]</sup> Herein, Phusion High Fidelity DNA polymerase (New England Biolabs) was applied with 20 ng of template DNA. First, PCR with single primers was run followed by a second PCR where primer pairs were mixed again. NNN codon degeneracy was employed to cover all 64 possible codons. Primer pairs used for PCR are listed in Table 1.

**Table 1 Primer sequences for site-saturation.**

Primer name	5'-3' sequence
L55-for	catgtgatttatgaaggtNNNgattgcggtgataattatg
L55-rev	cataattatcaccgcaatcNNNaccttcataaatcacatg
P92-for	gttgcatgtgttggNNNaatggttgggtg
P92-rev	ccaccacaaccattNNNaccaacacatgcaac
G118-for	gccttggcgactggttNNNctgggttatgatggtg
G118-rev	ccaccatcataaccagaNNNaaccagtcgccaaggc
L119-for	ggcgactggttggNNNggttatgatggtg
L119-rev	ccaccatcataaccNNNaccaaccagtcgcc
L262-for	gttattatgccggttggNNNggtgaccgaatctgtc
L262-rev	gacagattcggtgcaccNNNgccaaccggcataataac

Sites of saturation mutagenesis are highlighted in italics

Digestion of template DNA (pET22b-CPC2) was done by addition of 20 U DpnI (New England Biolabs) to 50  $\mu$ L PCR product and incubation at 37 °C overnight. Purified PCR products were transformed to *E. coli* BL21 (DE3) by electroporation and plated on agar plates containing 100  $\mu$ g mL<sup>-1</sup> ampicillin.



#### 3.4.3.5 Mutant Library Generation

Quality of the library was analyzed by sequencing seven random clones from each saturated position. Per amino acid position, about 240 clones represent all possible codons with a probability of 95 %.<sup>[25]</sup> High quality libraries (<30 % wild-type occurrence) were constructed by transferring single colonies from agar plate to 96-well microtiter plates (flat bottom, polystyrene) filled with 100  $\mu$ L LB medium supplemented with 100  $\mu$ g/mL ampicillin. Plates were tightly sealed and incubated (16 h, 37 °C, 900 rpm and 70 % humidity). For long-term storage, 100  $\mu$ L of 50 % (v/v) glycerol was added to each well and the libraries were stored at -80 °C.

#### 3.4.3.6 CPCR2 Protein Expression in Microtiter Plate

Expression in microtiter plates was performed by preparing a pre-culture using 10  $\mu$ L of glycerol stock to inoculate 140  $\mu$ L of LB medium supplied with ampicillin (100  $\mu$ g mL<sup>-1</sup>) in 96-well plates (flat bottom, polystyrene). Plates were closed with lids, tightly sealed and incubated for 16 hours (37 °C, 900 rpm and 70 % relative humidity). Then, 10  $\mu$ L of the pre-culture were transferred to 140  $\mu$ L TB medium (per litre: 12 g Tryptone, 24 g yeast extract, 4 mL glycerol, 0.017 mol L<sup>-1</sup> KH<sub>2</sub>PO<sub>4</sub>, 0.072 mol L<sup>-1</sup> K<sub>2</sub>HPO<sub>4</sub>) supplied with ampicillin 100  $\mu$ g/mL (V-bottom, polystyrene) and incubated (1 h, 37 °C, 900 rpm and 70 % relative humidity).

Expression was initiated by supplementing 10  $\mu$ L isopropylthiogalactoside (IPTG at) 0.1 mmol L<sup>-1</sup> final concentration. Subsequently, protein expression took place for 6-8 hours at 15 °C at 900 rpm. For storage at -20 °C, cells were pelleted (18350x g, 10 min, 4 °C) and medium was removed. For lysis, 150  $\mu$ L of lysis buffer (50 mmol L<sup>-1</sup> K<sub>2</sub>HPO<sub>4</sub>, 300 mmol L<sup>-1</sup> NaCl, 5 mg mL<sup>-1</sup> lysozyme, pH 8.0) was added in each well. Cell pellets were mechanically lysed by pipetting up and down 100 times applying a 96-well liquidator<sup>96</sup> pipetting tool (Steinbrenner Laborsysteme GmbH). Afterwards, the suspension was incubated (1 h, 37 °C, 900 rpm and 70 % relative humidity) to intensify enzymatic cell wall destruction by lysozyme.

#### 3.4.3.7 CPCR2 Protein Expression in Flasks

Batch expression of CPCR2 was carried out in 250 mL TB medium with ampicillin (100  $\mu$ g mL<sup>-1</sup>) inoculated with 4 mL of an overnight culture grown in LB medium with ampicillin (100  $\mu$ g mL<sup>-1</sup>; 37 °C, 250 rpm). When cell density reached 0.6-0.8 OD<sub>600</sub>, expression was induced by supplementing 0.1 mmol L<sup>-1</sup> IPTG. Final expression was carried out overnight (15 °C, 250 rpm). Cells were harvested by centrifugation (2820x g, 10 min, 4 °C) and resuspended in 4 volumes of lysis buffer (50 m mol L<sup>-1</sup> K<sub>2</sub>HPO<sub>4</sub>, 300 mmol L<sup>-1</sup> NaCl, pH 8.0). Mechanical lysis was performed by sonification 3 times (1 min, 40 % amplitude with 40 cycles, Bandelin M73 sonotrode). Supernatant containing the soluble CPCR2 was clarified by centrifugation (2820x g, 10 min, 4 °C) and use for subsequent experiments.

#### 3.4.3.8 CPCR2 Protein Purification

Crude cell extract was applied to affinity chromatography employing a streptavidin gravity column (*Strep-Tactin*<sup>®</sup> Sepharose, IBA TAGnology). Purification was performed according to the manufacturer's instructions. Elution fractions were analyzed by SDS-PAGE and CPCR2 concentrations were determined with the Bradford assay employing bovine serum albumin as standard. Fractions showing high enzyme activity were pooled and used for further measurements.

#### 3.4.3.9 CPCR2 Activity Assay in Microtiter Plate

The NADH depletion assay in microtiter plate format was performed spectrophotometrically (Tecan Infinite M1000). Here, 50  $\mu\text{L}$  of crude extract was mixed with 150  $\mu\text{L}$  of a substrate cocktail (see 3.4.6) in 100  $\text{mmol L}^{-1}$  TEA at pH 8.0. The reaction was initiated by addition of 50  $\mu\text{L}$  of 5  $\text{mmol L}^{-1}$  NADH and absorption was monitored at 340 nm for 5 min ( $\epsilon = 16,900 \text{ M}^{-1} \text{ cm}^{-1}$ ). Instrument and solutions were pre-warmed to 30  $^{\circ}\text{C}$ .

#### 3.4.3.10 CPCR2 Activity Assay in Cuvette

CPCR2 activity assay in cuvette format was carried out in a Cary 300 UV/Vis spectrophotometer (Varian). Varying concentrations of substrate were mixed with 0.3  $\text{mmol L}^{-1}$  NADH in 100  $\text{mmol L}^{-1}$  TEA, pH 8.0. The reaction was initiated by transferring 10  $\mu\text{L}$  of CPCR2 solution of appropriate dilution to the cuvette and flushing with 1 mL of the substrate solution. The absorption at 340 nm was monitored for 2 min at 30 $^{\circ}\text{C}$  ( $\epsilon = 16,900 \text{ M}^{-1} \text{ cm}^{-1}$ ).

#### 3.4.3.11 Determination of Kinetic Parameters $K_M$ and $v_{max}$

Kinetic characterizations of wtCPCR2 and CPCR2-L119M were carried out using the standard activity assay in cuvette-scale. 2-methyl cyclohexanone was used as substrate in concentrations ranging from 0 to 30  $\text{mmol L}^{-1}$  (0.1  $\text{mol L}^{-1}$  TEA, pH 8.0). Purified CPCR2 concentration were varied to determine initial activities and to calculate  $K_m$  and  $v_{max}$ . The data was fitted using SIMFIT, Version 6.3.2 and all measurements were conducted in triplicate.<sup>[26] [26]</sup>

#### 3.4.3.12 Determination of Temperature and pH-optimum

To determine the effect of temperature on the activity, CPCR2 assays were performed in cuvette format at temperatures from 18.5 to 47.8  $^{\circ}\text{C}$  with acetophenone as substrate. Twelve temperatures were taken into account and measurements were carried out in triplicates. To determine the kinetic parameters, enzyme assays were done in cuvette format with 2-methylcyclohexanone with concentrations ranging from 0 to 40  $\text{mmol L}^{-1}$ . At least ten different concentrations were applied for each data set and each set was performed in triplicates. To determine the effect of pH on activity, enzyme assays were performed in microtiter plate at pH 6.5 to 9.5 with acetophenone as substrate in triplicates.

### 3.4.3.13 Asymmetric Reduction of 2-methylcyclohexanone

For reduction of 2-MCHone, 40 mL buffer (100 mmol L<sup>-1</sup> TEA, pH 8.0) were mixed with 10 % (v/v) isopropanol, 10 mmol L<sup>-1</sup> NADH and 500 µL 2-MCHone (0.94 mmol L<sup>-1</sup>). Finally, purified wtCPCR2 (2 U) or CPCR2-L119M (30 U) were supplemented in purified form. The reaction was stirred (500 rpm, 30 °C) until maximum conversion was reached. Conversion was monitored by non-chiral GC. Educts and products were extracted 3 times with 50 mL CH<sub>2</sub>Cl<sub>2</sub>. Excess CH<sub>2</sub>Cl<sub>2</sub> and isopropanol were removed by evaporation under reduced pressure.

### 3.4.3.14 Determination of Conversion, Enantiomeric & Diastereomeric Excess

#### Non-chiral GC analysis

Conversion of 2-MCHone was monitored using Agilent GC device (HP5890 Series II) equipped with a flame ionization detector and a chiral column (FS-Cyclodex beta-I/P column 25 m, 0.25 mm, CS Chromatographie) at 10 psi nitrogen gas. The temperature program was: 120°C, 4 min, isothermal. Substrates were separated from products and typical retention times were determined for 2-MCHone (3.2 min), trans-2-MCHol (3.5 min) and cis-2-MCHol (3.7 min). The molecular identity of the individual peaks was validated by comparison with commercially available standards (racemic cis-2-MCHol, racemic trans-2-MCHol, purchased from Sigma-Aldrich).

#### Derivatization of 2-methyl cyclohexanols for chiral GC

Conversion mixtures were extracted with CH<sub>2</sub>Cl<sub>2</sub> (3 times; 50 mL), dried (MgSO<sub>4</sub>; 30 min), filtrated, concentrated to a final volume of ~500 µl and supplemented with 3 mL CH<sub>2</sub>Cl<sub>2</sub> (dried with MgSO<sub>4</sub>). Derivatisation was initiated by supplementing 2.8 mL of trifluoroacetic anhydride (excess in molarity: ~5-fold) and incubated (60 °C, 30 min; slowly stirred) under argon gas. Residual trifluoroacetic acid and CH<sub>2</sub>Cl<sub>2</sub> were removed subsequently by evaporation under reduced pressure. As control the identical procedure was performed for the commercial racemic mixture of *cis* and *trans* 2-MCHol (Sigma-Aldrich).

#### Chiral GC Analysis

Enantio- and diastereomeric excess of the biotransformation was determined by applying derivatized 2-MCHol. The instrument (Focus GC, Thermo Scientific) equipped with a Chirasil-Dex-CB column (25 m x 0.25 mm, CS Chromatographie) at 0.7 bar helium. The temperature program was: 50°C/1° min - 80°C/15 min – 160°C, 10 min.

The identity of the single peaks was validated by comparison of the peaks with GC-standards, which were synthesized earlier.

Typical retention times were determined for 1-(*S*), 2-(*R*) 2-MCHol (21.4 min), 1-(*R*), 2-(*S*) 2-MCHol (22.5 min), 1-(*S*), 2-(*S*) 2-MCHol (22.2 min), and 1-(*R*), 2-(*R*) 2-MCHol (22.9 min). Chiral standards for

all stereoisomers of 2-MCHol were produced according to Baldassarre *et al.* applying biotransformation of 500  $\mu\text{L}$  2-MCHone with 200 g chopped carrot root (*Daucus carota*) resuspended in 200 mL tap water.<sup>[19]</sup>

### 3.4.4 Results & Discussion

#### 3.4.4.1 Rational Site Selection

The reported crystal structure of a homologous ADH (35 % sequence identity) from *Sulfolobus solfataricus* (SsADH, PDB: 1R37<sup>[27]</sup>) was used as “closest relative” for selecting amino acid positions for site saturation mutagenesis. Furthermore, the comprehensive medium-chain dehydrogenase/reductase engineering database was consulted<sup>[14]</sup> and an alignment of 37 crystal structures of zinc-containing medium-chain ADHs was analyzed for variable regions within the Substrate-Recognition Site (SRS). Two such regions were recognized and termed SRSI (“ceiling”) & SRSII (“right wall”). Finally, five amino acid residues (L55, P92, G118, L119 and L262) within or near these regions were selected for semi-rational design of the substrate binding pocket and targeted in five single site saturation experiments (see Figure 2

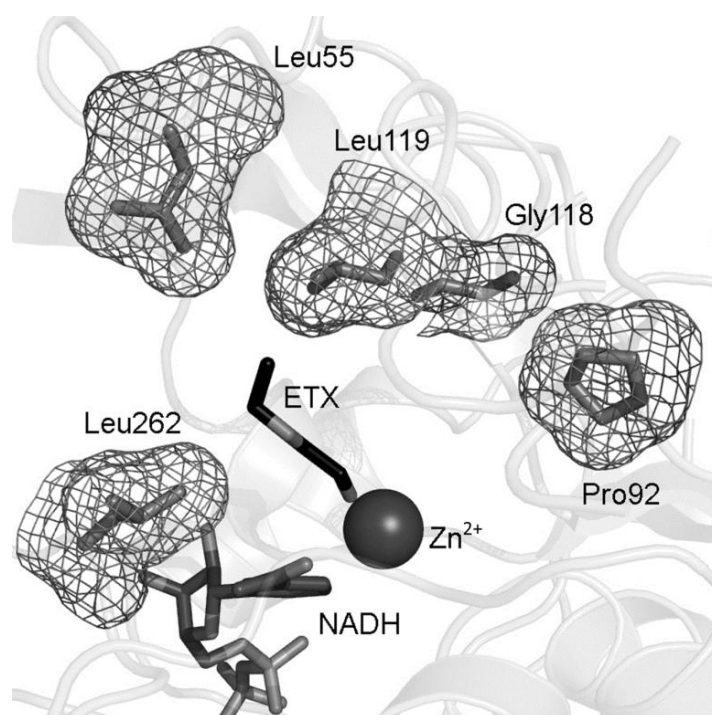


**Figure 2** Representation of the substrate binding pocket of wtCPCR2. The five amino acid residues selected for saturation mutagenesis are displayed as sticks surrounded by a mesh showing van-der-Vaals radii. The catalytic zinc ( $\text{Zn}^{2+}$ ) is depicted as black sphere and the substrate ethoxyethanol (ETX) and the cofactor NADH are represented as sticks. According to Knoll & Pleiss L55, G118 and L119 are located in SRSI and P92 in SRSII.<sup>[14]</sup> The amino acid L262 is at the entrance channel.

Amino acids L55, G118 and L119 are located in the SRSI region, amino acid P92 is found in the SRSII region and amino acid L262 is situated at the substrate entrance channel. Probing positions in four different regions (substrate entrance (L262), “ceiling” (Leu55, L119), “right wall” (P92), second

coordination sphere (G118) will reveal which regions are important for substrate acceptance in CPCR2.

Unique for wtCPCR2 is the occurrence of the amino acid proline at position 92 within SRSII; all related ADH-enzymes contain a tryptophan or a phenylalanine at the corresponding position. Mutations of this position had an impact on substrate acceptance in ADHs from horse liver (F93)<sup>[28]</sup>, yeast (W93)<sup>[29]</sup>, *Sulfolobus solfataricus* (W95)<sup>[30]</sup> and human liver (F93).<sup>[31]</sup>

Residues located in SRSI (“ceiling”) were reported to be variable among ADHs and held responsible for differences in substrate acceptance in individual ADHs.<sup>[14]</sup> The positions L55, G118, and L119 selected for saturation mutagenesis in wtCPCR2 correspond to L58, G119, and I120 in the closely related *SsADH* and are reported to exhibit substrate contact or to be in close proximity to the co-crystallized substrate.<sup>[32]</sup>

Amino acid L262 at the substrate entrance channel corresponds to amino acid L272 in *SsADH*, which is in direct contact with the substrate.<sup>[32]</sup> Mutation at this position exhibits impact on substrate acceptance like reduced activity on 2-butanol in ADH of *Thermoanaerobacter ethanolicus* (Y267G).<sup>[33]</sup> and a 7- to 10-fold increased activity for the substrates butanol, pentanol and hexanol in ADH1 from *S. cerevisiae* (Met294L)<sup>[34]</sup>, respectively.

#### 3.4.4.2 Screening with Acetophenone & 2-butanone

A first screening of the five libraries obtained from saturation mutagenesis was done with acetophenone as large and 2-butanone as small substrate. As wild type CPCR2 (wtCPCR2) accepts both substrates very well.<sup>[4]</sup> This was done to investigate the importance of the selected amino acids for the catalytic machinery. Sequencing of the seven most active clones from each library revealed that no exchanges occurred at positions 92, 118, 119 and 262 indicating that, with regard to the conversion of the two selected substrates, the amino acids placed in these positions in wtCPCR2 provide optimal performance. However, two variants with ~30 % higher activity towards 2-butanone than wtCPCR2 were identified after saturation mutagenesis on amino acid 55. Here, leucine was exchanged for phenylalanine and tryptophan. The activity of both variants on acetophenone was comparable to wild type.

The exchange from an aliphatic leucine to an aromatic phenylalanine or tryptophan narrows the available space in the substrate binding pocket and by this promotes conversion of the small substrate 2-butanone. This can be deduced from the finding of Green et al. that tight binding of small substrates by ADH1 from baker’s yeast is “disturbed” upon enlargement of the substrate binding pocket<sup>[16]</sup>, and the report of Ziegelmann-Fjeld *et al.*, where a more than ten times increased  $K_m$  for 2-butanol was found for a W267A variant of ADH from *Thermoanaerobacter ethanolicus*.<sup>[33]</sup> The finding

that reduction of acetophenone was not affected by reduction of the substrate site was somewhat surprising, but might be explained by probable beneficial interactions of the  $\pi$ -systems of the substrates and the amino side chains of phenylalanine and tryptophan.

#### 3.4.4.3 Screening with Poorly Accepted Substrates & Identification Improved Variants

For fast and efficient screening of the five libraries from site saturation mutagenesis for improved conversion of poor substrates, conversion of 14 different substrates by purified wtCPCR2 was determined (NADH depletion assay; see Table S1), and the substrates exhibiting less than 20 % activity relative to acetophenone were combined to four sets of substrate mixtures with a combination of three or four substrates each. Towards each set wtCPCR2 showed less than 15 % relative activity (see Table S2). The libraries from site-saturation mutagenesis were screened with these substrate mixtures for activity and variants with the highest activity were re-screened with single substrates of the respective mixture. Two variants from library L119 showed a significantly improved activity (~twofold) with 2-methyl cyclohexanone (2-MCHone) when compared to wild type.

Analysis of the DNA sequence of both variants revealed a nucleotide exchange from cytosine to adenine resulting in an amino acid replacement from leucine to methionine. Exchanges to methionine are generally rare events since this amino acid is encoded by only one nucleotide triplet. The substitution leucine to methionine is evolutionary the most conservative one, since it has the highest score of +2 in BLOSUM substitution matrix.<sup>[35]</sup>

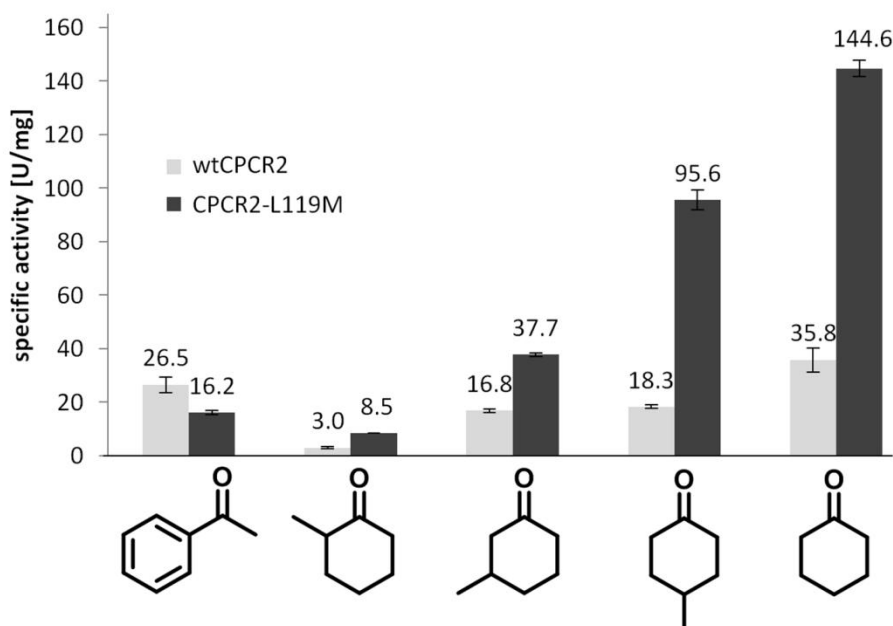


**Figure 3** Specific activities of wtCPCR2 & CPCR2-L119M on acetophenone and various cyclohexanones. Activities were determined at  $5 \text{ mmol L}^{-1}$  substrate concentration employing the standard NADH depletion assay; measurements were conducted in triplicate.

#### 3.4.4.4 Substrate Specificity and Selectivity of CPCR2-L119M

The variant CPCR2-L119M and wtCPCR2 were purified to homogeneity and analyzed in more detail concerning the substrate profile and catalytic parameters (SDS-PAGE; see Figure S1).

The catalytic activities towards acetophenone as reference substrate, cyclohexanone and substituted cyclohexanones are illustrated in Figure 3. Notably, highest activity is observed for non-substituted cyclohexanone and activity drops in the course of 4-methyl, 3-methyl and 2-methyl cyclohexanone. This trend is comparable between wtCPCR2 and variant L119M (e.g. wtCPCR2 from 3.0 (2-MCHone) to 18.3 U mg<sup>-1</sup> (4-MCHone) // L119M from 8.5 (2-MCHone) to 95.6 U mg<sup>-1</sup> (4-MCHone)). The most significant improvement of specific activity was achieved towards 4-methyl cyclohexanone (5.2-fold higher than of wtCPCR2).

**Table 2 Kinetic parameters of reduction of 2-MCHone with wtCPCR2 and CPCR2-L119M.**

Enzyme	$K_m$ [mmol <sup>-1</sup> ]	$v_{max}$ [U mg <sup>-1</sup> ]	$k_{cat}$ [sec <sup>-1</sup> ]	$k_{cat} K_m^{-1}$ [M <sup>-1</sup> sec <sup>-1</sup> ]
wtCPCR2	7.9 ± 1.3	4.6 ± 0.3	276	3.5 *10 <sup>4</sup>
CPCR2-L119M	9.7 ± 0.8	33.6 ± 1	2077	2.1 *10 <sup>5</sup>

The catalytic parameters for reduction of 2-MCHone were estimated by measuring initial rate activities. The  $K_m$  of CPCR2-L119M is similar to the one of wtCPCR2 (see Table 2), however,  $k_{cat}$  is more than 7-fold higher under substrate saturation conditions (see Table 2). Optima in temperature and pH remain unchanged when comparing wtCPCR2 and CPCR2-L119M (see Figure S2 & S3). Furthermore, the specific activity improvement of purified CPCR2-L119M towards 2-MCHone (see Figure 3), correlates well with the activity improvement found in the library at position 119 by screening crude cell extracts with the substrate set containing the screening substrate 2-MCHone.

Table 3 compares the kinetic parameters of wtCPCR2 and CPCR2-L119M for reduction of 2-MCHone with literature data for purified alcohol dehydrogenases demonstrating a notably superior specific activity of variant CPCR2-L119M (>3-fold; Table 3).

**Table 3 Kinetic parameters for reduction of 2-MCHone to 2-MCHol of purified alcohol dehydrogenases.**

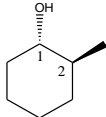
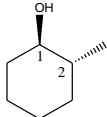
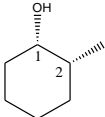
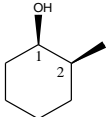
Species	Enzyme	$v_{max}$ [U mg <sup>-1</sup> ]	$K_m$ [mmol <sup>-1</sup> ]	$k_m/v_{max}$ [mmol (L mg U) <sup>-1</sup> ]	Substrate conc. [m mol <sup>-1</sup> ]	Source
<i>Candida parapsilosis</i>	wtCPCR2	4.6 ± 0.3	7.9 ± 1.3	0.58	40	this work
<i>Candida parapsilosis</i>	CPCR2-L119M	33.6 ± 1	9.7 ± 0.8	3.46	40	this work
<i>Thermus species</i> ATN1	TADH	6.97	-	-	20	[37]
<i>Commononas testosteroni</i>	QH-EDH	9.24	81	0.11	-	[38]
<i>Thermoanaerobium brockii</i>	-	6.0	-	-	150	[39]

Selectivity of wtCPCR2 and CPCR2-L119M was investigated in the reduction of 2-MCH on analytical scale. The detected relative amounts of the four possible products and enantiomeric and diastereomeric excess are depicted in Table 4.

It was found that for both wtCPCR2 and CPCR2-L119M about half the generated product was the *trans* 1-*R*,2-*R* isomer. This is surprising since wtCPCR2 produces in general (*S*)- rather than (*R*)-alcohols. A significant difference in selectivity of wtCPCR2 and CPCR2-L119M was found with regards to the *cis*-products (1-*R*,2-*S* & 1-*S*,2-*R*). In particular, variant CPCR2-L119M produced an about 3-fold higher amount of 1-*R*,2-*S* than wtCPCR2 resulting in a slightly higher enantiomeric excess.

For synthetic application of wtCPCR2 or CPCR2-L119M selectivity for 2-MCHone reduction is too low and needs to be improved. However, product mixtures of 2-MCHol were reported previously for horse liver ADH<sup>[36]</sup> and various whole cell biotransformations.<sup>[37]</sup>

**Table 4** Relative amounts of 2-MCHols produced with wtCPCR2 & CPCR2-L119M and *ee* (*R*) & *de trans*.

enantiomer [%]	<i>trans</i> 1- <i>S</i> ,2- <i>S</i>	<i>trans</i> 1- <i>R</i> ,2- <i>R</i>	<i>cis</i> 1- <i>S</i> ,2- <i>R</i>	<i>cis</i> 1- <i>R</i> ,2- <i>S</i>	<i>ee</i> 1- <i>R</i>	<i>de trans</i>
structure						
wtCPCR2	27.2	50.6	18.4	3.9	9.0	55.5
CPCR2-L119M	28.0	46.4	13.4	11.8	16.4	48.8

#### 3.4.4.5 Structure-function Relationships & Substrate Docking

A role of position 119 in substrate recognition of CPCR2 can be deduced from the corresponding position 141 in distantly related ADH isoenzymes from human liver were reported (29 % sequence identity). The ADH isoenzymes ( $\beta_1\beta_1//\sigma\sigma$ ) show different responses to pyrazole-like inhibitors, wherein the  $\sigma\sigma$  isoenzyme has low affinity to 4-methylpyrazole and the  $\beta_1\beta_1$  isoenzyme exhibits high affinity. This is modulated by position 141 as was shown by the exchange of M141 in  $\sigma\sigma$ -ADH to L141 as in native  $\beta_1\beta_1$ -ADH, which resulted in 35-fold increase in affinity to 4-methylpyrazole.<sup>[38]</sup> Additionally, the substrate spectrum of the  $\sigma\sigma$ -M141L variant towards primary alcohols ( $C_2$ -  $C_6$ ) was affected. Maximal activity was decreased for all employed alcohols and  $K_m$  values showed an increase from  $C_2$  to  $C_4$  and a decrease for  $C_5$  and  $C_6$ .

Inhibitory effects and changes in substrate specificity were attributed to changes of the available space within the substrate binding pocket by a M141L substitution and not to an altered transition state as suggested earlier.<sup>[38]</sup> Whether this is also the case for the CPCR2 variant can be investigated by docking 2-MCHone into the substrate binding pocket of wtCPCR2 and CPCR2-L119M.



The “best” active site mutation for increased activity towards 2-MCHone was the replacement of leucine to methionine at position 119. To elucidate structure-function relationships, substrate docking was performed for the screening substrate 2-MCHone in *pro-cis* orientation within the substrate binding pocket of wtCPCR2 and CPCR2-L119M based on PDB-1R37.<sup>[27]</sup>

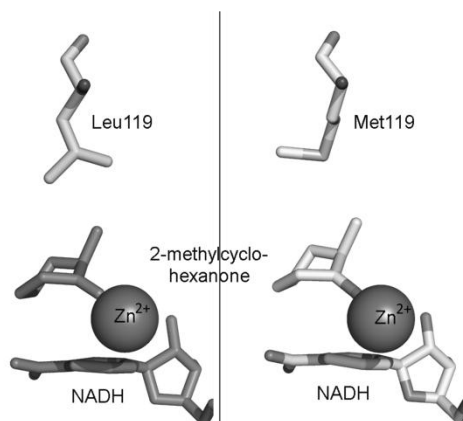


**Figure 4 Model 2-MCHone in the substrate binding pocket of wtCPCR2 and CPCR2-L119M.**

Figure 4 shows 2-MCHone, the catalytic zinc ion as well as the NADH cofactor and the amino acid residue 119. Computational studies revealed differences in the orientation of 2-MCHone and side chain conformation of amino acids at positions 119 in the variant enzymes. The positioning of 2-MCHone in CPCR2-L119M compared to wtCPCR2 is almost unaltered, but the terminal methyl group of the methionine in CPCR2-L119M points away from the 2-methyl group of 2-MCHone, whereas the isobutyl-side chain of leucine in wtCPCR2 sterically constrains the 2-methyl group of 2-MCHone. The replacement of leucine for methionine may therefore provide more flexibility to the binding and release of 2-, 3-, 4-MCHones and cyclohexanone resulting in higher catalytic activity of CPCR2-L119M (see Figure 3) as observed in the experimental studies. The volumes of the amino acids are; however, very similar: leucine =  $166.7 \text{ \AA}^3$ , methionine =  $162.9 \text{ \AA}^3$ .

Stabilization energies of MCHones and CHone related to the standard substrate acetophenone (see Table 5) indicate for both wtCPCR2 and CPCR2-L119M that cyclohexanone is preferred over the methyl-substituted cyclohexanones; the screening substrate 2-MCHone has the most unfavorable stabilization energy. This is in good agreement with the experimental data (see Figure 3).

Stabilization energies are between 6 and 26 kJ/mol lower in CPCR2-L119M than in wtCPCR2 and therefore considerably improved. Again this fits well to the catalytic performance of wtCPCR2 and CPCR2-L119M towards the examined substrates (Figure 3 and Table 5). Thus, there is a good correlation between calculated stabilizing energies and experimentally determined specific activities.

The computational study can also partially explain the enantiomeric preference of wtCPCR2 and CPCR2-L119M in the conversion of 2-MCHone (Table 4 and Figure 4). CPCR2-L119M yields 3-fold

more *cis*-1-*R*,2-*S* 2-MCHol (see Table 4) which can likely be attributed to the pro-*cis* orientation of the 2-MCHone in the binding pocket. The L119M substitution generates “free space” for the 2-methyl group of 2-MCHone since the branched iso-butyl side chain is replaced by a non-branched methionine side chain. However, for a detailed study, all binding modes of 2-MCHone (*cis*, *trans* isomers, chair and boat conformation) would have to be considered and a crystal structure in which cyclohexanol or similar substrates are bound to an ADH and that could serve as promising starting structure to elucidate enantiopreferences would be required; to our knowledge, there is no such structure to date.

**Table 5 Stabilization energies of different substrates in wtCPCR2 & CPCR2-L119M models relative to acetophenone.**

Substrate	wtCPCR2		CPCR2-L119M	
	kJ mol <sup>-1</sup>	U mg <sup>-1</sup>	kJ mol <sup>-1</sup>	U mg <sup>-1</sup>
Acetophenone	0	26.5	0	16.2
2-MCHone	1.5	3.0	-5.75	8.5
3-MCHone	-1.5	16.8	-13.4	37.7
4-MCHone	-0.25	18.3	-14.0	95.6
Cyclohexanone	-2.63	35.8	-29.2	144.6

### 3.4.5 Conclusion

This work represents the first study wherein amino acid positions of a carbonyl reductase from *Candida parapsilosis* (wtCPCR2) responsible for substrate recognition were rationally identified and subjected to saturation mutagenesis and screening. The screening system developed for this purpose is based on NADH-depletion and was optimized for homogeneous expression of wtCPCR2 in 96-well microtiter plates with a standard deviation of 15 %. It can most likely be employed for other ADHs with only minor modifications.

It was demonstrated that for broadening the substrate scope towards reduction of branched 2-MCHone the amino acid in position 119 plays a crucial role. Substitution of leucine for methionine in that position boosted the specific activity towards 2-MCHone by up to 7-fold. The variant CPCR2-L119M is ~3-fold more active in the conversion of 2-MCHone than any ADH investigated with this substrate so far. If selectivities can be further improved, CPCR2-L119M could become a synthetically attractive catalyst for the production of chiral cyclohexanol moieties occurring in complex compounds like menthol.

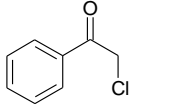
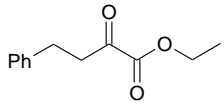
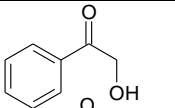
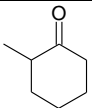
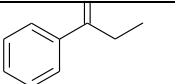
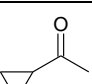
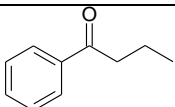
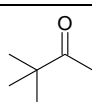
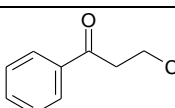
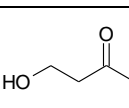
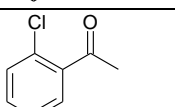
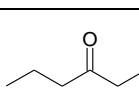
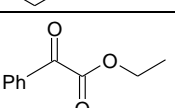
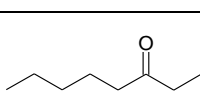
The effect of the single mutation L119M on activity and selectivity could partially be interpreted on the molecular level by comparing stabilization energies and taking the pro-*cis* orientation of 2-MCHone into account. Saturation mutagenesis at position 119 and the identified L119M substitution represent a first hint that a conservative substitution in close proximity to the active site could be important to broaden the substrate profile and/or preserve catalytic activity.

### 3.4.6 Supplementary Information

#### *Selection of screening substrates*

Fourteen single substrates were investigated with purified wtCPCR2 applying the standard cuvette scale activity test. Activity relative to acetophenone for every substrate was less than 20 % (see Table S1). Additionally, single substrates and combinations thereof were tested with wild type enzyme expressed in microtiter plate format as described in the materials and methods section. Herein, activities compared to acetophenone were always less than 20 % (see Table S1).

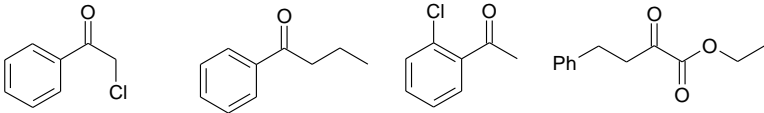
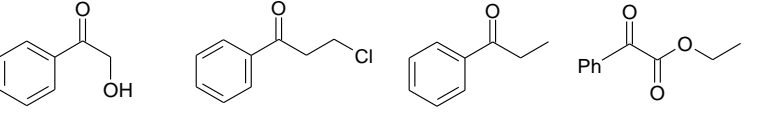
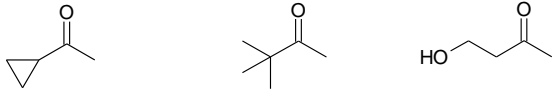
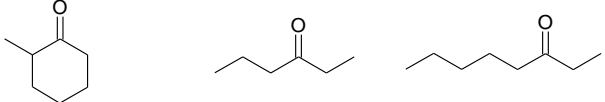
**Table S1** Activity of poorly accepted substrates relative to acetophenone. Measurements were performed with purified CPCR2 and in crude lysate.

no.	substrate	rel. act. with pure enzyme [%]	rel. act. with crude lysate [%]	no.	substrate	rel. act. with pure enzyme [%]	rel. act. with crude lysate [%]
1		17.9	2.8	8		8.3	2.7
2		8.4	27.6	9		0	-
3		7.9	6.5	10		17.5	-
4		3.4	0	11		4.7	-
5		10.4	2.5	12		6.7	-
6		11.1	10.7	13		10.0	-
7		8.1	5.5	14		8.0	-

Four sets of substrates were generated and cumulative activity of substrate combinations was determined under screening conditions (substrate concentration 5 mmol L<sup>-1</sup> each, crude lysate). Relative activities are summarized in Table S2.

Set 1, 3 & 4 showed no inactivation of CPCR2 when the assay was performed together with acetophenone, however, set 2 displayed a slight inactivation (70 % activity compared to pure acetophenone), which is most likely attributed to  $\beta$ -chloro propiophenone.

Table S2 Activity of substrate sets under screening conditions relative to acetophenone.

set no.	compounds	rel. act [%]
1		9.1
2		10.6
3		13.6
4		6.1

## Comparison of wtCPCR2 &amp; CPCR2-L119M

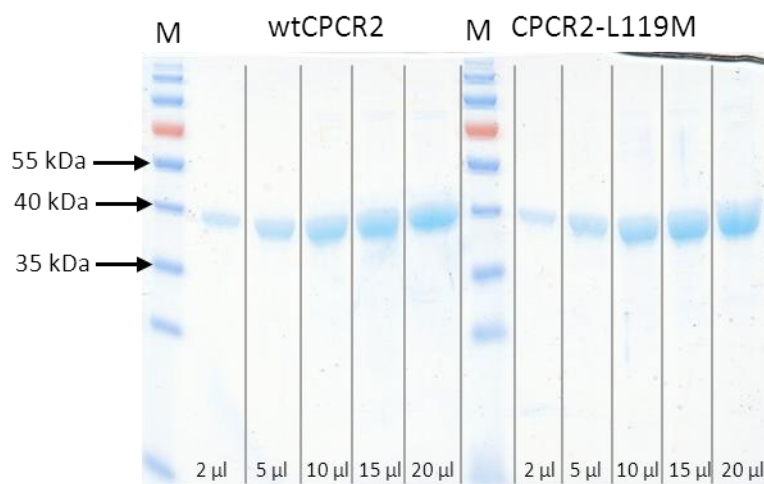


Figure S1 SDS-PAGE of wtCPCR2 and CPCR2-L119M of pooled elution fractions after strep-tag purification. M is protein weight standard (Fermentas PAGE Ruler #SM0671). Molecular weight of a CPCR2 monomer is 38.95 kDa.

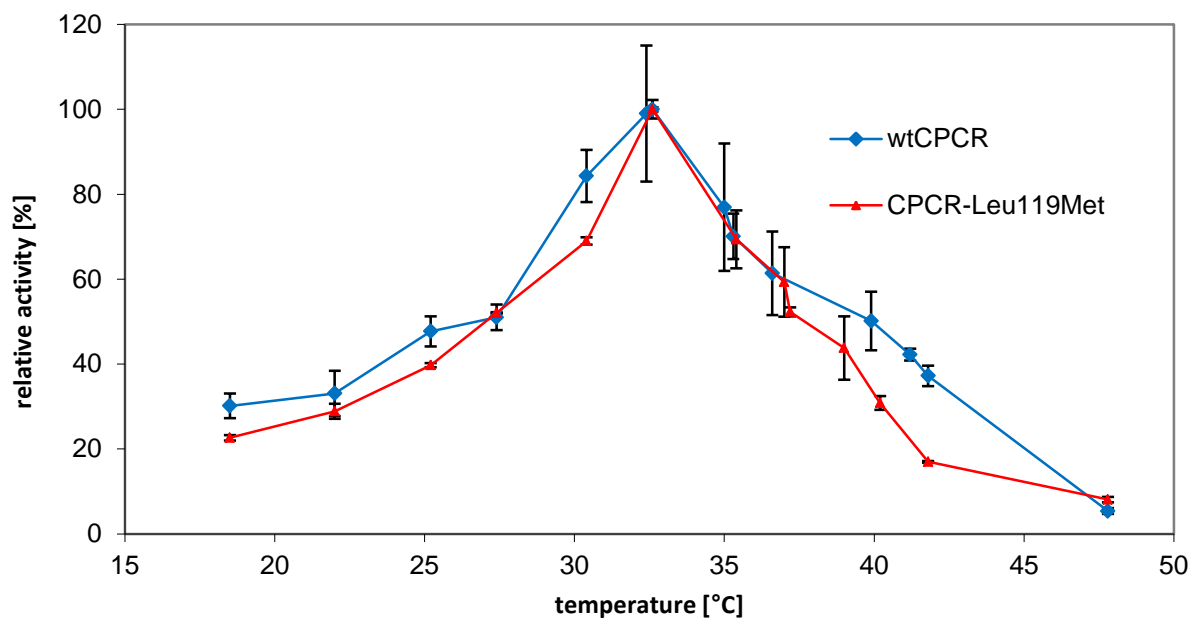


Figure S2 Comparison of the temperature optima of wtCPCR2 and CPCR2-L119M

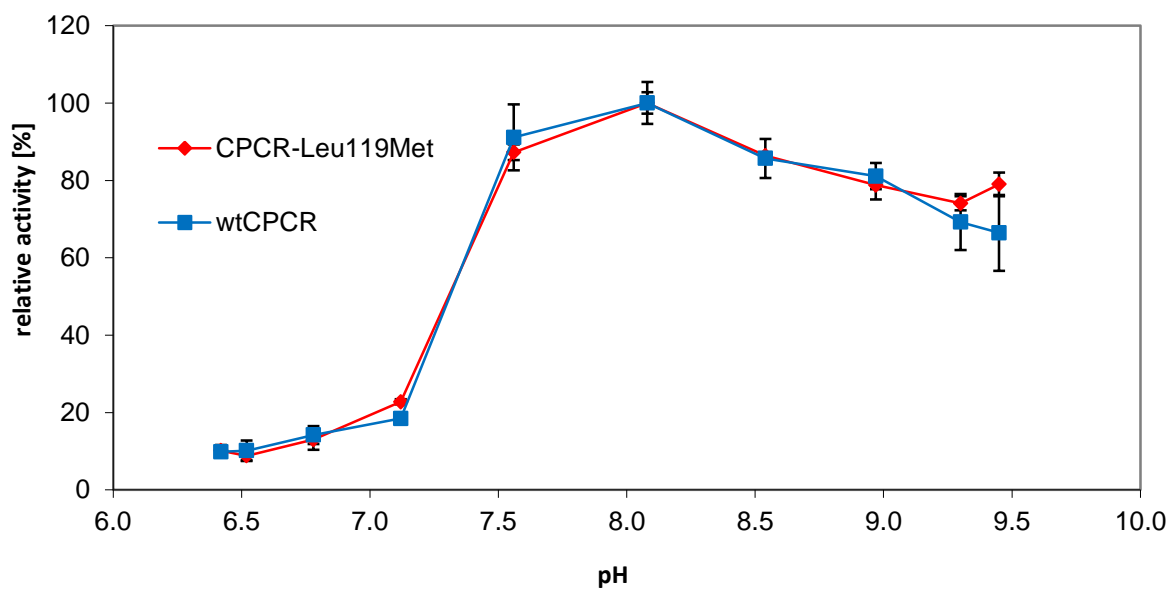


Figure S3 Comparison of the pH-optima for ketone reduction of wtCPCR2 and CPCR2-L119M

### 3.4.7 References

- [1] a) G. W. Huisman, J. Liang, A. Krebber, *Curr. Opin. Chem. Biol.* **2010**, *14*, 122-129; b) B. M. Nestl, B. A. Nebel, B. Hauer, *Curr. Opin. Chem. Biol.* **2011**, *15*, 187-193; c) R. Wohlgemuth, *Curr. Opin. Biotechnol.* **2010**, *21*, 713-724.
- [2] a) S. M. De Wildeman, T. Sonke, H. E. Schoemaker, O. May, *Acc. Chem. Res.* **2007**, *40*, 1260-1266; b) T. Matsuda, R. Yamanaka, K. Nakamura, *Tetrahedron: Asymmetry* **2009**, *20*, 513-557; c) R. N. Patel, *Coord. Chem. Rev.* **2008**, *252*, 659-701; d) R. Wohlgemuth, *Curr. Opin. Microbiol.* **2010**, *13*, 283-292; e) G. W. Zheng, J. H. Xu, *Curr. Opin. Biotechnol.* **2011**, *22*, 784-792.
- [3] A. Jakoblinnert, M. Bocola, M. Bhattacharjee, S. Steinsiek, M. Bönitz-Dulat, U. Schwaneberg, M. B. Ansorge-Schumacher, *Chembiochem* **2012**, *13*, 803-809.
- [4] J. Peters, T. Minuth, M. R. Kula, *Enzyme. Microb. Technol.* **1993**, *15*, 950-958.
- [5] H. Yamamoto, N. Kawada, A. Matsuyama, Y. Kobayashi, *Biosci. Biotechnol. Biochem.* **1999**, *63*, 1051-1055.
- [6] a) A. Matsuyama, H. Yamamoto, N. Kawada, Y. Kobayashi, *J. Mol. Catal. B: Enzymatic* **2001**, *11*, 513-521; b) H. Yamamoto, A. Matsuyama, Y. Kobayashi, *Biosci. Biotechnol. Biochem.* **2002**, *66*, 925-927.
- [7] H. Yamamoto, A. Matsuyama, Y. Kobayashi, *Biosci. Biotechnol. Biochem.* **2002**, *66*, 481-483.
- [8] T. Schubert, W. Hummel, M. R. Kula, M. Muller, *Eur. J. Org. Chem.* **2001**, 4181-4187.
- [9] S. Laue, L. Greiner, J. Wöltinger, A. Liese, *Adv. Synth. Catal.* **2001**, *6*, 343.
- [10] A. Liese, T. Zelinski, M. R. Kula, H. Kierkels, M. Karutz, U. Kragl, C. Wandrey, *J. Mol. Catal. B: Enzymatic* **1998**, *4*, 91-99.
- [11] A. van den Wittenboer, T. Schmidt, P. Muller, M. B. Ansorge-Schumacher, L. Greiner, *Biotechnol. J.* **2009**, *4*, 44-50.
- [12] A. Jakoblinnert, R. Mladenov, A. Paul, F. Sibilla, U. Schwaneberg, M. B. Ansorge-Schumacher, P. D. de Maria, *Chem. Commun.* **2011**, *47*, 12230-12232.
- [13] a) V. Prelog, *Pure Appl. Chem.* **1964**, *9*, 119-130; b) J. Peters, T. Minuth, M. R. Kula, *Biocatal. Biotransf.* **1993**, *8*, 31-46.
- [14] M. Knoll, J. Pleiss, *Protein Sci.* **2008**, *17*, 1689-1697.
- [15] H. Gröger, F. Chamouleau, N. Orogas, C. Rollmann, K. Drauz, W. Hummel, A. Weckbecker, O. May, *Angew. Chem. Int. Ed. Engl.* **2006**, *45*, 5677-5681.
- [16] D. W. Green, H. W. Sun, B. V. Plapp, *J. Biol. Chem.* **1993**, *268*, 7792-7798.
- [17] R. Machielsen, N. G. Leferink, A. Hendriks, S. J. Brouns, H. G. Hennemann, T. Dausmann, J. van der Oost, *Extremophiles* **2008**, *12*, 587-594.
- [18] J. Liang, J. Lalonde, B. Borup, V. Mitchell, E. Mundorff, N. Trinh, D. A. Kochre, R. N. Cherat, G. P. Ganesh, *Org. Proc. Res. & Dev.* **2010**, *14*, 193-198.
- [19] F. Baldassarre, G. Berton, C. Chiappe, F. Marioni, *J. Mol. Catal. B: Enzymatic* **2000**, *11*, 55-58.
- [20] E. Krieger, G. Koraimann, G. Vriend, *Proteins* **2002**, *47*, 393-402.
- [21] Y. Duan, C. Wu, S. Chowdhury, M. C. Lee, G. Xiong, W. Zhang, R. Yang, P. Cieplak, R. Luo, T. Lee, J. Caldwell, J. Wang, P. Kollman, *J. Comput. Chem.* **2003**, *24*, 1999-2012.
- [22] J. Wang, R. M. Wolf, J. W. Caldwell, P. A. Kollman, D. A. Case, *J. Comput. Chem.* **2004**, *25*, 1157-1174.
- [23] A. Jakalian, D. B. Jack, C. I. Bayly, *J. Comput. Chem.* **2002**, *23*, 1623-1641.
- [24] W. Wang, B. A. Malcolm, *Biotechniques* **1999**, *26*, 680-682.
- [25] A. E. Firth, W. M. Patrick, *Nucleic Acids Res.* **2008**, *36*, W281-285.

- [26] H. G. Holzhutter, A. Colosimo, *CABIOS* **1990**, *6*, 23-28.
- [27] L. Esposito, I. Bruno, F. Sica, C. A. Raia, A. Giordano, M. Rossi, L. Mazzarella, A. Zagari, *Biochem.* **2003**, *42*, 14397-14407.
- [28] a) B. V. Plapp, *Arch Biochem Biophys* **2010**, *493*, 3-12; b) J. K. Rubach, B. V. Plapp, *Biochem.* **2002**, *41*, 15770-15779.
- [29] E. H. Creaser, C. Murali, K. A. Britt, *Protein Eng.* **1990**, *3*, 523-526.
- [30] A. Pennacchio, L. Esposito, A. Zagari, M. Rossi, C. A. Raia, *Extremophiles* **2009**, *13*, 751-761.
- [31] T. D. Hurley, W. F. Bosron, *Biochem. Biophys. Res. Commun.* **1992**, *183*, 93-99.
- [32] L. Esposito, F. Sica, C. A. Raia, A. Giordano, M. Rossi, L. Mazzarella, A. Zagari, *J. Mol. Biol.* **2002**, *318*, 463-477.
- [33] K. I. Ziegelmann-Fjeld, M. M. Musa, R. S. Phillips, J. G. Zeikus, C. Vieille, *Protein Eng. Des. Sel.* **2007**, *20*, 47-55.
- [34] A. J. Ganzhorn, D. W. Green, A. D. Hershey, R. M. Gould, B. V. Plapp, *J. Biol. Chem.* **1987**, *262*, 3754-3761.
- [35] S. Henikoff, J. G. Henikoff, *Proc Natl Acad Sci U S A* **1992**, *89*, 10915-10919.
- [36] J. B. Jones, T. Takemura, *Can. J. Chem.* **1982**, *60*, 2950-2956.
- [37] a) R. M. De Conti, A. L. M. Porto, J. Augusto, R. Rodrigues, P. J. S. Moran, G. P. Manfio, A. J. Marsaioli, *J. Mol. Catal. B: Enzymatic* **2001**, *11*, 233-236; b) M. Kawamoto, T. Utsukihara, C. Abe, M. Sato, M. Saito, M. Koshimura, N. Kato, C. A. Horiuchi, *Biotechnol. Lett.* **2008**, *30*, 1655-1660; c) M. Miyazawa, S. Okamura, H. Kameoka, *J. Chem. Tech. Biotechnol.* **1996**, *65*, 171-165; d) H. Onishi, M. Doi, Y. Shuto, Y. Kinashita, *Biosci., Biotechnol., Biochem.* **1996**, *60*, 486-487; e) S. K. Padhi, I. A. Kaluzna, D. Buisson, R. Azerad, J. D. Stewart, *Tetrahedron: Asymmetry* **2007**, *18*, 2133-2138.
- [38] P. T. Xie, T. D. Hurley, *Protein Sci.* **1999**, *8*, 2639-2644.

**This chapter was reprinted from the publication “Reengineered carbonyl reductase for reducing methyl-substituted cyclohexanones” Jakoblinnert, A.; Wachtmeister, J.; Schukur, L.; Shivange, A.V.; Bocola, M.; Ansorge-Schumacher, M. B.\*, Schwaneberg, U.\* Protein Engineering, Design & Selection 26 (4): 291-298, 2013 with permission of Oxford University Press**

## 3.5 Design of a Carbonyl Reductase from *Candida parapsilosis* Towards Enhanced Activity & Stability

### 3.5.1 Abstract

The carbonyl reductase from *Candida parapsilosis* (CPCR2) is an industrially attractive biocatalyst for producing chiral alcohols from ketones. The homodimeric enzyme has a broad substrate spectrum and an excellent stereoselectivity, but is rapidly inactivated at aqueous-organic interfaces. The latter limits CPCR2's application in biphasic reaction media.

Reengineering the protein surface of CPCR2 yielded a variant CPCR2-(A275N, L276Q) with 1.5-fold increased activity, 1.5-fold higher interfacial stability (cyclohexane/buffer system), and increased thermal resistance ( $\Delta T_{50} = +2.7$  °C). Site-directed and site-saturation mutagenesis studies discovered that position 275 mainly influences stability and position 276 governs activity. After single site-saturation of position 275, amino acid exchanges to asparagine and threonine were discovered to be stabilizing. Interestingly, both positions are located at the dimer interface and close to the active site and computational analysis identified an inter-subunit hydrogen bond formation at position 275 to be responsible for stabilization.

Finally, the variant CPCR2-(A275S, L276Q) was found by simultaneous site-saturation of position 275 and 276. CPCR2-(A275S, L276Q) has compared to wtCPCR2 a 1.4-fold increased activity, a 1.5-fold higher interfacial stability, and improved thermal resistance ( $\Delta T_{50} = +5.2$  °C).

### 3.5.2 Introduction

Alcohol dehydrogenases (ADHs) are synthetically important enzymes for the production of optically pure alcohols, which are key intermediates for the synthesis of pharmaceuticals, agrochemicals, biomaterials and food ingredients.<sup>[1]</sup> The operation of ADHs in aqueous organic biphasic systems is often beneficial for process performance and downstream processing since, for instance, concentration of hydrophobic substrate molecules is increased and *in situ* product extraction from the organic phase is possible.<sup>[2]</sup> The application of ADHs for fine chemical synthesis in biphasic systems<sup>[1c, 3]</sup> is often limited by a low stability under process conditions, which determines process economics.<sup>[4]</sup> Process stability of isolated enzymes in aqueous organic reaction systems can be increased by protein engineering.<sup>[5]</sup> Protein engineering strategies comprise rational design, directed evolution or combined approaches, in which enzyme properties are tailored by amino acid exchanges.<sup>[6]</sup>

Rational protein engineering was mainly applied to alter substrate acceptance and selectivity of ADHs by changing amino acids in the substrate binding pocket. For instance, the substitution W110A in an ADH from *Thermoanaerobacter ethanolicus* enabled the conversion of benzylacetone which



was not converted by the wild type enzyme.<sup>[7]</sup> Stereoselectivity was inverted by single point mutations in ADHs from *Thermoanaerobacter ethanolicus* (I86A) and *Sporobolomyces salmonicolor* (Q245H, P, L).<sup>[8]</sup> Additionally, the preference for either NADH or NADPH as a cofactor was rationally reengineered for ADHs from *Lactobacillus brevis* as well as for the reductase S1 from *Candida magnoliae*.<sup>[9]</sup> Thermal resistance was increased for ADH from *Clostridium beijerinckii* by introduction of a proline.<sup>[10]</sup>

Also random protein engineering strategies consisting of iterative cycles of mutagenesis and subsequent screening of generated variants were employed for ADHs to improve activity, enantioselectivity, and stability. In detail, four rounds of directed evolution yielded a glyceraldehyde dehydrogenase variant with 26-fold improved activity on 2-hydroxybutanone.<sup>[11]</sup> Enantioselectivity for tetra-hydrothiophene-3-one was enhanced from 63 % to 99 % by eight rounds of evolution for ADH from *Lactobacillus kefir*.<sup>[12]</sup> Five mutagenesis and screening cycles yielded a ketoreductase with an overall process performance boost of 3000-fold.<sup>[5d]</sup> Higher resistance against elevated isopropanol concentrations (20 % (v/v)) was achieved for a phenylacetaldehyde reductase from *Rhodococcus sp.* ST-10.<sup>[13]</sup>

The carbonyl reductase from *Candida parapsilosis* DSM 70125 (CPCR2) was selected as protein engineering target due to its ability to produce a broad spectrum of enantiomerically pure alcohols.<sup>[14]</sup> The chiral products serve as important building blocks in chemical and pharmaceutical industries.<sup>[15]</sup> The purified CPCR2 enzyme has been applied previously in several non-conventional reaction systems such as microemulsions (composed of buffer and cyclohexane<sup>[16]</sup>) and biphasic systems (mixtures of buffer and organic solvent<sup>[17]</sup>). The latter reports demonstrated that CPCR2 is rapidly inactivated at aqueous organic interfaces limiting its application in such industrially relevant, biphasic systems.<sup>[16-17]</sup>

In this work, we reengineered CPCR2 towards enhanced activity and thermal resistance as well as increased stability in the presence of water-immiscible organic solvents. Eleven amino acid positions were rationally selected on basis of sequence alignments in order to replace surface-exposed amino acids from non-polar to polar. Two of the eleven positions (A275 and L276) proved to be beneficial and single as well simultaneous site-saturation mutagenesis of these two positions yielded CPCR2 variants with improved activity and increased thermal resistance. The CPCR2 variants were analyzed computationally and hypotheses on structure-function relationships were concluded.

### 3.5.3 Materials and Methods

#### 3.5.3.1 Chemicals, Oligo Nucleotides and Enzymes

All chemicals were purchased from Sigma (Steinheim, Germany), Aldrich (Steinheim, Germany), Fluka (Steinheim, Germany), Merck (Darmstadt, Germany) and Roth (Karlsruhe, Germany) if not stated otherwise. NADH was purchased from Jülich Chiral Solutions (Jülich, Germany). Primers were ordered from Sigma (Steinheim, Germany) or Eurofins MWG (Ebersberg, Germany). Restriction enzymes were purchased from Fermentas (St. Leon-Roth, Germany) if not stated differently.

#### 3.5.3.2 Cloning of CPCR2 and Generation of CPCR2 Variants

His-tagged CPCR2 constructs were used for purification, activity and stability determination of wild type CPCR2 (wtCPCR2) and its variants (see Supplementary Information Table S1). The His-tagged CPCR2 was replaced by a Strep-tagged CPCR2 with optimized codon usage for *E. coli* in order to increase expression levels and simplify protein purification to an one-step procedure. The Strep-tagged CPCR2 was used for all subsequent site-directed mutagenesis and site-saturation mutagenesis studies. The His-tagged and the Strep-tagged constructs of wtCPCR2 show very similar catalytic parameters (see Supplementary Information Table S3). Cloning, expression and purification of the His-tagged CPCR2 variants was performed as described previously.<sup>[14b, 18]</sup> The Strep-tagged CPCR2 was cloned and expressed as reported earlier.<sup>[14d]</sup> Strep-tag purification was carried out using 1 mL gravity flow columns purchased from IBA TAGnology (Göttingen, Germany). As elution buffer, 0.1 mol L<sup>-1</sup> triethanolamine (TEA), pH 8.0 and 2.5 mmol L<sup>-1</sup> desthiobiotin was used.

#### 3.5.3.3 Construction of CPCR2 Variants and Site-saturation Libraries

Site-directed mutagenesis of the His-tagged CPCR2 was performed according to the QuikChange<sup>®</sup> protocol (Stratagene, La Jolla, USA). Primer pairs used are listed in Supplementary Information Table S2. The general polymerase chain reaction (PCR) program was as follows: initial denaturation for 2 min at 95 °C, 25 cycles with 50 sec denaturation at 95 °C, 1 min annealing at 55 °C and 6.5 min elongation at 68 °C, final elongation for 7 min at 68 °C. PCR products were transformed into *E. coli* JM109 (DE3) using heat shock.<sup>[19]</sup>

All Strep-tagged CPCR2 site-directed mutagenesis variants and site-saturation libraries were constructed by using a two-step protocol for PCR adapted from Wang & Malcom.<sup>[20]</sup> Herein, Phusion High Fidelity DNA polymerase (New England Biolabs, Beverly, USA) was applied with 20-40 ng of wtCPCR2 DNA. In the first step, a PCR with forward and reverse primer in separate tubes was performed. The general PCR program for the first step was 95 °C initial denaturation for 5 min and three cycles: denaturation at 95 °C for 30 sec, primer annealing at 55 °C for 30-60 sec followed by elongation at 72 °C for 3-10 min. In the second step, primer pairs from the first step were mixed and a second PCR was carried out. PCR started with 95 °C initial denaturation for 5 min and 18-25 cycles:

denaturation at 95 °C for 30 sec, primer annealing at 55 °C for 30-60 sec followed by elongation at 72 °C for 3-10 min. Primer pairs used for PCR are listed in Supplementary Information Table S4.

Digestion of template DNA was performed by addition of 1  $\mu\text{L}$  *DpnI* (New England Biolabs) to 50  $\mu\text{L}$  PCR product and incubation at 37 °C overnight. Purified PCR products were transformed to commercial *E. coli*<sup>®</sup> BL21(DE3) (Lucigen, Middleton, USA) by electro-poration or heat shock according to the manufacturers manual. Transformation mixtures were spread on agar plates containing 100  $\mu\text{g mL}^{-1}$  ampicillin and grown overnight at 37 °C.

#### 3.5.3.4 *NADH-depletion Assays for CPCR2 Activity*

Cuvette-scale activity assays were carried out in a spectrophotometer with heatable cuvette chamber (Cary 300 UV/vis, Varian) using 1 mL plastic cuvettes. An assay solution was prepared (3 or 5 mmol  $\text{L}^{-1}$  acetophenone, 0.3 mmol  $\text{L}^{-1}$  NADH, 0.1 mol  $\text{L}^{-1}$  TEA, pH 8.0). The reaction was started by transferring 10  $\mu\text{L}$  of CPCR2 solution to the cuvette and rinsing with 990  $\mu\text{L}$  of the assay solution. Protein concentrations of purified CPCR2 protein were typically 25-100  $\mu\text{g mL}^{-1}$ . Absorption at 340 nm was monitored for 2 min at 30 °C. Enzyme solutions were diluted accordingly to obtain a linear decrease in absorption.

The activity assay in 96-well plate format was performed in a Sapphire M1000 spectrophotometer (Tecan). Here, 10-50  $\mu\text{L}$  of CPCR2 solution were mixed with 150  $\mu\text{L}$  substrate solution (8.33 mmol  $\text{L}^{-1}$  acetophenone, 0.1 mol  $\text{L}^{-1}$  TEA, pH 8.0). The reaction was started by addition of 50  $\mu\text{L}$  of 5 mmol  $\text{L}^{-1}$  NADH and absorption was monitored at 340 nm for 5 min. The micro titer plate chamber and the solutions were all heated up to 30 °C.

#### 3.5.3.5 *Kinetic Parameters, Stereoselectivity, $T_{50}$ -value and Interfacial Stability*

##### *Determination of $K_M$ & $k_{cat}$*

Kinetic characterizations of wtCPCR2 and its variants were carried out using the standard activity assay in cuvette-scale. Acetophenone was used as substrate in concentrations ranging from 0-30 mmol  $\text{L}^{-1}$  (0.1 mol  $\text{L}^{-1}$  TEA, pH 8.0). Purified CPCR2 enzyme was diluted accordingly to obtain a linear decrease. All measurements were conducted in triplicate. The data was fitted using SIMFIT, Version 6.3.2.<sup>[21]</sup> The first order rate constant  $k_{cat}$  was calculated by dividing  $v_{max}$ , deduced from the data fitting, by the CPCR2 concentration used in the assay.

##### *Determination of Stereoselectivity*

For determination of stereoselectivity 20 mL buffer (0.1 mol  $\text{L}^{-1}$  TEA, pH 8.0) were mixed with 2.5 % (v/v) isopropanol, 1 mmol  $\text{L}^{-1}$  NADH, 1 mmol  $\text{L}^{-1}$  dithiothreitol and 50 mmol  $\text{L}^{-1}$  acetophenone. Finally, purified CPCR2 (5 U) was supplemented. The reaction was stirred with 500 rpm at 30 °C for 24 h. Educts and products were extracted with 1 mL dichloromethane and subjected to chiral gas

chromatographic analysis. Enantiomeric excess was determined using an Agilent GC device (HP5890 Series II) equipped with a flame ionization detector (250 °C) and a chiral column (CP-ChiraSil-DEX CB 25 m, 0.25 mm, 2.5 µm, CS Chromatographie). Separation was performed at 10 psi N<sub>2</sub> with 120 °C isothermal for 30 min. Typical retention times were 10.5 min for acetophenone, 19.5 min for (*R*)-1-phenylethanol and 20.5 min for (*S*)-1-phenylethanol. Identification of the single peaks was done by comparison with authentic commercial standards. Enantiomeric excess was calculated by comparing the ratios of the peaks areas obtained from automated integration.

#### *Determination T<sub>50</sub>*

Residual activity of wtCPCR2 and its variants upon heat treatment was determined by transferring 50 µL purified CPCR2 into a 96-well plate (Thermowell-96<sup>®</sup> Corning). The plate was sealed and incubated at temperatures ranging from 37-60 °C for 20 min in a PCR cycler (Mastercycler pro S, Eppendorf). After incubation, 10-20 µL CPCR2 solution was subjected to the 96-well plate-scale activity assay. All measurements were conducted in triplicate. Data was fitted using the software ORIGIN version 7.0 applying a Boltzmann model. The temperature at, which 50 % of the initial activity was detected, was denoted T<sub>50</sub>-value.

#### *Determination of Interfacial Stability*

Interfacial stability of CPCR2 in the presence of a water-organic interface was monitored by overlaying 3 mL cyclohexane, *n*-heptane or methyl *tert*-butyl ether (MTBE) with 3 mL of CPCR2 solution (0.1 mol L<sup>-1</sup> TEA, pH 8.0). Protein concentrations were 50 µg mL<sup>-1</sup> for His-tagged CPCR2 and 100 µg mL<sup>-1</sup> for Strep-tagged CPCR2. The individual organic solvents and the aqueous buffer were saturated with each other beforehand. Incubation was performed at room temperature and 100 rpm stirring (5 mm Teflon coated stirrer bar). Aliquots were taken from the aqueous phase at regular time intervals until at least 75 % of activity was lost (2x half-life). Samples were subjected to the cuvette-scale activity assay. All measurements were at least performed in triplicate. Data was fitted with a model of first order decay using SIMFIT, Version 6.3.2.<sup>[21]</sup> Half-lives (*t*<sub>1/2</sub>) were calculated by dividing ln(2) by the apparent deactivation parameter (*k*<sub>app</sub>).

#### *Determination of Water Solubility of Solvents*

Solvent concentrations within the aqueous phase were determined from solvent-saturated buffer samples via GC-analysis using a HP5890 Series II (Agilent, Germany) equipped with a FS-FFAP-CB-0.5 column (CS-Chromatography, Germany). 1-butanol was used as internal standard and was added after sampling. Details of analysis: N<sub>2</sub> 0.25 bar; injector/flame ionization detector 200 °C; 45 °C for 3.5 min, 200 °C (20 °K min<sup>-1</sup>); typical retention times: MTBE 2.1 min, *n*-heptane 2.2 min, toluene 3.7 min, and 1-butanol 6.6 min.

### 3.5.3.6 Screening for Improved Stability

#### Screening for detergents

To identify a detergent, which effectively inactivates CPCR2 in crude *E. coli* lysate, TritonX100 as non-ionic, sodium dodecyl sulfate (SDS) as negatively charged, cetyltrimethyl ammonium bromide (CTAB) as positively charged and 3-[(3-cholramidopropyl)dimethyl-ammonio]-1-propanesulfonate (CHAPS) as zwitter ionic detergent were investigated with wtCPCR2 below the critical micelle concentration (cmc) and above. TritonX100 (cmc = 0.2-0.9) was used at 0.5 and 1 mmol L<sup>-1</sup>, SDS (cmc = 7-10 mmol L<sup>-1</sup>) at 0.5, 2 and 20 mmol L<sup>-1</sup>, CTAB (cmc = 1 mmol L<sup>-1</sup>) at 0.5 and 5 mmol L<sup>-1</sup>, CHAPS (cmc = 6-10 mmol L<sup>-1</sup>) at 2 and 20 mmol L<sup>-1</sup>.

For the stability assay, 10 units of CPCR2 from a crude *E. coli* extract were mixed in a final volume of 2 mL in glass vials with detergent solution at 30 °C and 100 rpm stirring (5 mm Teflon coated stirrer bar). Enzymatic activity was determined at regular time intervals using the cuvette-scale activity assay. Measurements were carried out in duplicate.

#### Screening for Detergent Stability

To find a SDS concentration for library screening, 20 µL crude wtCPCR2 lysate were incubated at 37 °C for 20 min with 20 µL SDS solution (0.1-2 mmol L<sup>-1</sup> SDS in 0.1mol L<sup>-1</sup> TEA, pH 8.0) in a 96-well plate and shaking (900 rpm, 70 % relative humidity). The residual CPCR2 activity was afterwards analyzed using the 96-well plate-scale activity assay.

For library screening, 20 µL of crude lysates were incubated with 20 µL of 1 mmol L<sup>-1</sup> SDS in 0.1 mol L<sup>-1</sup> TEA, pH 8.0 for 20 min in a multi titer plate shaker (900 rpm, 37 °C, 70 % relative humidity). Residual activity was quantified using the 96-well plate-scale activity assay.

#### Screening of Thermostability

The T<sub>50</sub>-value for wtCPCR2 in crude lysates was determined in the same way as described for purified CPCR2. For screening libraries, 50 µL of crude lysate was incubated for 20 min at 50 °C and cooled down to 4 °C before determination of residual activity applying the 96-well plate NADH-depletion assay.

#### Molecular Modeling

Structural basis for the modeling is the recently published homology model of wtCPCR2 based on the X-ray structure of *Sulfolobus solfataricus* ADH (PDB-code 1R37) with bound ethoxyethanol.<sup>[14b]</sup> We constructed relaxed models of CPCR2 with zinc-bound acetophenone in a reactive conformation according to the previously published procedure<sup>[14b]</sup> using Yasara Structure version 11.6.16 software<sup>[22]</sup> and employing the force field AMBER03<sup>[23]</sup> for the protein and GAFF<sup>[24]</sup> with AM1/BCC charges<sup>[25]</sup>

for the substrate. Stability calculation and dimer interaction energies were computed with FoldX Version 3.0 Beta 5.1 (c) <sup>[26]</sup> using the Yasara-FoldX plugin with standard settings. <sup>[27]</sup>

### 3.5.4 Results & Discussion

In the first paragraph the interfacial stability of wtCPCR2 is described. The second paragraph describes the generation of twelve rationally designed variants targeting the surface amino acids at positions 24, 26, 78, 79, 83, 222, 226, 275, 276, 307 and 308, which were subsequently screened for improved activity and/or interfacial stability. Positions 275 and 276 were selected for in-depth characterization since activities and interfacial stabilities were improved simultaneously. The concluding paragraph on computational analysis of the CPCR2 variants provides a first hypothesis on the role of the investigated amino acids on thermal resistance (position 275) and activity (position 276).

#### 3.5.4.1 Interfacial Stability of CPCR2

Purified wtCPCR2 was incubated in aqueous-organic biphasic systems with methyl tert-butyl ether (MTBE), cyclohexane and *n*-heptane as second phase as well as in monophasic systems composed of aqueous buffer saturated with the same solvents. Figure 1 shows stabilities of wtCPCR2 as half-life in mono- and biphasic systems. Inactivation in a monophasic system is termed “*molecular toxicity*” and inactivation at aqueous-organic interface is named “*phase toxicity*”. <sup>[28]</sup> The experimentally observed inactivation in biphasic systems comprises a combination of molecular toxicity and phase toxicity. Half-lives of wtCPCR2 show that the presence of cyclohexane and *n*-heptane in monophasic systems does not significantly affect the stability. However, MTBE reduces half-life significantly. This can likely be attributed to the considerably higher solubility of MTBE in aqueous buffer (668 mmol L<sup>-1</sup>) compared to cyclohexane and *n*-heptane (4 and 16 mmol L<sup>-1</sup>, respectively). Hence, for wtCPCR2 molecular toxicity correlates well with the solvent concentration in aqueous buffer. Such correlations of solvent concentration and enzyme stability have been reported for other enzyme classes. <sup>[29]</sup>

If a solvent-saturated buffer is overlaid with the same organic solvent a biphasic system with a distinct interface is generated. Upon comparison of enzyme stability in the solvent-saturated buffer with the corresponding biphasic system, the singular influence of the water/solvent interface (phase toxicity) can be estimated. Figure 1 displays that wtCPCR2 gets rapidly inactivated at the water/solvent interface. Its half-life drops up to 30-fold in presence of cyclohexane and *n*-heptane when compared to the half-life in buffer. Phase toxicity is less prominent with MTBE (twofold reduction).

The surface tensions of the organic solvents, which is 50.2 mN m<sup>-1</sup> for cyclohexane and *n*-heptane <sup>[30]</sup> but only 10.2 mN m<sup>-1</sup> for MTBE <sup>[30]</sup>, are in good correlation with the reduction in half-life and may account for the enzyme inactivation. The finding agrees with previous reports, in which a clear

correlation between the decrease in interfacial stability and increasing surface tension of solvents was observed for the protease papain.<sup>[31]</sup> As well, the ADHs from horse liver, *Lactobacillus brevis* and *Thermoanaerobium brockii* were shown to be, like wtCPCR2, relatively stable in presence of MTBE and unstable in emulsions with cyclohexane.<sup>[32]</sup> However, Gröger *et al.* reported *n*-heptane to be a better choice than MTBE as organic solvent for a biphasic system when an ADH from *Rhodococcus erythropolis* was employed jointly with a formate dehydrogenase from *Candida boidinii*.<sup>[2a]</sup> Mutants of CPCR2 were rationally designed, generated and analyzed in order to improve stability and obtain a deeper understanding of interfacial inactivation on the molecular level.

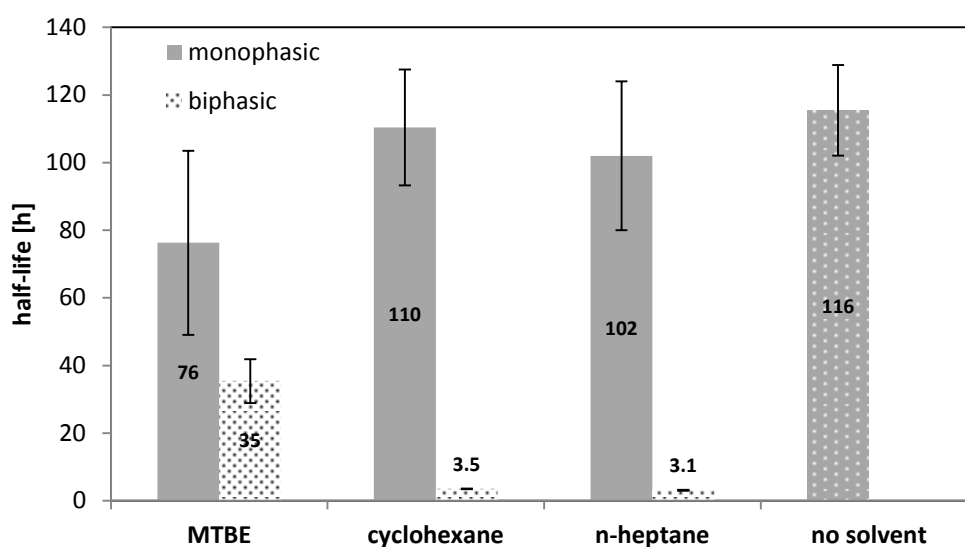


**Figure 1** Half-lives of CPCR2 in the presence of MTBE, cyclohexane and *n*-heptane in monophasic (solvent-saturated buffer) and biphasic systems. The numbers within the columns specify the average half-life in hours. Figure and results taken from PhD thesis A. van den Wittenboer, RWTH Aachen University 2009.<sup>[33]</sup>

#### 3.5.4.2 Rational Site Selection for CPCR2 Variants

Amino acid positions in wtCPCR2 for site-directed mutagenesis studies were selected following the hypothesis to decrease the extent of hydrophobic interactions with the organic solvent molecules by exchanging hydrophobic surface residues against hydrophilic residues. Preference was given to amino acid positions localized in flexible loop regions, which should ideally enable additional non-covalent interactions and thus reduce the susceptibility for structural rearrangements upon solvent exposure. Based on a protein sequence alignment of related ADHs originating from thermophile hosts and visual inspection of crystal structures (see Figure S 1), sites for site-directed mutagenesis were identified. Selected hydrophobic residues were exchanged against polar or charged residues with similar steric demand (see Table S1).

#### 3.5.4.3 Activity & Stability of Rationally Designed CPCR2 Variants

Twelve CPCR2 variants were generated, purified to homogeneity and investigated for specific activity using a NADH-depletion assay.<sup>[33]</sup> An improvement in specific activity compared to wtCPCR2 was

found for CPCR2-(A275N, L276Q); whereas most other variants exhibited lower activities (see Figure 2). In detail, the amino acid exchanges at positions 24, 26, 222, 226, 307 and 308 resulted in a loss of >80 % in specific activity. Mutation of positions 78, 79 and 83 was tolerated better, but relative specific activity values were still only 29 % for CPCR2-(V78S, I79K, V83E), 33 % for CPCR2-(V78S, I79T, V83S) and 86 % for CPCR2-(I79T, V83S), respectively.

The five most active CPCR2 variants for further studies were: CPCR2-(V78S, I79T, V83S), CPCR2-(I79T, V83S), CPCR2-(V78S, I79K, V83E), CPCR2-(A275N, L276Q) and CPCR2-(L307K, L308K). All five CPCR2 variants were subjected to stability experiments in mono- and biphasic systems in presence of MTBE, cyclohexane and *n*-heptane. Enantioselectivity of these variants remained unaltered for acetophenone as substrate when compared to wtCPCR2 (*ee* > 99 % with acetophenone, data not shown), whereas relative stability was decreased in monophasic systems especially in the presence *n*-heptane and cyclohexane (Figure 3, black bars).

On the contrary, considerable stabilization was observed in biphasic systems for the three variants CPCR2-(V78S, I79T, V83S), CPCR2-(I79T, V83S), and CPCR2-(A275N, L276Q) (see Figure 3, grey bars). Best improvement in interfacial stability was observed for the variant CPCR2-(I79T, V83S), which is significantly more stable in all investigated biphasic systems when compared to wtCPCR2.

Variant CPCR2-(A275N, L276Q) exhibits increased activity as well as increased interfacial stability in MTBE and cyclohexane (see Figure 2 and Figure 3). The respective amino acid substitutions at positions 275 and 276 were further analyzed by individually introducing both substitutions (A275N; L276Q) in wtCPCR2.

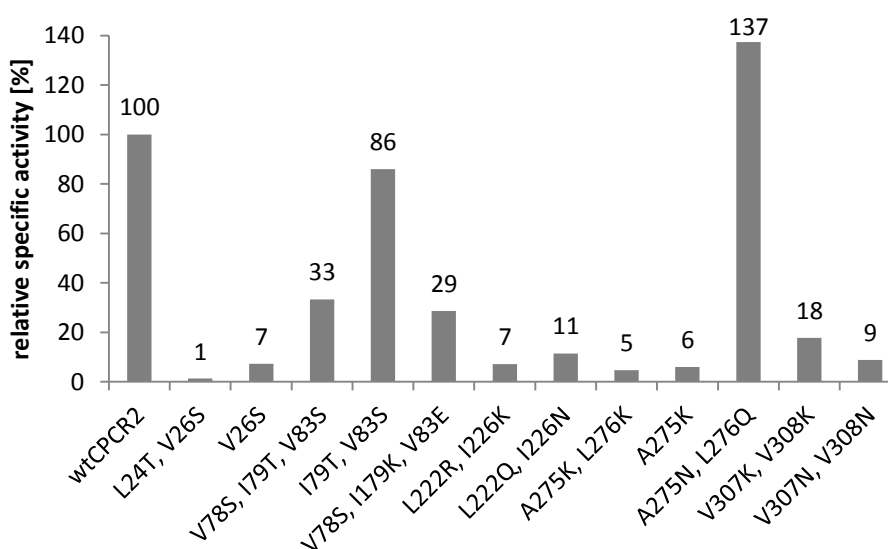


**Figure 2** Specific relative activities of purified CPCR2 variants in relation to wtCPCR2 in buffer (0.1 mol L<sup>-1</sup> TEA, pH 8; 5 mmol L<sup>-1</sup> acetophenone). Specific activity of wtCPCR2 in crude extract was 0.97 U mg<sup>-1</sup>. Figure and results taken from PhD thesis A. van den Wittenboer, RWTH Aachen University 2009.<sup>[33]</sup>



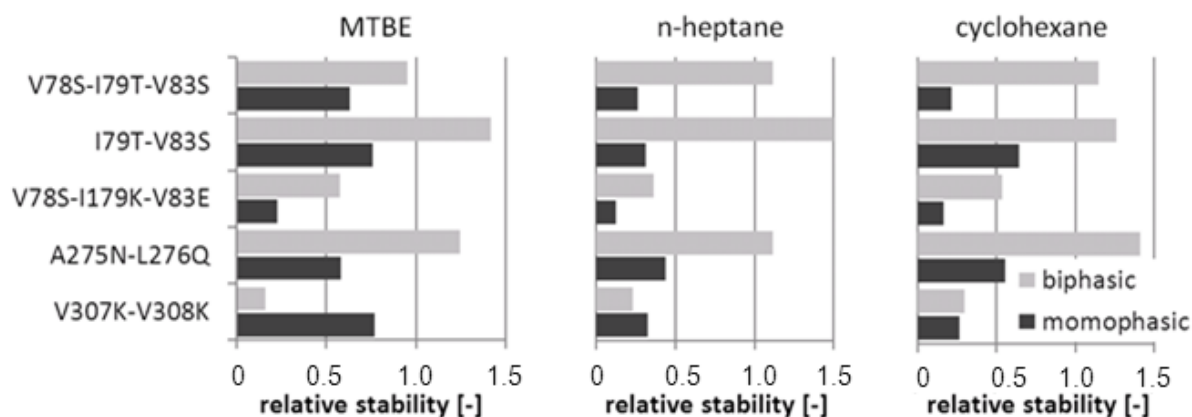


Figure 3 Relative stability of selected CPC2 variants in the presence of organic solvents. Relative stabilities are normalized to the half-lives of wtCPC2 in the corresponding mono- and biphasic systems (see Figure 1). Figure and results taken from PhD thesis A. van den Wittenboer, RWTH Aachen University 2009.<sup>[33]</sup>

#### 3.5.4.4 Cooperativity of Position 275 and 276 in CPC2

Figure 4 Fehler! Verweisquelle konnte nicht gefunden werden. shows the individual contributions of CPC2-(A275N) and CPC2-(L276Q) to the increase of relative activity and interfacial stability in the presence of cyclohexane. Cyclohexane was selected as organic solvent due to the strong improvements in relative stabilities in the corresponding biphasic system (see Figure 3).

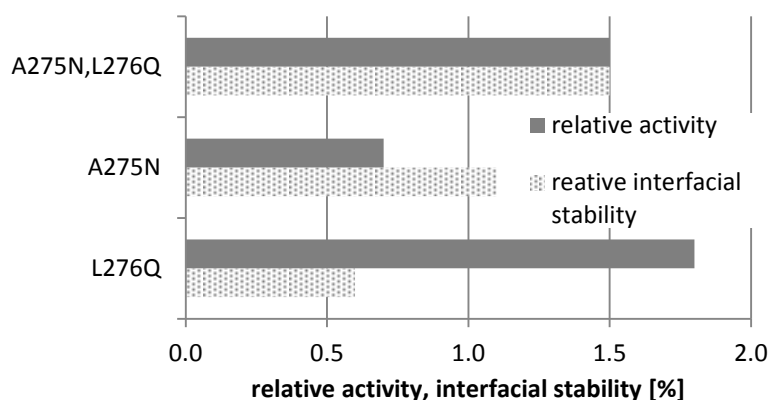


Figure 4 Relative activity in buffer and relative interfacial stability of CPC2-(A275N, L276Q), CPC2-(A275N), and CPC2-(L276Q) in a biphasic system with cyclohexane. Normalization was done to the activity of wtCPC2 in buffer (0.1 mol L<sup>-1</sup> TEA, pH 8; 5 mmol L<sup>-1</sup> acetophenone) and to interfacial stability of wtCPC2 determined in a biphasic system with cyclohexane. Specific activity of wtCPC2 was 25 U mg<sup>-1</sup>.

The analysis of the single amino acid exchanges on activity and interfacial stability demonstrated that CPC2-(A275N) is slightly more stable but significantly less active compared to wtCPC2. CPC2-(L276Q) is 1.8-fold more active but less stable in the biphasic cyclohexane/buffer system. CPC2-(A275N, L276Q) is ~1.5-fold more active and ~1.5-fold more stable than wtCPC2. Hence, position 275 influences preferentially interfacial stability while position 276 improves mainly activity. Site-saturation mutagenesis (SSM) of the positions A275 and L276 was performed with the individual single sites (sSSM) as well as with both site simultaneously (dSSM) in order to find out whether the

rationally designed variants (CPCR2-(A275N), CPCR2-(L276Q) and CPCR2-(A275N, L276Q)) represent the most beneficial amino acid substitutions for increased activity and interfacial stability.

#### 3.5.4.5 Screening Procedure of Increased Activity and Stability

Libraries of CPCR2 variants were screened for activity in crude *E. coli* lysates in 96-well plates employing a NADH-depletion assay previously adapted for this purpose.<sup>[34]</sup> The screening strategy comprised three steps: Firstly, initial activity was determined; secondly, residual activities were determined after incubation at elevated temperatures (50°C; 20 min) and thirdly, residual activities were determined after incubation in the presence of detergent (1 mmol L<sup>-1</sup> SDS; 20 min). To eliminate variations in protein expression levels, activity ratios were calculated.

Thermal resistance and SDS stability were selected as criteria for interfacial stability since crude cell lysates did not show inactivation of wtCPCR2 after overlaying and extensive incubation with organic solvents in 96-well micro titer plates. The latter can likely be attributed to interactions between the aqueous/organic interphase and proteins or membrane debris originating from *E. coli*. To validate the screening procedure, the variant CPCR2-(A275N, L276Q) served as a positive control since it was already proven to be more active and stable (see Figure 2 and Figure 3).

#### Screening assay for Improved Thermostability

For selection of an appropriate temperature for screen of wtCPCR2 for thermal resistance, the T<sub>50</sub>-values of wtCPCR2 and CPCR2-(A275N, L276Q) in crude *E. coli* lysate were determined by incubation at different temperatures for 20 min. Figure 5 shows the typical sigmoidal decrease in relative activity with increasing temperature and the T<sub>50</sub>-value defined as the temperature at which 50 % of residual enzymatic activity is left.<sup>[4b]</sup> CPCR2 wild type has a T<sub>50</sub>-value of 47.5 ± 0.74 °C and CPCR2-(A275N, L276Q) of T<sub>50</sub>= 50.2 ± 0.63 °C. The latter result gives the first indication that thermal resistance correlates with interfacial stability, since the T<sub>50</sub>-value of the positive control CPCR2-(A275N, L276Q) is increased (ΔT<sub>50</sub>= +2.7 °C) along with the interfacial stability (1.5-fold; Figure 3) when compared to wtCPCR2. A correlation between thermal resistance and interfacial stability was reported in other protein stabilization studies.<sup>[35]</sup>

In essence, incubation at 50 °C for 20 min was finally selected to screen for wtCPCR2 variants with improved interfacial stability. Residual activities were determined using the 96-well plate NADH-depletion assay.<sup>[14d]</sup> The standard deviation of the screening system was calculated to be 8.6 %. Screening systems with standard deviations below 14 % were routinely used to identify improved variants in 96-well microtiter plate format.<sup>[36]</sup>

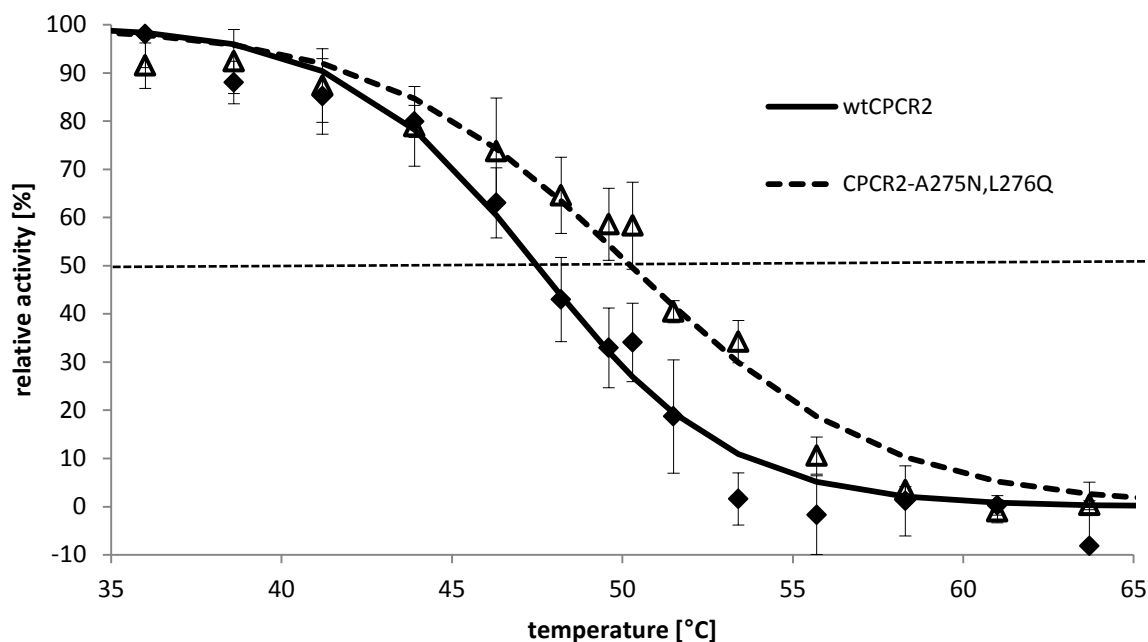


**Figure 5** Determination of  $T_{50}$ -value for wtCPCR2 and CPCR2-A275N-L276Q in crude lysates. The inactivation curves indicate that CPCR2-A275N-L276Q could be identified in crude cell extracts in screening campaigns to improve thermal resistance. The dotted line indicates 50 % of residual activity.

#### Screening Assay for Improved Detergent Stability

To establish screening conditions for detergent stability, four chemically different detergents were probed for their ability to inactivate wtCPCR2 above and below the critical micelle concentration (cmc). The NADH depletion assay in cuvettes revealed that all detergents inactivate wtCPCR2 in crude *E. coli* lysates at concentrations above their cmc (see Supplementary Information Figure S2). Sodium dodecyl sulfate (SDS) was identified as strong denaturant (50 % residual activity in 0.5 mmol L<sup>-1</sup> SDS; 30 min incubation). The non-ionic TritonX100 showed in contrast to SDS initial activation of CPCR2 at submicellar concentrations and the positively charged CTAB exhibits activity preserving properties below cmc since CPCR2 activity was unaltered for more than 30 h (see Supplementary Information **Fehler! Verweisquelle konnte nicht gefunden werden.**).

SDS was chosen for screening of CPCR2 crude lysates in 96-well plate-scale because it was reported to inactivate enzymes mainly by interactions with the hydrophobic part of the molecule thereby mimicking the interaction with water-immiscible organic solvents.<sup>[37]</sup> Different SDS concentrations (0.1, 0.25, 1 and 2 mmol L<sup>-1</sup>) were chosen to find conditions for CPCR2 inactivation. Incubation of crude wtCPCR2 lysate in micro titer plate for 20 min. demonstrated that 1 mmol L<sup>-1</sup> SDS reduced activity by half and was therefore chosen for further screening (data not shown). Standard deviation of the screening system was determined to be 6.5 %.

#### 3.5.4.6 *CPCR2 Variants Found by Screening*

CPCR2 SSM libraries were constructed and completeness calculated according to Patrick and Firth was high for all three libraries (see Supplementary Information Table S5).<sup>[38]</sup> Most promising clones identified from initial screening of the two sSSM as well as for the dSSM libraries of position 275 and 276 were rescreened in triplicate. Variants showing significant improvements in activity and/or stability were subjected to DNA sequencing.

Table 4 summarizes relative improvements in activity, thermal resistance and SDS stability of CPCR2 variants identified in screening of 275-sSSM-, 276-sSSM- and 275, 276-dSSM-libraries. From 275-sSSM, threonine and asparagine at position 275 exhibit significant improvements in thermal resistance and SDS stability. Notably, the previously generated variant CPCR2-(A275N), which exhibits higher interfacial stability than wtCPCR2 (see Figure 3), was identified in the library as more resistant to thermal and detergent inactivation. The positive correlation proves again that the screening strategy with incubation at an elevated temperature allows identifying interfacial stabilized CPCR2 variants in crude cell lysates. Screening of 275-sSSM proves that position 275 contributes, as previously suggested, to stability, whereas increases in activity were not significant.

Position 276 improves activity substantially especially for the exchanges to glutamine (2.1-fold), arginine (1.5-fold) and lysine (1.4-fold), whereas a significant stabilizing effect was not detected (see Table 4). The substitution pattern indicates that polar and positively charged amino acids at position 276 exhibit a positive effect on CPCR2 activity. Notably, stabilization towards SDS was not observed in 276-sSSM. Saturation mutagenesis of position 276 demonstrates its activity improving role as proposed earlier for CPCR2-(L276N) (see Figure 4). Like for position 275, the L276Q exchange was identified by the screening procedure as highly beneficial. The latter shows again the accuracy of the developed screening strategy and chosen conditions.

Simultaneous saturation at positions 275 and 276 resulted in CPCR2 variants with improved activity, thermal resistance, and detergent stability. The best combination found was CPCR2-(A275S, L276Q), which yielded improved activity (twofold), thermal resistance (twofold) and significantly higher stability in the presence of SDS (1.8-fold). Interestingly, at position 275 serine or threonine were found in 5 out of 7 sequenced variants indicating the importance of a hydroxyl group at this position. Methionine at position 276 was found to exhibit a substantial stabilizing effect when combined with serine, threonine or asparagine at position 275, whereas activity was improved only in combination with serine (see Table 4). Notably, the double mutant CPCR2-(A275N, L276Q), which was designed rationally before, was again identified by screening the dSSM library.

**Table 4** Relative improvements of CPCR2 variants compared to wtCPCR2 identified after rescreening in 96-well micro titer plate format. Measurements were performed in triplicates using the NADH depletion assay with crude cell lysates. For calculation of activity improvements, the activity ratios of the variants compared to wtCPCR2 were calculated ( $\text{act}_{\text{variant}}/\text{act}_{\text{wt}}$ ). Improvements in thermal resistance ( $\text{act}_{\text{Temp}}$ ) and SDS stability ( $\text{act}_{\text{SDS}}$ ) were determined by dividing the activities after treatment of the variants by the residual activity of wtCPCR2. Before forming the ratios, the residual activities were normalized with the activities before treatment to account for variation in expression levels. The best performing variant is in bold. The previously designed double mutant A275N, L276Q as well as wtCPCR2 are shaded in grey.

Variant	Relative activity $\text{act}_{\text{variant}}/\text{act}_{\text{wt}}$	Residual activity relative $\text{act}_{\text{Temp}}$	Residual activity relative $\text{act}_{\text{SDS}}$
wtCPCR2 (A275,L276)	1.00 ± 0.17	1.00 ± 0.10	1.00 ± 0.15
Ala275Thr	1.23 ± 0.44	1.61 ± 0.32	1.53 ± 0.27
Ala275Asn	0.97 ± 0.24	1.54 ± 0.04	1.58 ± 0.18
Leu276Gln	2.10 ± 0.30	1.17 ± 0.29	1.00 ± 0.35
Leu276Arg	1.54 ± 0.09	1.20 ± 0.21	0.96 ± 0.33
Leu276Lys	1.37 ± 0.15	0.83 ± 0.14	0.60 ± 0.01
<b>Ala275Ser,Leu276Gln</b>	<b>1.92 ± 0.05</b>	<b>1.96 ± 0.06</b>	<b>1.75 ± 0.44</b>
Ala275Asn,Leu276Gln	2.12 ± 0.29	1.38 ± 0.09	1.52 ± 0.12
Ala275Ser,Leu276Met	2.05 ± 0.17	1.40 ± 0.19	1.61 ± 0.32
Ala275Thr,Leu276Asn	2.33 ± 0.21	1.11 ± 0.42	1.49 ± 0.07
Ala275Ser,Leu276Arg	1.43 ± 0.11	1.26 ± 0.36	1.30 ± 0.10
Ala275Thr,Leu276Met	0.78 ± 0.21	1.85 ± 0.07	1.73 ± 0.29
Ala275Asn,Leu276Met	0.71 ± 0.01	1.60 ± 0.07	1.02 ± 0.25

Overall, the substitution patterns suggest that positions 275 and 276 in CPCR2 tolerate mutations to polar amino acids like serine, threonine, asparagine or glutamine. Basic as well as amide amino acids at position 276 appear to have positive effects on activity. The three rationally designed variants (CPCR2-(A275N), CPCR2-(L276Q) and CPCR2-(A275N, L276Q)) were identified by screening the corresponding SSM libraries. The trends in activity and stability deduced from screening in crude lysates resemble the results obtained for the purified variants generated beforehand validating the rationality within the screening and selection strategy.

For a detailed analysis, the most beneficial variants CPCR2-(A275T) and CPCR2-(L276Q) as well as the best double mutant CPCR2-(A275S, L276Q) were selected for in-depth characterization. The variant CPCR2-A275S was not identified by site-saturation in the screening system, despite that the dSSM of position 275 and 276 demonstrated the A275S substitution being a very beneficial one (see Table 4). Thus, the CPCR2-(A275S) variant was generated by site-directed mutagenesis applying the same conditions as for sSSM-275 library construction.

### 3.5.4.7 Characterization of Purified CPCR2 Variants

The variants CPCR2-(A275T), CPCR2-(A275S), CPCR2-(L276Q) and CPCR2-(A275S, L276Q) were selected for characterization in comparison to wtCPCR2. All variants were purified and analyzed in terms of kinetic performance ( $K_M$ ,  $k_{cat}$ ), stereoselectivity ( $ee$ ), interfacial stability ( $t_{1/2}$ ), and thermal resistance ( $T_{50}$ ).

**Table 5 Comparison of catalytic and stability parameters of wtCPCR2, CPCR2-A275S and most beneficial variants identified by screening SSM libraries of positions 275, 276.**

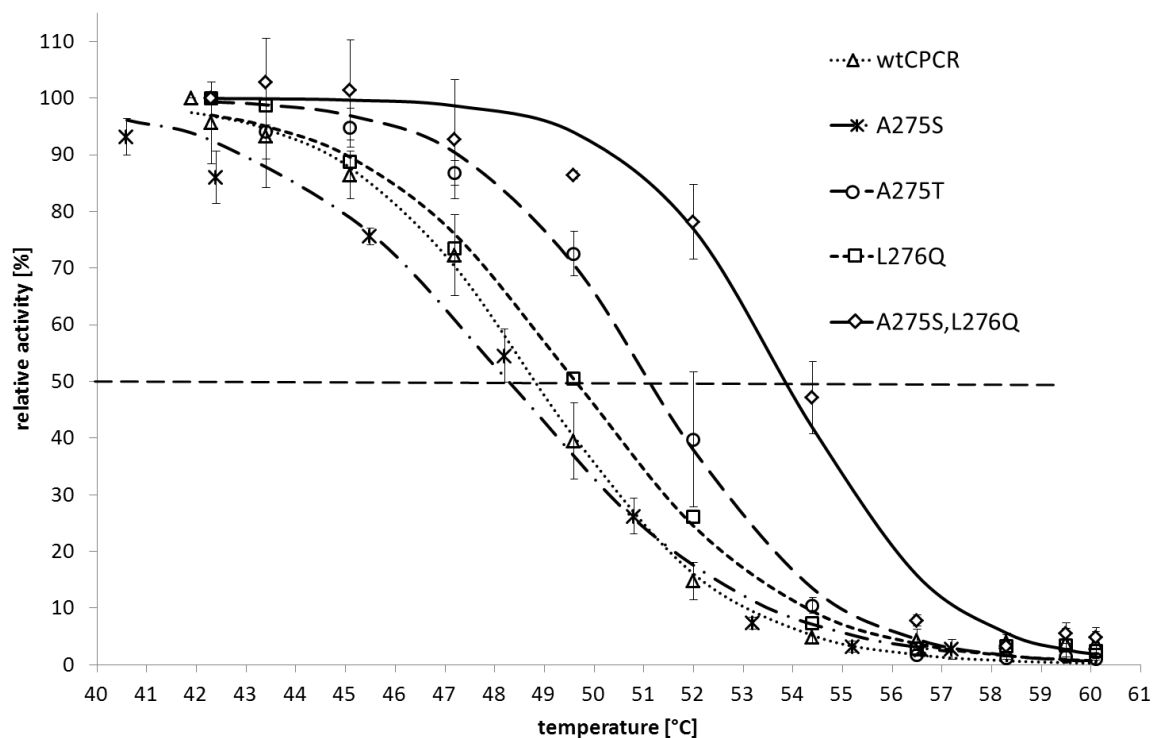
CPCR2 variant	$K_M$ [mol L <sup>-1</sup> ]	$v_{max}$ [U mg <sup>-1</sup> ]	$k_{cat}$ [s <sup>-1</sup> ]	$ee$ S [%]	$t_{1/2}$ [h]	$T_{50}$ [°C]
wtCPCR2	0.20 ±0.03	53.2 ±0.9	3213	>99	5.87 ±0.28	48.8 ±0.1
CPCR2-A275S	0.53 ±0.05	56.0 ±0.8	3186	>99	2.05 ±0.07	48.4 ±0.4
CPCR2-A275T	0.21 ±0.03	46.3 ±0.8	2678	>99	4.49 ±0.11	51.4 ±0.1
CPCR2-L276Q	0.72 ±0.06	72.6 ±1.4	4305	>99	3.17 ±0.06	49.3 ±0.2
CPCR2-A275S-L276Q	0.71 ±0.07	74.8 ±1.7	4773	>99	8.96 ±0.38	54.0 ±0.3

Table 5 lists the catalytic and stability parameters for the purified wtCPCR2 and selected CPCR2 variants determined with acetophenone as substrate. The performance values demonstrate that  $K_M$ -values are higher for all variants except CPCR2-(A275T). Particularly,  $K_M$ -values increased almost threefold for variants with glutamine at position 276 (CPCR2-(L276Q), CPCR2-(S275S, L276Q)). Furthermore, specific activity is raised for the same variants by a factor of 1.4 as deduced from the turnover frequency  $k_{cat}$ . Stereoselectivity ( $ee$ ) was not changed for any of the variants listed in Table 5.

Increased  $K_M$ -values accompanied by increased  $k_{cat}$  were observed before for mutants of ADHs of *Sulfolobus solfataricus* (SsADH). The effect was explained by a faster cofactor release as a direct consequence of the major weakening of a binary enzyme complex.<sup>[39]</sup>

In summary, the performance characterization of purified wtCPCR2 and variants in Table 5 matches well with the results of crude cell lysates from screening of the SSM libraries. For instance CPCR2-(L276Q) and CPCR2-(S275S, L276Q) exhibited highest activity in crude extracts as well as after purification.

Stability of CPCR2 variants was evaluated by analysis of thermal inactivation ( $T_{50}$ -value) and stability in the presence of a cyclohexane-buffer interface (half-life in h). Figure 6 depicts the stabilities determined for wtCPCR2 and variants. Thermal resistance is significantly improved for CPCR2-(A275T) ( $\Delta T_{50} = +2.6^\circ\text{C}$ ) and CPCR2-(A275S, L276Q) ( $\Delta T_{50} = +5.2^\circ\text{C}$ ), whereas  $T_{50}$ -values for all other variants are similar to the ones of wtCPCR2 (see also Table 5; error bars). Surprisingly the single substitution A275S does not provide an increased thermal resistance when compared to wtCPCR2. The substitution A275S is, however, found in the most stable variant (CPCR2-(A275S, L276Q)).



**Figure 6** Thermal inactivation curves of purified wtCPCR2 and selected variants. The black horizontal dashed line indicates 50 % residual relative activity.

Comparative analysis of the half-life indicates that thermal resistance and interfacial stability do not necessarily correlate as shown in Table 5. The double mutant CPCR2-(A275S, L276Q) showed as expected the highest thermal resistance and highest increased half-life (1.5-fold). CPCR2-(A275T) shows the second highest thermal resistance ( $\Delta T_{50} = +2.6^{\circ}\text{C}$ ); however, the half-life is 20 % reduced when compared to wtCPCR2.

Characterization of the CPCR2-(A275S) variant proves that a serine at position 275 is not improving thermal resistance or activity and would consequently not be identified as beneficial variant in the screening systems. Serine at position 275 is therefore only beneficial in combination with the substitutions to glutamine, methionine or arginine at position 276 (see Table 4). The double mutant CPCR2-(A275S, L276Q) was identified by dSSM showing a similar activity increase than the rationally designed variant CPCR2-N/Q but a significantly higher thermal resistance (CPCR2-(A275N, L276Q):  $\Delta T_{50} = +2.6^{\circ}\text{C}$ , CPCR2-(A275S, L276Q):  $\Delta T_{50} = +5.2^{\circ}\text{C}$ ). Thus, simultaneous site-saturation yielded a better performing CPCR2 variant.

#### 3.5.4.8 Computational Analysis of the Mutations

Amino acid substitutions at positions 275 and 276 were analyzed *in silico* with FoldX to evaluate results obtained from screening experiments. For computational analysis, a previously generated dimeric homology model was used.<sup>[14b]</sup> Furthermore, the computational output was discussed in the

context of experimental results. Relations to protein structures from related ADHs were used to explain the observed increase in interfacial stability and activity.

#### *Fold-X analysis of beneficial positions 275 & 276*

FoldX analysis provides insights on stabilization energies ( $\Delta\Delta G$ ) of CPCR2 upon site-saturation mutagenesis at position 275 and/or 276 (see Supplementary Information Table S6).

and Table S7, respectively). The highest stabilization energy was calculated for threonine at position 275 ( $\Delta\Delta G = -1.37 \text{ kJ mol}^{-1}$ ), which could mainly be attributed to dimer stabilization (see Supplementary Information Table S6). CPCR2-(A275T) was as calculated by FoldX found to be the most stable variant also in screening 275-sSSM. The other stabilizing substitutions A275M ( $\Delta G = -0.66 \text{ kJ mol}^{-1}$ ) and A275C ( $\Delta\Delta G = -0.56 \text{ kJ mol}^{-1}$ ) did not show up within the micro titer plate screening experiments, probably due to reduced activity. The stable variant CPCR2-(A275N) (see Table 4), was calculated to have a slight destabilizing effect ( $\Delta\Delta G = +0.07 \text{ kJ mol}^{-1}$ ). Thus, both FoldX and experimental data demonstrates that position 275 is a hot spot for stabilization of CPCR2.

FoldX analysis of position 276 showed that considerable stabilization could only be detected for CPCR2-(L276F) ( $\Delta\Delta G = -0.54 \text{ kJ mol}^{-1}$ ) and CPCR2-(L276M) ( $\Delta\Delta G = -0.19 \text{ kJ mol}^{-1}$ ) (see Supplementary Information Table S7). Most other amino acids at this position were considered to destabilize. FoldX calculation and experimental results are hence in good agreement (see Table 4). The stabilized variants CPCR2-(L276F) or CPCR2-(L276M) were; however, not identified in the screening.

FoldX analysis calculated that the combination CPCR2-(A275T, L276M) would be the most stabilized one (see Table 6). Experimentally, the variant CPCR2-(A275T, L276M) scored second with respect to stability (see Table 4). The other double mutants were calculated to be or destabilized or slightly stabilized.

**Table 6** FoldX calculations of improved CPCR2 double mutants found by screening-

Rank	Mutation Pos Ala 275	Mutation Pos Leu 276	Average $\Delta\Delta G \text{ (kcal mol}^{-1}\text{)}$	Complex stability $\Delta\Delta G \text{ (kcal mol}^{-1}\text{)}$
1	Ser	Gln	0.84	0.48
2	Asn	Gln	-0.09	0.65
3	Ser	Met	0.58	-0.42
4	Thr	Asn	0.39	-0.22
5	Ser	Arg	2.52	1.35
6	Thr	Met	-0.58	-1.51
7	Asn	Met	0.74	0.56

Single substitutions calculated by FoldX analysis reflect well the results obtained for SSM and stability screening. Double substitutions were not reliably identified by computational analysis. The latter can



partially be attributed to the fact that in FoldX calculations the backbone is not flexible and since both positions are neighboring each other it is likely that the backbone geometry was altered.

In FoldX, also interaction energies of the dynamic monomer-dimer equilibrium were calculated (complex stability). This analysis showed that mutations at position 275 contribute to a stabilization of the dimeric state (see Table S6 and Table S7).

#### 3.5.4.9 Hypotheses of activating or stabilizing role of position 275 and 276 in *CPCR2*

##### *Impact of position 275 on dimer stabilization*

Amino acid 275 is located at the dimer interface of wtCPCR2 according to the homology model<sup>[14b]</sup>, and FoldX analysis as well as experimental results from SSM identified CPCR2-(A275T) as most stabilizing substitution. Distinct energy contributions to overall stabilization derived from FoldX analysis indicated the formation of an inter-subunit hydrogen bond between the side chain of T275 and the backbone of the second monomer A.

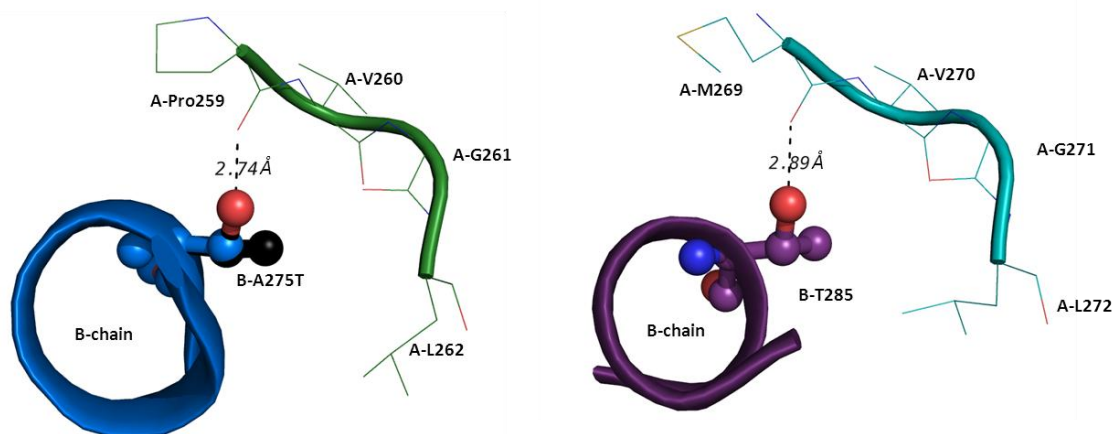


**Figure 7** Dimer interaction of CPCR2 homology model (left) and the SsADH crystal structure (right). The A-chain of CPCR2 is colored in green and the B-chain is shown in blue. Threonine (black ball and stick) at position 275 forms a hydrogen bond to the backbone oxygen of A-P259. The wtCPCR2 amino acid A275 is represented in blue ball and stick mode. Other interacting residues are depicted in lines. In SsADH, the chain of monomer A is colored in cyan and the monomer B is shown in purple. T285 forms a hydrogen bond with the backbone oxygen of A-M269 analogous to CPCR2-(A275T).

Figure 7 shows the inter-subunit interactions of monomer B (blue) with monomer A (green) in the homodimeric wtCPCR2 superimposed with CPCR2-(A275T). It is evident that the replacement to threonine at position 275 (black) leads to a hydrogen bond formation with the backbone oxygen of P259 in monomer A as acceptor (A-P275, distance 2.74 Å, see Figure 7, left). Alanine in wtCPCR2 (B-A275) could not establish such a hydrogen bond. A corresponding hydrogen bond between B-T285 and A-M269 is present in the crystal structure of the related SsADH (see Figure 7, right), which originates from a hyperthermophilic host.<sup>[40]</sup> SsADH is considerably more stable than wtCPCR2 ( $T_{50} = 95^{\circ}\text{C}$ ; 30

min).<sup>[39b]</sup> Notably, all stabilizing substitutions inCPCR2 double mutants at position 275 can serve as hydrogen bond donor namely serine, threonine and glutamine (see Table 4). The latter finding suggests that the formation of this inter-subunit hydrogen bond is a key to stabilize CPCR2 (see Figure 7) and can be found in thermostable zinc-containing dimeric ADHs like SsADH.

Fostering of inter-subunit interactions can be responsible for the difference in stability of dehydrogenases. A comparison of an ADH from thermophilic *Thermoanaerobacter brockii* (TbADH) and an ADH from mesophilic *Clostridium beijerinckii* with 75 % sequence identity revealed that the structural determinants strengthening the interface of the subunits are mainly responsible for the higher thermostability of TbADH.<sup>[41]</sup> Assessment of crystal structures of four related malate dehydrogenases (MDH) with largely different thermal stabilities showed the importance of the subunit interfaces of the oligomers for stability.<sup>[42]</sup> Mutational analyses of the thermostable MDH from *Chloroflexus aurantiacus* again demonstrated how subunit interactions contribute to stability by introduction of an inter-dimer disulfide bond ( $\Delta T_m = +15^\circ\text{C}$ ) or removal of inter-dimer salt bridges ( $\Delta T_m = -26.8^\circ\text{C}$ ).<sup>[43]</sup> Importance of the oligomeric state for stability of dehydrogenases was reported additionally for ADH from *Clostridium beijerinckii*<sup>[10]</sup>, glucose-6-phosphate dehydrogenase from *Aquifexaeolicus*<sup>[44]</sup> and glucose dehydrogenase from *Bacillus megaterium*.<sup>[45]</sup>

#### *Role of Position 276 on CPCR2 Activity & Stability*

The amino acid position L276 in wtCPCR2 aligns with L286 in the structurally related SsADH. Together with T285, the amino acid L286 is positioned at the dimer interface and is located in a short helix ( $\alpha\text{F}$ ; 280-288).<sup>[40, 46]</sup> The crystal structure of SsADH reveals that L286 has several inter-subunit interactions and constitutes a part of the substrate binding pocket of the monomer A.<sup>[40]</sup> The inter-subunit interactions within SsADH and CPCR2 differ significantly as residue B-L286 forms inter-subunit interactions with F49, L52 and L295 of monomer A in dimeric SsADH. The corresponding amino acid B-L276 in CPCR2 has only A-F285 (L295 in SsADH) as interaction partner as deduced from the dimeric homology model.<sup>[14b]</sup> Furthermore, L286 in SsADH was shown to have direct contact with C<sub>3</sub> and C<sub>4</sub> of the co-crystallized substrate ethoxyethanol so that similar interactions can be expected for CPCR2.<sup>[47]</sup>

Results from 276-sSSM showed an increase in activity (up to twofold) without substantial stabilization or destabilization of CPCR2 (see Table 4). Increased activity was found by replacing the hydrophobic leucine with glutamine, arginine or lysine (L276Q, L276R and L276K) proving that a polar and charged nature is a prerequisite for improved activity. Consistently, FoldX analysis did not predict a stabilizing effect for three beneficial substitutions (see Supplementary Information Table S7). A role of position 276 in boosting activity has not been reported for ADHs until now.

Position 276 preserves this role in the most active double mutant CPCR2-(A275T, L276N) despite neighboring position T275, which governs thermal resistance of CPCR2. Notably for hydrolases activity and thermal resistance have been improved simultaneously in contrast to dehydrogenases.<sup>[48]</sup> Improving both properties simultaneously is on the molecular level challenging since high activity requires in general high flexibility and high thermal resistance requires strong interactions (rigidity).<sup>[49]</sup> A comparison of the sSSM of position 275, position 276 and dSSM yielded that best combination of the sSSM (A275T; L276Q) is quite similar to the best result of dSSM (CPCR2-(A275S, L276Q)). In contrast to sSSM experiments, the simultaneous exchanges (A275N, L276Q), (A275S, L276M), (A275T, L276N) and (A275S, L276R) proved to be beneficial for activity and also stability (see Table 4). A more detailed analysis on intra- and intermolecular interactions affecting stability and activity require crystals of CPCR2 and the generated variants.

To our best knowledge, there is only one report on improving activity by reengineering the subunit interface of ADHs. Plapp and co-workers constructed a variant of ADH from horse liver with three substitutions at the dimer interface, which activated the enzyme by allowing more rapid conformational changes that accompany coenzyme binding, probably due to movement of the loop containing the mutations.<sup>[50]</sup>

### 3.5.5 Conclusion

In essence, CPCR2 was stabilized and activated by rational and semi-rational introduction of surface amino acid mutations. To our knowledge, the current report is the first one on activation of an ADH by mutagenesis of an inter-subunit residue which in contact or in close proximity to the substrate. The developed 96-well multi titer plate screening strategy can likely be used for other dehydrogenases to improve thermal resistance, catalytic activity and other properties.

The amino acid positions A275 and L276 were identified as key residues for improving thermal resistance (A275) and activity (L276). Interestingly, the simultaneous saturation of the neighboring amino acid positions resulted in variants improved in thermal resistance as well as in activity. The best double mutant CPCR2-A275S/L276Q showed 1.4-fold higher activity, 1.5-fold increased half-life in aqueous-organic biphasic system and  $\Delta T_{50}$  of +5.2°C.

The inter-subunit interactions of position 275 proved to govern thermal resistance, which is likely a general option for increasing thermal resistance of ADHs with similar fold. In addition, the  $\alpha$ F-helix (280-288 in SsADH) located at the dimer interface plays an important role for ADH activity in general and might represent a preferred reengineering target for improving  $k_{cat}$  values of ADH. The semi-rational engineering strategy and the developed screening strategy demonstrate that key performance parameter of CPCR2 can rapidly be improved to match application demands.

### 3.5.6 Supplementary Information

**Table S1** CPCR2 variants generated from selected surface amino acids

No.	Variant	No.	Variant
1	CPCR2-(L24T, V26S)	7	CPCR2-(L222Q, I226K)
2	CPCR2-(V26S)	8	CPCR2-(A275K, L276K)
3	CPCR2-(V78S, I79T, V83S)	9	CPCR2-(A275K)
4	CPCR2-(I79T, V83S)	10	CPCR2-(A275N, L276Q)
5	CPCR2-(V78S, I79K, V83E)	11	CPCR2-(V307K, V308K)
6	CPCR2-(L222R, I226K)	12	CPCR2-(V307N, V308N)

**Table S2** Primer sequences for site-directed mutagenesis of NhisCPCR2.

Primer name	5'-3' sequence
L24T,V26S_fwd	AATTTGAGAAATGATACCCCTTCTCACAAGCCC
L24T,V26S_rev	GGGCTTGTGAGAAGGGGTATCATTTCTCAAATT
V26S_fwd	AATTTGAGAAATGATTTGCCTTCTCACAAGCCC
V26S_rev	GGGCTTGTGAGAAGGCAAATCATTTCTCAAATT
V78S,I79T,V83S_fwd	GGTGATGATTCTACCAACTACAAGTCTGGTGATCG
V78S,I79T,V83S_rev	CGATCACCAGACTTGTAGTTGGTAGAATCATCACC
I79T,V83S_for	GGTGATGATGTCACCAACTACAAGTCTGGTGATCG
I79T,V83S_rev	CGATCACCAGACTTGTAGTTGGTGACATCATCACC
V78S,I79K,V83E_fwd	GGTGATGATTCTAAAAACTACAAGGAAGGTGATCG
V78S,I79K,V83E_rev	CGATCACCTTCCTTGTAGTTTTTTAGAATCATCACC
L222Q,I226N_fwd	GTTTATGAAACACAGCCAGAATCCAACCTCTCCTGGC
L222Q,I226N_rev	GCCAGGAGAGTTGGATTCTGGCTGTGTTTCATAAAC
A275K,L276K_fwd	GGAGATTTGAAAAAAGAGAAATTCGAATC
A275K,L276K_rev	GATTCGAATTTCTCTTTTTTTCAAATCTCC
A275K_fwd_fwd	GGAGATTTGAAATTGAGAGAAATTCGAATC
A275K_fwd_rev	GATTCGAATTTCTCTCAATTTCAAATCTCC
A275N,L276Q_fwd	GGAGATTTGAACCAGAGAGAAATTCGAATC
A275N,L276Q_rev	GATTCGAATTTCTCTCTGGTTCAAATCTCC
V307K,V308K_fwd	GAAGGTAAAGTTAAACCCAAAAAAGAAGTGCC
V307K,V308K_rev	GGCACTTCTTTTTTTGGGTTTAACTTTACCTTC
V307N,V308N_fwd	AGTGAAGGTAAAAACAAACCCAACAACAGAAGTGCC
V307N,V308N_rev	GGCACTTCTGTTGTTGGGTTTGTTTTTACCTTCACT

Nucleotides different from wild-type sequence are highlighted in bold.

**Table S3** Comparison of His-tagged CPCR2 and Strep-tagged CPCR2

parameter	His-tagged wtCPCR2	Strep-tagged wtCPCR2
$v_{\max}$ [U/mg]	56.5	53.2
$K_M$	0.128	0.201

Table S4 Primers applied for site-saturation of CstrepCPCR2.

Primer name	5'-3' sequence
A275N_fwd	CTGGGTGATCTGAATCTGCGTGAAATTCG
A275N_rev	CGAATTTACGCAGATTCAGATCACCCAG
A275S_fwd	CTGGGTGATCTGTGCTGCGTGAAATTCG
A275S_rev	CGAATTTACGCAGCGACAGATCACCCAG
L276Q_fwd	GGTATCTGGCACAGCGTGAAATTCG
L276Q_rev	CGAATTTACGCTGTGCCAGATCACC
A275-SSM_fwd	GGTATCTGGCANNScgtgaaattcg
A275-SSM_rev	CGAATTTACGSNNTGCCAGATCACC
L276-SSM_fwd	CTGGGTGATCTGNNSCTGCGTGAAATTCG
L276-SSM_rev	CGAATTTACGCAGSNNCAGATCACCCAG
A275-L276 dSSM-for	CTTTAATCTGGGTGATCTGNNSNNSCGTGAAATTCGTATTC
A275-L276 dSSM-rev	GAATACGAATTTACGSNNSNNCAGATCACCCAGATTAAGA

Nucleotides different from wild-type sequence are highlighted in bold. N stands for all four nucleotides and S stands for G and C.

Figure S 1 Protein sequence alignment of pdb entries most related to CPCR2. Upper digits refers to CPCR2 numbering, lower digits refer to automatic numbering created by alignment.

	10	20	30	40	50	60
<b>CPCR2</b>	<b>MSIPSSQYGFVFNKQSGLNLRNDLPVHKPKAGQLLLKVDVAVGLCHSDLHVIYEG</b> -----					
1R37	-----MRAVRLVEIGKPLSLQEI	GV	PKPKG	PQVLI	KVEAAGV	<b>CHSDVHMRQGRF</b> GNLRI
2EER	-----MRAMRLVEIGKPLKLEDI	PI	PKPKGS	QVLI	KIEAAGV	<b>CHSDVHMRQGR</b> -GNLRI
1RJW	-----MKAADVVEQFKEPLKIKEVE	KPTIS	YGEV	LVRI	KACG	<b>VCHTDLHAAHGDPVK</b> ---
2XAA	-----MKAQYQTEIGSEPVVVDI	PT	PTPG	PEIL	LKVTAAG	<b>LCHSDIFVMDMPAAQ</b> ---
				<b>24 26</b>		
	70	80	90	100	110	120
<b>CPCR2</b>	<b>---LDCGDNYVMGHEIAGTVAAVGDDVINYKVGDRVACVGNP-GCGGCKYCRGAIDNVCK</b>					
1R37	VEDLGVKLPVTL <b>GHEI</b> AGKIEEV	GV	DEVV	GYSK	<b>GD</b> LVAVNPWQ-GE	<b>GN</b> CYYCRIGEEHLCD
2EER	VEDLGVKLPVTL <b>GHEI</b> AGRIEIV	GV	DEVV	YSK	<b>GD</b> LVAVNPWE-GE	<b>GN</b> CYYCRIGEEHLCD
1RJW	-----PKLPLIP <b>GHEG</b> VGV	I	VEEV	GPV	THLKV	<b>GD</b> RVGIPWLYSAC <b>GH</b> CDYCLSGQETLCE
2XAA	---YAYGLPLTL <b>GHEG</b> VGV	T	VAEL	EGVT	GFGV	<b>GD</b> AVAVYGPW-GCGACHACARGRENYCT
				<b>78,79 83</b>		
	130	140	150	160	170	180
<b>CPCR2</b>	<b>NAFGDWFG---LGVDGGYQQYLLVTR---PRNLSRIPDNVSADVAASSTDAVLTTPYHAIK</b>					
1R37	SPR--WLGI-N--FDGAYAEY	VIVPH---	YKMY	KLRR-	INAVE	<b>AA</b> PLTCSG <b>ITTYRAVR</b>
2EER	SPR--WLGI-N--YDGAYAEY	VIVPH---	YKLY	KLRR-	LSAVE	<b>AA</b> PLTCSG <b>VTTYRAVR</b>
1RJW	HQKN--AG---YSVDGGYAEY	CRAAADY	VVKI	PDNLS---	FEE	<b>AA</b> PIFCAG <b>VTTYKALK</b>
2XAA	RAADLGITPPGLGSPG	SMAYMIVDS---	ARHL	VPIGD-	LDPVA	<b>AA</b> PLTDAGL <b>TPYHAIS</b>
	190	200	210	220	230	240
<b>CPCR2</b>	<b>--MAQVS-PTSNNILLIG-AGGLGGNAIQVAKAFG-AKVTVLDKKKEARDQAKKLGADAVY</b>					
1R37	KAS--LDP	P	K	T	L	L
2EER	KAS--LDP	S	K	T	L	L
1RJW	VTS--AK-PGE	W	V	A	I	Y
2XAA	RVLPLLG-PG	S	T	A	V	V
	250	260	270	280	290	300
<b>CPCR2</b>	<b>ET-----LPESISPGSFSACFDVSVQATFDVCQKYVEPKGVIIMPVGLGAPNLSF</b>					
1R37	NASM-QD-PLAE	IRRI	TESK	GVDA	VIDL	NNSEK
2EER	NASS-QD-PVSE	IRRI	TQ	KG	ADA	VIDL
1RJW	NPLKED---AA	F	M	K	E	K
2XAA	KSGAGAA---DA	I	R	L	T	G
				<b>222 226</b>		
	310	320	330	340	350	360
<b>CPCR2</b>	<b>N-LGDLALREIRILGSFWGTTNDLDDVLKLVSEGVKVPVRSACL-KELPEYIEKLRNA</b>					
1R37	H-APLITL	SEI	Q	F	V	G
2EER	H-APLITL	NE	V	Q	F	I
1RJW	IPI	F	D	T	V	L
2XAA	V-GFFM	I	P	F	G	S
		<b>275, 276</b>			<b>307, 308</b>	
				<b>370</b>		
<b>CPCR2</b>	<b>YE-GRVVFNP--- CR Candida parapsilosis</b>				<b>336aa</b>	
1R37	AI-GRQVLIP---	ADH Sulfolobus solfataricus			345aa (34% seqID)	
2EER	AV-GRQVLP---	ADH Sulfolobus tokodaii			347aa (35% seqID)	
1RJW	IN-GRVVLTL	EDK ADH Bacillus stearothermophilus			339aa (33% seqID)	
2XAA	IR-GRGVVVP---	ADH-A Rhodococcus ruber			345aa (35% seqID)	

Table S5 Number of clones and completeness of each library (NNS-codon degeneracy and  $P_c = 95\%$ <sup>[41]</sup>).

Library	Number of clones	Completeness [%]
275 SSM	172	99.7
276 SSM	172	99.7
275/276 dSSM	747	73.2

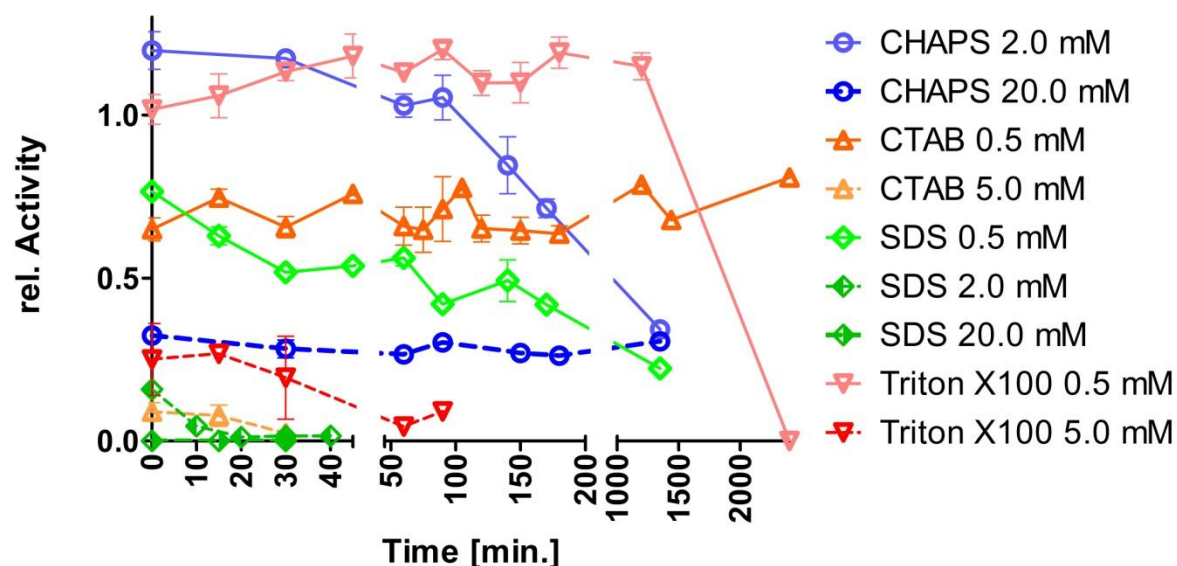


Figure S2 Relative activity of wtCPCR2 cell-free lysate after incubation with different detergents below and above the critical micelle concentration (cmc).

Table S6 Energies calculated by FoldX for in silico saturation of position 275 in CPCR2.

Entry	Mutation	Average	complex	Corrected
	Pos 275	ddG (kcal/mol)	stability ddG (kcal/mol)	average ddG (kcal/mol)
1	275THR	-0.61	-1.37	-1.37
2	275MET	-0.52	-1.06	-0.66
3	275CYS	-0.2	-0.56	-0.56
4	275SER	0.7	-0.05	-0.05
wt 5	275ALA	0	0	0
6	275ASN	-0.07	0.07	0.07
7	275VAL	0.23	0.13	0.13
8	275LYS	0.88	-0.01	0.48
9	275GLY	0.79	0.5	0.5
10	275ARG	0.98	0.74	0.74
11	275GLN	2.02	0.69	0.95
12	275LEU	1.09	0.03	1.73
13	275ASP	2.54	2.02	2.02
14	275GLU	4.22	2.78	2.78
15	275PHE	2.95	2.12	3.1
16	275HIS	3.86	2.75	3.28
17	275ILE	3.26	1.6	3.96
18	275TYR	4.56	3.68	5.08
19	275PRO	5.9	1.58	6.01
20	275TRP	9.82	5.18	9.87

**Table S7** Energies calculated by FoldX for in silico saturation of position 276 in CPR2.

Entry	Mutation	Average	complex stability	Corrected average
	Pos 276	ddG (kcal/mol)	ddG (kcal/mol)	ddG (kcal/mol)
1	276PHE	-0.31	-0.54	-0.54
2	276MET	-0.02	-0.19	-0.19
3	276ILE	0.11	-0.06	-0.06
wt 4	276LEU	-0.01	-0.03	-0.03
5	276TYR	0.73	0.09	0.34
6	276ASN	0.72	0.51	0.51
7	276GLN	0.47	0.62	0.62
8	276VAL	1	0.66	0.66
9	276THR	1.06	0.91	0.91
10	276HIS	1.79	1.21	1.21
11	276ARG	1.53	1.3	1.3
12	276LYS	2	1.43	1.43
13	276TRP	1.72	0.28	1.44
14	276ALA	1.39	1.44	1.44
15	276CYS	1.85	1.45	1.45
16	276SER	1.89	1.54	1.54
17	276GLU	2.02	2.08	2.08
18	276ASP	2.36	2.36	2.36
19	276GLY	2.84	2.67	2.67
20	276PRO	1.53	1.32	3.07

**This chapter was reproduced from the publication “Design of an Activity and Stability Improved Carbonyl Reductase from *Candida parapsilosis*”** Jakoblinnert, A.; van den Wittenboer, A.; Shivange, A. V.; Bocola, M.; Heffele, L.; Ansorge-Schumacher, M. B.\*; Schwaneberg, U.\* *Journal of Biotechnology*, 165: 52-62, 2013 **with permission from Elsevier**

### 3.5.7 References

- [1] a G. W. Zheng, J. H. Xu, *Curr. Opin. Biotechnol.* **2011**, *22*, 784-792; b G. W. Huisman, J. Liang, A. Krebber, *Curr. Opin. Chem. Biol.* **2010**, *14*, 122-129; c M. Musa, R. S. Phillips, *Catal. Sci. Technol.* **2011**, *1*, 1311-1323.
- [2] a H. Gröger, W. Hummel, C. Rollmann, F. Chamouveau, H. Hüsken, H. Werner, C. Wunderlich, K. Abokitse, K. Drauz, S. Buchholz, *Tetrahedron* **2004**, *60*; b P. Müller, B. L. Bangasser, L. Greiner, S. Na'amnieh, P. S. Bäuerlein, D. Vogt, C. Müller, *The Open Catalysis Journal* **2011**, *4*, 113-116.
- [3] G. A. Strohmeier, H. Pichler, O. May, M. Gruber-Khadjawi, *Chem. Rev.* **2011**, *111*, 4141-4164.
- [4] a A. S. Bommarius, J. M. Broering, J. F. Chaparro-Riggers, K. M. Polizzi, *Curr. Opin. Biotechnol.* **2006**, *17*, 606-610; b K. M. Polizzi, A. S. Bommarius, J. M. Broering, J. F. Chaparro-Riggers, *Curr. Opin. Chem. Biol.* **2007**, *11*, 220-225.
- [5] a V. G. Eijsink, S. Gaseidnes, T. V. Borchert, B. van den Burg, *Biomol. Eng.* **2005**, *22*, 21-30; b V. G. Eijsink, A. Bjork, S. Gaseidnes, R. Sirevag, B. Synstad, B. van den Burg, G. Vriend, *J. Biotechnol.* **2004**, *113*, 105-120; c C. K. Savile, J. M. Janey, E. C. Mundorff, J. C. Moore, S. Tam, W. R. Jarvis, J. C. Colbeck, A. Krebber, F. J. Fleitz, J. Brands, P. N. Devine, G. W. Huisman, G. J. Hughes, *Science* **2010**, *329*, 305-309; d J. Liang, J. Lalonde, B. Borup, V. Mitchell, E. Mundorff, N. Trinh, D. A. Kochre, R. N. Cherat, G. P. Ganesh, *Organic Proc. Res. Dev.* **2010**, *14*, 193-198.
- [6] a A. V. Shivange, J. Marienhagen, H. Mundhada, A. Schenk, U. Schwaneberg, *Curr. Opin. Chem. Biol.* **2009**; b T. S. Wong, D. Roccatano, M. Zacharias, U. Schwaneberg, *J. Mol. Biol.* **2006**, *355*, 858-871.
- [7] K. I. Ziegelmann-Fjeld, M. M. Musa, R. S. Phillips, J. G. Zeikus, C. Vieille, *Protein Eng. Des. Sel.* **2007**, *20*, 47-55.
- [8] a M. M. Musa, N. Lott, M. Laivenieks, L. Watanabe, C. Vieille, R. S. Phillips, *ChemCatChem* **2009**, *1*, 89-93; b D. Zhu, Y. Yang, S. Majkowicz, T. Hsin-Yuan Pan, K. Kantardjieff, L. Ling Hua, *Org. Lett.* **2008**, *10*, 525-528.
- [9] a R. Machielsen, L. L. Looger, J. Raedts, S. Dijkhuizen, W. Hummel, H.-G. Hennemann, T. Dausmann, J. van der Oost, *Eng. Life Sci.* **2009**, *9*, 38-44; b S. Morikawa, T. Nakai, Y. Yasohara, H. Nanba, N. Kizaki, J. Hasegawa, *Biosci. Biotechnol. Biochem.* **2005**, *69*, 544-552; c N. H. Schlieben, K. Niefind, J. Muller, B. Riebel, W. Hummel, D. Schomburg, *J. Mol. Biol.* **2005**, *349*, 801-813.
- [10] E. Goihberg, O. Dym, S. Tel-Or, I. Levin, M. Peretz, Y. Burstein, *Proteins* **2007**, *66*, 196-204.
- [11] H. Zhang, G. T. Lountos, C. B. Ching, R. Jiang, *Appl. Microbiol. Biotechnol.* **2010**, *88*, 117-124.
- [12] J. Liang, E. Mundorff, R. Voladri, S. J. Jenne, L. Gilson, A. Conway, A. Krebber, J. Wong, S. Truesdell, J. Lalonde, *Org. Proc. Res. Dev.* **2010**, *14*, 188-192.
- [13] a Y. Makino, T. Dairi, N. Itoh, *Appl. Microbiol. Biotechnol.* **2007**, *77*, 833-843; b Y. Makino, K. Inoue, T. Dairi, N. Itoh, *Appl. Environ. Microbiol.* **2005**, *71*, 4713-4720.
- [14] a J. Peters, T. Minuth, M. R. Kula, *Enzyme Microb. Technol.* **1993**, *15*, 950-958; b A. Jakoblinnert, M. Bocola, M. Bhattacharjee, S. Steinsiek, M. Bönitz-Dulat, U. Schwaneberg, M. B. Ansorge-Schumacher, *ChemBiochem* **2012**, *13*, 803-809; c A. Jakoblinnert, R. Mladenov, A. Paul, F. Sibilla, U. Schwaneberg, M. B. Ansorge-Schumacher, P. D. de Maria, *Chem. Commun.* **2011**, *47*, 12230-12232; d C. Lensink, E. Rijnberg, J. G. de Vries, *J. Mol. Catal. A: Chem.* **1997**, 199-207.
- [15] a S. M. De Wildeman, T. Sonke, H. E. Schoemaker, O. May, *Acc. Chem. Res.* **2007**, *40*, 1260-1266; b R. N. Patel, *Coord. Chem. Rev.* **2008**, *252*, 659-701.
- [16] B. Orlich, H. Berger, M. Lade, R. Schomacker, *Biotechnol. Bioeng.* **2000**, *70*, 638-646.
- [17] A. van den Wittenboer, T. Schmidt, P. Muller, M. B. Ansorge-Schumacher, L. Greiner, *Biotechnol. J.* **2009**, *4*, 44-50.
- [18] M. Bhattacharjee, PhD thesis, RWTH Aachen (Aachen), **2006**.
- [19] J. Sambrook, D. Russell, W., *Molecular Biology: A Laboratory Manual, Vol. 1-3*, 3 ed., CSH Press, Cold Spring Harbor, **2000**.
- [20] W. Wang, B. A. Malcolm, *Biotechniques* **1999**, *26*, 680-682.



- [21] H. G. Holzhutter, A. Colosimo, *Comput. Appl. Biosci.* **1990**, *6*, 23-28.
- [22] E. Krieger, G. Koraimann, G. Vriend, *Proteins* **2002**, *47*, 393-402.
- [23] Y. Duan, C. Wu, S. Chowdhury, M. C. Lee, G. Xiong, W. Zhang, R. Yang, P. Cieplak, R. Luo, T. Lee, J. Caldwell, J. Wang, P. Kollman, *J. Comput. Chem.* **2003**, *24*, 1999-2012.
- [24] J. Wang, R. M. Wolf, J. W. Caldwell, P. A. Kollman, D. A. Case, *J. Comput. Chem.* **2004**, *25*, 1157-1174.
- [25] A. Jakalian, D. B. Jack, C. I. Bayly, *J. Comput. Chem.* **2002**, *23*, 1623-1641.
- [26] R. Guerois, J. E. Nielsen, L. Serrano, *J. Mol. Biol.* **2002**, *320*, 369-387.
- [27] J. Van Durme, J. Delgado, F. Stricher, L. Serrano, J. Schymkowitz, F. Rousseau, *Bioinformatics* **2011**, *27*, 1711-1712.
- [28] M. H. Vermue, J. Tramper, *Pure & Appl. Chem.* **1995**, *67*, 345-373.
- [29] V. V. Mozhaev, Y. L. Khmel'nitsky, M. V. Sergeeva, A. B. Belova, N. L. Klyachko, A. V. Levashov, K. Martinek, *Eur. J. Biochem.* **1989**, *184*, 597-602.
- [30] A. A. Freitas, F. H. Quina, F. A. Carroll, *J. Phys. Chem.* **1997**, *101*, 7488-7493.
- [31] K. Fan, P. Ouyang, X. Wu, Z. Lu, *Enzyme Microb. Technol.* **2001**, *28*, 3-7.
- [32] M. Villela-Filho, T. Stillger, M. Muller, A. Liese, C. Wandrey, *Angew. Chem. (Int. Ed.)* **2003**, *42*, 2993-2996.
- [33] A. van den Wittenboer, PhD thesis, RWTH Aachen, **2009**.
- [34] A. Jakobinnert, J. Wachtmeister, L. Schukur, A. V. Shivange, M. Bocola, M. B. Ansorge-Schumacher, U. Schwaneberg, *Protein Eng. Des. Sel.* **2013**, *accepted*.
- [35] a M. T. Reetz, P. Soni, L. Fernandez, Y. Gumulya, J. D. Carballeira, *Chem. Commun.* **2010**, *46*, 8657-8658; b J. Hao, A. Berry, *Protein Eng. Des. Sel.* **2004**, *17*, 689-697; c C. Ó. Fágáin, *Enzyme Microb. Technol.* **2003**, *33*, 137-149; d E. Vazquez-Figueroa, V. Yeh, J. M. Broering, J. F. Chaparro-Riggers, A. S. Bommarius, *Protein Eng. Des. Sel.* **2008**, *21*, 673-680.
- [36] a K. L. Tee, U. Schwaneberg, *Angew. Chem. (Int. Ed.)* **2006**, *45*, 5380-5383; b K. L. Tee, U. Schwaneberg, *Comb. Chem. High Throughput Screen.* **2007**, *10*, 197-217.
- [37] A. K. Bhuyan, *Biopolymers* **2009**, *93*, 186-199.
- [38] W. M. Patrick, A. E. Firth, J. M. Blackburn, *Protein Eng.* **2003**, *16*, 451-457.
- [39] a A. Giordano, R. Cannio, F. La Cara, S. Bartolucci, M. Rossi, C. A. Raia, *Biochemistry* **1999**, *38*, 3043-3054; b A. Pennacchio, L. Esposito, A. Zagari, M. Rossi, C. A. Raia, *Extremophiles* **2009**, *13*, 751-761.
- [40] L. Esposito, F. Sica, C. A. Raia, A. Giordano, M. Rossi, L. Mazzarella, A. Zagari, *J. Mol. Biol.* **2002**, *318*, 463-477.
- [41] Y. Korkhin, A. J. Kalb, M. Peretz, O. Bogin, Y. Burstein, F. Frolow, *Protein science : a publication of the Protein Society* **1999**, *8*, 1241-1249.
- [42] B. Dalhus, M. Saarinen, U. H. Sauer, P. Eklund, K. Johansson, A. Karlsson, S. Ramaswamy, A. Bjork, B. Synstad, K. Naterstad, R. Sirevag, H. Eklund, *J. Mol. Biol.* **2002**, *318*, 707-721.
- [43] a A. Björk, D. Mantzilas, R. Sirevag, V. G. Eijsink, *FEBS Lett.* **2003**, *553*, 423-426; b A. Björk, B. Dalhus, D. Mantzilas, V. G. Eijsink, R. Sirevag, *J. Mol. Biol.* **2003**, *334*, 811-821.
- [44] M. Nakka, R. B. Iyer, L. G. Bachas, *Protein J.* **2006**, *25*, 17-21.
- [45] S. H. Baik, F. Michel, N. Aghajari, R. Haser, S. Harayama, *Appl. Environ. Microb.* **2005**, *71*, 3285-3293.
- [46] L. Esposito, I. Bruno, F. Sica, C. A. Raia, A. Giordano, M. Rossi, L. Mazzarella, A. Zagari, *FEBS Lett.* **2003**, *539*, 14-18.
- [47] L. Esposito, I. Bruno, F. Sica, C. A. Raia, A. Giordano, M. Rossi, L. Mazzarella, A. Zagari, *Biochemistry* **2003**, *42*, 14397-14407.
- [48] H. Mihara, H. Muramatsu, R. Kakutani, M. Yasuda, M. Ueda, T. Kurihara, N. Esaki, *FEBS J.* **2005**, *272*, 1117-1123.
- [49] W. Tang, X. Zhang, *Chem. Rev.* **2003**, *103*, 3029-3070.
- [50] F. Strasser, J. Dey, M. R. Eftink, B. V. Plapp, *Arch. Biochem. Biophys.* **1998**, *358*, 369-376.

## 4. Conclusion

The European Union commission has identified Industrial Biotechnology as one of the five key enabling technologies for the EU according to the recent report “*Preparing for our future: Developing a common strategy for key enabling technologies in the EU*”, Brussels, 30.09.2009. Based on this evaluation, the importance of research in the field of Industrial or White Biotechnology for the society becomes evident. In the development towards a greener industry, biocatalysis plays a vital role in order to replace old-fashioned chemical processes by more sustainable and cost-efficient ones exploiting the synthetic potential of Nature.

Recent progress in genome sequencing, gene synthesis, bioinformatics as well as metabolic and protein engineering are truly revolutionary and will fuel the translation of science and technology into standard industrial practice. However, further efforts have to be made to switch to a bio-based economy. One way to foster this constitutes the smart integration of biocatalytic steps in complex synthesis routes by reaction designs, which are compatible with the existing processes. Herein, the aqueous environment, often vital for biocatalytic transformations, comprises several drawbacks and biocatalysis in non-aqueous systems is demanded. Another approach is to tailor the biocatalyst to match the performance parameters rendering a process economically feasible. Protein engineering is the most appropriate tool to achieve this goal and this technology will constantly augment our basic understanding how biocatalysts function on the molecular level.

In this thesis, the carbonyl reductases from the yeast *Candida parapsilosis* (CPCRs) present the central theme. To make this biocatalyst more attractive for industrial application, the paths of reaction engineering as well as protein engineering were followed resulting in the development of a novel concept for the manufacture of chiral alcohols and a substantial improvement of PCR catalytic properties.

In the age of rapid DNA sequencing, where massive accumulation of sequence information overwhelms the processing and storing of this data, the link between the actual biological function and the DNA sequence becomes even more indispensable. One contribution to achieve this is presented in this work, where the ketone reducing activity of *Candida parapsilosis* could be allocated to two distinct isoenzymes, now termed PCR1 and PCR2. The two enzymes were made recombinant by classical biochemical methods; additionally homology models were generated and tested for an array of indicator substrates using advanced methods of computational chemistry. By testing the elaborate hypothesis in the lab, the allocation of a small substrate scope to PCR1 and a larger substrate scope to PCR2 was possible. PCR1 was characterized biochemically for the first time and the sequence, connected to its function, is now freely accessible in the GeneBank data base

(accession number: JQ659192.1). This interdisciplinary approach constitutes a fast and efficient methodology to differentiate between two isoenzymes. In future, this might contribute improving the investigation sequence-function relationships in similar systems.

Biocatalysis is generally carried out in dilute aqueous media as Nature evolved microorganisms and enzymes to optimally function in hydrous environments. However, chemists perform reactions almost exclusively in organic solvents instead of water due to practical reasons like high substrate solubility, easy evaporation and reduction of side-reactions. The pioneering work of Klivanov in the 1980s; however, demonstrated that biocatalysts can also work in pure organic solvents. Whereas much attention was drawn to investigate the phenomena like activity, selectivity and stability of isolated enzymes in this non-natural environment, whole cells as biocatalysts were almost neglected. Nevertheless, whole cells comprise significant advantages as cofactors are intrinsically provided and recycled, enzymes are protected and cells are cheap to produce; but the perception that whole cells categorically need water to perform biocatalysis prevented extensive research on their catalytic potential in pure organic media.

In this thesis, recombinant CPCR2 was employed in *E. coli* whole cells for asymmetric reduction of ketones to produce chiral alcohols. This is particularly beneficial since the enzyme must not be purified and the cofactor NADH, needed in stoichiometric amounts, is provided by the cell and efficiently recycled. The new aspect, presented here, is the operation of this whole cell biocatalyst in a system composed of neat organic substrates (isopropanol and acetophenone) and lacking any bulk water or other organic solvent. It was rather unexpected that virtually dry cells perform efficiently the stereoselective reduction of acetophenone in isopropanol, which acts as cosubstrate for cofactor recycling. As a main trigger for biocatalytic activity, water activity of the organic medium and the catalyst was identified and full conversion could be obtained by removal of the co-product acetone. To this end, up to 500 g L<sup>-1</sup> enantiopure alcohol (*ee* >99 %) could be produced applying this system rendering the concept competitive to other processes for chiral alcohol production. However, reaction times of two weeks are much too long for an industrial application. Since the thermodynamic equilibrium impedes the reaction rather than the biocatalyst activity or stability, the reaction times might be shortened by smart reaction engineering promoting in situ (co-) product removal for fast and complete conversion.

The system was expanded to two more ketone reducing enzymes, namely alcohol dehydrogenases from *Rhodococcus erythropolis* (ReADH) and *Lactobacillus brevis* (LbADH), wherein ReADH exhibits *Prelog's* specificity and depends on NADH like CPCR2 but is more thermostable. LbADH has opposite stereoselectivity and depends on NADPH unlike CPCR2 and ReADH. Gratifyingly, both enzymes performed well as whole cell catalysts in the neat substrate system with analogous dependence on water activity like CPCR2. This finding implies that the concept may be transferred to even more

alcohol dehydrogenases, which are recombinantly available. Furthermore, an array of structurally diverse ketones was reduced to the corresponding alcohols by all three catalysts mostly at  $ee >98\%$ . This suggests that the substrate scope of the enzymes reported for aqueous systems can be fully exploited also in neat substrates. Nevertheless, selectivity for small ketones was only moderate leaving room for optimization for instance by adaption of reaction parameters.

As factors hampering initial reaction rates, mass transfer across the cell membrane as well as cofactor availability were identified. Herein, twofold rate acceleration was achieved by cell permeabilization and addition of NADH resulted in 2.7-fold increased reaction rate. From these findings, it may be inferred that the performance of the whole cell catalysts can be substantially elevated by proper pre-treatment. However, since whole cells comprise a complex system the underlying molecular reasons for the observed effects are only accessible indirectly making it difficult to rationalize the optimization approaches. Former experiments performed in neat substrates, showed that the catalyst was extremely stable under process conditions. This was verified by repeated batch operation and cell recycling, wherein biocatalytic performance was nearly unchanged within five batches. The striking process stability renders the neat substrate system suitable for continuous operation mode and thus broadens its applicability.

As presented in this thesis, it was possible to produce (*S*)-alcohols by application of CPCR2 or ReADH and the (*R*)-alcohols with LbADH by reduction of ketones. To complete the synthetic toolbox, asymmetric oxidation (racemate resolution) is missing, where one of the enantiomers is oxidized to the ketone leaving the other enantiomer behind. This was achieved by simply exchanging isopropanol by acetone and driving the reaction towards oxidation. However, the yield of a racemate resolution is limited to 50 % as only one enantiomer takes part in the reaction. To overcome this limitation, CPCR2 was operated in oxidation mode to produce the ketone from the unwanted (*S*)-alcohol; and after this, LbADH was utilized in reduction mode to yield up to 100 % (*R*)-alcohol. As a consequence of the sequential use of oxidation and reduction exploiting the stereocomplementary of the enzymes, quantitative conversion (96.1 %) at high enantioselectivity ( $ee = 96.5\%$  *R*) was achieved. This demonstrates the compatibility and especially the flexibility of the neat substrate system with respect to the reaction direction, tunable by the cosubstrate, and stereoselectivity, adjustable by the choice of catalyst.

The neat substrate system, developed in this thesis, is very much competitive with existing processes with regard to substrate load ( $500\text{ g L}^{-1}$ ), selectivity ( $ee >99\%$ ), sustainability and cost-effectiveness. Product work-up is very straightforward since cells can be filtered off and co-products are easily removed by evaporation. A key feature constitutes also the tool-box character of the reaction system, wherein the starting material and the stereospecific outcome are freely selectable. Certainly, the prolonged reaction time is in the focus of optimization and full conversion within one day is

envisaged. Strikingly, inhibition phenomena, due to the exceedingly high substrate and product concentrations, could not be observed so far. For industrial application of this system in production plants, regulations for genetically modified microorganisms (GMO), as used here, may inhibit the fast translation into practice. Hence, also non-GMOs might be tested in the neat substrates to circumvent this obstacle.

Protein engineering is a powerful tool to make enzymes fit for applications in industrial processes. The carbonyl reductase CPCR2 is already an attractive enzyme for organic synthesis due to its broad substrate scope and high stereoselectivity; however, some ketones are only poorly accepted and stability in biphasic systems is particularly low. Therefore, two semi-rational approaches were undertaken, one to broaden the substrate scope of CPCR2 and the second to make the enzyme more stable and resistant in the presence of water-organic interfaces.

In this thesis, the recombinant CPCR2 was subjected to saturation mutagenesis and screening for the first time. To achieve this, a protein expression procedure and activity-based screening strategy were successfully developed for microtiter plates. Saturation of five single amino acid positions, located in the substrate binding pocket (55, 92, 118, 119 & 262), and screening with 14 poorly converted substrates led to one CPCR2 variant with altered substrate acceptance. A CPCR2 variant (CPCR2-L119M) with the rare substitution from leucine to methionine at position 119 exhibited more than 7-fold improved turn over with 2-methyl cyclohexanone in comparison to wild type CPCR2, whereas selectivity was not altered significantly. Relative to other alcohol dehydrogenases from literature, CPCR2-L119M showed superior activity for this substrate. Sequencing of active clones of the other four positions revealed only little flexibility with respect to alternative amino acids. In a screening with well-accepted substrates the only improved variants were found at position 55 (L55F, L55W); whereas the other positions (92, 118, 119 & 262) seem to be strongly conserved.

CPCR2-L119M was tested for acceptance of substrates with similar structure like cyclohexanone as well as 3- methyl and 4-methyl cyclohexanone. The relative activity profile was similar to that of the wild type, but absolute activity was substantially improved for CPCR2-L119M but decreased for acetophenone. This indicates that the adaption of the enzyme towards the flexible cyclohexanone ring plays the most important role for the alteration of the substrate scope. Molecular modeling of 2-methyl cyclohexanone into the substrate binding pocket of the wild type and the variant showed a steric constraint of the substrate molecule and the branched leucine in the wild type enzyme. This constraint was not observed in CPCR2-L119M as the side chain is more flexible allowing a proper positioning of the substrate for catalysis. The flexibility of the side chain is mostly likely responsible for the difference in acceptance of cyclohexanone moieties.

To explain the differences in acceptance of all the cyclohexanone isomers and, in particular, the selectivity of CPCR2 for these substrates, a more sophisticated computational approach including

extensive molecular dynamics calculations has to be carried out. Crystallization of CPCR2 is currently attempted and may provide a high resolution crystal structure making more accurate modeling possible. On the basis of this, further campaigns to enlarge the substrate spectrum of CPCR2 targeting new amino acid positions may be undertaken. The selectivity of the wild type CPCR2 as well as of the variant with 2-methyl cyclohexanone as substrate are very low ( $ee < 16\%$  1-R &  $de < 55\%$  trans) and needs to be improved.

CPCR2 was also mutated on the surface to achieve stabilization at water-organic interfaces. Rational selection and mutagenesis of several surface exposed amino acids led to the variant CPCR2-(A275N, L276Q), which was improved in stability and also unexpectedly in activity. Usually, activity and stability display antagonists in protein engineering since mutations with higher activity are thought to enhance protein flexibility, whereas stabilizing mutations are believed to make the protein more rigid. However, the two adjacent amino acid positions were found to act cooperatively, wherein position 275 promotes stability and position 276 has an activating effect on CPCR2.

Single and double site saturation of these positions confirmed this initial finding and lead to the identification of a superior double variant CPCR2-(A275S, L276Q), which appeared from screening at elevated temperatures and in the presence of SDS. A more stable single variant was identified (CPCR2-A275T) as well as a variant with twofold improved activity (CPCR2-L276Q). Moreover, the general assumption that thermo- and solvent stability are positively correlated was confirmed for CPCR2 by testing the thermostable variants in a cyclohexane-buffer system.

Investigations on the structural level exhibit that the two mutations are located at the dimer interface and close to the active site, wherein position 275 is in hydrogen bonding distance to the other monomer and the amino acid at position 276 has direct contact with the substrate. Thus the structural model intuitively explains the effect of the substitutions. In silico site saturation and stability assessment using FoldX supported the experimental results as CPCR-A275T was identified as the most stable variant forming a hydrogen bond with the other monomer. All other amino acids found in stabilized variants are hydrogen bond donors as well; thus the inter-subunit hydrogen bond can be regarded as the general stabilizing interaction in CPCR2 variants.

The two positions 275 and 276 located at the dimer interface were never targeted by protein engineering in other alcohol dehydrogenases of this class but clearly constitute interesting spots for deeper investigation. For instance, further stabilization might be achieved by introduction of a salt bridge or targeting adjacent amino acids. Similar to other reports, this study shows that enhancing the interactions of the monomers promotes enzyme stability. In particular, stabilization of CPCR2 was achieved together with simultaneous activation.

For this reason, the impact of position 276 on CPCR2 activation might be examined more closely by QM/MM simulations of the protein-ligand complex. Here, arginine, lysine and methionine were found to promote activity but the underlying mechanism for activation is still unclear. To get a glimpse on the importance of this position 276 in catalysis, the effect on substrate scope and selectivity of CPCR2 variants might be tested in future.

The successful development of the “neat substrate system” for the manufacture of molar amounts of chiral alcohols, which is flexible with respect to the catalyst, the substrates, the stereoselectivity and the starting material, is one main outcome of this thesis. Surprisingly, the biocatalyst exhibits very high stereoselectivity and stability in pure substrate, which is most important for translation of this concept into industrial application. On the first glance, the high stability of the CPCR2 catalyst in the “neat substrate system” seems to make the development of a more stable CPCR2 for operation in organic media obsolete. But, so far, high stereoselectivity for 2-butanol could only be achieved with pure enzyme. Thus, a CPCR2 enzyme variant stable in biphasic reactor systems is still valuable. Protein engineering, as a second main result, was demonstrated to be applicable to CPCR2 and substantial improvements with respect to enlargement of the substrate scope and enzyme stability were achieved. Ultimately, in this thesis several successful approaches to enlarge the tool box of chiral alcohols accessible by asymmetric ketone reduction with CPCR2 were demonstrated and may lead to the development of sustainable industrial biocatalytic processes in the future.

## 5 Appendix

### 5.1 List of Abbreviations

Abbreviation	Meaning
A	alanine
A	adenine nucleotide base
Å	Ångström
ADH	alcohol dehydrogenase
ADPR	adenosine diphosphoribose
Ala	alanine
AMP	adenosine mono phosphate
Amp/amp	Ampicillin
APS	ammonium persulfate
Arg	arginine
Asn	asparagine
aw	water activity
BLAST	basic local alignment search tool
C	cysteine
C	cytosine nucleotide base
C.	Candida
CAST	combinatorial active site design
CCTCC	China Center for Type Culture Collection
CHAPS	3-[(3-Cholramidopropyl)dimethyl-ammonio]-1-propanesulfonate
Cl	chlor
cmc	critical micelle concentration
CO <sub>2</sub>	carbon dioxide
CPCR	Candida parapsilosis carbonyl reductase
CpSADH	carbonyl reductase secondary alcohol dehydrogenase
CR	carbonyl reductase
CTAB	cetyl trimethyl ammonium bromide
Cys	cysteine
D	aspartic acid
d	day
DCM	dichloro methane
DMSO	dimethylsulfoxide
DNA	deoxyribonucleic acid
dNTP	deoxyribonucleotide
DSM	Dutch State Mining
DSMZ	Deutsche Sammlung von Mikroorganismen und Zellkulturen
dSSM	double site saturation mutagenesis
DTT	dithiothreitol
E	glutamic acid
E	Escherichia
E. coli	Escherichia coli
EC	Enzyme Commission
EDTA	ethyl diamine tetraacetic acid
ee	enantiomeric excess
epPCR	error prone polymerase chain reaction
F	phenylalanine
FACS	fluorescence activated cell sorting
FDA	Food and Drug Association
FDH	formate dehydrogenase



Abbreviation	Meaning
Fig	Figure
FPLC	fast protein liquid chromatography
G	guanine nucleotide base
G	glycine
GC	gas chromatography
Gln	glutamine
Glu	glutamic acid
GLUE-IT	GLUE including translation
Gly	glycine
H	histidine
h	hour
His	histidine
HLADH	horse liver alcohol dehydrogenase
HTS	high throughput screening
I	isoleucine
Ile	isoleucine
IPTG	isopropyl $\beta$ -D-1-thiogalactopyranoside
K	lysine
kb	kilobases
kcat	turnover number of an enzyme, first-order rate constant
kDa	kilodalton
Km	affinity constant in Michaelis Menten kinetics
L	leucine
lac	lactose
LB	lysogeny broth
LbADH	Lactobacillus brevis alcohol dehydrogenase
LDR	long chain dehydrogenase/reductase
Leu	leucine
LPS	lipopolysaccharide
Lys	lysine
M	methionine
MCS	multiple cloning site
MDR	medium-chain dehydrogenases/reductases
Met	methionine
min	minute
MTBE	methyl-tert. butyl ether
MTP	microtiterplate
N	asparagine
Na	sodium
NAD <sup>+</sup>	nicotinamide adenine dinucleotide, oxidized
NADH	nicotinamide adenine dinucleotide, reduced
NADPH	nicotinamide adenine dinucleotide phosphate
NDT	degenerated nucelotide triplet
nm	nanometer
NNK	degenerated nucelotide triplet
NNN	degenerated nucelotide triplet
NNS	degenerated nucelotide triplet
OD	optical density
opt	optimum
orf	open reading frame
P	proline
PAGE	polyachrylamide gel electrophoresis
PCR	polymerase chain reaction
PDB/pdb	protein data bank

Abbreviation	Meaning
PF	protein family
Phe	phenylalanine
Pi	inorganic phosphate
PMSF	phenylmethanesulfonylfluorid
Pro	proline
ProSAR	<i>Protein Sequence Activity Relationships</i>
PSI	position-specific iterated
PSSM	position-specific scoring matrix
Q	glutamine
R	arginine
ReADH	Rhodococcus erythropolis alcohol dehydrogenase
RNA	ribonucleic acid
S	serine
SBP	substrate binding pocket
SDM	site-directed mutagenesis
SDR	short chain dehydrogenase/reductase
SDS	sodium dodecyl sulfate
Ser	Serine
SeSaM	Sequence Saturation Mutagenesis
SOC	super optimal broth
sp.	species
SsADH	<i>Sulfolobus solfataricus alcohol dehydrogenase</i>
SSM	site saturation mutagenesis
StEP	staggered extension process
Strep	streptavidin
T	threonine
T	thymine nucleotide base
Tab	Table
TAE	Tris base-acetic acid-EDTA
TB	terrific broth
TbADH	Thermoanaerobacter brockii alcohol dehydrogenase
TEA	triethanolamine
TEMED	N, N, N', N'-tetramethylethylenediamine
temp	temperature
TeSADH	Thermoanaerobacter ethanolicus secondary alcohol dehydrogenase
TEV	tobacco etch virus
Tris	Tris(hydroxymethyl)-aminomethan
tRNA	transfer ribonucleic acid
Trp	tryptophane
Tyr	tyrosine
U	unit
UV	Ultraviolet
V	valine
Val	valine
W	tryptophane
WT/wt	wild type
X	random amino acid
Y	tyrosine
YADH1	yeast alcohol dehydrogenase 1
YT	yeast extract tryptone
Z	zinc
Zn	zinc

## 5.2 List of Figures

### Figures from Chapter 1

Figure 1 Examples for different biocatalytic routes for the production of alcohols.....	4
Figure 2 Deracemization of secondary alcohol.....	5
Figure 3 Cofactor regeneration systems for alcohol dehydrogenases.....	7
Figure 4 Mechanism and enantioselectivity of alcohol dehydrogenases. ....	16
Figure 5 Overall structure of dimeric alcohol dehydrogenase and Rossmann-fold.....	17
Figure 6 Catalytic and structural zinc in horse liver alcohol dehydrogenase. ....	18
Figure 7 General architecture of an alcohol dehydrogenase and overview of substrate spectrum of commonly used alcohol dehydrogenases.....	18
Figure 8 Proposed model of the substrate binding pocket of <i>Candida parapsilosis</i> carbonyl reductase.....	20
Figure 9 Scheme of the three steps in a directed evolution experiment.....	27
Scheme 1 Interconversion of a ketone to the corresponding alcohol with NAD(P)H.....	6

### Figures from Chapter 2

Figure 1 Vector map of pET22b(+) vector from Novagen (Cat. No. 69744-3).....	39
Figure 2 Design of CPCR construct.....	40
Figure 3 Principle of a single amino acid exchange using the QuikChange® method.....	41
Figure 4 Standard operation procedure for CPCR expression in multititer plate.....	44
Figure 5 Standard operation procedure for cell lysis of CPCR in microtiter plate scale.....	46
Figure 6 Typical inactivation profile of an enzyme to determine $T_{50}$ -value.....	49
Figure 7 Screening strategy to find CPCR variants with increased activity and stability.....	51
Figure 8 Setup for equilibration to fixed $a_w$ -values of substrate solutions & cells with saturated salt solutions.....	53

### Figures from Chapter 3.1

Figure 1 Alignment of CPCR1 with ADH 1 and ADH 2 from <i>C. albicans</i> and ADH1 from bakers' yeast.....	61
Figure 2 A) Binding site of the CPCR1 model with bound 2,2,2-trifluoroethanol (magenta) and B) binding site of the CPSADH-model with bound ethoxyethanol (magenta). Catalytic residues around $Zn^{2+}$ and NADH are represented in ball and stick, all other residues in stick representation. Residues from the monomer B are colored red. Binding sites of C) CPCR1 model and D) CpSADH model in van der Waals representation.....	64
Figure 3 A) The bar diagram represents relative volumetric enzyme activities of three different CPCR preparations for ethyl 5-oxohexanoate, methyl-3-oxovalerate cyclohexanone and acetophenone. B) The bar diagram depicts the calculated relative activation energies ( $\Delta E$ ) for the same substrates for the two CPCR homology models.....	65
Figure S1 Coomassie stained SDS-PAGE of CPCR.....	66
Figure S 2 CPCR1 & CpSADH quaternary structures are modelled as tetramers.....	67
Figure S 3 Sequence alignment of CPCR1 and CpSADH with the homologous.....	67
Scheme 1 Sample compounds from the substrate range of CPCR.....	56

### Figures from Chapter 3.2

Figure 1 Biocatalytic reduction of acetophenone using lyophilized <i>E. coli</i> cells.....	72
Figure 2 Conversion of acetophenone by <i>E. coli</i> whole cells overexpressing CPCR in solvent-free conditions.....	73
Figure 3 Initial reaction rate of acetophenone in neat substrates employing <i>E. coli</i> whole cells.....	74
Figure 4 Biocatalytic reduction of 3-butyn-2-one using lyophilized <i>E. coli</i> cells.....	75

**Figures from Chapter 3.3**

Figure 1 Dependence on water activity of three different ADH whole cell catalysts in neat substrates .....	86
Figure 2 Reaction rate in pure isopropanol and acetophenone (ratio 9:1) with <i>E. coli</i> whole cells overexpressing CPCR2 after treatment with different permeabilizing agents. ....	91
Figure 3 Reaction rate in pure isopropanol and acetophenone (ratio 9:1) with <i>E. coli</i> whole cells overexpressing CPCR2 after resuspension in NAD <sup>+</sup> -solutions.....	92
Figure 4 Relative reaction rates in pure isopropanol and acetophenone (ratio 9:1) with <i>E. coli</i> whole cells overexpressing CPCR2 operated at different temperatures for 24h. ....	93
Figure 5 Operational stability of the whole catalyst in the standard reaction system in repeated batch mode..	94
Figure 6 Sequential deracemization of 1-phenylethanol by consecutive use of two whole cell catalysts with opposing stereoselectivity. ....	96
Figure 7 Conversion and enantioselectivity of sequential deracemization of 1-phenylethanol. The arrows indicate removal of coproduct and replenishment with fresh cosubstrate. ....	96
Scheme 1 Deracemization: Racemic starting material is subjected to asymmetric oxidation where only one enantiomer is converted by ADH1 to the ketone.....	82

**Figures from Chapter 3.4**

Figure 1 Substrates tested with CPCR2 relative to ethyl 5-oxo-hexanoate.....	104
Figure 2 Representation of the substrate binding pocket of CPCR2.....	110
Figure 3 Specific activities of wtCPCR2 & CPCR2-L119M on acetophenone and various cyclohexanones.....	112
Figure 4 Model 2-MCHone in the substrate binding pocket of wtCPCR2 and CPCR2-L119M.....	115
Figure S 1 SDS-PAGE of wtCPCR2 and CPCR-L119M .....	118
Figure S 2 Comparison of the temperature optima of wtCPCR2 and CPCR2-L119M.....	119
Figure S 3 Comparison of the pH-optima for ketone reduction of wtCPCR2 and CPCR2-L119M.....	119

**Figures from Chapter 3.5**

Figure 1 Half-lives of CPCR2 in the presence of MTBE, cyclohexane and <i>n</i> -heptane in monophasic (solvent-saturated buffer) and biphasic systems. ....	129
Figure 2 Specific relative activities of purified CPCR2 variants in relation to wtCPCR2 in buffer (0.1 mol L <sup>-1</sup> TEA, pH 8; 5 mmol L <sup>-1</sup> acetophenone). Specific activity of wtCPCR2 in crude extract was 0.97 U mg <sup>-1</sup> . ....	130
Figure 3 Relative stability of selected CPCR2 variants in the presence of organic solvents. Relative stabilities are normalized to the half-lives of wtCPCR2 in the corresponding mono- and biphasic.....	131
Figure 4 Relative activity in buffer and relative interfacial stability of CPCR2-(A275N, L276Q), CPCR2-(A275N), and CPCR2-(L276Q) in a biphasic system with cyclohexane. ....	131
Figure 5 Determination of T <sub>50</sub> -value for wtCPCR2 and CPCR2-A275N-L276Q in crude lysates. ....	133
Figure 6 Thermal inactivation curves of purified wtCPCR2 and selected variants. The black horizontal dashed line indicates 50 % residual relative activity. ....	137
Figure 7 Dimer interaction of CPCR2homology model (left) and the <i>Ss</i> ADH crystal structure (right). The A-chain of CPCR2 is colored in green and the B-chain is shown in blue.....	139
Figure S1 Protein sequence alignment of pdb entries most related to CPCR2. Upper digits refers to CPCR2 numbering, lower digits refer to automatic numbering created by alignment .....	143
Figure S2 Relative activity of wtCPCR2 cell-free lysate after incubation with different detergents below and above the critical micelle concentration (cmc) .....	145

## 5.3 List of Tables

### Tables from Chapter 1

Table 1 Selected large-scale biotransformations, adapted from <sup>[2]</sup> .....	1
Table 2 Biocatalytic asymmetric reduction of C=O compounds in industrial scale (>1kg) .....	9
Table 3 Biocatalytic asymmetric reduction in preparative scale (<1 kg).....	10
Table 4 Temperature and pH optimum for CPCR preparation .....	21
Table 5 Stability of CPCR preparations under different conditions. ....	22
Table 6 Recombinant carbonyl reductases from various <i>Candida parapsilosis</i> type strains compered to CPCR .	22
Table 7 Applications of CPCR in preparative scale and in different reaction setups. ....	23
Table 8 Patents published for reductive activities of <i>Candida parapsilosis</i> .....	24
Table 9 Recent achievements in protein engineering towards improvement of various properties with random, rational and combined methods.....	24

### Tables from Chapter 2

Table 1 Properties and applied concentrations of selected detergents for CPCR2 inactivation. ....	50
Table 2 Composition of saturated salt solutions and water activity at 30°C, taken from <sup>[10]</sup> . ....	53

### Tables from Chapter 3.1

Table 1 Measured and published biochemical features of carbonyl reductase from <i>Candida parapsilosis</i> .....	60
Table 2 Results from sequence alignment and modeling parameters.....	63
Table S1 Conversion by partially purified CPCR preparation of selected substrates.....	68
Table S2 Comparison of active site residues of CPCR1 and CpSADH with according X-templates.....	69
Table S3 CPCR1: Calculated energy-values given in kJ/mol .....	69
Table S4 CpSADH: Calculated energy-values given in kJ/mol .....	69

### Tables from Chapter 3.3

Table 1 Comparison of enzymes selected for application in the neat substrate system.....	79
Table 2 Benchmark substrates selected for reduction in the neat substrate system.....	80
Table 3 Price comparison of ketones with their corresponding alcohols in racemic and enantiopure form. ....	81
Table 4 Concentrations of agents used for permeabilization of <i>E. coli</i> whole cells.....	83
Table 5 Conditions for gas chromatographic separation of ketone/alcohol pairs and typical retention times. .	84
Table 6 Conversion & enantioselectivity ( <i>ee</i> meas.) of structurally different substrates by LbADH, ReADH and CPCR2 whole cell catalysts in neat substrates. ....	87
Table 7 Enantiomeric excess of 2-butanone with CPCR2 in different reaction systems.....	88

### Tables from Chapter 3.4

Table 1 Primer sequences for site-saturation.....	106
Table 2 Kinetic parameters of reduction of 2-MCHone with wtCPCR2 and CPCR2-L119M.....	113
Table 3 Kinetic parameters for reduction of 2-MCHone to 2-MCHol of purified alcohol dehydrogenases.....	113
Table 4 Relative amounts of 2-MCHols produced with wtCPCR2 & CPCR2-L119M and <i>ee R</i> & <i>de trans</i> .....	114
Table 5 Stabilization energies of different substrates in wtCPCR2 & CPCR2-L119M models.....	116
Table S1 Activity of poorly accepted substrates relative to acetophenone.....	117
Table S2 Activity of substrate sets under screening conditions relative to acetophenone.....	118

**Tables from Chapter 3.5**

Table 1 Relative improvements of CPCR2 variants compared to wtCPCR2 identified in rescreening. ....	135
Table 2 Comparison of catalytic and stability parameters of wtCPCR2 and its variants.....	136
Table 3 FoldX calculations of improved CPCR2 double mutants found by screening.....	138
Table S1 Table S1 CPCR2 variants generated from selected surface amino acids.....	142
Table S2 Primers applied for site-saturation of NhisCPCR2. ....	142
Table S3 Comparison of His-tagged CPCR2 and Strep-tagged CPCR2.....	142
Table S4 Primers applied for site-saturation of CstrepCPCR2.....	143
Table S5 Number of clones and completeness of each library (NNS-codon degeneracy and $P_c = 95\%^{[41]}$ ).....	144
Table S6 Energies calculated by FoldX for in silico saturation of position 275 in CPCR2.....	144
Table S7 Energies calculated by FoldX for in silico saturation of position 276 in CPCR2 .....	145